AD-A114 033 JOINT TACTICAL COMMUNICATIONS OFFICE FORT MONMOUTH NJ F/G 9/4
MULTIPLEXED NOISE CODES - A UNIQUE CODE CLASS.(U)
APR 82 F S GUTLEBER.
UNCLASSIFIED TTO-ENG-002-82 NL

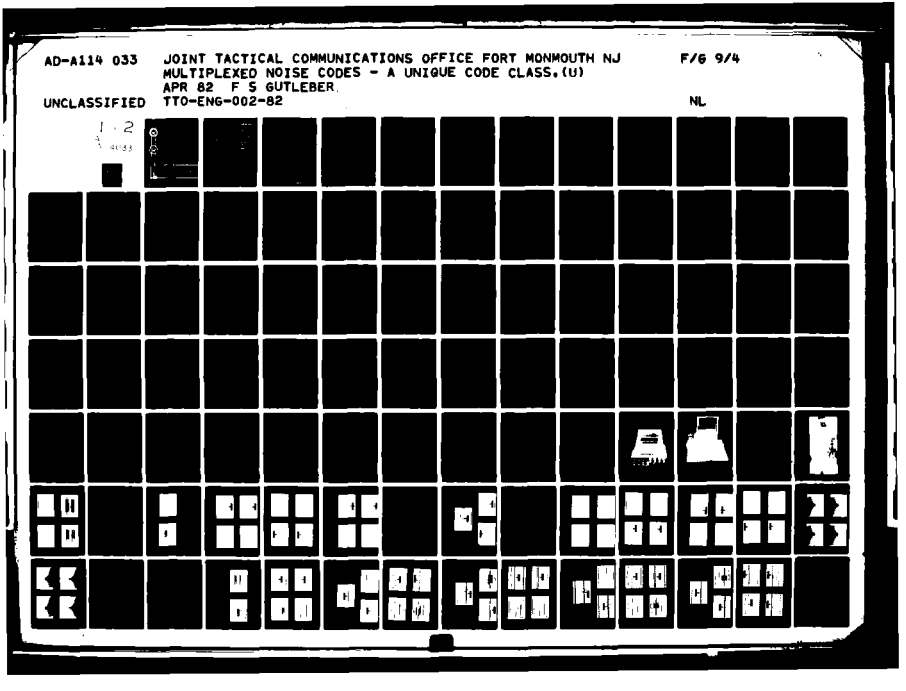

(12)

TTO-ENG-002-82

SECRETARY OF THE ARMY'S
RESEARCH AND STUDY FELLOWSHIP
FINAL REPORT

MULTIPLEXED NOISE CODES
—A UNIQUE CODE CLASS—

BY FRANK S. GUTLEBER

APRIL 1982

USA-USN-USAF-USMC

JOINT TACTICAL COMMUNICATIONS OFFICE
FORT MONMOUTH, N.J.

UNCLASSIFIED

SECURITY CLASSIFICATION OF THIS PAGE (When Data Entered)

REPORT DOCUMENTATION PAGE	READ INSTRUCTIONS BEFORE COMPLETING FORM
1. REPORT NUMBER: TTO-ENG-002-82	2. GOVT ACCESSION NO.: AD-A114 033
	3. RECIPIENT'S CATALOG NUMBER:
4. TITLE (and Subtitle): MULTIPLEXED NOISE CODES - A UNIQUE CODE CLASS -	5. TYPE OF REPORT & PERIOD COVERED: Secretary of the Army's Research and Study Fellowship Final Report, 1 Oct 80-1 Oct81
	6. PERFORMING ORG. REPORT NUMBER:
7. AUTHOR(s): FRANK S. GUTLEBER	8. CONTRACT OR GRANT NUMBER(s):
9. PERFORMING ORGANIZATION NAME AND ADDRESS: Joint Tactical Communications Office(TRI-TAC) ATTN: TT-E-SS 197 Rance Avenue Tinton Falls, NJ 07724	10. PROGRAM ELEMENT, PROJECT, TASK AREA & WORK UNIT NUMBERS:
11. CONTROLLING OFFICE NAME AND ADDRESS:	12. REPORT DATE: April 1982
	13. NUMBER OF PAGES: 163
14. MONITORING AGENCY NAME & ADDRESS(if different from Controlling Office):	15. SECURITY CLASS. (of this report): UNCLASSIFIED
	15a. DECLASSIFICATION/DOWNGRADING SCHEDULE:

16. DISTRIBUTION STATEMENT (of this Report)

Approved for public release; distribution unlimited.

17. DISTRIBUTION STATEMENT (of the abstract entered in Block 20, if different from Report)

18. SUPPLEMENTARY NOTES

19. KEY WORDS (Continue on reverse side if necessary and identify by block number)

Spread Spectrum; Coding; Multiple-Access; Orthogonal Coding; Signal Waveform Design; Impulse Autocorrelation Function; ECCM

20. ABSTRACT (Continue on reverse side if necessary and identify by block number)

The contents of this paper comprises a treatise on spread spectrum multiplexed noise codes which were first conceived about 20 years ago but have not received much publicity to date. Multiplexed noise codes are codes formed with mate code pairs which, when orthogonally multiplexed, transmitted, and detected in a matched filter, possess an impulse autocorrelation function (i.e., noise-like codes which compress to a single impulse containing no sidelobes). The fundamental requirement for achieving this desirable result is

cont

DD FORM 1 JAN 73 1473 EDITION OF 1 NOV 65 IS OBSOLETE

UNCLASSIFIED

SECURITY CLASSIFICATION OF THIS PAGE (When Data Entered)

20.(Cont'd)
that the autocorrelation function of the two codes forming a mate pair must be of equal magnitude and opposite sense for all values of time outside of the main lobe.

The various fundamental concepts which define the requirements for obtaining lobeless compression, an orthogonal noise code subclass, and basic general code expansion concepts are described and theoretically verified. In addition, a relatively complete coverage of the various unique attributes inherent in multiplexed noise codes is disclosed. In essence, a practical unified theory and explanation of these codes is presented to teach the principles involved and illustrate the magnitude of the gains that are realizable from codes that are capable of compressing to a lobeless impulse and which are available in abundance. The theoretical treatment demonstrates that the concepts and applications are all technically sound.

Utilizing the various concepts established, an orthogonal subset of multiplexed noise codes (32 bit mate pair codes) was implemented, actively using shift registers and passively using SAW device technology, and tested in appropriate test configurations to verify that the theoretical performance can be obtained with practical hardware. Excellent results were realized for both autocorrelation and crosscorrelation function measurements which established the feasibility of obtaining orthogonal multiple-access operation. This capability was then demonstrated by performing TDMA and CDMA tests where in the TDMA version, all the users employ the same noise code but select different available time slots and in the CDMA version, the same single available time slot is used by everyone in the system with a different unique noise code assigned to each user. An interference rejection capability in excess of 46 db (40,000/1) was obtained for both the TDMA and CDMA configurations. Other tests demonstrated that C.W. or pulse interference can be totally eliminated while retaining the desired signal at its peak detected level using an interference canceler in conjunction with multiplexed noise codes. The fact that multiplexed noise codes automatically provide a power gain margin or protection ratio equal to the number of code bits N was also experimentally confirmed. The various tests were specifically selected to (1) demonstrate that multiplexed noise codes can compress to an essentially lobeless impulse using state-of-the-art hardware and (2) to provide confidence in their utility as an optimum design solution for advanced communications systems.

TABLE OF CONTENTS

		PAGE
1.	Introduction	1
2.	Research Objectives	3
3.	Theory	5
	a. Concept Description	5
	b. Characteristics	14
	(1) Code Expansion with Transposed Codes	14
	(2) Available Code Quantity	17
	(3) Orthogonal Noise Code Subsets	18
	(4) Orthogonal Code Mate Pairs	30
	(5) Correlation Statistics	32
	(6) C.W. and Pulse Interference Rejection Potential	34
4.	Test Configurations and Results	42
	a. General Considerations	42
	b. Active Configurations	54
	(1) Implementation	54
	(2) Autocorrelation Function Measurements	54
	(3) Crosscorrelation Function Measurements	60
	(4) Multiplexed Noise Code Spectrum	67
	(5) Multiple-Access Tests	67
	• Orthogonal TDMA Concept	67
	• Orthogonal CDMA Concept	86
	(6) C.W. Interference Canceling Test	102
	c. Passive (SAW Device) Configurations	108
	(1) Implementation	108
	(2) Autocorrelation Function Measurements	111
	(3) Multiplexed Noise Code Spectrum	111
	(4) Future Plans	117
5.	Equipment List	118
6.	Conclusions	120
7.	Recommendations	122
	Acknowledgements	123

PAGE

Appendix A - General Code Mate Pair Expansion Concept 124

Appendix B - Interference Canceling Spread Spectrum System Concepts . . 127

Appendix C - An Orthogonal Spread Spectrum TDMA Mobile Subscriber Access System 140

Appendix D - An Orthogonal CDMA System 148

Appendix E - A Multiplexed Noise Coded Switching System 155

Bibliography 160

Related Patents 163

LIST OF TABLES

TABLE		PAGE
1	Sub Class of 4 Bit Multiplexed Noise Codes with Zero Crosscorrelation at τ=0 (Code Set #1).	.20
2	Sub Class of 8 Bit Multiplexed Noise Codes with Zero Crosscorrelation at τ=0 (Code Set #2).	.21
3	Crosscorrelation Function Values at τ=0 for Code Set #1. . .	.23
D1	Sub Class of 4 Bit Multiplexed Noise Codes with Zero Crosscorrelation at τ=0 (Code Set #1).	.152
D2	Sub Class of 8 Bit Multiplexed Noise Codes with Zero Crosscorrelation at τ=0 (Code Set #2).	.153

LIST OF ILLUSTRATIONS

FIGURE		PAGE
1	C. W. Interference Canceling Spread Spectrum System.	36
2	Autocorrelation Function of Code Pair A_1B_1.	43
3	Autocorrelation Function of Code Pair A_2B_2.	44
4	Autocorrelation Function of Code Pair A_3B_3.	45
5	Autocorrelation Function of Code Pair A_4B_4.	46
6	Autocorrelation Function of Code Pair A_6B_6.	47
7	Shift Register Code Generator/Correlation Detector (Top). .	55
8	Shift Register Code Generator/Correlation Detector (Bottom)	56
9	Autocorrelation & Crosscorrelation Test Configuration . . .	57
10	Test Configuration for Autocorrelation/Crosscorrelation Function Measurements.	58
11	Generated & Phase Modulated Code Pair A_4B_4.	59
12	Autocorrelation Function Value at $\tau=0$ for Code Pair A_4B_4. .	61
13	Autocorrelation Function Value at $\tau=6$ and $\tau=9$ for Code Pair A_4B_4.	62
14	Autocorrelation Function Value at $\tau=4$ and $\tau=12$ for Code Pair A_4B_4.	63
15	Autocorrelation Function Value at $\tau=20$ and $\tau=28$ for Code Pair A_4B_4.	64
16	Autocorrelation Function Calculation at $\tau=9$.	65
17	Autocorrelation Function Value for Code Pair A_4B_4 at $\tau=4$. .	66
18	Generated Multiplexed Noise Code Pairs.	68
19	Crosscorrelation of A_4B_4 vs A_2B_2 (a&b) and A_4B_4 vs A_6B_6 (c&d) at $\tau=0$.	69

FIGURE		PAGE
20	Crosscorrelation of A_4B_4 vs A_3B_3 (a&b) and A_2B_2 vs A_6B_6 (c&d) at τ=0.	70
21	Crosscorrelation of A_2B_2 vs A_3B_3 (a&b) and A_6B_6 vs A_3B_3 (c&d) at τ=0.	71
22	Multiplexed Noise Code Spectrum.	72
23	Multiplexed Noise Code Spectrum.	73
24	Multiple Access Test Configuration (2 Users).	75
25	Signal Plus Interference (2nd User) Performance.	76
26	Signal Plus Interference (2nd User) Performance τ=5.	77
27	Signal Plus Interference (2nd User) Performance τ=5.	78
28	Signal Plus Interference (2nd User) Performance τ=-1.	79
29	Signal Plus Interference (2nd User) Performance τ=-1.	80
30	Signal Plus Interference (2nd User) Performance τ=11.	81
31	Signal Plus Interference (2nd User) Performance τ=11.	82
32	Signal Plus Interference (2nd User) Performance τ=20.	83
33	Signal Plus Interference (2nd User) Performance τ=20.	84
34	Signal Plus Interference (2nd User) Performance τ=8.	85
35	Multiple Access Test Configuration (2 Users).	88
36	Signal Plus Interference (2nd User) Performance A_4B_4 vs A_6B_6. . .	89
37	Signal Plus Interference (2nd User) Performance A_3B_3 vs A_6B_6. . .	90
38	Signal Plus Interference (2nd User) Performance A_4B_4 vs A_3B_3. . .	91
39	Signal Plus Interference (2nd User) Performance A_4B_4 vs A_3B_3. . .	92
40	Multiple Access Test Configuration (3 Users).	94
41	Test Configuration for Multiple-access Tests (3 Users).	95
42	Signal Plus Multiple Interference Performance (A_3B_3+A_6B_6) vs A_4B_4.	96

FIGURE		PAGE
43	Signal Plus Multiple Interference Performance (A_3B_3+A_6B_6) vs A_4B_4.	97
44	Signal Plus Multiple Interference Performance (A_3B_3+A_4B_4) vs A_6B_6.	98
45	Signal Plus Multiple Interference Performance (A_3B_3+A_4B_4) vs A_6B_6.	99
46	Signal Plus Multiple Interference Performance (A_4B_4+A_6B_6) vs A_3B_3.	100
47	Signal Plus Multiple Interference Performance (A_4B_4+A_6B_6) vs A_3B_3.	101
48	C. W. Interference Canceling Test.	103
49	C. W. Interference Canceling Spread Spectrum System Performance.	104
50	C. W. Interference Canceling Spread Spectrum System Performance.	105
51	C. W. Interference in Output with Delay Path Disconnected and Signal Removed.	107
52	Surface Acoustic Wave Code Generator/Compressor (metal can enclosure).	109
53	Surface Acoustic Wave Code Generator/Compressor (machined enclosure).	110
54	Autocorrelation Function Test Configuration.	112
55	Test Configuration for Autocorrelation Function Measurements. .	113
56	Composite (Summed) Compressed Multiplexed Noise Code Pair A_4B_4..	114
57	SAW Device Generation & Compression of Code Pair A_4B_4.	115
58	Multiplexed Noise Code Spectrum (SAW Code Generator).	116
B1	C. W. Interference Canceling Spread Spectrum System.	128
B2	Pulse Interference Canceling Spread Spectrum System.	134
B3	Pulse Interference Canceling Spread Spectrum System.	137
C1	Ground Mobile Access System Employing Orthogonal TDMA.	141
C2	Loop Back Synchronous Timing Subsystem.	142
C3	Multiplexed Code Transceiver.	145

FIGURE		PAGE
D1	Ground Mobile Access System Employing Orthogonal CDMA.	149
D2	Multiplexed Code Transceiver.	151
E1	Multiplexed Noise Coded Switching System.	157
E2	Line-to-Line Switch Operation.	158

1. INTRODUCTION

Reflecting on the many advances made in the general field of coding over the last four decades reveals that a single common structure repeatedly surfaces as the optimum solution for one reason or another. In order to simultaneously meet numerous different critical requirements, wide bandwidth (spread spectrum) noise coded signals have been shown to provide the optimum solution. That is, the most desirable codes available in general have an approximately uniform frequency spectrum, are essentially constant in amplitude and compress to a narrow-pulse (whose width equals the reciprocal of the spread bandwidth) with low sidelobes (ideally with zero sidelobes) when detected with a matched filter. If an application involves a doppler shift of the signal, then the optimum solution becomes a code which provides a compressed pulse in the ambiguity diagram containing low level sidelobes in both time or range and doppler frequency or velocity. Again, the noise like coded structure predominates and is in fact necessary to simultaneously provide the required degree of compression (or equivalently resolution) in both time and doppler frequency.

Performance essentially becomes optimum for systems that utilize noise like codes in general (as evidenced by the more recent extensive use of spread spectrum noise like codes) since

- Maximum resolution is provided or ambiguity is minimized by approximating the ideal (thumbtack) ambiguity diagram.
- Range (time) and velocity (doppler frequency) accuracy measurements are simultaneously maximized.
- Anti-Jam (A/J) protection is the best achievable and employing a noise code forces an enemy to employ wideband noise jamming.
- Low Probability of Intercept (LPI) or covert communications is the best achievable.
- Unambiguous maximum timing accuracy is obtained (time jitter is minimized).
- Transmission efficiency for communications systems is optimum and approaches Shannon's performance limit using orthogonal noise codes in a biorthogonal (M' ary) PCM system.
- Anti-multipath RAKE diversity can be utilized which provides an optimum and effective means for countering the signal fades experienced over tropospheric or ionospheric transmission links.

The most widely understood and utilized noise like code class to date is the popular direct sequence maximal length shift register codes which are generally referred to as pseudo-noise (P-N) codes. These codes have found wide application since they are easily generated with shift registers,

possess a periodic autocorrelation function with sidelobes down by (1/N) from the main lobe for an N bit code, and have a spectrum that is spread to $(1/\tau)$ where τ is equal to the pulse width of the compressed code. In spite of these very desirable properties and the codes numerous applications in existing and contemplated systems, however, they have limitations which render them undesirable or impractical for the more stringent requirements of some future communications systems. The major disadvantages of P-N codes are that the sidelobes are down by only $\approx 1/\sqrt{N}$ when the codes are used as an aperiodic structure, only non-orthogonal spread spectrum multiple-access is feasible, and even more significant is the fact that the quantity of available unique (i.e., different) codes for moderate time-bandwidth products (TxW=N) are very limited. For example, a 31 and 63 bit code length are each constrained to only 6 codes and there are only 18 available codes for a code length of 127. Even a 1023 bit length provides only 60 unique codes which still renders it impractical for many applications.

Not so well known and understood, but much more cogent are multiplexed noise codes which are the subject of this research program. These codes (as a class) were first conceived by myself about 20 years ago, but have not received much publicity to date. The Golay Binary Complementary Sequence Codes which are a subset of my general multiplexed noise codes have received some limited attention but have also not been highly publicized or tested to establish their full potential. Multiplexed noise codes overcome the major disadvantages noted above for direct sequence P-N codes since lobeless compression is realized using aperiodic codes, orthogonal code subsets exist, and the available quantity of unique codes for this class is inordinately large for moderate code lengths n. These characteristics permit implementing orthogonal (zero self-interference) multiple-access systems, totally canceling C.W. and/or pulse interference or jamming, and prevent an enemy from utilizing intelligent jamming. In addition, the advantages itemized for noise codes in general are all realized for multiplexed noise codes. Other applications that utilize multiplexed noise codes in some unique manner are described in several of the references listed in the bibliography.

2. RESEARCH OBJECTIVES

The overall objective of the research program is to construct and test brassboard models which will prove the efficacy and practicality of employing multiplexed noise codes in several novel applications in the communications field that capitalize on its unique characteristics. The capability to compress to an essentially lobeless impulse for an aperiodic structure, cross-correlate to a near zero amplitude using orthogonal subsets and possess a noise like spread spectrum is to be verified for codes implemented with practical hardware. Their application in various novel communication systems will then be demonstrated using appropriate test configurations to provide confidence in their utility as an optimum design solution for advanced communications systems.

More specifically, the program will first involve constructing active and/or passive code mate pair generators and matched filter detectors. These code generators/matched filters will then be tested in appropriate test configurations to verify they:

- o Compress to an essentially lobeless impulse or have a measured auto-correlation function whose values are significantly lower that the square root of the time bandwidth product.

- o Cross correlate to near zero ($< -40db$) amplitude relative to the peak output of the desired signal using an orthogonal code subset.

- o Possess a noise like spectrum that is spread by the time-bandwidth product or equivalently the number of code bits n to provide a gain margin equal to n.

Armed with positive test results for the above characteristics, system tests will then be established to verify the feasibility of utilizing the implemented code generators and matched filters in orthogonal time division and code division multiple access (TDMA and CDMA) system applications. The coded and modulated signals of several users will be combined and detected in a filter matched to the desired signal to measure the interference rejection capability that can be realized when using practical hardware. In the TDMA version, all the users employ the same code but different available time slots whereas in the CDMA version, the same single available time slot is employed, but each user is assigned a different unique noise code belonging to an orthogonal subset. The CDMA tests will also verify what performance is realizable when multiplexed codes are used in a switching application.

In addition, the C.W. interference rejection potential of multiplexed noise codes will be measured. Theoretically, a C.W. or pulse interferer or jammer can be nulled out or cancelled completely with no loss at all in the received level of the desired signal. Since multiplexed noise codes compress to a lobeless impulse, a delay greater than one code bit would not interfere with the detection of the desired signal while providing a coherent replica of the interference that can be subtracted from the input interference.

Concurrent with implementing and conducting performance verification tests using multiplexed noise-codes, its related theory will be expanded upon to establish other important properties and to formulate general proofs for the various developed code expansion formulas.

3. THEORY

a. CONCEPT DESCRIPTION

Multiplexed noise codes are codes formed with mate code pairs which when orthogonally multiplexed and detected in a matched filter possesses an impulse autocorrelation function (i.e., noise like codes which compress to a single impulse containing no lobes). The fundamental requirement for achieving this desirable result is that the autocorrelation function of the two codes forming a mate pair must be of equal magnitude and opposite sense for all values of time outside of the main lobe. Expressed mathematically; for two mate pair codes a and b

$$\phi_a(\tau) = -\phi_b(\tau)$$

$$\text{for all } \tau \neq 0 \qquad (1)$$

where $\phi_a(\tau)$ = autocorrelation function of code a

$\phi_b(\tau)$ = autocorrelation function of code b

When two codes meet this requirement, then the simple linear sum of their matched filter outputs results in compressing the code structure into a single lobeless impulse. As a simple illustration, consider the following elementary code pair which satisfies the requirements of equation (1).

code a = 1 0 0 0

code b = 1 0 1 1

where: 0 indicates +1

1 indicates -1

The matched filter output for each code of the pair produces the autocorrelation function of the input code sequence and the linear sum of the two matched filter outputs yields the composite autocorrelation function that is the sum of the individual autocorrelation functions.

i.e., $\phi_T(\tau) = \phi_a(\tau) + \phi_b(\tau)$

An easy method of calculating the autocorrelation function of any binary code involves a graphic means which essentially performs the operating functions of a passive pulse compressor (matched filter). The classical pulse compression filter for each of the code pairs is illustrated below.

For code a = 1 0 0 0

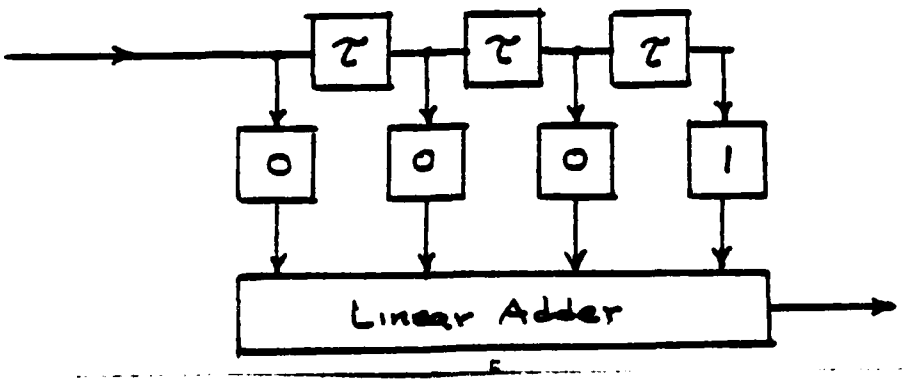

For code b = 1 0 1 1

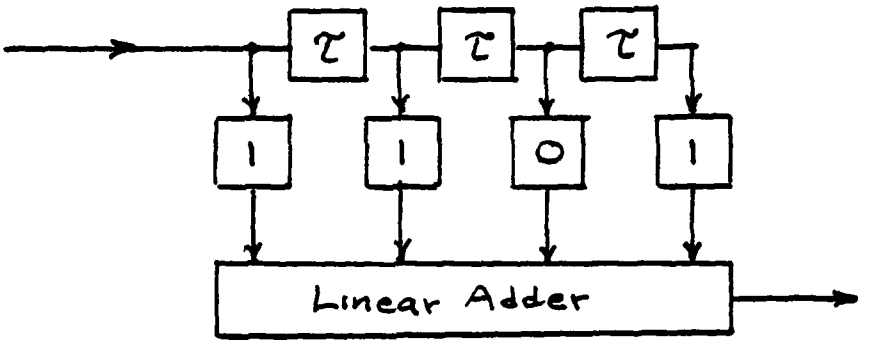

where:

the functional blocks containing τ represents a delay of τ that is equal to the code bit width

the functional blocks containing "1" or "0" identify a phase operation where 1 signifies a phase reversal and 0 signifies no phase reversal.

Graphically performing the operations illustrated in the functional block diagram for code a results in the following:

$$
\begin{array}{r}
1\ 0\ 0\ 0 \\
\quad 1\ 0\ 0\ 0 \\
\quad\quad 1\ 0\ 0\ 0 \\
\quad\quad\quad 0\ 1\ 1\ 1 \\
\hline
\phi_a(\tau) = 1 \cdot 0\ 0^4 0 \cdot 1 \\
\qquad\qquad\quad \uparrow_{\tau = 0}
\end{array}
$$

where:

the exponent represents the amplitude

i.e., $0^K = +K$

$1^K = -K$

A dot represents a zero amplitude.

Note that the matched filter phase inverts each of the delayed inputs only when it is required to provide an "0" or +1 at $\tau = 0$. This results when the phase reversals match the input code sequence in reverse order.

Compressing code (b) in its corresponding matched filter yields:

$$
\begin{array}{r}
0\ 1\ 0\ 0 \\
\quad 0\ 1\ 0\ 0 \\
\quad\quad 1\ 0\ 1\ 1 \\
\quad\quad\quad 0\ 1\ 0\ 0 \\
\hline
\phi_b(\tau) = 0 \cdot 1\ 0^4 1 \cdot 0 \\
\qquad\qquad\quad \uparrow_{\tau = 0}
\end{array}
$$

And the linear sum of the individually compressed codes results in a lobeless impulse as expected.

$$\phi_a(\tau) = 1 \cdot 0\ 0^4 0 \cdot 1$$

$$\phi_b(\tau) = 0 \cdot 1\ 0^4 1 \cdot 0$$

$$\phi_T(\tau) = \cdots 0^8 \cdots$$

$$\uparrow \tau = 0$$

The corresponding time diagrams for the compressed signals are shown below.

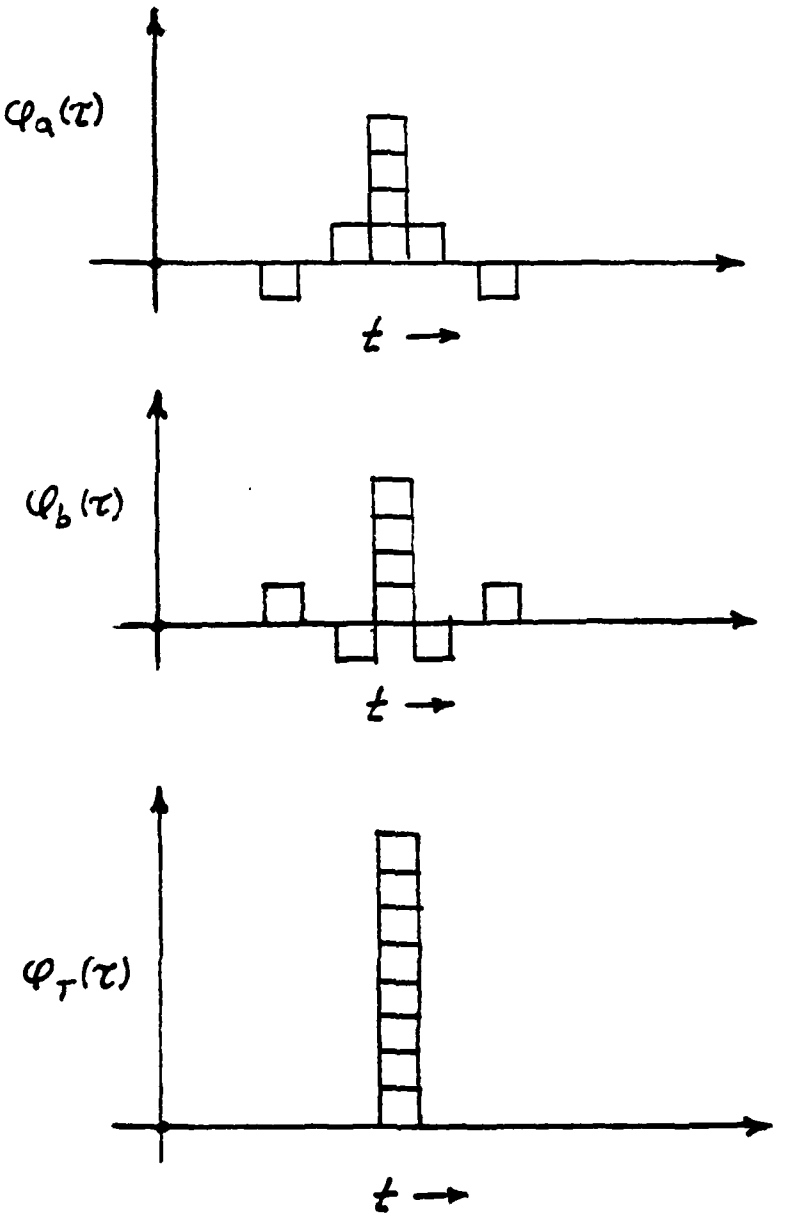

The implications associated with compressing a noise code to a lobeless impulse as compared with obtaining lobes of low level (such as is realized with direct sequence P-N codes) is very significant since this provides orthogonal noise code sets. That is, noise codes are available whose crosscorrelation value is zero. This eliminates the only real disadvantage associated with noise codes, namely, interference from close proximity users in a multiple-access communications system application (usually referred to as the "near/far ratio" problem).

The second most important attribute pertaining to the general class of multiplexed noise codes is that there is practically an inexhaustible supply of different unique codes for moderate time bandwidth products or code lengths n (i.e., n = 100 to n = 1000). The large available quantity results from the many different general methods that have been conceived for expanding any code mate pair into a new mate pair with twice as many code bits. The basic but general code expansion concepts are described below.

For a given code mate pair a and b, a new code pair A and B can be generated in accordance with the following paired relationships.

$$A_1 = a\,(t),\ b\,(t+\tau) \qquad (2)$$
$$B_1 = a\,(t),\ \overline{b\,(t+\tau)}$$

$$A_2 = b\,(t),\ a\,(t+\tau) \qquad (3)$$
$$B_2 = b\,(t),\ \overline{a\,(t+\tau)}$$

where: $\overline{x}$ = complement of code x

(1011 becomes 0100)

τ = a time delay of τ sec.

Since any code and its inverse has the same autocorrelation function, the following paired equations identify six additional expansion equations.

$$A_3 = a\,(t),\ \underline{b\,(t+\tau)} \qquad (4)$$
$$B_3 = a\,(t),\ \overline{\underline{b\,(t+\tau)}}$$

$$A_4 = \underline{b\,(t)},\ a\,(t+\tau) \qquad (5)$$
$$B_4 = \underline{b\,(t)},\ \overline{a\,(t+\tau)}$$

$$A_5 = \underline{a\,(t)},\ b\,(t+\tau) \qquad (6)$$
$$B_5 = \underline{a\,(t)},\ \overline{b\,(t+\tau)}$$

$$A_6 = b\,(t),\ \underline{a\,(t+\tau)} \qquad (7)$$
$$B_6 = b\,(t),\ \overline{\underline{a\,(t+\tau)}}$$

$$A_7 = \underset{\sim}{a}(t),\ \underset{\sim}{b}(t+\tau)$$
$$B_7 = \underset{\sim}{a}(t),\ \overline{\underset{\sim}{b}(t+\tau)} \qquad (8)$$

$$A_8 = \underset{\sim}{b}(t),\ \underset{\sim}{a}(t+\tau)$$
$$B_8 = \underset{\sim}{b}(t),\ \overline{\underset{\sim}{a}(t+\tau)} \qquad (9)$$

where:

$\underset{\sim}{x}$ = inverted digit sequence for code x
(i.e., 1011 becomes 1101)

Of major significance is the fact that τ can have any value from zero to infinity and still guarantee an expanded code mate pair. The time delay τ would, however, be limited to a maximum value that is constrained by the processing time utilized in any given application. In addition, τ would be confined to specific integral multiple values of the code bit width for codes that are constrained to a constant amplitude (i.e., binary). In spite of these restrictions, the available guantity of unique codes still remains extremely large.

A general proof which confirms that codes expanded in accordance with equations (2) through (9) results in another mate pair is contained in Appendix A. A simple heuristic proof is presented below.

Consider the following general code pair A and B which is expanded in accordance with the general basic expansion formula from code pair a and b.

$$A = a(t),\ b(t+\tau)$$
$$B = a(t),\ \overline{b(t+\tau)}$$

The autocorrelation and crosscorrelation processes experienced between the a and b codes when detecting A and B with a matched filter (or pulse compression filter) can be represented graphically as shown below.

For code A

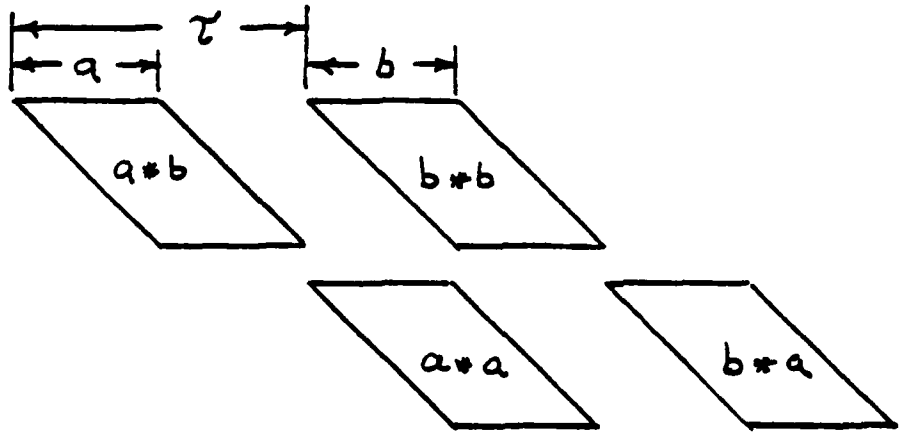

For code B

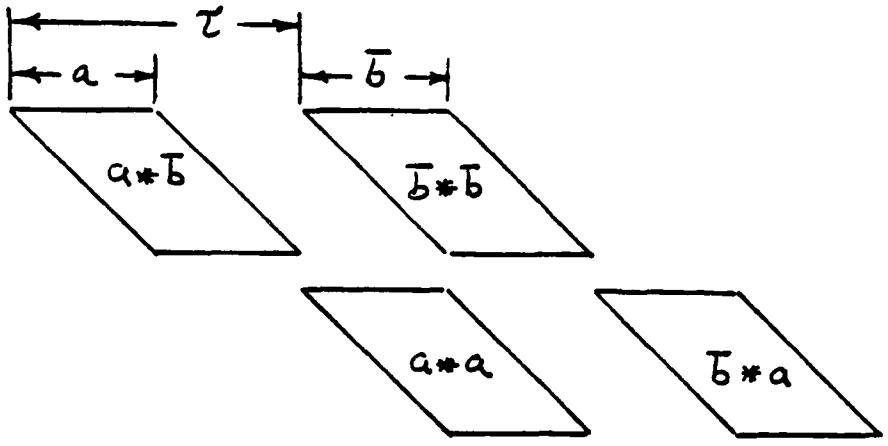

where:

x*x = autocorrelation function of code x

x*y = cross correlation function of code x with code y

And summing the appropriate autocorrelation and cross correlation functions results in

$$a*a + b*b \tag{10}$$

$$a*a + \bar{b}*\bar{b} \tag{11}$$

$$a*b + a*\bar{b} \tag{12}$$

$$b*a + \bar{b}*a \tag{13}$$

Now since a and b form a code mate pair by definition we have

$$a*a + b*b = 0 \quad \text{for all } \tau \neq 0 \tag{14}$$

And

$$a*a + \bar{b}*\bar{b} = 0 \quad \text{for all } \tau \neq 0 \tag{15}$$

Also since

$$a*\bar{b} = -a*b \tag{16}$$

and

$$\bar{b}*a = -b*a \tag{17}$$

Then

$$a*b + a*\bar{b} = 0 \tag{18}$$

and

$$b*a + \bar{b}*a = 0 \tag{19}$$

Hence the autocorrelation function of $B[\phi_B(\tau)]$ is of equal magnitude and opposite sense to the autocorrelation function of $A[\phi_A(\tau)]$ for all $\tau \neq 0$.

Note that τ can have any value and when it is less than the length of code a, partial or complete interleaving occurs between the b and a codes during the code expansion process.

The following example will help to clarify the flexibility inherent in the general expansion formulas and verify that the expanded code pair does indeed compress to a lobeless impulse.

The most basic elementary code pair a and b is

code a = 10
code b = 00

Although not specifically stated, any code structure can be symmetrically gapped without changing its autocorrelation function characteristics. That is, a and b can be lengthened as follows:

$a_0 = 1 \cdot \cdot \cdot 0$
$b_0 = 0 \cdot \cdot \cdot 0$

where:

The dot signifies a zero amplitude whose width is the same as the individual code bit width.

The autocorrelation function of code a_0 is now

$$\begin{array}{r} 1 \cdot \cdot \cdot 0 \\ 0 \cdot \cdot \cdot 1 \\ \hline \end{array}$$
$$\phi_{a_0}(\tau) = 1 \cdot \cdot \cdot 0^2 \cdot \cdot \cdot 1$$

And the autocorrelation function of code b_0 is

$$\begin{array}{r} 0 \cdot \cdot \cdot 0 \\ 0 \cdot \cdot \cdot 0 \\ \hline \end{array}$$
$$\phi_{b_0}(\tau) = 0 \cdot \cdot \cdot 0^2 \cdot \cdot \cdot 0$$

Hence:

$$\phi_{b_0}(\tau) = -\phi_{a_0}(\tau)$$
for all $\tau \neq 0$

Delaying code b_0 by 1 code bit ($\tau = 1$) and utilizing equation (2) results in

$$\begin{array}{r} 1 \cdot \cdot \cdot 0 \\ 0 \cdot \cdot \cdot 0 \\ \hline \end{array}$$
$$a_1 = 1\ 0 \cdot \cdot 0\ 0$$

$$
\begin{array}{rl}
 & 1 \cdots 0 \\
 & \quad 1 \cdots 1 \\
\hline
b_1 = & 1\,1 \cdots 0\,1
\end{array}
$$

Now applying equation (7) with $\tau = 3$ yields

$$
\begin{array}{rl}
 & 1\,1 \cdots 0\,1 \\
 & \quad\; 0\,0 \cdots 0\,1 \\
\hline
a_2 = & 1\,1\,0\,0\,0\,1\,0\,1
\end{array}
$$

$$
\begin{array}{rl}
 & 1\,1 \cdots 0\,1 \\
 & \quad\; 1\,1 \cdots 1\,0 \\
\hline
b_2 = & 1\,1\,1\,1\,0\,1\,1\,0
\end{array}
$$

a_2 and b_2 are a guaranteed 8 bit code pair since the general expansion formulas identified by equations (2) through (9) were utilized to generate them. Let us confirm that they are in fact a mate pair by determining their autocorrelation functions.

For code a_2 we have

$$
\begin{array}{l}
0\,0\,1\,1\,1\,0\,1\,0 \\
\quad 1\,1\,0\,0\,0\,1\,0\,1 \\
\quad\;\; 0\,0\,1\,1\,1\,0\,1\,0 \\
\quad\;\;\; 1\,1\,0\,0\,0\,1\,0\,1 \\
\quad\;\;\;\; 1\,1\,0\,0\,0\,1\,0\,1 \\
\quad\;\;\;\;\; 1\,1\,0\,0\,0\,1\,0\,1 \\
\quad\;\;\;\;\;\; 0\,0\,1\,1\,1\,0\,1\,0 \\
\hline
\quad\;\;\;\;\;\;\; 0\,0\,1\,1\,1\,0\,1\,0
\end{array}
$$

$$\phi_{a_2}(\tau) = 0 \cdot 1 \cdot 1^3 \cdot 1\,0^8 1 \cdot 1^3 \cdot 1 \cdot 0$$

And for code b_2

$$
\begin{array}{r}
1\ 1\ 1\ 1\ 0\ 1\ 1\ 0 \\
\quad 0\ 0\ 0\ 0\ 1\ 0\ 0\ 1 \\
\quad\quad 0\ 0\ 0\ 0\ 1\ 0\ 0\ 1 \\
\quad\quad\quad 1\ 1\ 1\ 1\ 0\ 1\ 1\ 0 \\
\quad\quad\quad\quad 0\ 0\ 0\ 0\ 1\ 0\ 0\ 1 \\
\quad\quad\quad\quad\quad 0\ 0\ 0\ 0\ 1\ 0\ 0\ 1 \\
\quad\quad\quad\quad\quad\quad 0\ 0\ 0\ 0\ 1\ 0\ 0\ 1 \\
\quad\quad\quad\quad\quad\quad\quad 0\ 0\ 0\ 0\ 1\ 0\ 0\ 1 \\
\hline
\end{array}
$$

$$\phi_{b_2}(\tau) = 1 \cdot 0 \cdot 0^3 \cdot 0\ 0^8 0 \cdot 0^3 \cdot 0 \cdot 1$$

And we see that $\phi_{b2}(\tau) = -\phi_{a2}(\tau)$ for all $\tau \neq 0$; therefore, the requirement for forming a mate pair has been retained as a and b were expanded to a_2 and b_2.

It must be mentioned here that the general concepts established by equations (1) through (9) are not confined to binary structures or codes. Any generated n bit code can be multi-amplitude as a result of having code bits of amplitude ± 1 overlap or by not having all of the gaps filled in during the code generation process.

As a simple illustration, let $\tau = 1$ (one code bit width) for the following two bit code pair.

$$\begin{array}{l} a = 1\ 0 \\ b = 0\ 0 \end{array}$$

Employing equation (2) yields:

$$
\begin{array}{rl}
1\ 0 & = a \\
0\ 0 & = b \\
\hline
1\ 0^2 0 & = A
\end{array}
\qquad
\begin{array}{rl}
1\ 0 & = a \\
1\ 1 & = \bar{b} \\
\hline
1 \cdot 1 & = B
\end{array}
$$

For confirmation that A and B are a mate pair, their respective autocorrelation functions will be established.

Pulse compressing code A:

$$\begin{array}{r} 1\ 0^2 0 \\ 1^2 0^4 0^2 \\ 0\ 1^2 1 \\ \hline 1 \cdot 0^6 \cdot 1 = \end{array} \quad \phi_A(\tau)$$

And pulse compressing code B:

$$\begin{array}{r} 0 \cdot 0 \\ \cdot \\ 0 \cdot 0 \\ \hline 0 \cdot 0^2 \cdot 0 = \end{array} \quad \phi_B(\tau)$$

which proves that the resultant expanded multi-amplitude code pairs satisfy the requirement for being a mate pair.

Note that the 2nd row for obtaining $\phi_A(\tau)$ is multiplied by 2 and that the second row for obtaining $\phi_B(\tau)$ is zero. This conforms to matching the code bits in reverse order which must be both in phase and amplitude.

b. CHARACTERISTICS

The basic concepts, defining equations and proofs that establish the fundamental elements associated with multiplexed noise codes has been presented. They are aperiodic, compress to a lobeless impulse, and are available in an extremely large quantity even for moderate time-bandwidth products. Other attributes which are also very advantageous and unique will now be addressed.

(1) Code Expansion with Transposed Codes

The basic code expansion equations (2 through 9) all involve delaying the same code of the initial pair when forming each code of the new expanded pair. The following set of code expansion equations enables each expanded code to begin with each different code of the initial mate pair provided that the delayed codes are inverted. Complementing one of the delayed and inverted codes then guarantees a new expanded code mate pair.

Expressed mathematically :

For a given code mate pair a and b,

$$\begin{aligned} A_1 &= a(t),\ \underbrace{b(t+\tau)} \\ B_1 &= b(t),\ \overline{\underbrace{a(t+\tau)}} \end{aligned} \qquad (20)$$

$$A_2 = b(t),\ \underset{\sim}{a}(t+\tau)$$
$$B_2 = a(t),\ \overline{\underset{\sim}{b}(t+\tau)} \qquad (21)$$

where as before:

$\underset{\sim}{x}$ = inverse of x
$\overline{x}$ = complement of x

And since any code and its inverse has the same autocorrelation function, the following paired equations identify six additional expansion equations that will meet the requirements for forming a mate pair.

$$A_3 = \underset{\sim}{a}(t),\ \underset{\sim}{b}(t+\tau)$$
$$B_3 = b(t),\ \overline{a(t+\tau)} \qquad (22)$$

$$A_4 = b(t),\ a(t+\tau)$$
$$B_4 = \underset{\sim}{a}(t),\ \overline{\underset{\sim}{b}(t+\tau)} \qquad (23)$$

$$A_5 = a(t),\ b(t+\tau)$$
$$B_5 = \underset{\sim}{b}(t),\ \overline{\underset{\sim}{a}(t+\tau)} \qquad (24)$$

$$A_6 = \underset{\sim}{b}(t),\ \underset{\sim}{a}(t+\tau)$$
$$B_6 = a(t),\ \overline{b(t+\tau)} \qquad (25)$$

$$A_7 = \underset{\sim}{a}(t),\ b(t+\tau)$$
$$B_7 = \underset{\sim}{b}(t),\ \overline{a(t+\tau)} \qquad (26)$$

$$A_8 = \underset{\sim}{b}(t),\ a(t+\tau)$$
$$B_8 = \underset{\sim}{a}(t),\ \overline{b(t+\tau)} \qquad (27)$$

A simple heuristic proof which demonstrates that the above set of 8 equations guarantees forming a new mate pair is readily achieved in a manner analogous to that employed for the basic set of expansion equations.

The general expansion formula for the above set of equations is:

$$A = a(t),\ \underset{\sim}{b}(t+\tau)$$
$$B = b(t),\ \overline{\underset{\sim}{a}(t+\tau)}$$

And the autocorrelation and crosscorrelation process experienced between the a and b codes when detecting A and B with a matched filter (or pulse compression filter) can be represented graphically as shown below.

For code A

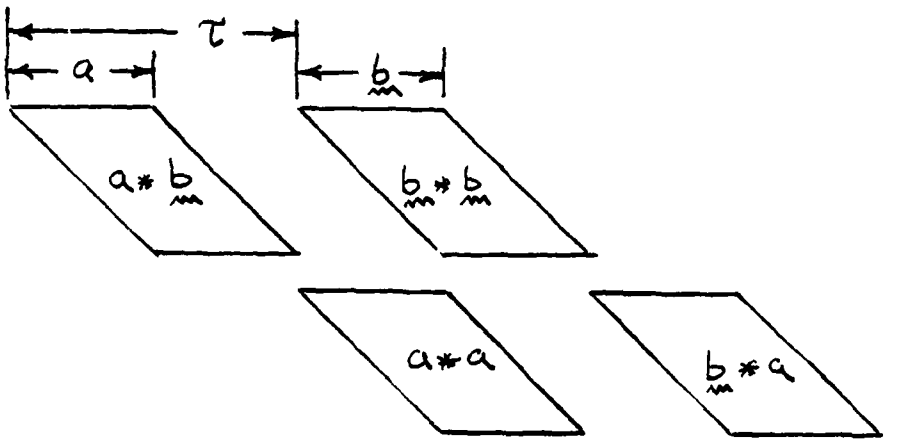

For code B

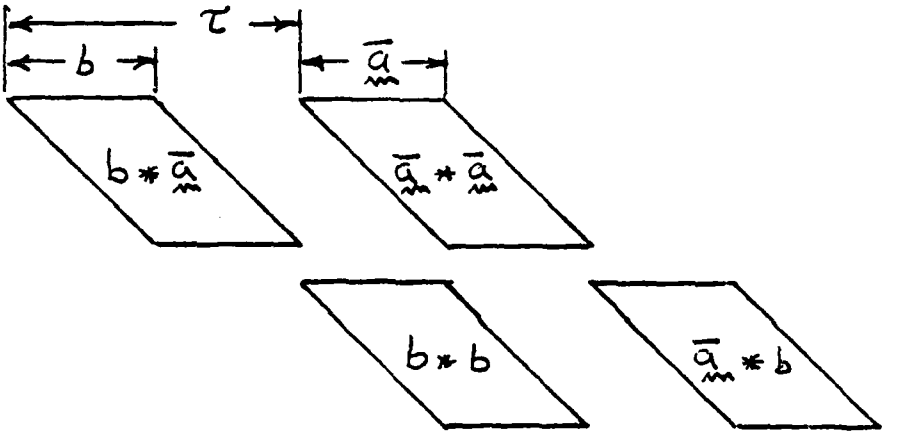

where as before:

x*x = autocorrelation function of x

x*y = crosscorrelation function of code x with code y

Summing the appropriate autocorrelation and crosscorrelation functions results in:

$$a*a + b*b \tag{28}$$

$$\bar{a}*\bar{a} + b*b \tag{29}$$

$$a*b + b*\bar{a} \tag{30}$$

$$b*a + \bar{a}*b \tag{31}$$

Since a and b form a code mate pair by definition, then:

$$a*a + b*b = 0 \quad \text{for all } \tau \neq 0 \tag{32}$$

And

$$\bar{a}*\bar{a} + b*b = 0 \quad \text{for all } \tau \neq 0 \tag{33}$$

Also, since

$$a*b = b*a \tag{34}$$

And

$$b*\bar{a} = -b*a \tag{35}$$

Then

$$a*b + b*\bar{a} = 0 \tag{36}$$

Likewise, since

$$b*a = a*b \tag{37}$$

And

$$\bar{a}*b = -a*b \tag{38}$$

Then

$$b*a + \bar{a}*b = 0 \tag{39}$$

Hence, the autocorrelation function of B $[\phi_B(\tau)]$ is guaranteed to be of equal magnitude and opposite sense to the autocorrelation function of A $[\phi_A(\tau)]$ for all $\tau \neq 0$. At $\tau = 0$, $\phi_T(0) = \phi_A(0) + \phi_B(0) = 4n$

where n = number of code bits in a and b.

Equations (20) through (27) identify a second set of 8 general expansion formulas that can be utilized to generate multiplexed noise codes as an iterative expansion process. We therefore now have 16 expansion equations that can be utilized with different delays (τ) at each code doubling process in a code generator.

(2) Available Code Quantity

Although a precise equation identifying what quantity of multiplexed noise codes exist for any given code length has not been determined, the following facts are presented to establish that the number is extremely large. The 16 derived expansion equations actually identify 32 different combinations of mate pair codes a and b that can be utilized at each code doubling stage of a code generator since either one of the delayed codes can be complemented when expanding

a mate pair. Also, it can be readily shown that there are K! different ways of grouping the code bits when constrained to a binary structure where K equals the number of code doubling stages employed to generate an n bit code ($n = 2^K$). This would result in a quantity of codes Q given by

$$Q = 32^{K-1} \times K!$$

if none of the codes were duplicated in the expansion process. Code expansion during the initial code generation stages, however (i.e., 2 bits are doubled to 4 and 4 to 8), in many situations has a code equal to its inverse which initially reduces the available number of legitimate equations that can be utilized. Even if one postulated that the number of equations averaged out to 8, then Q would become about a half million for a modest 32 bit length mate code pair.

$$2^K = 32$$

$$K = 5$$

and

$$Q = 8^4 \times 5!$$

$$= 491, 520$$

Such a large quantity is rather extraordinary when compared to the fact that only 6 unique codes exist for a 63 bit length direct sequence maximal length shift register P-N code.

If one employed a multi-amplitude multiplexed noise code in a system by either allowing gaps or by allowing bit overlap during the code generation, then the quantity of available codes would be increased by another substantially large factor.

Having an exceptionally large available quantity of codes for moderate code lengths (i.e., 100 to 1000) is critically important for many practical applications that address ECCM, LPI, Multiple-Access, Communication and Switching. This comprises one of the major attributes inherent in the multiplexed noise code class and it does not exist for any other known present state-of-the-art code class. Direct sequence codes are exceptionally limited in quantity and the so called Gold codes are simple time permutations of the existing Direct Sequence Codes.

(3) Orthogonal Noise Code Sub Sets

Another unique and important property of the multiplexed noise code class is that sub classes exist whereby the crosscorrelation between any two codes of the subclass is zero at $\tau = 0$. Although spurious lobes exist whose averaged (rms) value has an amplitude that is lower than the peak main lobe by a factor equal to the square root of the code sequence length (i.e., the time-bandwidth product), the absence of any cross correlation value of over lapped codes (i.e., $\tau = 0$) enables the implementation of orthogonal systems which utilize different noise codes. Some examples would be a mobile

subscriber multiple-access system, a satellite multiple-access system or a tactical switch.

Hand calculations of the crosscorrelation function at $\tau = 0$ of four and eight bit mate code pairs (8 bit and 16 bit noise codes) resulted in identifying 8 unique codes for the four bit code pairs and 16 unique codes for the 8 bit code pairs whose crosscorrelation value between any two or more codes of the subclass was zero. The specific codes forming the subclasses are shown in Tables 1 and 2. The codes identified in Table 1 form a subclass of 4-bit multiplexed codes and the codes identified in Table 2 form a subclass of 8-bit multiplexed codes.

Verification of orthogonality is established by showing that the crosscorrelation between any 2 or more codes identified in either tables 1 or 2 is zero at $\tau = 0$. Consider first the code subclass presented in table 1.

The cross-correlation function of codes 2 and 1 at $\tau = 0$ is readily determined as follows:

$$\begin{array}{rl} & 1\ 0\ 0\ 0 \\ \times & 0\ 0\ 1\ 0 \\ \hline \Sigma & - + - + = 0 = \phi_{a_2\, a_1}(0) \end{array}$$

$$\begin{array}{rl} & 1\ 0\ 1\ 1 \\ \times & 1\ 1\ 1\ 0 \\ \hline \Sigma & + - + - = 0 = \phi_{b_2\, b_1}(0) \end{array}$$

$$\phi_{21}(0) = \phi_{a_2\, a_1}(0) + \phi_{b_2\, b_1}(0)$$

$$= 0 + 0 = 0$$

Where

$\phi_{a_2\, a_1}(0)$ = Crosscorrelation function value between codes a_2 and a_1 at $\tau = 0$

$\phi_{b_2\, b_1}(0)$ = Crosscorrelation function value between codes b_1 and b_2 at $\tau = 0$

$\phi_{21}(0)$ = Total crosscorrelation function value between multiplexed code pairs 2 and 1 at $\tau = 0$

Code Pair No.	Code a	Code b
1	1 0 0 0	1 0 1 1
2	0 0 1 0	1 1 1 0
3	0 1 0 0	0 1 1 1
4	0 0 0 1	1 1 0 1
5	1 0 0 0	0 1 0 0
6	0 0 1 0	0 0 0 1
7	0 1 0 0	1 0 0 0
8	0 0 0 1	0 0 1 0

Table 1 - Sub Class of 4 Bit Multiplexed Noise Codes with Zero Crosscorrelation at $\tau = 0$ (Code Set #1)

Code Pair No.	Code a	Code b
1	1 0 1 0 0 0 1 1	1 0 0 1 0 0 0 0
2	1 0 0 0 0 1 0 0	1 0 0 0 1 0 1 1
3	0 1 0 0 1 0 0 0	1 0 1 1 1 0 0 0
4	0 0 0 1 0 0 1 0	0 0 0 1 1 1 0 1
5	1 1 0 1 0 0 0 1	1 1 0 1 1 1 1 0
6	1 1 1 1 0 1 1 0	0 0 1 1 1 0 1 0
7	0 1 0 0 0 1 1 1	0 1 0 0 1 0 0 0
8	0 1 1 1 0 1 0 0	1 0 0 0 0 1 0 0
9	0 1 1 1 1 0 1 1	1 0 0 0 1 0 1 1
10	1 1 1 0 1 1 0 1	0 0 0 1 1 1 0 1
11	0 0 1 0 1 1 1 0	1 1 0 1 1 1 1 0
12	1 0 1 1 1 0 0 0	0 1 0 0 1 0 0 0
13	0 0 1 0 0 0 0 1	0 0 1 0 1 1 1 0
14	1 1 1 0 0 0 1 0	1 1 1 0 1 1 0 1
15	0 0 1 1 0 1 0 1	1 1 1 1 1 0 0 1
16	1 0 0 1 1 1 1 1	1 0 1 0 1 1 0 0

Table 2 - Sub Class of 8 Bit Multiplexed

Noise Codes with Zero Crosscorrelation at $\tau = 0$

(Code Set #2)

And

$$1 \times 0 = -1$$

$$0 \times 1 = -1$$

$$1 \times 1 = +1$$

$$0 \times 0 = +1$$

In a like manner, the crosscorrelation function value at $\tau = 0$ was calculated for all 28 possible combinations. The results are shown in table 3 which verifies that the crosscorrelation values between any 2 or more codes is zero (i.e., the codes are orthogonal or totally non-interfering) at $\tau = 0$.

As a more dramatic illustration and for further clarification, consider a situation where eight codes exist at the same time. For code pair no. 1, the potential interference of codes 2 through 8 would be as follows.

The input to a code compressor matched to code pair no. 1 would be:

For the code a matched filter input

$$\begin{array}{r} 0\ 0\ 1\ 0 \\ 0\ 1\ 0\ 0 \\ 0\ 0\ 0\ 1 \\ 1\ 0\ 0\ 0 \\ 0\ 0\ 1\ 0 \\ 0\ 1\ 0\ 0 \\ 0\ 0\ 0\ 1 \\ \hline \end{array}$$

$\Sigma = 0^5 0^3 0^3 0^3$

For the code b matched filter input

$$\begin{array}{r} 1\ 1\ 1\ 0 \\ 0\ 1\ 1\ 1 \\ 1\ 1\ 0\ 1 \\ 0\ 1\ 0\ 0 \\ 0\ 0\ 0\ 1 \\ 1\ 0\ 0\ 0 \\ 0\ 0\ 1\ 0 \\ \hline \end{array}$$

$\Sigma = 0\ 1\ 0\ 0$

1	0	0	0			1	0	1	1								
0	1	0	0			0	1	1	1								
-	-	+	+	•		-	-	+	+	=	0	=	$\varphi_{31}(0)$				
1	0	0	0			1	0	1	1								
0	0	0	1			1	1	0	1								
-	+	+	-	•		+	-	-	+	=	0	=	$\varphi_{41}(0)$				
1	0	0	0			1	0	1	1								
1	0	0	0			0	1	0	0								
+	+	+	+	•		-	-	-	-	=	0	=	$\varphi_{51}(0)$				
1	0	0	0			1	0	1	1								
0	0	1	0			0	0	0	1								
-	+	-	+	•		-	+	-	+	=	0	=	$\varphi_{61}(0)$				
1	0	0	0			1	0	1	1								
0	1	0	0			1	0	0	0								
-	-	+	+	•		+	+	-	-	=	0	=	$\varphi_{71}(0)$				
1	0	0	0			1	0	1	1								
0	0	0	1			0	0	1	0								
-	+	+	-	•		-	+	+	-	=	0	=	$\varphi_{81}(0)$				
0	0	1	0			1	1	1	0								
0	1	0	0			0	1	1	1								
+	-	-	+	•		-	+	+	-	=	0	=	$\varphi_{32}(0)$				
0	0	1	0			1	1	1	0								
0	0	0	1			1	1	0	1								
+	+	-	-	•		+	+	-	-	=	0	=	$\varphi_{42}(0)$				
0	0	1	0			1	1	1	0								
1	0	0	0			0	1	0	0								
-	+	-	+	•		-	+	-	+	=	0	=	$\varphi_{52}(0)$				

TABLE 3 - Crosscorrelation Function Values at $\tau = 0$
For Code Set #1 Note $\varphi_{xy}(0) = \varphi_{yx}(0)$

0	0	1	0				1	1	1	0						
0	0	1	0				0	0	0	1						
+	+	+	+	•			-	-	-	-	=	0	=	$\varphi_{62}(0)$		
0	0	1	0				1	1	1	0						
0	1	0	0				1	0	0	0						
+	-	-	+	•			+	-	-	+	=	0	=	$\varphi_{72}(0)$		
0	0	1	0				1	1	1	0						
0	0	0	1				0	0	1	0						
+	+	-	-	•			-	-	+	+	=	0	=	$\varphi_{82}(0)$		
0	1	0	0				0	1	1	1						
0	0	0	1				1	1	0	1						
+	-	+	-	•			-	+	-	+	=	0	=	$\varphi_{43}(0)$		
0	1	0	0				0	1	1	1						
1	0	0	0				0	1	0	0						
-	-	+	+	•			+	+	-	-	=	0	=	$\varphi_{53}(0)$		
0	1	0	0				0	1	1	1						
0	0	1	0				0	0	0	1						
+	-	-	+	•			+	-	-	+	=	0	=	$\varphi_{63}(0)$		
0	1	0	0				0	1	1	1						
0	1	0	0				1	0	0	0						
+	+	+	+	•			-	-	-	-	=	0	=	$\varphi_{73}(0)$		
0	1	0	0				0	1	1	1						
0	0	0	1				0	0	1	0						
+	-	+	-	•			+	-	+	-	=	0	=	$\varphi_{83}(0)$		
0	0	0	1				1	1	0	1						
1	0	0	0				0	1	0	0						
-	+	+	-	•			-	+	+	-	=	0	=	$\varphi_{54}(0)$		

TABLE 3 (Cont'd)

0	0	0	1					1	1	0	1						
0	0	1	0					0	0	0	1						
+	+	-	-	•				-	-	+	+	=	0	=	$\varphi_{64}(0)$		
0	0	0	1					1	1	0	1						
0	1	0	0					1	0	0	0						
+	-	+	-	•				+	-	+	-	=	0	=	$\varphi_{74}(0)$		
0	0	0	1					1	1	0	1						
0	0	0	1					0	0	1	0						
+	+	+	+	•				-	-	-	-	=	0	=	$\varphi_{84}(0)$		
1	0	0	0					0	1	0	0						
0	0	1	0					0	0	0	1						
-	+	-	+	•				+	-	+	-	=	0	=	$\varphi_{65}(0)$		
1	0	0	0					0	1	0	0						
0	1	0	0					1	0	0	0						
-	-	+	+	•				-	-	+	+	=	0	=	$\varphi_{75}(0)$		
1	0	0	0					0	1	0	0						
0	0	0	1					0	0	1	0						
-	+	+	-	•				+	-	-	+	=	0	=	$\varphi_{85}(0)$		
0	0	1	0					0	0	0	1						
0	1	0	0					1	0	0	0						
+	-	-	+	•				-	+	+	-	=	0	=	$\varphi_{76}(0)$		
0	0	1	0					0	0	0	1						
0	0	0	1					0	0	1	0						
+	+	-	-	•				+	+	-	-	=	0	=	$\varphi_{86}(0)$		
0	1	0	0					1	0	0	0						
0	0	0	1					0	0	1	0						
+	-	+	-	•				-	+	-	+	=	0	=	$\varphi_{87}(0)$		

TABLE 3 (Cont'd)

where

The exponent indicates the amplitude

$0 = +1$

$1 = -1$

And the output of the matched filters for code pair no. 1 would be

For the code a matched filter output

$$
\begin{array}{cccccccc}
0^5 & 0^3 & 0^3 & 0^3 & & & & \\
 & 0^5 & 0^3 & 0^3 & 0^3 & & & \\
 & & 0^5 & 0^3 & 0^3 & 0^3 & & \\
 & & & 1^5 & 1^3 & 1^3 & 1^3 & \\
\hline
0^5 & 0^8 & 0^{11} & 0^4 & 0^3 & \cdot & 1^3 & = \phi_{a_1}(\tau)
\end{array}
$$

For the code b matched filter output

$$
\begin{array}{cccccccc}
1 & 0 & 1 & 1 & & & & \\
 & 1 & 0 & 1 & 1 & & & \\
 & & 0 & 1 & 0 & 0 & & \\
 & & & 1 & 0 & 1 & 1 & \\
\hline
1 & \cdot & 0 & 1^4 & 0 & \cdot & 1 & = \phi_{b_1}(\tau)
\end{array}
$$

Or the composit summed output would result in

$$
\begin{array}{cccccccc}
0^5 & 0^8 & 0^{11} & 0^4 & 0^3 & \cdot & 1^3 & \\
1 & \cdot & 0 & 1^4 & 0 & \cdot & 1 & \\
\hline
0^4 & 0^8 & 0^{12} & \cdot & 0^4 & \cdot & 1^4 & = \phi_{T_1}(\tau)
\end{array}
$$

$\tau = 0$

The center time slot corresponds to $\tau = 0$ and is where all the other codes of the system would be totally non-interfering. The desired output signal would simply linearly sum with the total input and compress to its peak value of 8 at $\tau = 0$. The interference that is indicated by the lobes of the compressed signal would be gated out in any real system application or it would cause no interference at all. It is important to note that although this illustrated example used the same amplitude for each interfering pair, the actual amplitudes could all be different and theoretically have any value with the same result.

A similar exercise for the code class identified in Table 2 (Code Set # 2) would reveal identical results. Rather than present the crosscorrelation function values for all of the 66 possible combinations, however, some typical sample situations will be illustrated. This will suffice to demonstrate and clarify that this 8 bit code set can indeed operate as an orthogonal code set.

Referring to Table 2, consider code pairs 5 and 7 existing simultaneously with code pair number 4. The inputs to a filter matched to code pair no. 4 is then

For the code a matched filter input

code #5 1 1 0 1 0 0 0 1
code #7 0 1 0 0 0 1 1 1

$\Sigma =$ $\cdot\ 1^2 0^2 \cdot\ 0^2 \cdot\ \cdot\ 1^2$

For the code b matched filter input

code #5 1 1 0 1 1 1 1 0
code #7 0 1 0 0 1 0 0 0

$\Sigma =$ $\cdot\ 1^2 0^2 \cdot\ 1^2 \cdot\ \cdot\ 0^2$

And the output of the matched filters for code pair no. 4 would be

For the code a matched filter output

$$
\begin{array}{l}
1^2\ 0^2\ \cdot\ 0^2\ \cdot\ \cdot\ 1^2 \\
\quad 0^2\ 1^2\ \cdot\ 1^2\ \cdot\ \cdot\ 0^2 \\
\quad\quad 1^2\ 0^2\ \cdot\ 0^2\ \cdot\ \cdot\ 1^2 \\
\quad\quad\quad 1^2\ 0^2\ \cdot\ 0^2\ \cdot\ \cdot\ 1^2 \\
\quad\quad\quad\quad 0^2\ 1^2\ \cdot\ 1^2\ \cdot\ \cdot\ 0^2 \\
\quad\quad\quad\quad\quad 1^2\ 0^2\ \cdot\ 0^2\ \cdot\ \cdot\ 1^2 \\
\quad\quad\quad\quad\quad\quad 1^2\ 0^2\ \cdot\ 0^2\ \cdot\ \cdot\ 1^2 \\
\quad\quad\quad\quad\quad\quad\quad 1^2\ 0^2\ \cdot\ 0^2\ \cdot\ \cdot\ 1^2 \\
\hline
1^2\ 0^4\ 1^4\ 0^2\ 0^2\ 1^2\ \cdot\ \cdot\ 0^2\ \cdot\ 0^4\ 1^2\ 1^2\ 1^2 \ = \ \phi_{a_4}(\tau)
\end{array}
$$

For the code b matched filter output

$$
\begin{array}{cccccccccccccccccc}
0^2 & 1^2 & \cdot & 0^2 & \cdot & \cdot & 1^2 & & & & & & & & & & & \\
 & 1^2 & 0^2 & \cdot & 1^2 & \cdot & \cdot & 0^2 & & & & & & & & & & \\
 & & 0^2 & 1^2 & \cdot & 0^2 & \cdot & \cdot & 1^2 & & & & & & & & & \\
 & & & 0^2 & 1^2 & \cdot & 0^2 & \cdot & \cdot & 1^2 & & & & & & & & \\
 & & & & 0^2 & 1^2 & \cdot & 0^2 & \cdot & \cdot & 1^2 & & & & & & & \\
 & & & & & 1^2 & 0^2 & \cdot & 1^2 & \cdot & \cdot & 0^2 & & & & & & \\
 & & & & & & 1^2 & 0^2 & \cdot & 1^2 & \cdot & \cdot & 0^2 & & & & & \\
 & & & & & & & 1^2 & 0^2 & \cdot & 1^2 & \cdot & \cdot & 0^2 & & & & \\
\hline
0^2 & 1^4 & 0^4 & 0^2 & 1^2 & 1^2 & \cdot & 0^4 & 1^2 & 1^4 & 1^4 & 0^2 & 0^2 & 0^2 & = & \phi_{b_4}(\tau) & &
\end{array}
$$

Or the composit summed output of the filter matched to code pair no. 4 is

$$
\begin{array}{cccccccccccccccc}
1^2 & 0^4 & 1^4 & 0^2 & 0^2 & 1^2 & \cdot & \cdot & 0^2 & \cdot & 0^4 & 1^2 & 1^2 & 1^2 & & \\
0^2 & 1^4 & 0^4 & 0^2 & 1^2 & 1^2 & \cdot & 0^4 & 1^2 & 1^4 & 1^4 & 0^2 & 0^2 & 0^2 & & \\
\hline
\cdot & \cdot & \cdot & 0^4 & \cdot & 1^4 & \cdot & 0^4 & \cdot & 1^4 & \cdot & \cdot & \cdot & \cdot & = & \phi_{T_4}(\tau)
\end{array}
$$

$\tau = 0$

which verifies that there would be no interference from the simultaneous presence of code pairs 5 and 7 against code pair number 4.

Consider next the presence of code pairs 6 through 12 existing simultaneously when pulse compressing code pair no. 1. The input to the filter matched to code pair no. 1 is

For the code a matched filter input

$$
\begin{array}{cccccccc}
1 & 1 & 1 & 1 & 0 & 1 & 1 & 0 \\
0 & 1 & 0 & 0 & 0 & 1 & 1 & 1 \\
0 & 1 & 1 & 1 & 0 & 1 & 0 & 0 \\
0 & 1 & 1 & 1 & 1 & 0 & 1 & 1 \\
1 & 1 & 1 & 0 & 1 & 1 & 0 & 1 \\
0 & 0 & 1 & 0 & 1 & 1 & 1 & 0 \\
1 & 0 & 1 & 1 & 1 & 0 & 0 & 0 \\
\hline
0 & 1^3 & 1^5 & 1 & 1 & 1^3 & 1 & 0
\end{array}
\quad = \Sigma
$$

For the code b matched filter input

$$
\begin{array}{cccccccc}
0 & 0 & 1 & 1 & 1 & 0 & 1 & 0 \\
0 & 1 & 0 & 0 & 1 & 0 & 0 & 0 \\
1 & 0 & 0 & 0 & 0 & 1 & 0 & 0 \\
1 & 0 & 0 & 0 & 1 & 0 & 1 & 1 \\
0 & 0 & 0 & 1 & 1 & 1 & 0 & 1 \\
1 & 1 & 0 & 1 & 1 & 1 & 1 & 0 \\
0 & 1 & 0 & 0 & 1 & 0 & 0 & 0 \\
\hline
\Sigma = 0 & 0 & 0^5 & 0 & 1^5 & 0 & 0 & 0^3
\end{array}
$$

The output of the matched filters for code pair no. 1 would therefore be

For the code a matched filter output

$$
\begin{array}{cccccccccccccc}
1 & 0^3 & 0^5 & 0 & 0 & 0^3 & 0 & 1 & & & & & & \\
 & 1 & 0^3 & 0^5 & 0 & 0 & 0^3 & 0 & 1 & & & & & \\
 & & 0 & 1^3 & 1^5 & 1 & 1 & 1^3 & 1 & 0 & & & & \\
 & & & 0 & 1^3 & 1^5 & 1 & 1 & 1^3 & 1 & 0 & & & \\
 & & & & 0 & 1^3 & 1^5 & 1 & 1 & 1^3 & 1 & 0 & & \\
 & & & & & 1 & 0^3 & 0^5 & 0 & 0 & 0^3 & 0 & 1 & \\
 & & & & & & 0 & 1^3 & 1^5 & 1 & 1 & 1^3 & 1 & 0 \\
 & & & & & & & 1 & 0^3 & 0^5 & 0 & 0 & 0^3 & 0 \quad 1 \\
\hline
1 & 0^2 & 0^9 & 0^4 & 1^5 & 1^6 & 0 & 1^4 & 1^7 & 0^2 & 0^3 & \cdot & 0 & 0^2 \quad 1 = \phi_{a_1}(\tau)
\end{array}
$$

For the code b matched filter output

$$
\begin{array}{cccccccccccccc}
0 & 0 & 0^5 & 0 & 1^5 & 0 & 0 & 0^3 & & & & & & \\
 & 0 & 0 & 0^5 & 0 & 1^5 & 0 & 0 & 0^3 & & & & & \\
 & & 0 & 0 & 0^5 & 0 & 1^5 & 0 & 0 & 0^3 & & & & \\
 & & & 0 & 0 & 0^5 & 0 & 1^5 & 0 & 0 & 0^3 & & & \\
 & & & & 1 & 1 & 1^5 & 1 & 0^5 & 1 & 1 & 1^3 & & \\
 & & & & & 0 & 0 & 0^5 & 0 & 1^5 & 0 & 0 & 0^3 & \\
 & & & & & & 0 & 0 & 0^5 & 0 & 1^5 & 0 & 0 & 0^3 \\
 & & & & & & & 1 & 1 & 1^5 & 1 & 0^5 & 1 & 1 \quad 1^3 \\
\hline
0 & 0^2 & 0^7 & 0^8 & 0 & 0^2 & 1^4 & 0^4 & 0^{15} & 1^6 & 1^3 & 0^4 & 0^3 & 0^2 \quad 1^3 = \phi_{b_1}(\tau)
\end{array}
$$

Or the composit summed output of the filters matched to code pair no. 1 is

$$\begin{array}{l} 0\ \ 0^2\ 0^7\ 0^8\ 0\ \ 0^2\ 1^4\ 0^4\ 0^{15}1^6\ 1^3\ 0^4\ 0^3\ 0^2\ 1^3 \\ 1\ \ 0^2\ 0^9\ 0^4\ 1^5\ 1^6\ 0\ \ 1^4\ 1^7\ 0^2\ 0^3\ \cdot\ \ 0\ \ 0^2\ 1 \\ \hline \cdot\ \ 0^4\ 0^{16}0^{12}1^4\ 1^4\ 0^3\ \cdot\ \ 0^8\ 1^4\ \cdot\ \ 0^4\ 0^4\ 0^4\ 1^2 = \phi_{T_1}(\tau) \end{array}$$

$\tau = 0$

And again we see that orthogonal operation is obtained. The output of a filter matched to code pair no. 1 would be completely free of interference even though code pairs 6 through 12 were simultaneously present. For those still skeptical, a close inspection of Table 2 reveals that each possible combination of any 2 code pairs have 8 bits of the 16 opposite in sense which is tantamount to yielding a crosscorrelation value of zero at $\tau = 0$.

A new conceptual approach for obtaining orthogonal operation using noise codes was demonstrated. This was the result of discovering that code subclasses of multiplexed noise codes exist that has the unique property of having a crosscorrelation value of zero at $\tau = 0$ between all of the codes of the subclass. The two subclasses identified which were for four bit and eight bit code mate pairs verify the existence of subclasses of codes with the required unique property and demonstrates the associated operational capability. Establishing multiplexed noise code subclasses for code lengths greater than 16 requires the utilization of a computer and allocated research time and funds.

(4) *Orthogonal Code Mate Pairs*

Another important discovery concerning multiplexed noise codes is that for any given mate pair a and b, a second mate pair exists a' and b' that is completely orthogonal to the first pair. The crosscorrelation function between the two pairs is zero for all values of τ. The orthogonal mate pair is related to a mate pair a and b by the following pair of equations.

For a given mate pair code a and b

Its orthogonal mate pair, code a' and b' is given by

$$\begin{aligned} a' &= \underset{\sim}{b} \\ b' &= \underset{\sim}{\bar{a}} \end{aligned} \tag{40}$$

A simple general heuristic proof verifying the orthogonality between the two code mate pairs is presented below.

The crosscorrelation function operation between the two code pairs can be presented graphically as shown below.

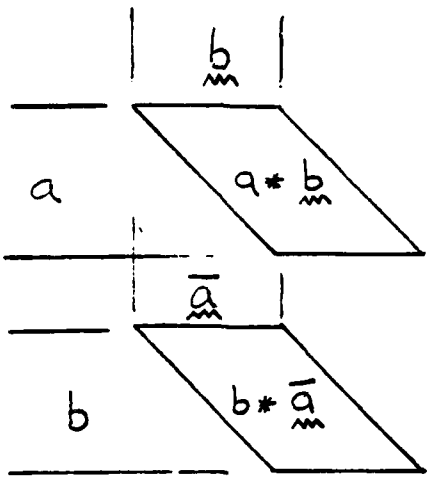

And the composite summed output of the above filter matched to a' and b' with a and b present would be:

$$a*\underset{\sim}{b} + b*\bar{\underset{\sim}{a}} \tag{41}$$

Now since

$$a*\underset{\sim}{b} = b*\underset{\sim}{a} \tag{42}$$

and

$$b*\bar{\underset{\sim}{a}} = -b*\underset{\sim}{a} \tag{43}$$

Then

$$a*\underset{\sim}{b} + b*\bar{\underset{\sim}{a}} = 0 \tag{44}$$

Let us demonstrate the orthogonality between two code mate pairs that satisfies equation (40) using an example

Consider the following 8 bit mate code pair a and b

a = 1 0 1 0 0 0 1 1

b = 1 0 0 1 0 0 0 0

Then from equation (40)

a'= 0 0 0 0 1 0 0 1

b'= 0 0 1 1 1 0 1 0

And crosscorrelating the code pair a and b with a' and b' results in the following:

Crosscorrelating a with a' yields

$$
\begin{array}{l}
0\ 1\ 0\ 1\ 1\ 1\ 0\ 0 \\
\quad 1\ 0\ 1\ 0\ 0\ 0\ 1\ 1 \\
\quad\quad 1\ 0\ 1\ 0\ 0\ 0\ 1\ 1 \\
\quad\quad\quad 0\ 1\ 0\ 1\ 1\ 1\ 0\ 0 \\
\quad\quad\quad\quad 1\ 0\ 1\ 0\ 0\ 0\ 1\ 1 \\
\quad\quad\quad\quad\quad 1\ 0\ 1\ 0\ 0\ 0\ 1\ 1 \\
\quad\quad\quad\quad\quad\quad 1\ 0\ 1\ 0\ 0\ 0\ 1\ 1 \\
\quad\quad\quad\quad\quad\quad\quad 1\ 0\ 1\ 0\ 0\ 0\ 1\ 1 \\
\hline
\phi_{aa'}(\tau) = \quad 0\ 1^2 0 \cdot 1^3 0^2 0 \cdot 1\ 0^2 0^3 \cdot 1\ 1^2 1
\end{array}
$$

And crosscorrelating b with b' yields

$$
\begin{array}{l}
1\ 0\ 0\ 1\ 0\ 0\ 0\ 0 \\
\quad 0\ 1\ 1\ 0\ 1\ 1\ 1\ 1 \\
\quad\quad 1\ 0\ 0\ 1\ 0\ 0\ 0\ 0 \\
\quad\quad\quad 0\ 1\ 1\ 0\ 1\ 1\ 1\ 1 \\
\quad\quad\quad\quad 0\ 1\ 1\ 0\ 1\ 1\ 1\ 1 \\
\quad\quad\quad\quad\quad 0\ 1\ 1\ 0\ 1\ 1\ 1\ 1 \\
\quad\quad\quad\quad\quad\quad 1\ 0\ 0\ 1\ 0\ 0\ 0\ 0 \\
\quad\quad\quad\quad\quad\quad\quad 1\ 0\ 0\ 1\ 0\ 0\ 0\ 0 \\
\hline
\phi_{bb'}(\tau) = \quad 1\ 0^2 1 \cdot 0^3 1^2 1 \cdot 0\ 1^2 1^3 \cdot 0\ 0^2 0
\end{array}
$$

The composit output crosscorrelation is given by the sum of $\phi_{aa'}(\tau)$ and $\phi_{bb'}(\tau)$ or

$$
\begin{array}{rl}
\phi_{aa'}(\tau) = & 0\ 1^2 0 \cdot 1^3 0^2 0 \cdot 1\ 0^2 0^3 \cdot 1\ 1^2 1 \\
\phi_{bb'}(\tau) = & 1\ 0^2 1 \cdot 0^3 1^2 1 \cdot 0\ 1^2 1^3 \cdot 0\ 0^2 0 \\
\hline
\phi_{aa'bb'}(\tau) = & \cdots\cdots\cdots\cdots\cdots\cdots
\end{array}
$$

Hence the crosscorrelation between the two code mate pairs is zero everywhere and they are therefore completely orthogonal to each other.

An important point to be made concerning the guaranteed existence of this one totally orthogonal mate pair for each existing mate pair is that there is no penalty incurred due to the requirement to employ two orthogonal channels in practical applications. Both orthogonal code mate pairs can be utilized to retain 2n available orthogonal levels where n is the number of bits per code.

(5) Correlation Statistics

Another important discovery concerning multiplexed noise codes is that

the individual mate codes have noise like characteristics. This became evident when the lobe structure for many calculated autocorrelation functions of mate codes was seen to be similar in appearance to that for the direct sequence P-N codes. Tentative confirmation of this desirable trait was made by generating 68 - 32 bit mate code pairs (or 136 individual 32 bit codes), determining their specific autocorrelation functions and then calculating the rms value of their lobes. These were then compared to the rms and peak values of the 6 unique 31 bit direct sequence P-N codes. In all cases, the rms value σ of the lobes for the mate pair codes was essentially equal to the rms value σ of the lobes for the P-N codes.

The maximum and minimum values of σ were

For 32 bit mate pair codes

$2.15 < \sigma < 2.38$

For 31 bit direct sequence P-N codes

$2.12 < \sigma < 2.57$

The peak values of the lobes for the individual 32 bit mate codes was also comparable to the peak lobe values of the direct sequence code 31 bit code.

The 32 bit mate pair codes had peak values distributed as shown in the table below:

PEAK AMPLITUDE	QUANTITY
9	40
7	48
6	24
5	8
4	16
	TOTAL: 136

The six 31 bit P-N codes had the following distribution

PEAK AMPLITUDE	QUANTITY
5	5
4	1
	TOTAL: 6

Note that 16 of the 136 generated mate codes had a peak amplitude as low as the only single available P-N code and that 24 mate codes had an amplitude equal to or less than the six P-N codes. Also, 48 of the codes are only very slightly larger having an amplitude that is equal to or less than 6 which is only .8 db greater and 96 are equal to or less than 7 which is 1.5 db larger than for the 6 P-N codes. Although the remaining 40 which have a peak amplitude of 9 corresponds to a peak lobe level 2.5 db larger, this is accompanied by a corresponding reduction in the level of the remaining lobes.

Since the generated codes whose autocorrelation function and rms side lobe levels has been calculated actually represents only a small fraction of those available, it could be conjectured that a quantity of individual mate codes significantly greater than the available quantity of direct sequence codes exist whose peak value is equal to or less than that of the direct sequence codes. This then provides another distinct class of individual noise codes that would have direct application in systems.

Additional confirmation of the noise like characteristics for individual mate codes was accomplished by calculating the crosscorrelation functions for a selected group of five mate code pairs. This provided 20 different cross-correlation function results (10 different combinations between the a codes and 10 different combinations between the b codes) whose rms value of the lobes was calculated and is shown below.

$$3.70 < \sigma_{rms} < 4.15$$

For comparison, the crosscorrelation function was determined and σ_{rms} computed for the different possible combinations between 3 of the P-N codes. In this case, the results were as shown below.

$$3.70 < \sigma_{rms} < 4.17$$

Again the statistical resemblance is evident.

It would be of significant value to pursue further the noise like characteristics of the individual mate codes but this is beyond the scope and intent of this research study.

The much more important and powerful property of mate codes is their ability to compress to a lobeless impulse. Today's technology is more than sufficient to provide the frequency stabilities and phase coherence that is necessary to implement operational systems that will achieve cancellation of the lobes of opposite phase that exist for the two separate mate codes. Although one would not expect to obtain lobes of zero amplitude (∞ db attenuation) with practical hardware, it is expected that lobes whose amplitude is orders of magnitude less than what can be achieved for the state-of-the-art P-N codes is realizable.

(6) C.W. and Pulse Interference Rejection Potential

The complete cancelation of C.W. and/or pulse interference with no loss at all in the received level of the desired signal is possible for any spread spectrum system that utilizes multiplexed noise codes. This unique result is realizable since these codes compress to a lobeless impulse. A delay equal to or greater than one code bit width τ for the signal would not interfere with the signal detection operation while permiting a replica of the interference to be obtained. This is then readily adjusted in phase and subtracted from the signal plus interference to provide an interference free signal.

Although the implementation details would be different for canceling pulse or C.W. interference and would also depend whether active or passive matched filter detection was utilized, the principle is the same in all cases. The concept will be clarified for a C.W. interference canceler that utilizes a passive (pulse compression) matched filter for detection. The implementation details for a C.W. interference canceler that employs active coherent detection and for a pulse interference canceler using active and passive detection is illustrated and described in Appendix B.

The hardware implementation for the C.W. interference canceler that employs pulse compression consists of a variable delay line (whose order of magnitude is equal to the compressed code bit width τ) and a linear adder. A functional block diagram of the canceler as utilized in a transmission link is presented in figure 1. During the presence of interference at any carrier frequency in the input bandwidth of the system, the delay device ($\tau + \varepsilon$) is varied in delay until the phase of the output interference is exactly 180^0 out of phase with its phase at the input. Adding the input to the output then totally cancels the interference while the output peak signal level remains unchanged. This retention of the signal is readily demonstrated with an example.

Consider the following 8 bit multiplexed noise code pair

Code a 1 0 0 0 0 1 0 0

Code b 0 0 1 0 1 1 1 0

where:

0 signifies +1

1 signifies -1

Compressing code a in a matched filter results in

```
1 0 0 0 0 1 0 0
  1 0 0 0 0 1 0 0
    0 1 1 1 1 0 1 1
      1 0 0 0 0 1 0 0
        1 0 0 0 0 1 0 0
          1 0 0 0 0 1 0 0
            1 0 0 0 0 1 0 0
              1 0 0 0 0 1 0 0
                0 1 1 1 1 0 1 1
-----------------------------------
1 . 0^3. 0 . 0 0^8 0 . 0 . 0^3. 1  = φ_a(τ)
```

where: The exponent identifies the amplitude

NOTE: The time scale for the C.W. Interference is expanded for clarity. In general, the C.W. period would be a small fraction of the compressed pulse width.

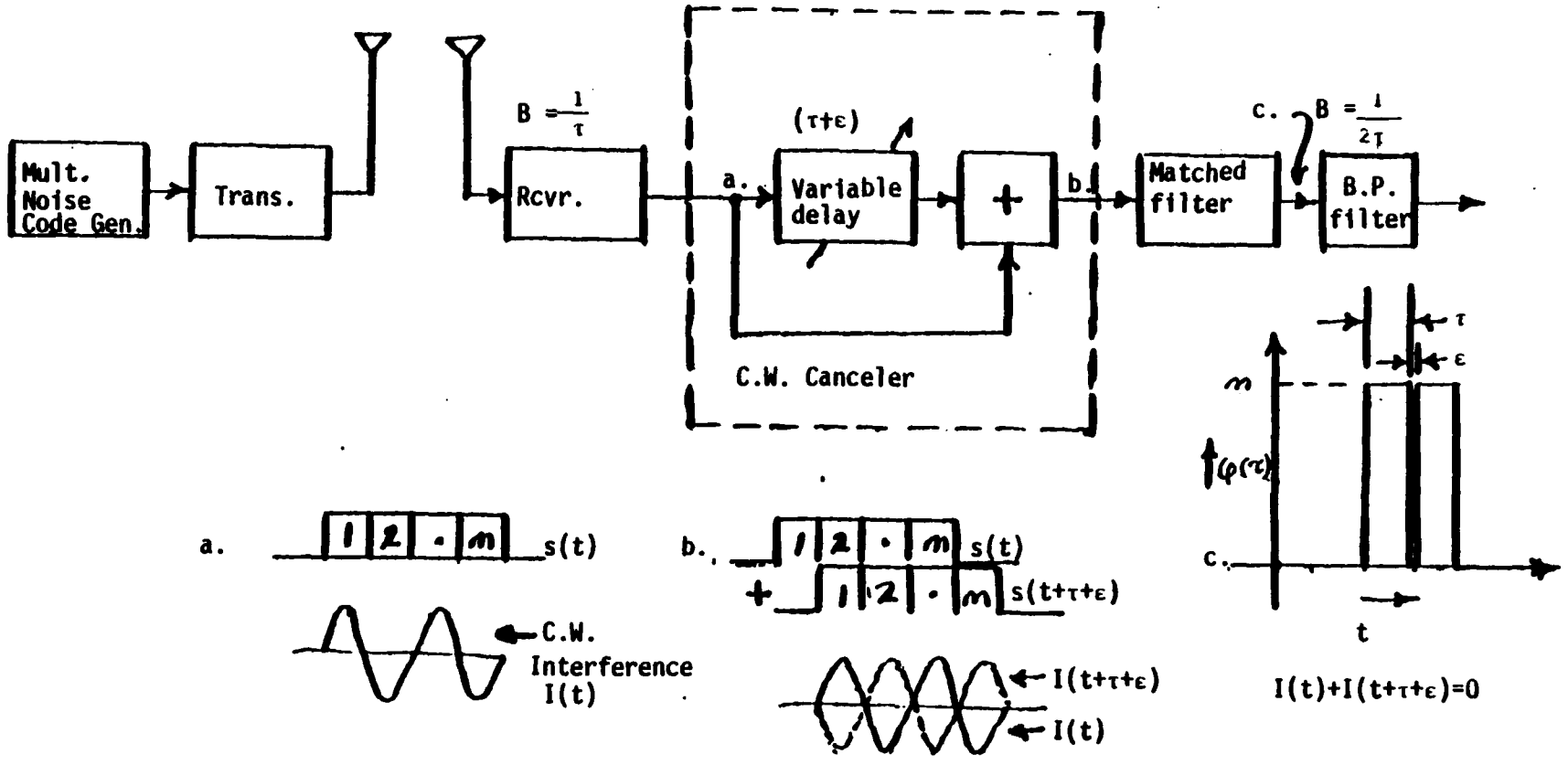

FIGURE 1 - C.W. INTERFERENCE CANCELING SPREAD SPECTRUM SYSTEM

And compressing code b in a matched filter yields

$$
\begin{array}{r}
0\ 0\ 1\ 0\ 1\ 1\ 1\ 0 \\
1\ 1\ 0\ 1\ 0\ 0\ 0\ 1 \\
1\ 1\ 0\ 1\ 0\ 0\ 0\ 1 \\
1\ 1\ 0\ 1\ 0\ 0\ 0\ 1 \\
0\ 0\ 1\ 0\ 1\ 1\ 1\ 0 \\
1\ 1\ 0\ 1\ 0\ 0\ 0\ 1 \\
0\ 0\ 1\ 0\ 1\ 1\ 1\ 0 \\
0\ 0\ 1\ 0\ 1\ 1\ 1\ 0 \\
\hline
0\ .\ 1^3\ .\ 1\ .\ 1\ 0^8\ 1\ .\ 1\ .\ 1^3\ .\ 0 = \varphi_b(\tau)
\end{array}
$$

The composite compressed output consists of the linear addition of $\varphi_a(\tau)$ and $\varphi_b(\tau)$ which produces

$$
\begin{array}{rl}
 & 1\ .\ 0^3\ .\ 0\ .\ 0\ 0^8\ 0\ .\ 0\ .\ 0^3\ .\ 1 = \varphi_a(\tau) \\
 & 0\ .\ 1^3\ .\ 1\ .\ 1\ 0^8\ 1\ .\ 1\ .\ 1^3\ .\ 0 = \varphi_b(\tau) \\
\Sigma = & \ .\ .\ .\ .\ .\ .\ .\ .\ 0^{16}\ .\ .\ .\ .\ .\ .\ .\ = \varphi_T(\tau)
\end{array}
$$

When the interference canceler is interposed between the output of the receiver and the input to the matched filter with the delay equal to 1 code bit width, the input signal becomes

For the code a signal we have

$$
\begin{array}{rl}
 & 1\ 0\ 0\ 0\ 0\ 1\ 0\ 0 = a(t) \\
 & \ \ 1\ 0\ 0\ 0\ 0\ 1\ 0\ 0 = a(t+\tau) \\
\Sigma = & 1\ .\ 0^2\ 0^2\ 0^2\ .\ .\ 0^2\ 0
\end{array}
$$

For the code b signal we have

$$
\begin{array}{rl}
 & 0\ 0\ 1\ 0\ 1\ 1\ 1\ 0 = b(t) \\
 & \ \ 0\ 0\ 1\ 0\ 1\ 1\ 1\ 0 = b(t+\tau) \\
\Sigma = & 0\ 0^2\ .\ .\ .\ 1^2\ 1^2\ .\ 0
\end{array}
$$

And the compressed signal now becomes

Compressing the summed code a

$$
\begin{array}{cccccccccccccccc}
1 & . & 0^2 & 0^2 & 0^2 & . & . & 0^2 & 0 & & & & & & & \\
 & 1 & . & 0^2 & 0^2 & 0^2 & . & . & 0^2 & 0 & & & & & & \\
 & & 0 & . & 1^2 & 1^2 & 1^2 & . & . & 1^2 & 1 & & & & & \\
 & & & 1 & . & 0^2 & 0^2 & 0^2 & . & . & 0^2 & 0 & & & & \\
 & & & & 1 & . & 0^2 & 0^2 & 0^2 & . & . & 0^2 & 0 & & & \\
 & & & & & 1 & . & 0^2 & 0^2 & 0^2 & . & . & 0^2 & 0 & & \\
 & & & & & & 1 & . & 0^2 & 0^2 & 0^2 & . & . & 0^2 & 0 & \\
 & & & & & & & 0 & . & 1^2 & 1^2 & 1^2 & . & . & 1^2 & 1 \\
\hline
1 & 1 & 0^3 & 0^3 & 0 & 0 & 0 & 0^9 & 0^9 & 0 & 0 & 0 & 0^3 & 0^3 & 1 & 1
\end{array}
= \varphi_a(\tau)
$$

Compressing the summed code b

$$
\begin{array}{cccccccccccccccc}
0 & 0^2 & . & . & . & 1^2 & 1^2 & . & 0 & & & & & & & \\
 & 1 & 1^2 & . & . & . & 0^2 & 0^2 & . & 1 & & & & & & \\
 & & 1 & 1^2 & . & . & . & 0^2 & 0^2 & . & 1 & & & & & \\
 & & & 1 & 1^2 & . & . & . & 0^2 & 0^2 & . & 1 & & & & \\
 & & & & 0 & 0^2 & . & . & . & 1^2 & 1^2 & . & 0 & & & \\
 & & & & & 1 & 1^2 & . & . & . & 0^2 & 0^2 & . & 1 & & \\
 & & & & & & 0 & 0^2 & . & . & . & 1^2 & 1^2 & . & 0 & \\
 & & & & & & & 0 & 0^2 & . & . & . & 1^2 & 1^2 & . & 0 \\
\hline
0 & 0 & 1^3 & 1^3 & 1 & 1 & 1 & 0^7 & 0^7 & 1 & 1 & 1 & 1^3 & 1^3 & 0 & 0
\end{array}
= \varphi_b(\tau)
$$

Which results in the following composite output

$$
\begin{array}{cccccccccccccccc}
1 & 1 & 0^3 & 0^3 & 0 & 0 & 0 & 0^9 & 0^9 & 0 & 0 & 0 & 0^3 & 0^3 & 1 & 1 \\
0 & 0 & 1^3 & 1^3 & 1 & 1 & 1 & 0^7 & 0^7 & 1 & 1 & 1 & 1^3 & 1^3 & 0 & 0 \\
\hline
. & . & . & . & . & . & . & 0^{16} & 0^{16} & . & . & . & . & . & . & .
\end{array}
= \varphi_T(\tau)
$$

Note that the peak value of the signal remains at a level of 16 (the same as without the interposed interference canceler) and that the pulse width of the main lobe doubles. The compressed pulse still remains lobeless.

In general, the additional vernier delay "ε" represents a small additional increment that is much less than τ which is employed to render the C.W. interference 180^0 out of phase with the input. That this would not change the above result can be demonstrated by adding a fractional part of the pulse width τ to the delay.

Consider a delay equal to 1.5τ for the code pair illustrated.

The code a signal then becomes

$\rightarrow|\quad|\leftarrow \tau$

$$\begin{array}{cccccccccccccccc} 1 & 1 & 0 & 0 & 0 & 0 & 0 & 0 & 0 & 0 & 1 & 1 & 0 & 0 & 0 & 0 \\ & & & 1 & 1 & 0 & 0 & 0 & 0 & 0 & 0 & 0 & 1 & 1 & 0 & 0 & 0 & 0 \end{array} \quad \begin{array}{l} = a(t) \\ = a(t+1.5\tau) \end{array}$$

$$\Sigma = \quad 1\ 1\ 0\ .\ .\ 0^2\ 0^2\ 0^2\ 0^2\ 0^2\ .\ .\ 0^2\ .\ .\ 0^2\ 0\ 0\ 0$$

where: Each code bit is presented as 2 bits to facilitate demonstrating the effect of a 1.5 bit delay (ε=.5τ)

And the code b signal becomes

$$\begin{array}{cccccccccccccccc} 0 & 0 & 0 & 0 & 1 & 1 & 0 & 0 & 1 & 1 & 1 & 1 & 1 & 1 & 0 & 0 \\ & & & 0 & 0 & 0 & 0 & 1 & 1 & 0 & 0 & 1 & 1 & 1 & 1 & 1 & 1 & 0 & 0 \end{array} \quad \begin{array}{l} = b(t) \\ = b(t+1.5\tau) \end{array}$$

$$\Sigma = \quad 0\ 0\ 0\ 0^2\ .\ .\ 0^2\ .\ 1^2\ .\ .\ 1^2\ 1^2\ 1^2\ .\ .\ 1\ 0\ 0$$

Compressing the summed code a

$$\begin{array}{l} 1\ 1\ 0\ .\ .\ 0^2 0^2 0^2 0^2 0^2 .\ .\ 0^2 .\ .\ 0^2 0\ 0 \\ \quad 1\ 1\ 0\ .\ .\ 0^2 0^2 0^2 0^2 0^2 .\ .\ 0^2 .\ .\ 0^2 0\ 0 \\ \quad\quad 0\ 0\ 1\ .\ .\ 1^2 1^2 1^2 1^2 1^2 .\ .\ 1^2 .\ .\ 1^2 1\ 1 \\ \quad\quad\quad 1\ 1\ 0\ .\ .\ 0^2 0^2 0^2 0^2 0^2 .\ .\ 0^2 .\ .\ 0^2 0\ 0 \\ \quad\quad\quad\quad 1\ 1\ 0\ .\ .\ 0^2 0^2 0^2 0^2 0^2 .\ .\ 0^2 .\ .\ 0^2 0\ 0 \\ \quad\quad\quad\quad\quad 1\ 1\ 0\ .\ .\ 0^2 0^2 0^2 0^2 0^2 .\ .\ 0^2 .\ .\ 0^2 0\ 0 \\ \quad\quad\quad\quad\quad\quad 1\ 1\ 0\ .\ .\ 0^2 0^2 0^2 0^2 0^2 .\ .\ 0^2 .\ .\ 0^2 0\ 0 \\ \quad\quad\quad\quad\quad\quad\quad 1\ 1\ 0\ .\ .\ 0^2 0^2 0^2 0^2 0^2 .\ .\ 0^2 .\ .\ 0^2 0\ 0 \\ \quad\quad\quad\quad\quad\quad\quad\quad 0\ 0\ 1\ .\ .\ 1^2 1^2 1^2 1^2 1^2 .\ .\ 1^2 .\ .\ 1^2 1\ 1 \\ \hline 1\ 1\ .\ 1\ 0^2 0^3 .\ 0^3 0^4 0\ .\ 0\ 0^2 0\ 0^8 0^9 0^2 0^9 0^8 0\ 0^2 0\ .\ 0\ 0^4 0^3 .\ 0^3 0^2 1\ .\ 1\ 1 \end{array} = \varphi_a(\tau)$$

Compressing the summed code b

$$0\ 0\ 0\ 0^{2}.\ .\ 0^{2}.\ 1^{2}.\ .\ 1^{2}1^{2}1^{2}.\ .\ 1\ 0\ 0$$
$$1\ 1\ 1\ 1^{2}.\ .\ 1^{2}.\ 0^{2}.\ .\ 0^{2}0^{2}0^{2}.\ .\ 0\ 1\ 1$$
$$1\ 1\ 1\ 1^{2}.\ .\ 1^{2}.\ 0^{2}.\ .\ 0^{2}0^{2}0^{2}.\ .\ 0\ 1\ 1$$
$$1\ 1\ 1\ 1^{2}.\ .\ 1^{2}.\ 0^{2}.\ .\ 0^{2}0^{2}0^{2}.\ .\ 0\ 1\ 1$$
$$0\ 0\ 0\ 0^{2}.\ .\ 0^{2}.\ 1^{2}.\ .\ 1^{2}1^{2}1^{2}.\ .\ 1\ 0\ 0$$
$$1\ 1\ 1\ 1^{2}.\ .\ 1^{2}.\ 0^{2}.\ .\ 0^{2}0^{2}0^{2}.\ .\ 0\ 1\ 1$$
$$0\ 0\ 0\ 0^{2}.\ .\ 0^{2}.\ 1^{2}.\ .\ 1^{2}1^{2}1^{2}.\ .\ 1\ 0\ 0$$
$$\underline{0\ 0\ 0\ 0^{2}.\ .\ 0^{2}.\ 1^{2}.\ .\ 1^{2}1^{2}1^{2}.\ .\ 1\ 0\ 0}$$
$$0\ 0\ .\ 0\ 1^{2}1^{3}.\ 1^{3}1^{4}1\ .\ 1\ 1^{2}1\ 0^{8}0^{7}1^{2}0^{7}0^{8}1\ 1^{2}1\ .\ 1\ 1^{4}1^{3}.\ 1^{3}1^{2}0\ .\ 0\ 0 = \varphi_b(\tau)$$

Add the addition of $\varphi_a(\tau)$ with $\varphi_b(\tau)$ yields

$$1\ 1\ .\ 1\ 0^{2}0^{3}.\ 0^{3}0^{4}0\ .\ 0\ 0^{2}0\ 0^{8}0^{9}0^{2}0^{9}0^{8}0\ 0^{2}0\ .\ .\ 0\ 0^{4}0^{3}.\ 0^{3}0^{2}1\ .\ 1\ 1$$
$$\underline{0\ 0\ .\ 0\ 1^{2}1^{3}.\ 1^{3}1^{4}1\ .\ 1\ 1^{2}1\ 0^{8}0^{7}1^{2}0^{7}0^{8}1\ 1^{2}1\ .\ 1\ 1^{4}1^{3}.\ 1^{3}1^{2}0\ .\ 0\ 0}$$
$$.\ .\ .\ .\ .\ .\ .\ .\ .\ .\ .\ .\ .\ .\ .\ 0^{16}0^{16}.\ 0^{16}0^{16}.\ .\ .\ .\ .\ .\ .\ .\ .\ .\ .\ .\ .\ .\ .\ . = \varphi_T(\tau)$$

$$\Delta = \varepsilon = .5\,\tau$$

Or it is evident from the above example that the additional delay "ε" does not affect the result. Since in general $\varepsilon \ll \tau$ for a practical system, complete cancellation of any C.W. frequency in the input bandwidth can be achieved (i.e., ∞ db attenuation of C.W. interference) with no loss at all in the signal level. Since the final pulse width "τ" is essentially doubled, then the output can be filtered further in a bandwidth B equal to $1/2\tau$ to reduce the output noise by an additional 3db. The end result is that no loss at all is reflected in the output (S/N) level while the C.W. interference is totally eliminated. In addition, lobeless compression is retained.

It should be evident that several C.W. cancelers of the type illustrated can be utilized in tandem to totally eliminate multiple C.W. interference. Each canceler would double the pulse width if the (S/N) level is to be retained. If it is more important not to lose available compressed time slots in some specific application, then each additional canceler could delay the signal by $\tau + \varepsilon_i$ (rather than $2\tau + \varepsilon_2$, $4\tau + \varepsilon_3$, etc.). The peak signal level would be retained but each canceler would double the noise power. In all cases, the C.W. interference would be attenuated by ∞ .

It should also be mentioned that slowly varying C.W. could be readily accommodated by forming a closed loop whereby the output interference level would be continuously monitored and the variable delay $(\tau + \varepsilon)$ adjusted until the interference was nulled in some type of standard null detector. A practical system would in fact require some type of interference monitor while adjusting the delay to affect a null.

4. TEST CONFIGURATIONS AND RESULTS

a. General Considerations

The primary thrust of the tests performed on this research program was to determine if near zero autocorrelation function sidelobes and crosscorrelation function values for an orthogonal code subset can be realized when multiplexed noise code generators and matched filter detectors are implemented with practical hardware, and if sufficiently low values can be obtained, what degree of interference rejection can be realized when the codes are utilized in a TDMA or CDMA multiple-access configuration. Theoretically, orthogonal (zero self-interference) multiple-access operation is realizable using multiplexed noise codes.

To accomplish these and other objectives as previously noted, system design parameters were chosen that are typical in existing and contemplated communications systems. A code length of 64 bits (32 bit mate code pairs) was utilized to provide a structure that conformed to available quartz substrates (for SAW device fabrication) while providing a minimum A/J gain margin of about 20 db. Using the general expansion formulas, 68-32 bit mate code pairs were generated. A subset of 5 mate pairs was then identified which represented typical lobe patterns for the individual mate codes and which formed an orthogonal group. The crosscorrelation function at $\tau=0$ between any two of the 5 code pairs is equal to zero. The selected codes and their autocorrelation functions are shown in figures 2 through 6. All of the codes that were implemented for this research program were selected from these codes which facilitated performing multiple-access tests in either a TDMA version (the same code using different selected time slots) or in a CDMA version (different codes all using the same time slot).

Before describing the implementation and testing details, the basic differences between passive code generation/compression and active code generation/correlation detection will be clarified.

- Passive code generation/compression

The passive configuration provides a true pulse compression operation whereby a wide coded pulse compresses down to a narrow pulse whose width is equal to the reciprocal of the spread spectrum bandwidth. For a binary code structure, the code is simply generated by delaying an input pulse by multiples of the code bit width with a tapped delay device and summing all the outputs with each output inverted or not inverted as necessary to form the desired code. The same device becomes a pulse compressor by simply feeding the generated code into the opposite end of the structure.

MULTIPLEXED NOISE CODE PAIR NO. 1

A_1 1 0 1 0 1 0 0 1 1 1 0 0 1 1 1 1 0 0 0 0 0 0 1 1 0 1 1 0 0 1 0 1

B_1 1 0 1 0 0 1 1 0 1 1 0 0 0 0 0 0 0 0 0 0 1 1 0 0 0 1 1 0 1 0 1 0

$$\sigma_{A1} = \sigma_{B1} = \sqrt{\frac{144}{31}} = 2.15$$

$$\sigma_{\tau} = 0$$

$$\varphi_{B1}(\tau) = -\varphi_{A1}(\tau)$$

for all $\tau \neq 0$

	0	1	0	1	0	1	1	0	0	0	1	1	0	0	0	0	1	1	1	1	1	1	0	0	1	0	0	1	1	0	1	0
	1	0	1	0	1	0	0	1	1	1	0	0	1	1	1	1	0	0	0	0	0	0	1	1	0	1	1	0	0	1	0	
		0	1	0	1	0	1	1	0	0	0	1	1	0	0	0	0	1	1	1	1	1	1	0	0	1	0	0	1	1	0	
			1	0	1	0	1	0	0	1	1	1	0	0	1	1	1	1	0	0	0	0	0	0	1	1	0	1	1	0	0	
				1	0	1	0	1	0	0	1	1	1	0	0	1	1	1	1	0	0	0	0	0	1	1	0	1	1	0	0	
					1	0	1	0	1	0	0	1	1	1	0	0	1	1	1	1	0	0	0	0	0	1	1	0	1	1	0	
						0	1	0	1	0	1	1	0	0	0	1	1	0	0	0	0	1	1	1	1	1	1	0	0	1	0	
							0	1	0	1	0	1	1	0	0	0	1	1	0	0	0	0	1	1	1	1	1	1	0	0	1	0
								1	0	1	0	1	0	0	1	1	1	0	0	1	1	1	1	0	0	0	0	0	0	1	1	0
									0	1	0	1	0	1	1	0	0	0	1	1	0	0	0	1	1	1	1	1	1	0	0	
										0	1	0	1	0	1	1	0	0	0	1	1	0	0	0	1	1	1	1	1	1	0	
											1	0	1	0	1	0	0	1	1	1	0	0	1	1	1	1	0	0	0	0	0	0	
												1	0	1	0	1	0	0	1	1	1	0	0	1	1	1	1	0	0	0	0	0	
													1	0	1	0	1	0	0	1	1	1	0	0	1	1	1	1	0	0	0	0	
														1	0	1	0	1	0	0	1	1	1	0	0	1	1	1	1	0	0	0	
															1	0	1	0	1	0	0	1	1	1	0	0	1	1	1	1	0	0	
																1	0	1	0	1	0	0	1	1	1	0	0	1	1	1	1	0	
																	0	1	0	1	0	1	1	0	0	0	1	1	0	0	0	
																		0	1	0	1	0	1	1	0	0	0	1	1	0	0	
																			0	1	0	1	0	1	1	0	0	0	1	1	0	
																				0	1	0	1	0	1	1	0	0	0	1	1	
																					0	1	0	1	0	1	1	0	0	0	1	
																						0	1	0	1	0	1	1	0	0	0	
																							0	1	0	1	0	1	1	0	0	
																								0	1	0	1	0	1	1	0	
																									0	1	0	1	0	1	1	
																										0	1	0	1	0	1	
																											0	1	0	1	0	
																												0	1	0	1	
																													0	1	0	
																														0	1	
																															0	

$$\varphi_{A_1}(\tau) = \overset{2\,3\,4\,3\,2}{0\,1\,0\,1\,0\,1\,0} \cdot \overset{2\;\;4\;\;2}{0\,0\,1\,1\,1\,0\,0} \cdot \overset{2\;\;4\;\;2}{1\,0\,0\,1\,0\,0\,1} \cdot \overset{2\,3\,4\,3\,2}{1\,1\,1\,1\,1\,1\,1\,0} \quad 32$$

FIGURE 2 - AUTOCORRELATION FUNCTION OF CODE PAIR A_1B_1

MULTIPLEXED NOISE CODE PAIR NO. 2

A_2 0 0 0 1 1 1 1 0 0 0 1 0 0 0 1 0 0 1 0 0 1 0 1 1 0 1 1 1 1 0 1 1 1

B_2 1 1 1 0 1 1 1 0 1 1 0 1 0 0 1 0 1 0 1 1 1 0 1 1 1 0 0 0 0 1 1 1

$$\sigma_{A2} = \sigma_{B2} = \sqrt{\frac{144}{31}} = 2.15$$

$$\sigma_T = 0$$

$$\varphi_{B2}(\tau) = -\varphi_{A2}(\tau)$$

for all $\tau \neq 0$

τ	1	2	3	4	5	6	7	8	9	10	11	12	13	14	15	16	17	18	19	20	21	22	23	24	25	26	27	28	29	30	31	32
$\varphi_{A2}(\tau)$	1	1	1	·	0	0	1	·	1	1	0	·	0	1	0	·	1	1	1	·	1	1	0	·	0	0	1	·	0	1	0	0

FIGURE 3 - AUTOCORRELATION FUNCTION OF CODE PAIR A_2B_2

MULTIPLEXED NOISE CODE PAIR NO. 3

A_3 1 1 1 1 0 0 1 1 1 1 0 0 0 0 0 0 0 1 0 1 0 1 1 0 0 1 1 0 0 1 0 1

B_3 0 1 0 1 1 0 0 1 0 1 1 0 1 0 1 0 1 1 1 1 1 1 0 0 1 1 0 0 1 1 1 1

$\sigma_{A3} = \sigma_{B3} = \sqrt{\frac{144}{31}} = 2.15$

$\sigma_T = 0$

$\varphi_{B3}(\tau) = -\varphi_{A3}(\tau)$

for all $\tau \neq 0$

$\varphi_{A3}(\tau) =$	0	·	0	·	1	·	0	·	0	·	1	·	0	·	1	·	1	·	1	·	1	·	1	·	1	·	1	·	0	0	3	32

FIGURE 4 - AUTOCORRELATION FUNCTION OF CODE PAIR A_3B_3

MULTIPLEXED NOISE CODE PAIR NO. 4

A_4 1 0 1 0 1 1 1 1 1 0 0 1 1 1 0 0 1 1 0 0 1 0 0 1 1 1 1 1 1 0 1 0

B_4 0 1 0 1 1 1 1 1 0 1 1 0 1 1 0 0 0 0 1 1 1 0 0 1 0 0 0 0 1 0 1 0

$$\sigma_{A4} = \sigma_{B4} = \sqrt{\frac{144}{31}} = 2.15$$

$$\sigma_T = 0$$

$$\varphi_{B6}(\tau) = -\varphi_{A6}(\tau)$$

for all $\tau \neq 0$

$$\varphi_{A4}(\tau) = 1\,0\,1\,0\,1\,0\,1 \cdot 0\,0\,0\,0\,0\,0\,0 \cdot 1\,1\,0\,0\,0\,1\,1 \cdot 0\,1\,1\,0\,1\,1\,0\,0$$

$$2\;3\;4\;3\;2 \qquad 2\;3\;4\;3\;2 \qquad 2\;4\;2 \qquad 2\;4\;2\;32$$

FIGURE 5 - AUTOCORRELATION FUNCTION OF CODE PAIR A_4B_4

MULTIPLEXED NOISE CODE PAIR NO. 6

A_6 1 0 1 1 1 0 0 0 1 0 1 1 0 1 1 1 0 1 0 0 0 1 1 1 1 0 1 1 0 1 1 1

B_6 0 0 0 1 0 0 1 0 0 0 0 1 1 1 0 1 1 1 1 0 1 1 0 1 0 0 0 1 1 1 0 1

$$\sigma_{A6} = \sigma_{B6} = \sqrt{\frac{176}{31}} = 2.38$$

$$\sigma_\tau = 0$$

$$\varphi_{B6}(\tau) = -\varphi_{A6}(\tau)$$

for all $\tau \neq 0$

τ	1	2	3	4	5	6	7	8	9	10	11	12	13	14	15	16	17	18	19	20	21	22	23	24	25	26	27	28	29	30	31	32
$\varphi_{A6}(\tau)$	0	0	0	1	0	0	0	1	0	0	1	1	0	0	0	0	1	1	0	0	0	1	0	0	1	0	0	0	1	1	1	0

FIGURE 6 - AUTOCORRELATION FUNCTION OF CODE PAIR A_6B_6

As an illustration consider the passive generation/compression of the 5 bit Barker Code - 00010. The code generator would be configured as shown in the sketch below.

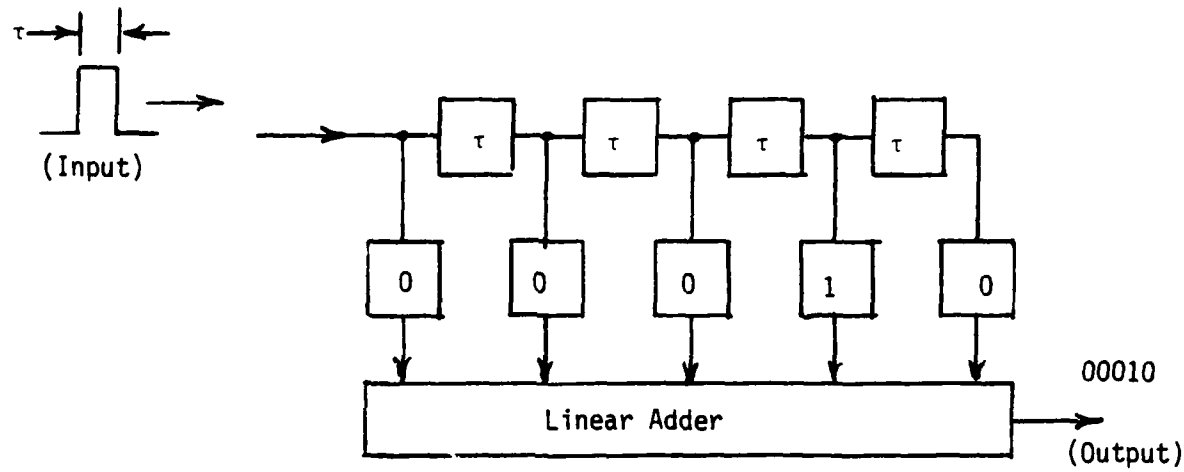

where: The functional blocks identified as τ represent a delay of τ that is equal to the code bit width

The functional blocks containing a "1" or "0" identify a phase operation where "1" signifies a phase reversal and "0" signifies no phase reversal.

The pulse compression filter for the 5 bit Barker Code is illustrated below.

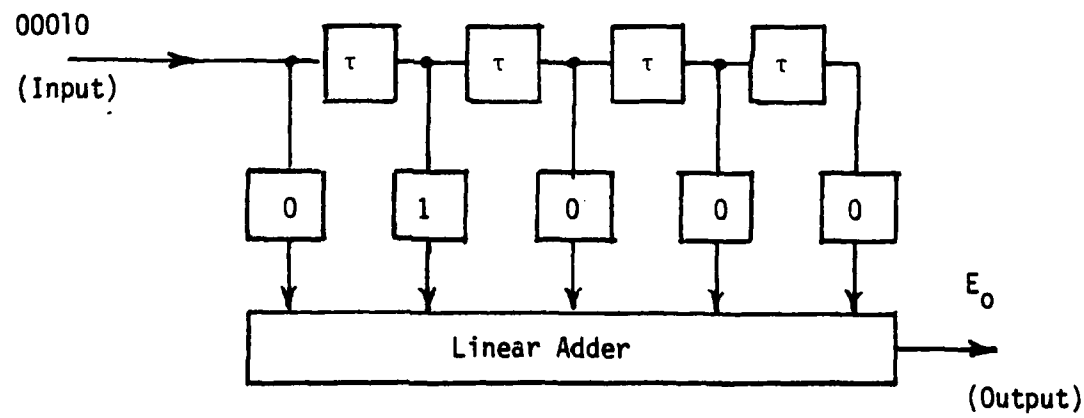

Graphically performing the operations identified in the previous functional block diagram results in the following compressed code.

$$
\begin{array}{ccccccccccc}
 & 0 & 0 & 0 & 1 & 0 & & & & & \\
 & & 1 & 1 & 1 & 0 & 1 & & & & \\
 & & & 0 & 0 & 0 & 1 & 0 & & & \\
 & & & & 0 & 0 & 0 & 1 & 0 & & \\
 & & & & & 0 & 0 & 0 & 1 & 0 & \\
\hline
E_0 = & 0 & \cdot & 0 & \cdot & 0^5 & \cdot & 0 & \cdot & 0 & = \varphi(\tau)
\end{array}
$$

where as previously noted: The exponent represents the amplitude,
i.e. $0^K = +K$
$1^K = -K$

A dot represents a zero amplitude
$\varphi(\tau)$ = autocorrelation function.

Note that the pulse compressor (matched filter) phase inverts each of the delayed inputs only when it is required to provide an "0" or +1 at τ=0. This results when the phase reversals match the input code sequence in reverse order. An inspection of the generator and compressor show them to be identical in form; the only difference being which side of the tapped delay device is used for the input.

The corresponding time diagrams for the generated and compressed Barker Code is shown below.

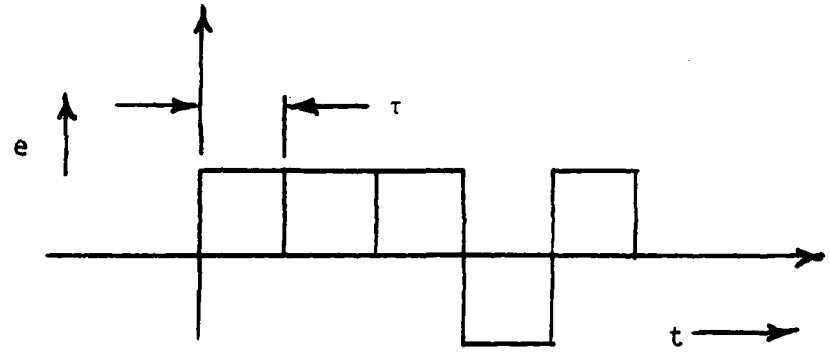

Generated Code

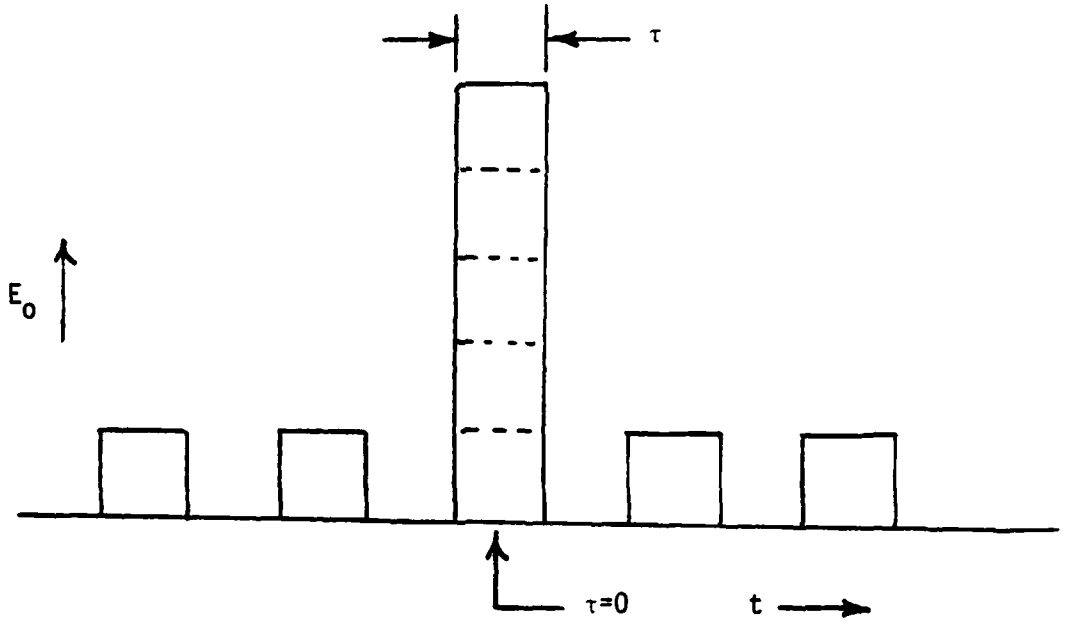

Compressed Code

- Active code generation/correlation detection.

When active code generation/correlation detection is employed, the mechanics are quite different even though both the passive and active methods provide optimum matched filter detection of the desired signal. A classical active code generator would utilize an n bit shift register and simply hard wire the desired states of each binary element of the shift register. A clock then sequentially shifts the code out of the register using shift load and clock inhibit control signals. A functional block diagram of the code generator is illustrated below.

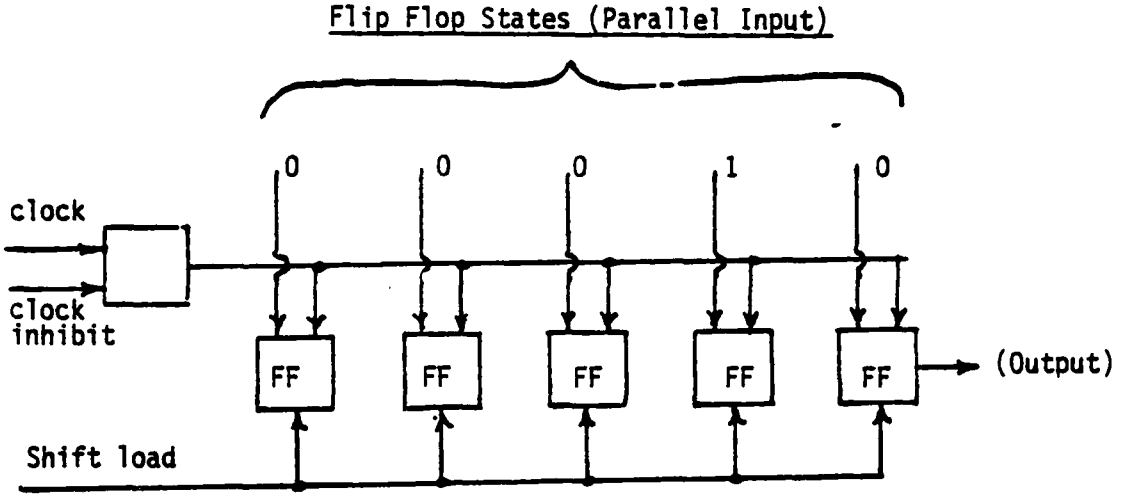

Code Generator

Active correlation (coherent) detection is obtained using a multiplier and integrator as is defined by the autocorrelation function equation.

$$\varphi_s(\tau) = \int_{-\infty}^{\infty} s(t)\, s(t+\tau)dt \qquad (45)$$

where: $\varphi_s(\tau)$ = autocorrelation function of s(t)

The value for $\varphi_s(\tau)$ peaks at $\tau=0$ and is analogous to optimum matched filter detection of the signal.

A functional block diagram of a correlation detector is shown below.

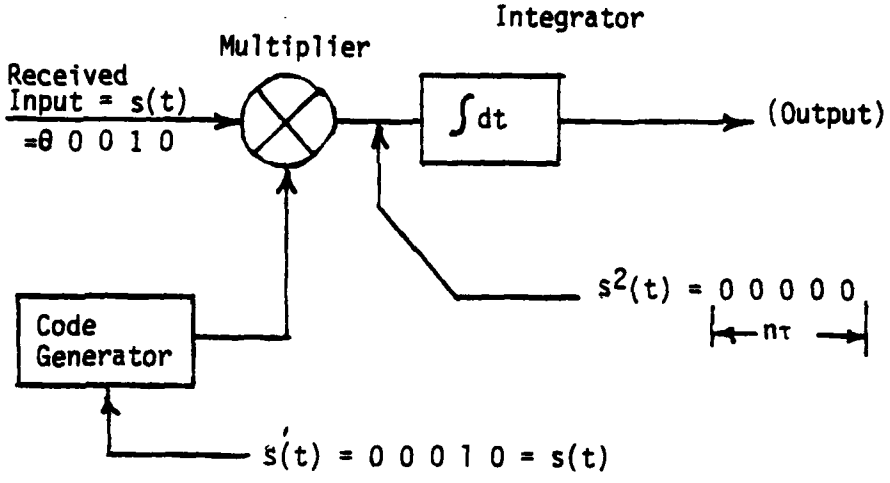

Correlation Detector

Fundamentally (at $\tau=0$), the correlation detector translates all of the code bits to +1 (i.e. d-c during the presence of the coded signal) which can then be integrated to its maximum possible value. There is no time compression at all (as was the case for passive matched filter detection) since the output time duration of the processed signal is the same as that of the input coded signal. It is the bandwidth that is compressed by the time-bandwidth product (i.e. the number of code bits) of the spread spectrum signal when correlation or coherent detection is utilized.

For a digital signal such as employed here, the autocorrelation function becomes:

$$\varphi_s(\tau) = \sum_{i=1}^{i=n-\tau} a_i a_{i+\tau} \qquad (46)$$

Its value for different values of τ is readily calculated from equation (46) which is accomplished below for the 5 bit Barker Code.

At $\tau=0$

$$\begin{array}{r} 0\ 0\ 0\ 1\ 0 \\ \times\ 0\ 0\ 0\ 1\ 0 \\ \hline \Sigma\ +\ +\ +\ +\ + \end{array} = +5 = \varphi_s(0)$$

where: 0x0 = +1
1x1 = +1
0x1 = -1
1x0 = -1

At $\tau=1$

$$\begin{array}{r} 0\ 0\ 0\ 1\ 0 \\ \times\ 0\ 0\ 0\ 1\ 0 \\ \hline \Sigma\ +\ +\ -\ - \end{array} = 0 = \varphi_s(1)$$

At $\tau = 2$

$$\begin{array}{r} 0\ 0\ 0\ 1\ 0 \\ \times\quad 0\ 0\ 0\ 1\ 0 \\ \hline \Sigma\quad +\ -\ + \end{array} = +1 = \varphi_s(2)$$

At $\tau = 3$

$$\begin{array}{r} 0\ 0\ 0\ 1\ 0 \\ \times\quad\ 0\ 0\ 0\ 1\ 0 \\ \hline \Sigma\quad\ -\ + \end{array} = 0 = \varphi_s(3)$$

At $\tau = 4$

$$\begin{array}{r} 0\ 0\ 0\ 1\ 0 \\ \times\quad\ \ 0\ 0\ 0\ 1\ 0 \\ \hline \Sigma\quad\ \ + \end{array} = +1 = \varphi_s(4)$$

Since an autocorrelation function is an even function, it is not necessary to calculate $\varphi_s(\tau)$ for negative values of τ. A plot of $\varphi_s(\tau)$ is shown below.

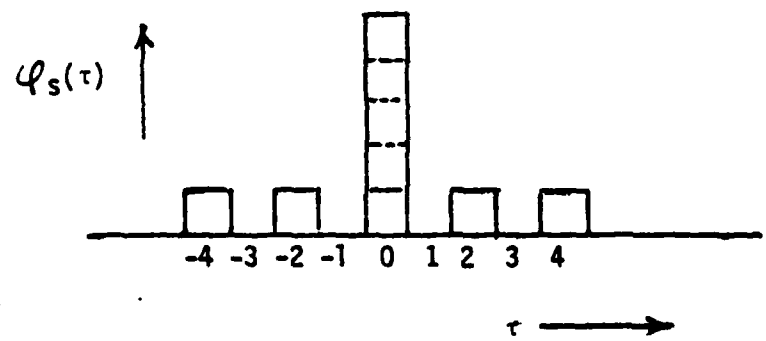

And we see that this result is exactly the same as that obtained for the passive (pulse compression) matched filter.

b. Active Configurations

(1) Implementation

Several active code generators were fabricated using TTL 8 bit shift registers (DM 74165N) in tandem to provide 32 bit binary mate code pairs. The parallel inputs to the shift register were wired to their respective appropriate states, as illustrated in the previous paragraph, to generate the code pairs contained in figures 2 through 6. A photograph of one of these generators is shown in figures 7 and 8. These fabricated code generators were utilized in conjunction with an available Digital Data Simulator, Model 900SP which is manufactured by Moxon Incorporated, to provide the binary multiplexed noise codes required for the various tests performed on this research project.

All of the tests were conducted at RF which required converting the zero to 5 volt binary coded signal provided by the code generators to bipolar video and then bi-phase modulating a 30MHz RF carrier with the bipolar video signal. Double balanced mixers were utilized to provide the phase modulation function. The correlation detector comprised Merrimac (Model PCM-3) phase detectors as the coherent multiplier and a R-C low pass filter to perform the required integration.

(2) Autocorrelation Function Measurements

A functional block diagram of the test configuration that was utilized for obtaining measurements of the autocorrelation function is presented in figure 9. Two independent code generators (A_1B_1 and A_2B_2) are bi-phase modulated, gated using an RF switch and applied to phase detectors (multipliers). The output of the phase detectors (one for the Channel A code pair and one for the channel B code pair) are then linearly added and integrated to provide the measured value of the autocorrelation function at some specific value of delay τ which corresponds to the time difference between the two generated code pairs. Both code generators are timed from the same clock with a variable delay control contained in one of the generators (code generator no. 1) which enabled stepping the time difference between the two codes in integral multiples of the code bit pulse width τ.

A photograph of the physical test configuration employed which corresponds to the functional block diagram illustrated in figure 9 is shown in figure 10. An itemized list of the major test equipment and components used to implement the test set-up illustrated is contained in paragraph 5. The code generators, integrator and linear adder were fabricated in-house at the Electronic Technology and Devices (ET&D) Laboratory and the remaining items comprised available test equipment and purchased (off the shelf) components.

Code pair A_4B_4 was utilized for this test. The output of both of the code generators provided a two state (0 to +5V) binary coded signal (codes A_4 and B_4) whose bit rate was chosen to be 1 Mb/s. A photograph of these generated codes is shown in figure 11 along with the 30 MHz RF carrier that is bi-phase modulated by the codes. With these phase modulated signals providing the inputs to the correlation detector, their relative time

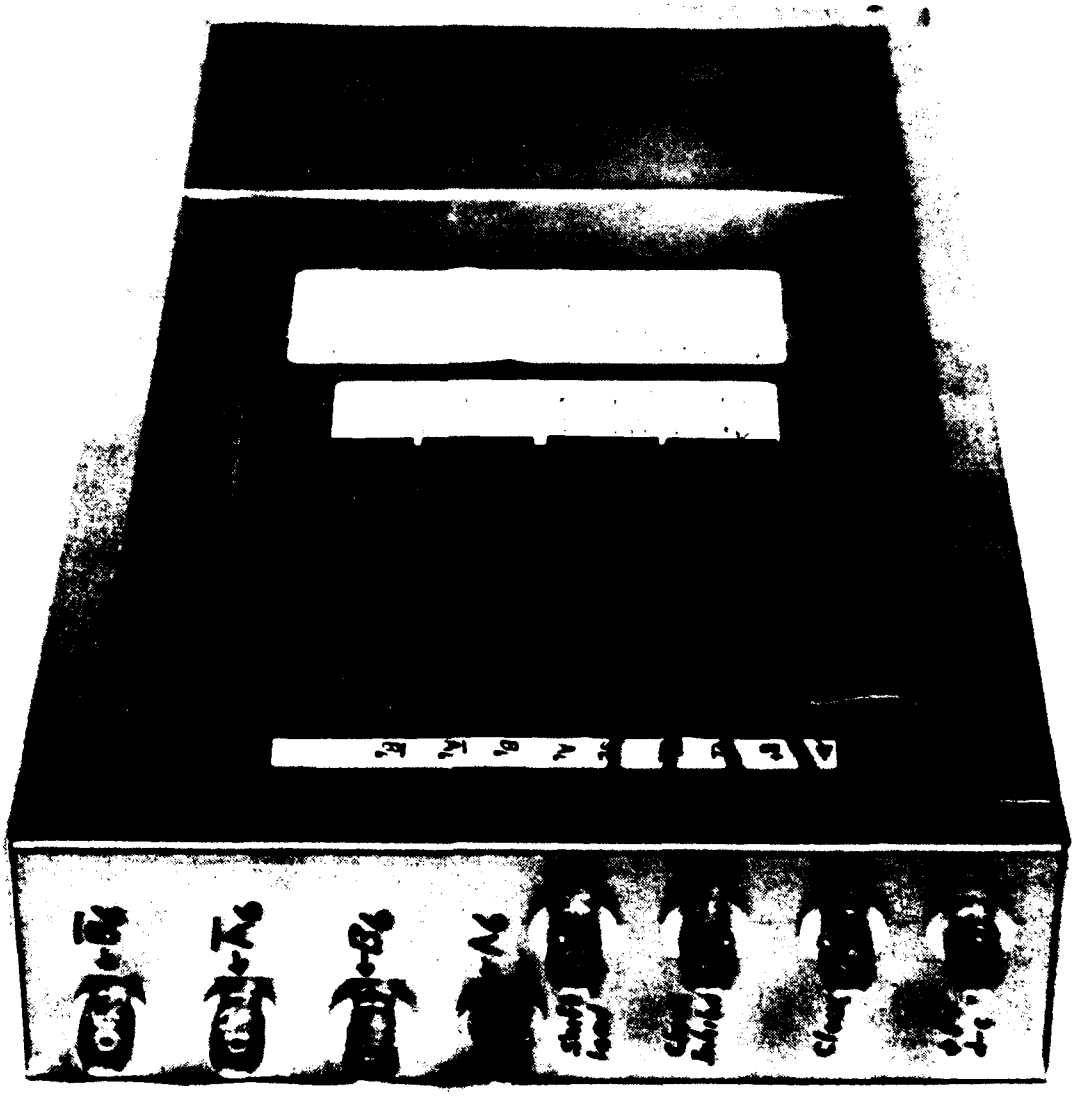

Figure 7 - Shift Register Code Generator/Correlation Detector (Top)

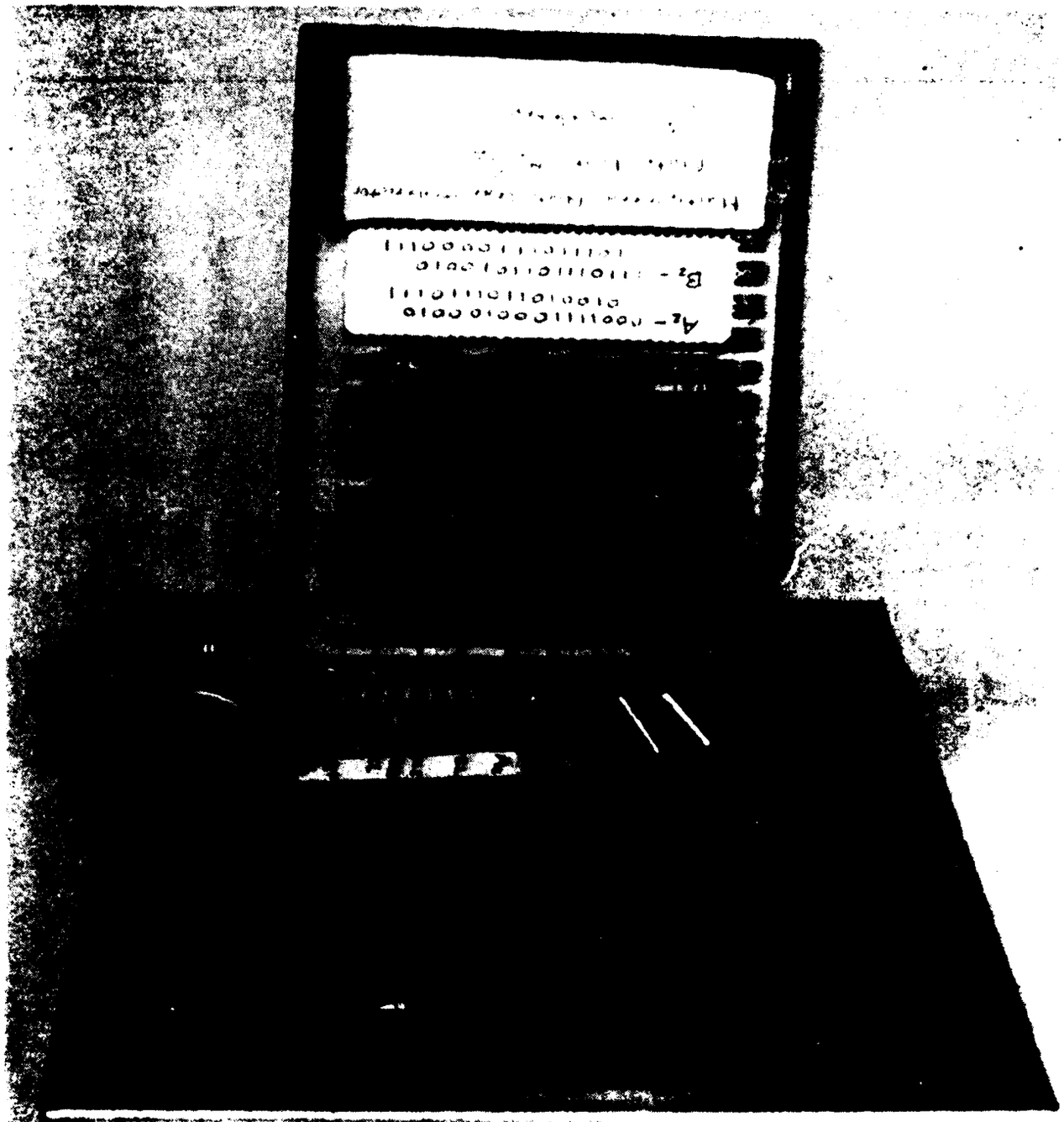

Figure 3 - Shift Register Code Generator/Correlation Detector (Bottom)

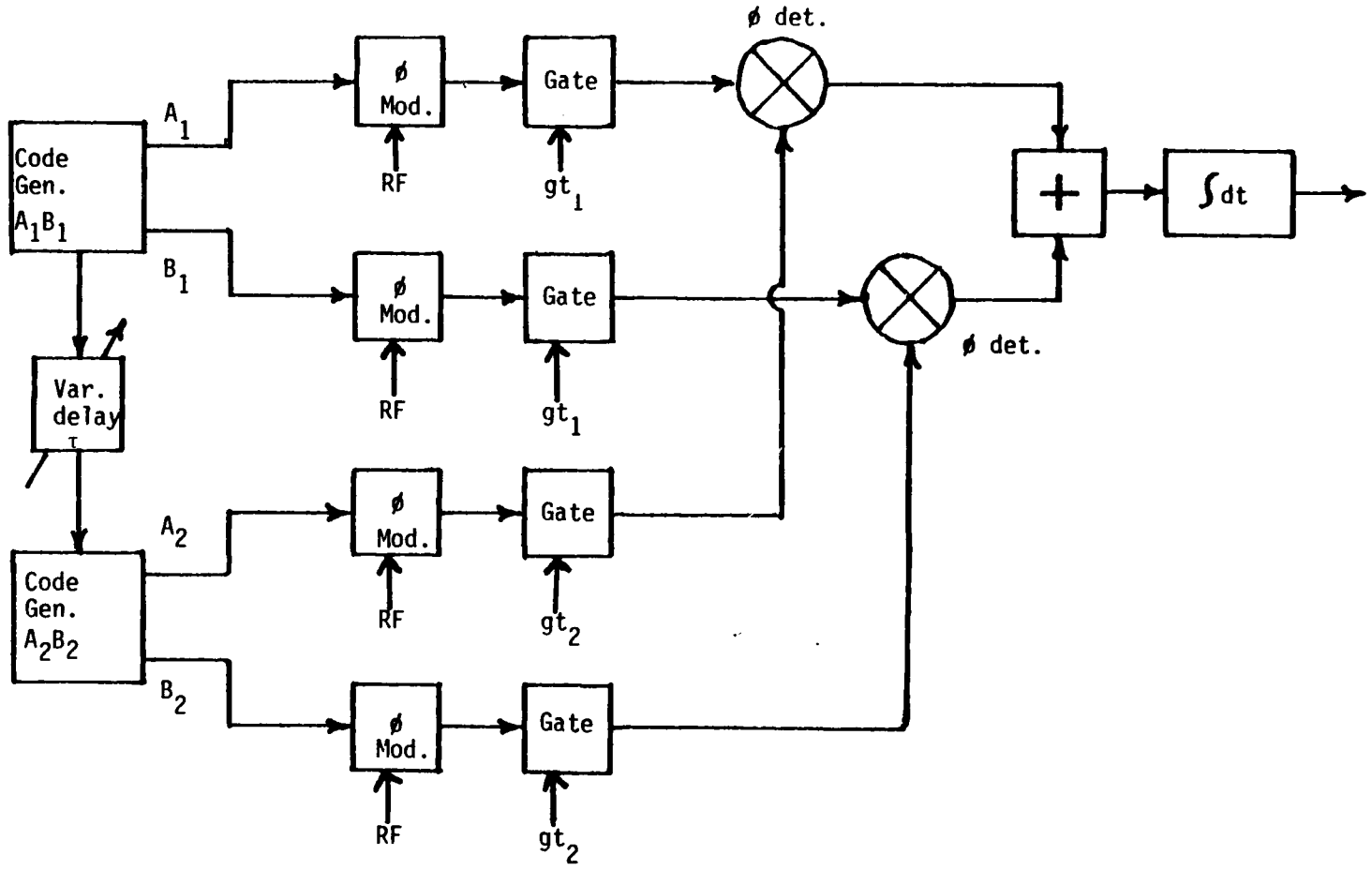

FIGURE 9 - AUTOCORRELATION & CROSSCORRELATION TEST CONFIGURATION

Figure 10 - Test Configuration for Autocorrelation/Crosscorrelation Function Measurements

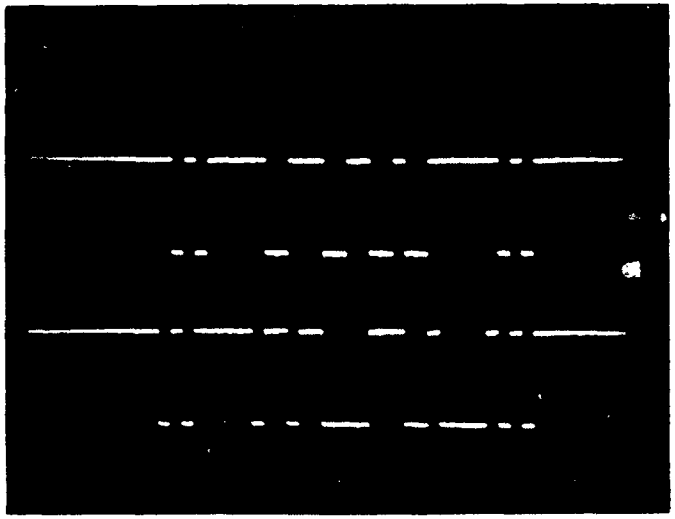

a. CODE GENERATOR #1 OUTPUTS
CODE A ON TOP / CODE B ON BOTTOM
X SCALE - 5 us/div

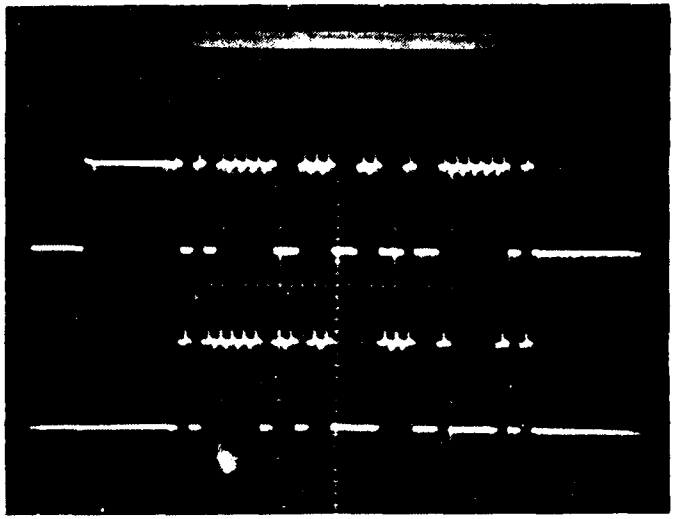

b. CODE GENERATOR #2 OUTPUTS
CODE A ON TOP / CODE B ON BOTTOM
X SCALE - 5 us/div

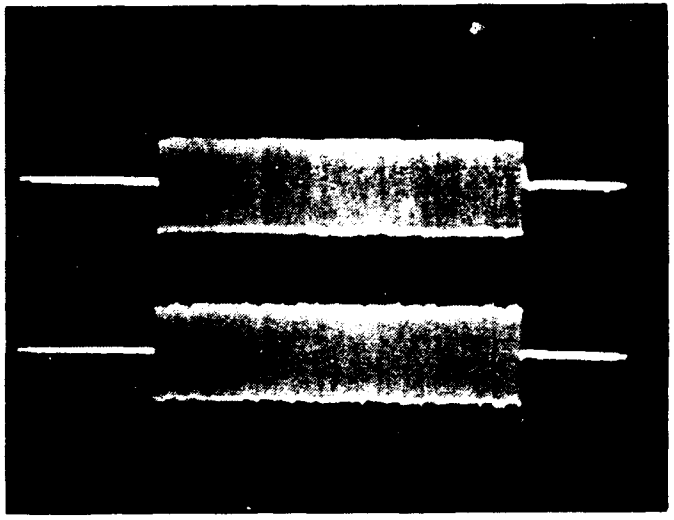

c. PHASE MODULATED OUTPUT OF CODE PAIR #1
CODE A ON TOP / CODE B ON BOTTOM
X SCALE - 5 us/div

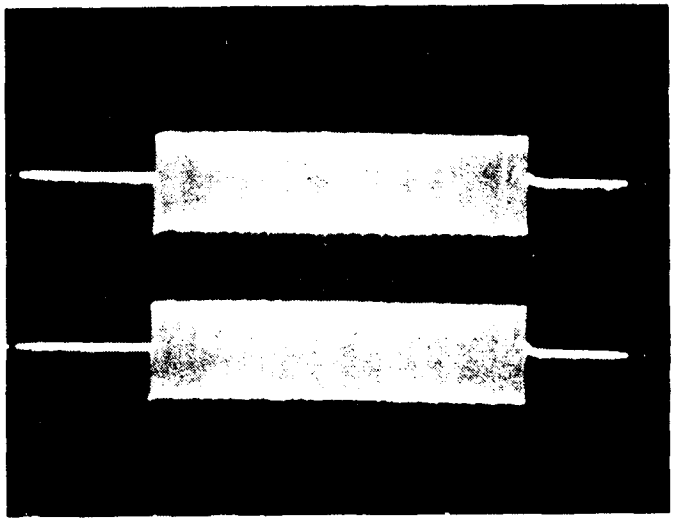

d. PHASE MODULATED OUTPUT OF CODE PAIR #2
CODE A ON TOP / CODE B ON BOTTOM
X SCALE - 5 us/div

FIGURE 11- GENERATED & PHASE MODULATED CODE PAIR A_4 B_4

difference (τ) was varied and the autocorrelation function value measured at the integrator output for all values of τ using a calibrated oscilloscope. The largest measured sidelobe value occurred at τ=6 and was 40db below the peak signal level. The peak detected signal was measured to be 32mv as shown in figure 12a (this occurs at τ=0) and the measured value of the autocorrelation function at τ=6 is .3mv as shown in figure 13a. The measurement is made at the sample point which corresponds to the end of the processing time of the coded information bit. An operating system would sample the output at this point using a narrow gate and then detect the signal using a threshold detector. For all of the photographs taken at the integrator output in this test, the grid line of the x axis corresponds to zero volts. The phase detector output of code A is shown at the bottom of these photos using a dual trace to identify the location of the sample point and a photo of the integrator input is provided to illustrate how the operating function of the multiplier and summing networks perform.

Most of the measured autocorrelation function values (i.e. equivalent sidelobe levels) were down by about 50db as shown in figure 13c for τ=9. In order to conserve film and time, the recorded values were restricted to measuring (τ) at values of τ corresponding to the largest lobe (τ=6), a value typical of the amplitude of most of the lobes (τ=9), and the four values of τ corresponding to the theoretically largest lobe value for the individual codes of the mate pairs A_4B_4(τ=4, 12, 20 and 28). The measured and recorded autocorrelation function values for τ=4 and 12 are presented in figure 14 and figure 15 shows the results at τ=20 and 28. The lobe values at τ=4, 12, 20 and 28 were all down by more than 40db, ranging from 42 to 44db.

The measured autocorrelation function values are very impressive when compared to the best results one can achieve, even theoretically, using state of the art direct sequence P-N codes. A 63 bit P-N code has its largest theoretical sidelobe down by only 19db.

In order to further demonstrate how close the measured performance using hardware compares to theory, the theoretical manipulations involved in calculating the autocorrelation function at τ=9 was accomplished. The results which are presented in figure 16 are essentially the same as was obtained for the measured value at τ=9 as presented in figure 13c and d. There is a very close resemblance between theory and practice at the phase detector output, the integrator input and the integrator output.

To illustrate the cancellation operation experienced when using the code mate pairs, a photo was taken of the integrator output for τ=4 with the code B_4 input removed, then with the code A_4 input removed and then with both inputs connected. The result is shown in figure 17.

(3) Crosscorrelation Function Measurements

The same basic hardware was utilized for the crosscorrelation function measurements as was employed in obtaining the autocorrelation function measurements. The only differences being that the code generators provided different codes and the variable delay is not necessary. Both codes were time coincident (τ=0) for all of the crosscorrelation tests performed.

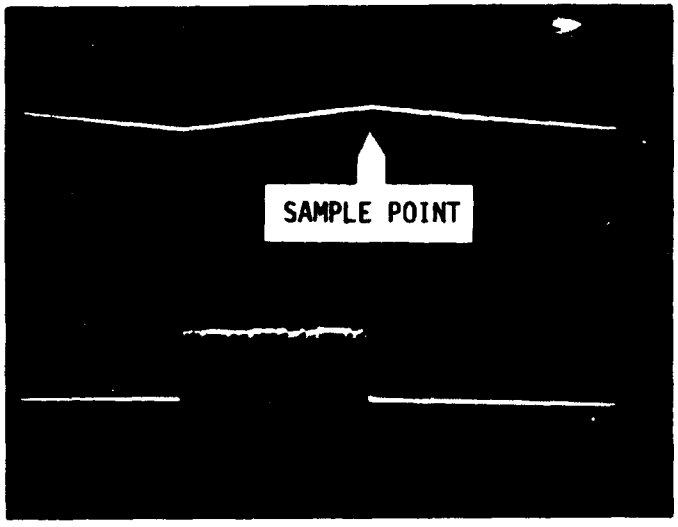

a. PEAK INTEGRATOR OUTPUT τ =0 (TOP)
INTEGRATOR INPUT AT τ = 0 (BOT)
X SCALE - 10 us/div
Y SCALE - 10 mv/div(TOP) 50mv/div(BOT)

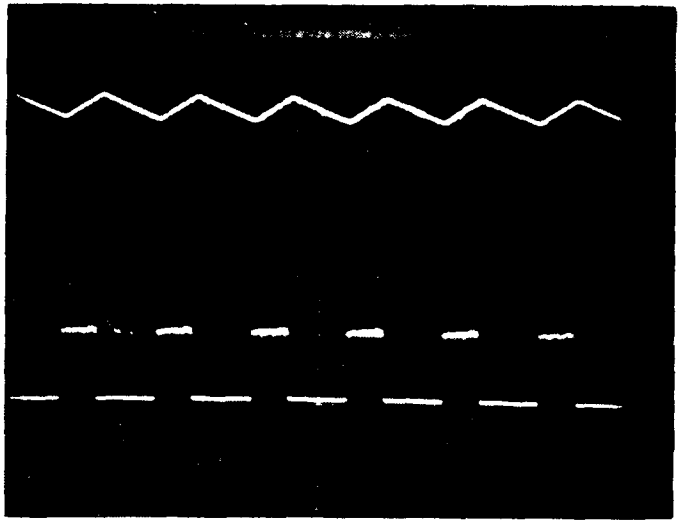

b. PEAK INTEGRATOR OUTPUT AT τ = 0 (TOP)
INTEGRATOR INPUT AT τ = 0 (BOT)
X SCALE - 50 us/div
Y SCALE - 10 mv/div (TOP) 50 mv/div(BOT)

FIGURE 12 - AUTOCORRELATION FUNCTION VALUE AT τ=0 FOR CODE PAIR A4 B_4

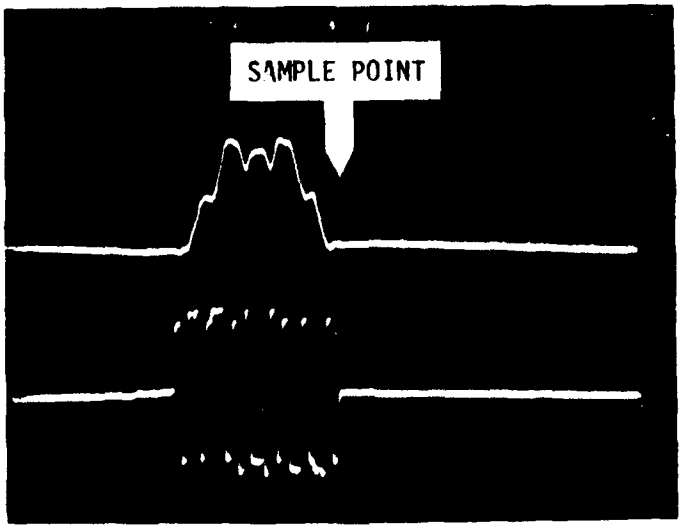

a. INTEGRATOR OUTPUT AT τ= 6 (TOP)
PHASE DETECTOR OUTPUT OF CODE A AT τ=6(BOT)
X SCALE - 10 us/div
Y SCALE - 0.5mv/div(TOP)

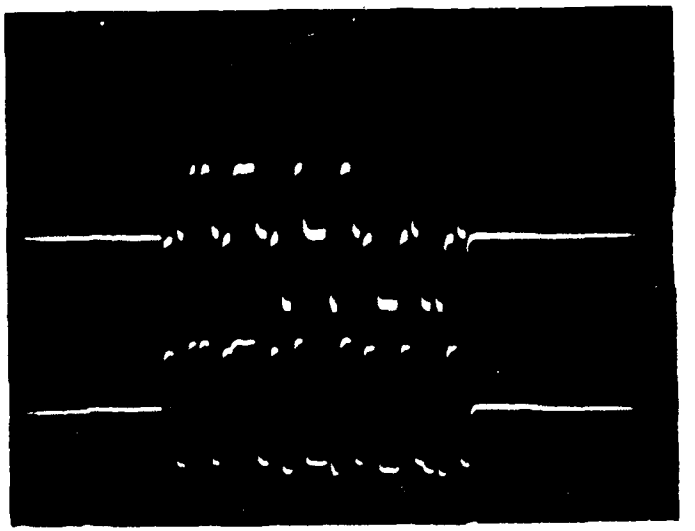

b. INTEGRATOR INPUT AT τ=6 (TOP)
PHASE DETECTOR OUTPUT OF CODE A AT τ=6(BOT)
X SCALE - 5 us/div
Y SCALE - 50 mv/div

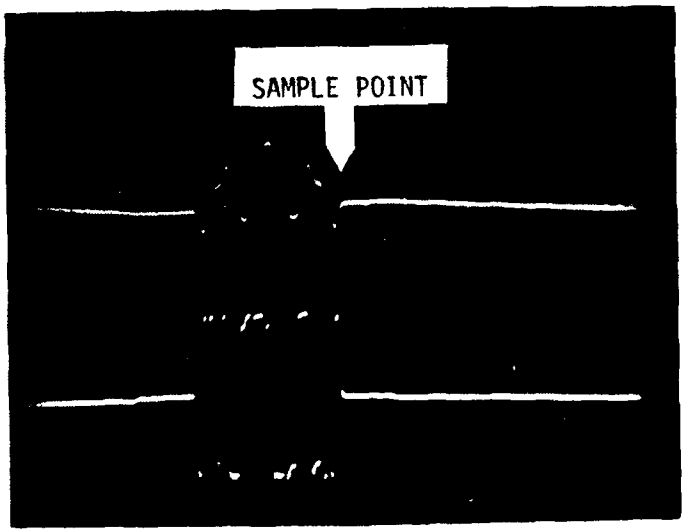

c. INTEGRATOR OUTPUT AT τ= 9 (TOP) (TYPICAL)
PHASE DETECTOR OUTPUT OF CODE A AT τ=9(BOT)
X SCALE - 10 us/div
Y SCALE - 0.5 mv/div(TOP)

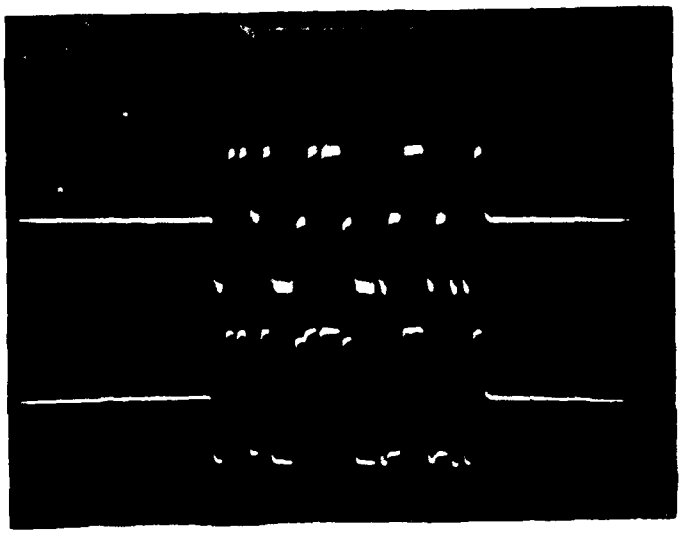

d. INTEGRATOR INPUT AT τ= 9 (TOP) (TYPICAL)
PHASE DETECTOR OUTPUT OF CODE A AT τ=9(BOT)
X SCALE - 5 us/div
Y SCALE - 50 mv/div

FIGURE 13 - AUTOCORRELATION FUNCTION VALUE AT τ= 6 AND τ=9 FOR CODE PAIR A4 B4

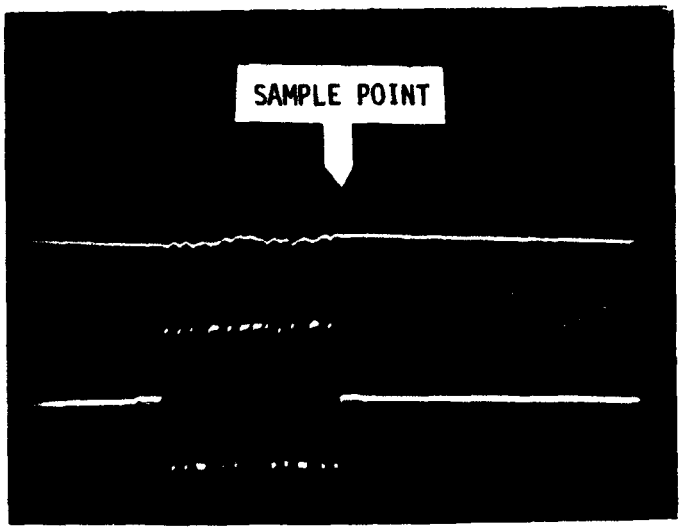

a. INTEGRATOR OUTPUT AT τ = 4 (TOP)
PHASE DETECTOR OUTPUT OF CODE A AT τ = 4 (BOT)
X SCALE - 10 us/div
Y SCALE - 0.5 mv/div(TOP)

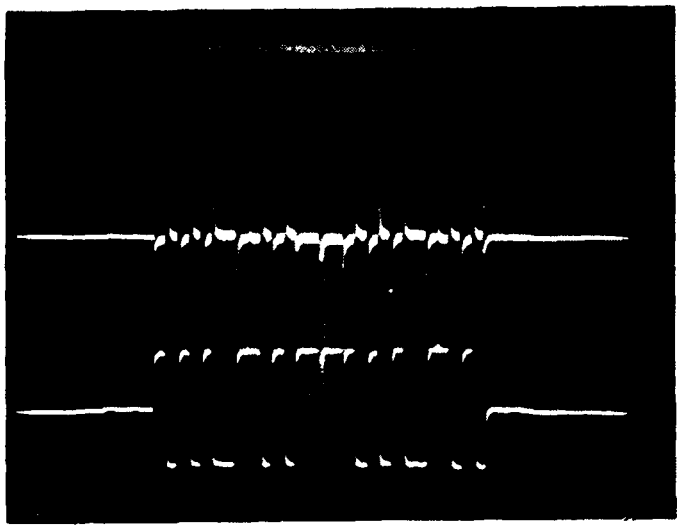

b. INTEGRATOR INPUT AT τ=4 (TOP)
PHASE DETECTOR OUTPUT OF CODE A AT τ= 4 (BOT)
X SCALE - 5 us/div
Y SCALE - 50 mv/div

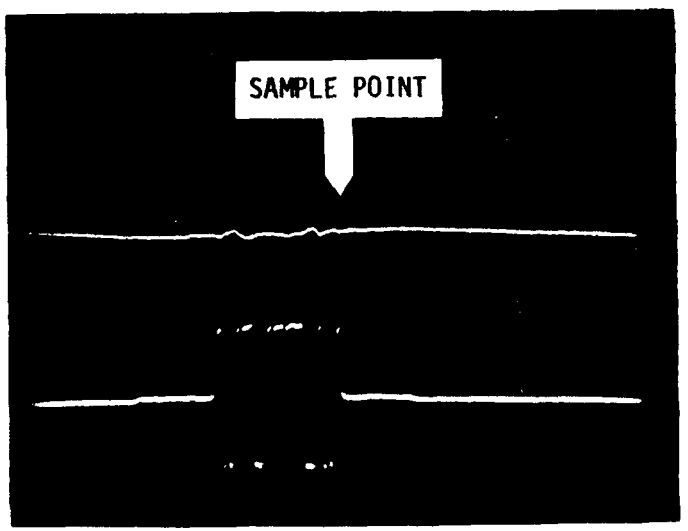

c. INTEGRATOR OUTPUT AT τ=12 (TOP)
PHASE DETECTOR OUTPUT OF CODE A AT τ= 12(BOT)
X SCALE - 10 us/div
Y SCALE - 0.5 mv/div(TOP)

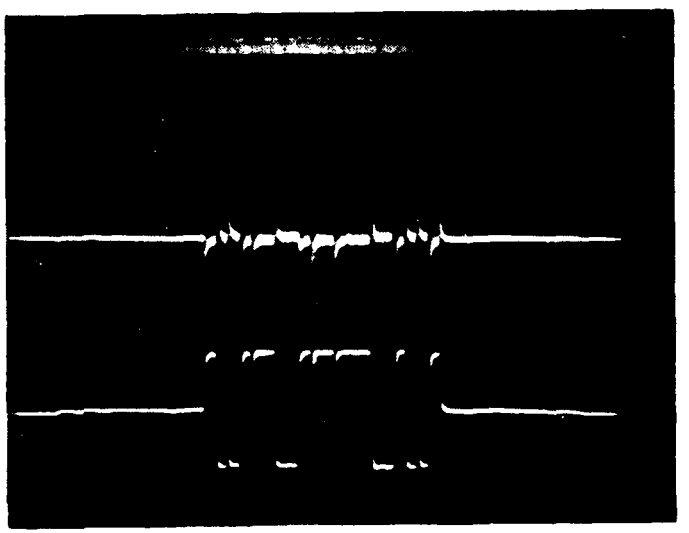

d. INTEGRATOR INPUT AT τ= 12 (TOP)
PHASE DETECTOR OUTPUT OF CODE A AT τ= 12(BOT)
X SCALE - 5 us/div
Y SCALE - 50 mv/div

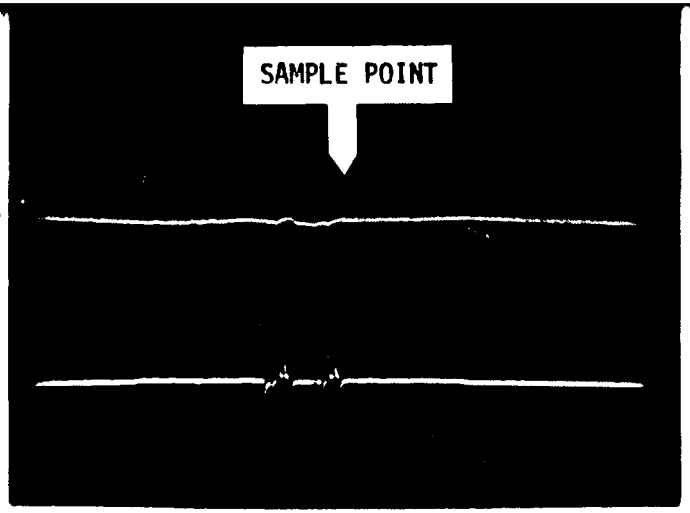

a. INTEGRATOR OUTPUT AT τ= 20 (TOP)
INTEGRATOR INPUT AT τ= 20 (BOT)
X SCALE - 10 us/div
Y SCALE - 0.5 mv/div(TOP)

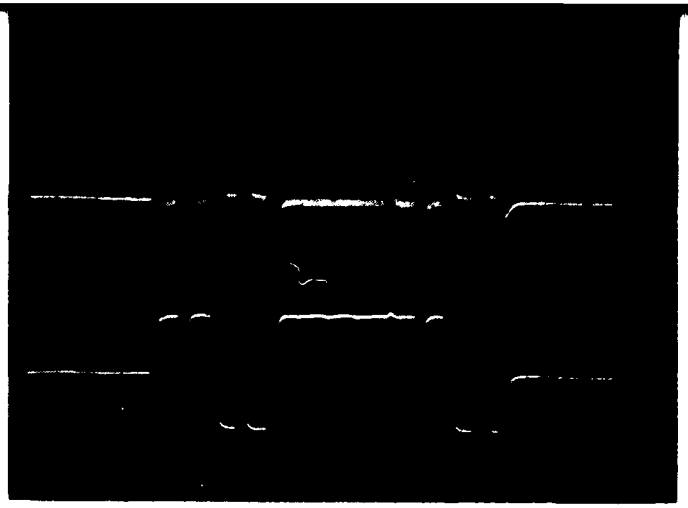

b. INTEGRATOR INPUT AT τ= 20 (TOP)
PHASE DETECTOR OUTPUT OF CODE A AT τ=20(BOT)
X SCALE - 2 us/div
Y SCALE - 50 mv/div

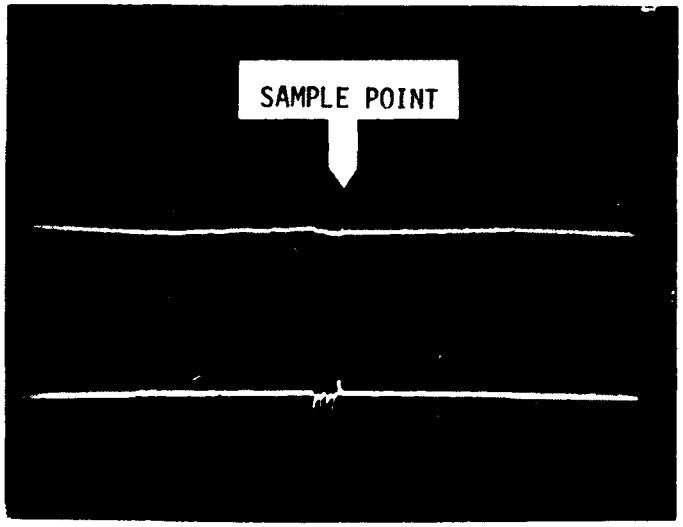

c. INTEGRATOR OUTPUT AT τ= 28 (TOP)
INTEGRATOR INPUT AT τ= 28 (BOT)
X SCALE - 10 us/div
Y SCALE - 0.5 mv/div(TOP)

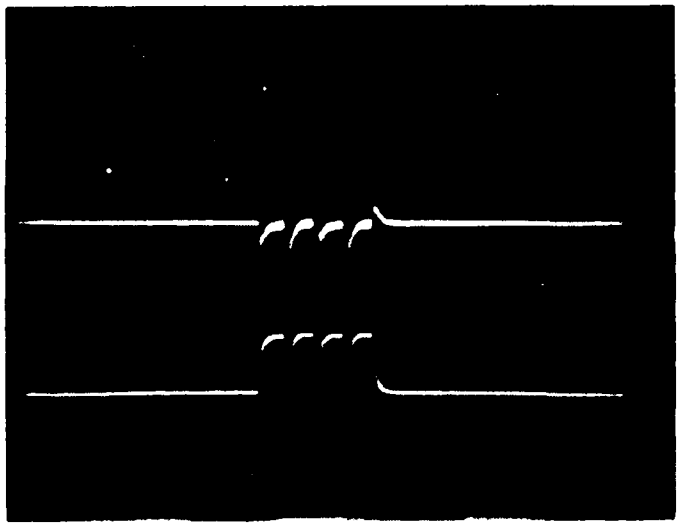

d. INTEGRATOR INPUT AT τ= 28 (TOP)
PHASE DETECTOR OUTPUT OF CODE A AT τ=28(BOT)
X SCALE - 2 us/div
Y SCALE - 50 mv/div

FIGURE 15 - AUTOCORRELATION FUNCTION VALUE AT τ=20 and τ=28 FOR CODE PAIR A_4 B_4

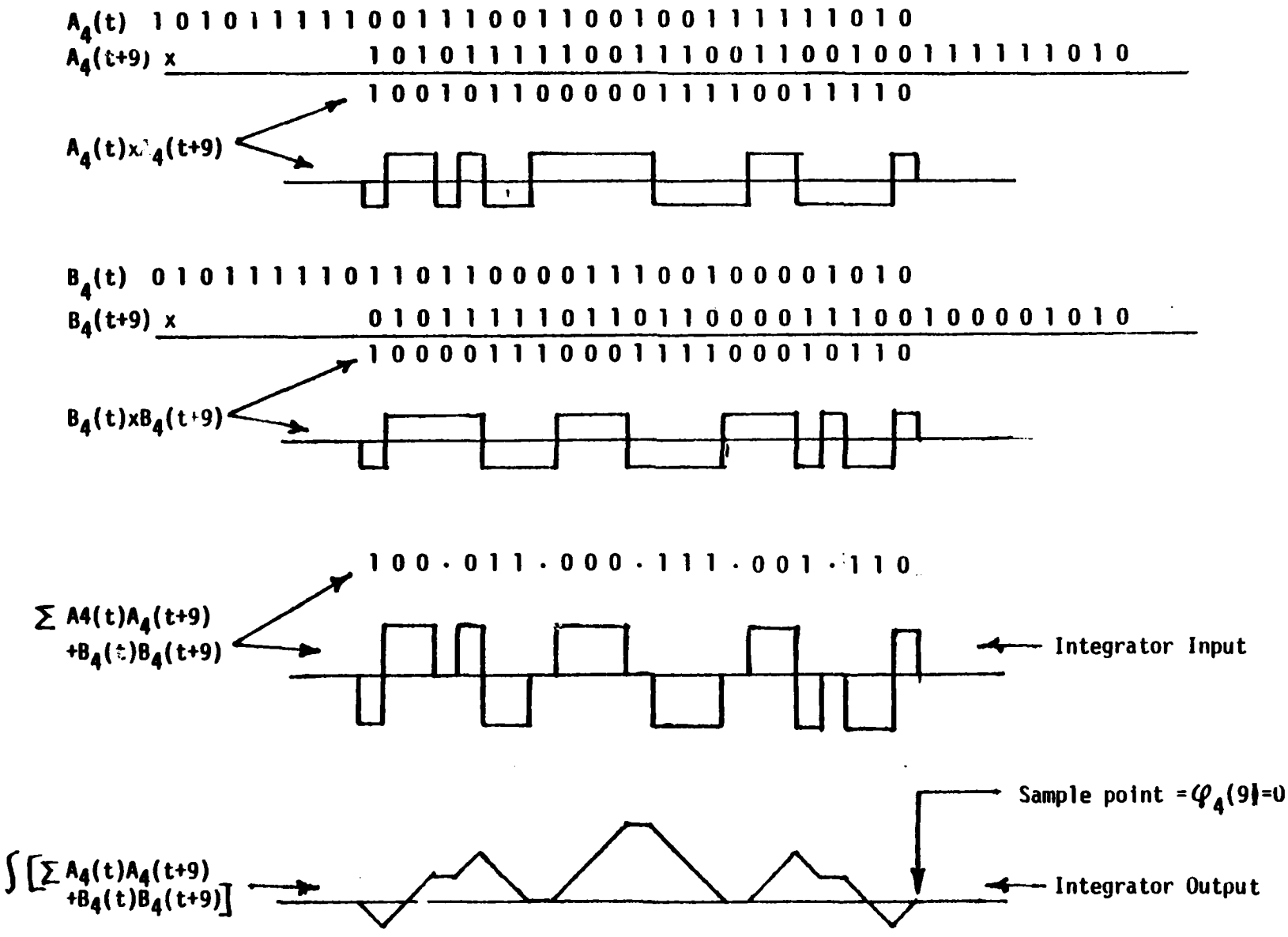

FIGURE 16 - AUTOCORRELATION FUNCTION CALCULATION AT $\tau = 9$

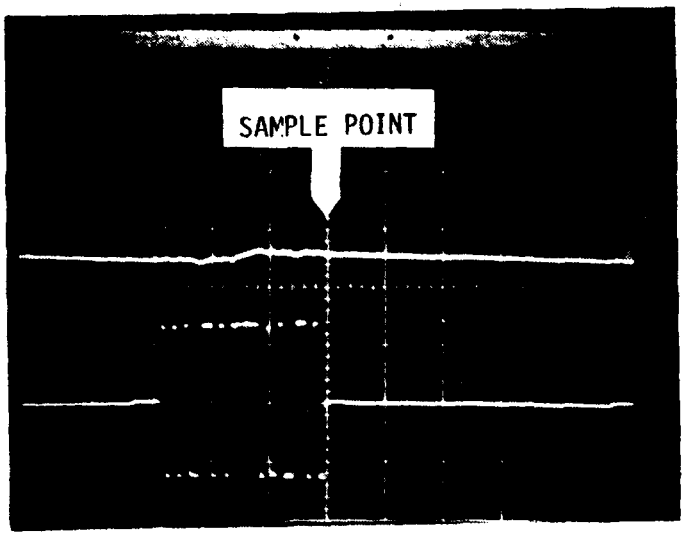

a. INTEGRATOR OUTPUT FOR CODE A ONLY AT τ=4(TOP)
PHASE DETECTOR OUTPUT OF CODE A AT τ=4(BOT)
X SCALE - 10 us/div
Y SCALE - 5 mv/div (TOP) 50 mv/div (BOT)

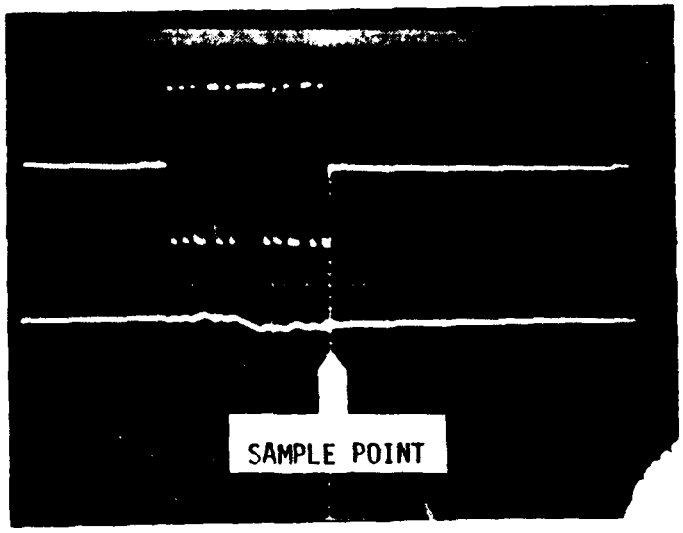

b. INTEGRATOR OUTPUT FOR CODE B AT τ= 4 (BOT)
PHASE DETECTOR OUTPUT OF CODE A AT τ=4(TOP)
X SCALE - 10 us/div
Y SCALE - 5 mv/div (BOT) 50 mv/div (TOP)

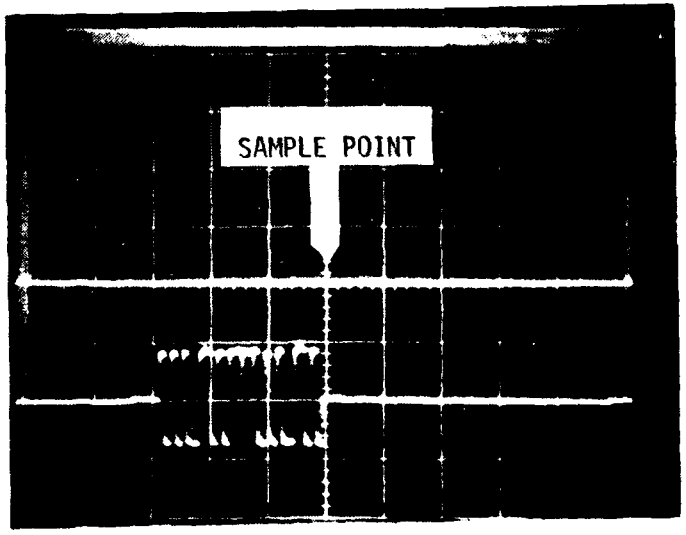

c. INTEGRATOR OUTPUT AT τ= 4 (TOP)
PHASE DETECTOR OUTPUT OF CODE A AT τ=4(BOT)
X SCALE - 10 us/div
Y SCALE - 5 mv/div (TOP) 50 mv/div (BOT)

FIGURE 17 - AUTOCORRELATION FUNCTION VALUE FOR CODE PAIR A_4 B_4 AT τ= 4

The four code pairs (A_4B_4, A_2B_2, A_3B_3 and A_6B_6) of the orthogonal subset were employed in this test configuration.[3] They are shown in figure 18 as generated binary codes which are utilized to phase modulate the RF carrier. As time coincident biphase modulated codes, they provide the inputs to the correlation detector. Using all the 6 possible different combinations between them, the crosscorrelation function at $\tau=0$ was measured using a calibrated oscilloscope and taking pictures of the integrator output. As was the case for the autocorrelation function tests, pictures were also taken of the phase detector output on a dual beam trace to accurately identify the measurement time or sample point, and a picture of the integrator input is provided to illustrate how the operating functions of the multiplier and summing networks perform. The results are shown in figures 19, 20 and 21. In all cases, the measured crosscorrelation value was greater than 60db below the peak output level of the desired signal. A more sensitive scale than that used for the pictures was necessary in making the actual measurement as a result of achieving almost totally orthogonal operation. An interference attenuation of 60db corresponds to a voltage ratio of 1000/1 or a power ration of 10^6/1. These results are very impressive and demonstrate that the orthogonal code subclasses should perform very well in switching and/or orthogonal multiple-access applications.

(4) Multiplexed Noise Code Spectrum

A photograph was taken of the spectrum for code pairs A_3B_3, A_4B_4, and A_6B_6 using an AIL Model 707 Spectrum Analyzer. The results are shown in figures 22 and 23 where it can be seen that in all cases the spectrum is spread from the information bandwidth of 31.2KHz ($10^6 \div 32$) to 1MHz. In addition, the envelope of the spectrum possesses lobes that correspond to a sinx/x function as it should. An expanded scale (3MHz/div) was used to obtain the spectrum for code pair A_6B_6 (in addition to the normal scale of 1MHz/div) to show the far out frequency domain sidelobes. Since the spectrum does indeed spread by a factor of 32 for the multiplexed noise codes, then an A/J protection ration of 64 (32 for each code of the pair) would be realized against any form of jamming or interference signal structure. This is confirmed in a C.W. interference test (paragraph 4b(6)) that was also performed as part of the research program.

(5) Multiple-Access Tests

. Orthogonal TDMA Concept

Since multiplexed noise codes compress to a lobeless impulse, they can be utilized to provide orthogonal (zero-self-interference) operation in a TDMA multiple-access system. The performance that can be obtained depends directly on how low or how close to zero the autocorrelation function sidelobes are for code generators and matched filters that are implemented with practical hardware. The excellent results obtained for the autocorrelation function measurements indicate that near orthogonal multiple-access operation should be feasible. To confirm this, several multiple-access system tests were performed with two users simultaneously occupying the same spread spectrum frequency band but different selected time slots.

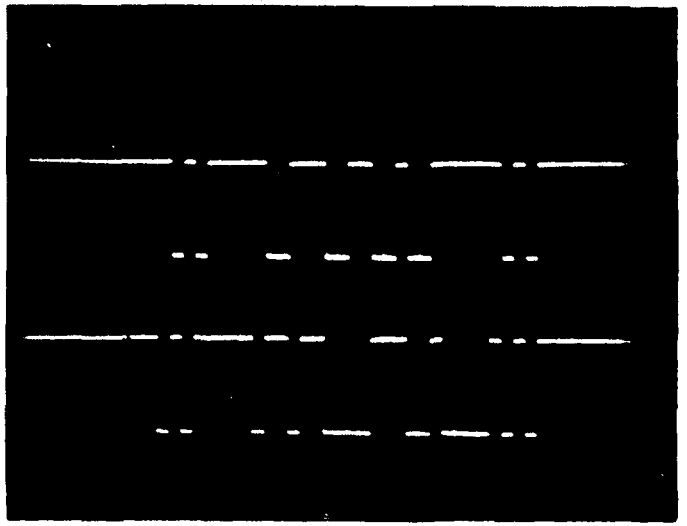

a. CODE A_4 (TOP)
CODE B_4 (BOT)

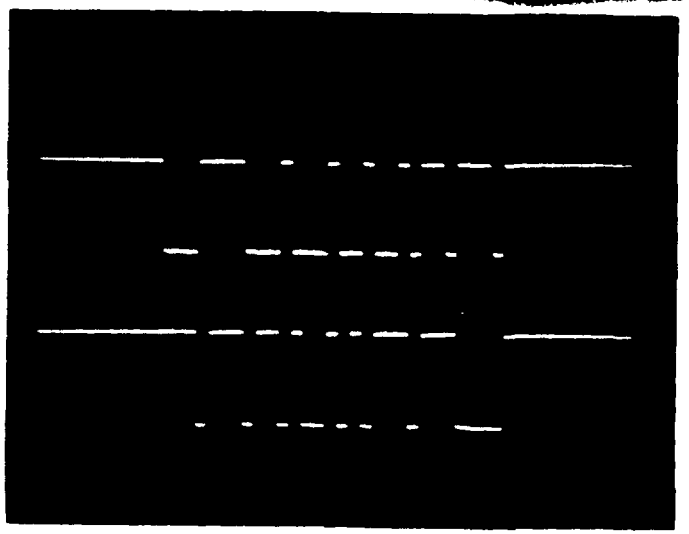

b. CODE A_2 (TOP)
CODE B_2 (BOT)

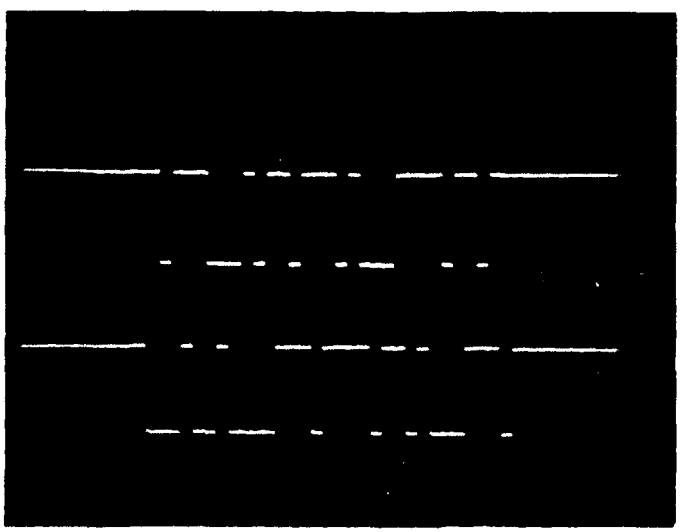

c. CODE A_6 (TOP)
CODE B_6 (BOT)

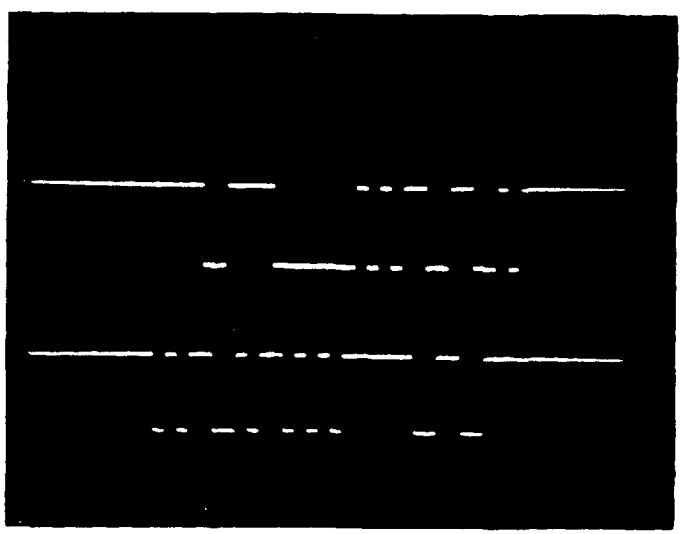

d. CODE A_3 (TOP)
CODE B_3 (BOT)

FIGURE 18 - GENERATED MULTIPLEXED NOISE CODE PAIRS

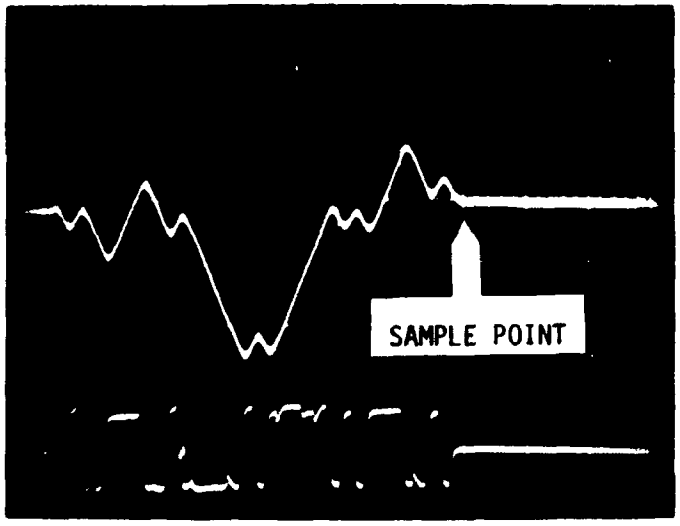

a. INTEGRATOR OUTPUT (TOP)
PHASE DETECTOR OUTPUT OF CODE A (BOT)
X SCALE - 5 us/div
Y SCALE - .5 mv/div(TOP) 50 mv/div(BOT)

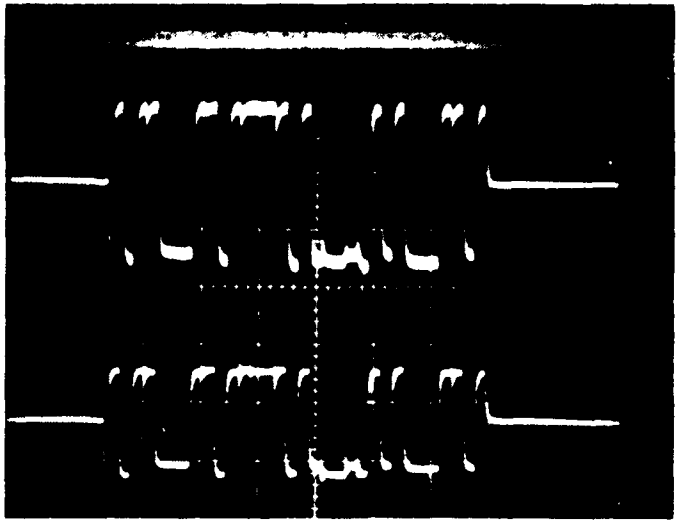

b. INTEGRATOR INPUT (TOP)
PHASE DETECTOR OUTPUT OF CODE A (BOT)
X SCALE - 5 us/div
Y SCALE - 50 mv/div

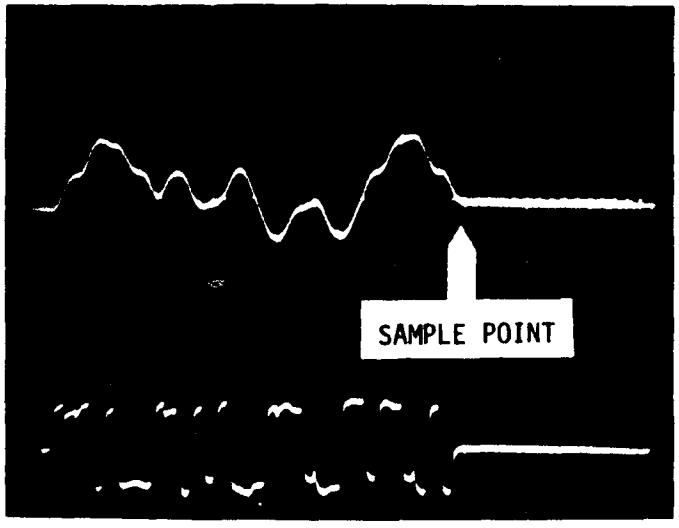

c. INTEGRATOR OUTPUT (TOP)
PHASE DETECTOR OUTPUT OF CODE A(BOT)
X + Y SCALES - SAME AS ABOVE

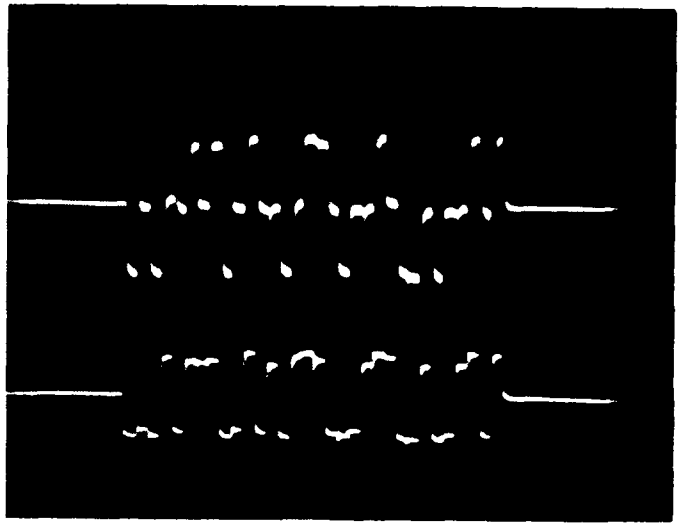

d. INTEGRATOR INPUT (TOP)
PHASE DETECTOR OUTPUT OF CODE A (BOT)
X + Y SCALES - SAME AS ABOVE

FIGURE 19 - CROSSCORRELATION OF A_4 B_4 vs A_2 B_2 (a&b) and A_4 b_4 vs A_6 B_6 (c&d) AT $\tau = 0$

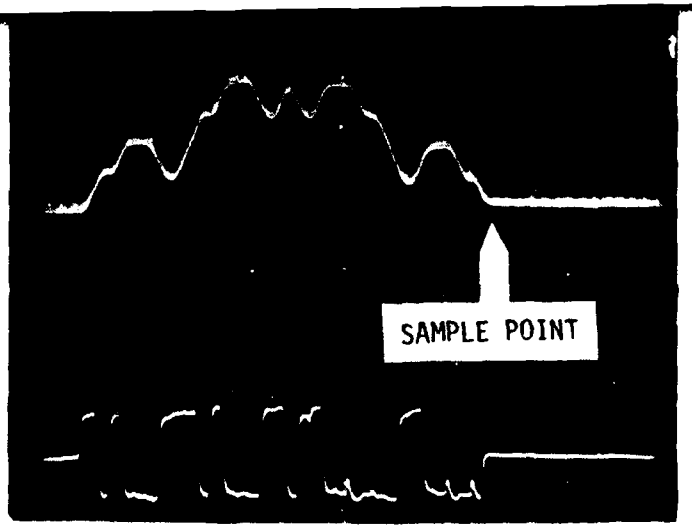

a. INTEGRATOR OUTPUT (TOP)
PHASE DETECTOR OUTPUT OF CODE A (BOT)
X SCALE - 5 us/div
Y SCALE - .5 mv/div(TOP) 50 mv/div(BOT)

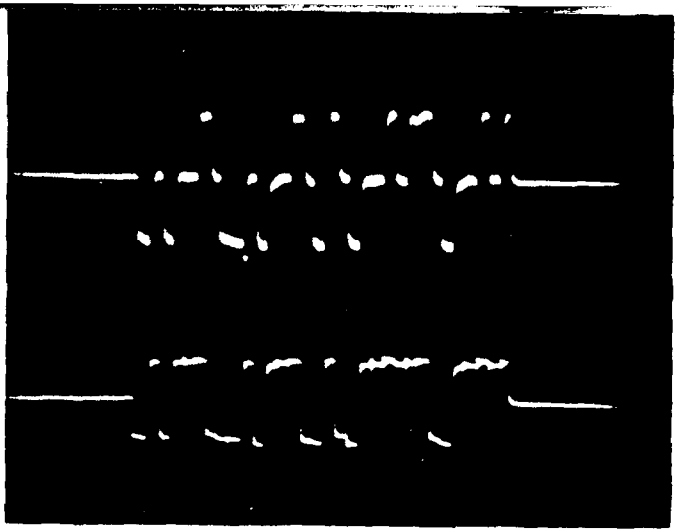

b. INTEGRATOR INPUT (TOP)
PHASE DETECTOR OUTPUT OF CODE A (BOT)
X SCALE - 5 us/div
Y SCALE - 50 mv/div

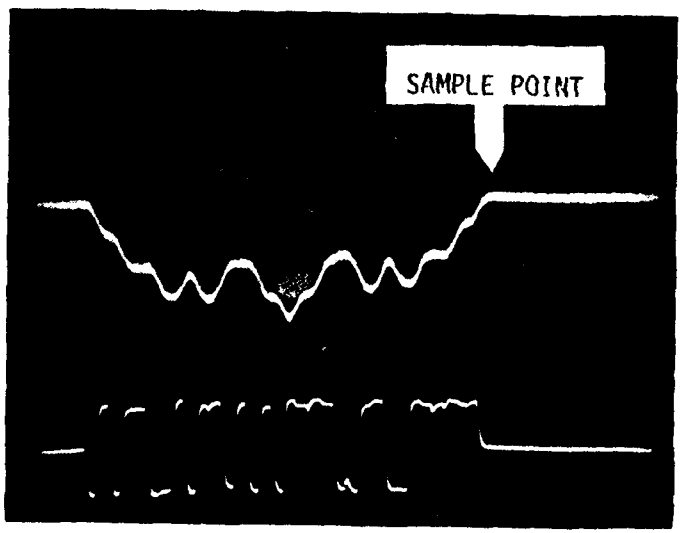

c. INTEGRATOR OUTPUT (TOP)
PHASE DETECTOR OUTPUT OF CODE A(BOT)
X + Y SCALES - SAME AS ABOVE

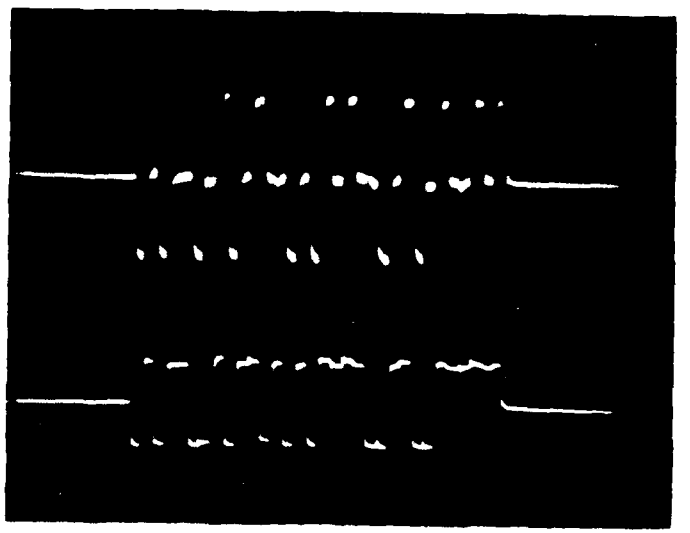

d. INTEGRATOR INPUT (TOP)
PHASE DETECTOR OUTPUT OF CODE A (BOT)
X + Y SCALES - SAME AS ABOVE

FIGURE 20 - CROSSCORRELATION OF A_4 B_4 vs A_3 B_3 (a&b) and A_2 B_2 vs A_6 B_6 (c&d) AT $\tau = 0$

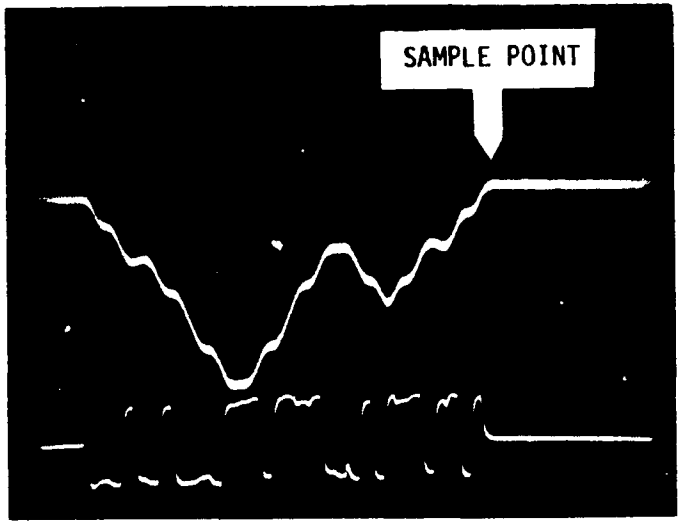

a. INTEGRATOR OUTPUT (TOP)
PHASE DETECTOR OUTPUT OF CODE A (BOT)
X SCALE - 5 us/div
Y SCALE - .5 mv/div(TOP) 50 mv/div(BOT)

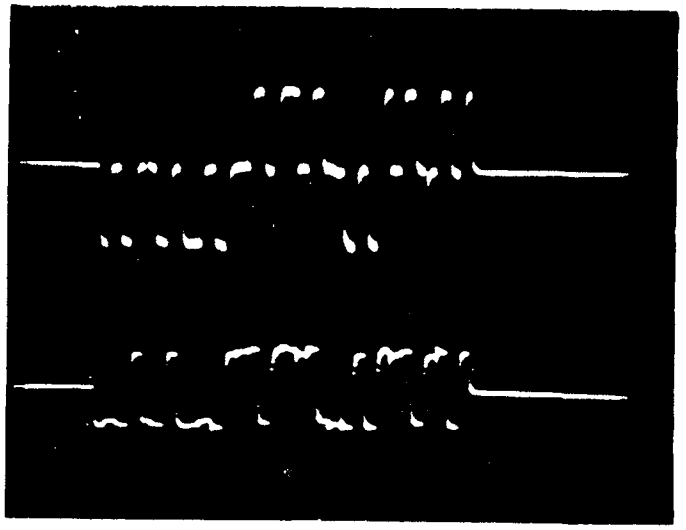

b. INTEGRATOR INPUT (TOP)
PHASE DETECTOR OUTPUT OF CODE A (BOT)
X SCALE - 5 us/div
Y SCALE - 50 mv/div

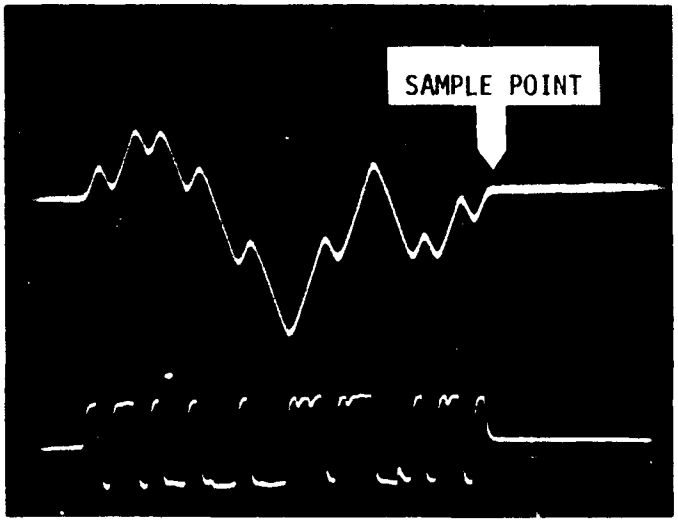

c. INTEGRATOR OUTPUT (TOP)
PHASE DETECTOR OUTPUT OF CODE A(BOT)
X + Y SCALES - SAME AS ABOVE

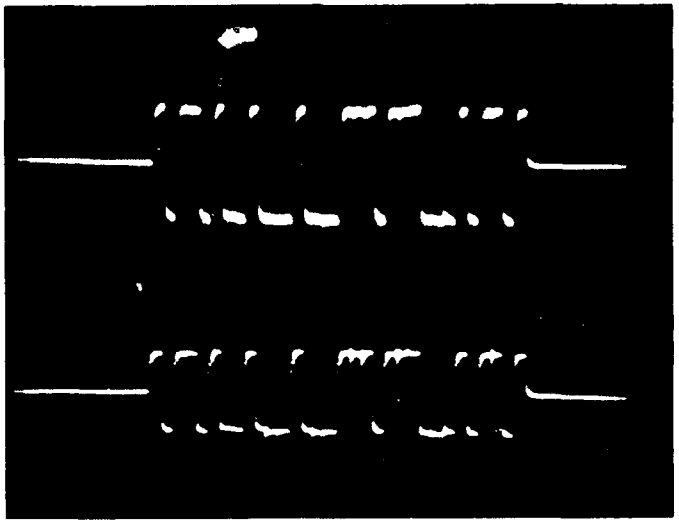

d. INTEGRATOR INPUT (TOP)
PHASE DETECTOR OUTPUT OF CODE A (BOT)
X + Y SCALES - SAME AS ABOVE

FIGURE 21 - CROSSCORRELATION OF A_2 B_2 vs A_3 B_3 (a&b) and A_6 B_6 vs A_3 B_3 (c&d) AT $\tau = 0$

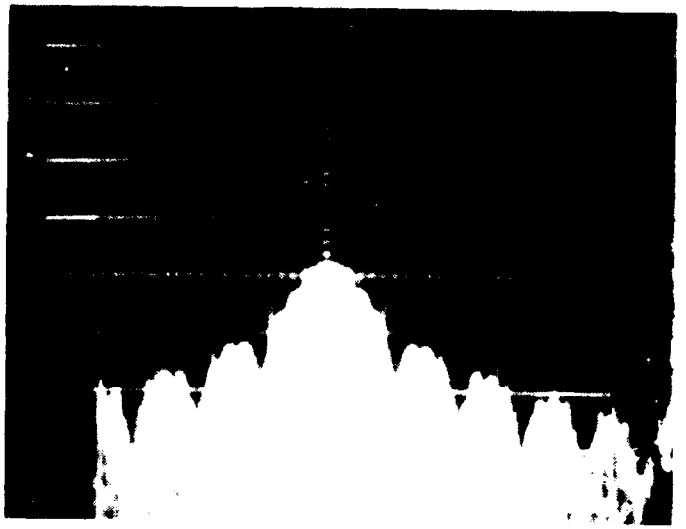

a. Code A_3

X Scale - 1 MHz/div
Y Scale - 10db/div

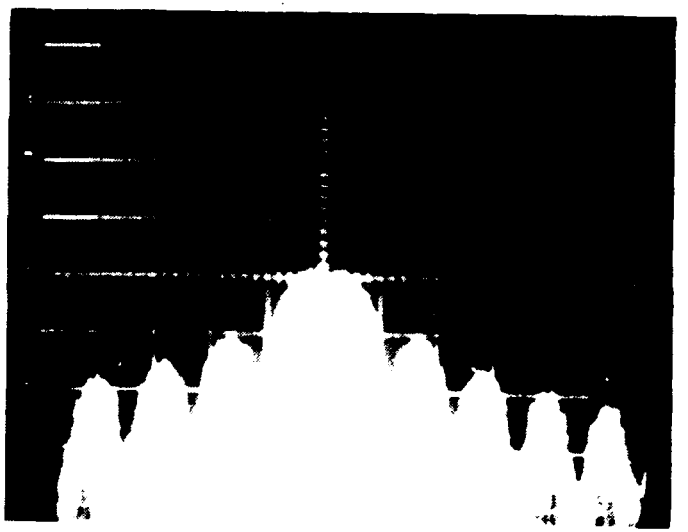

b. Code B_3

X Scale - 1 MHz/div
Y Scale - 10db/div

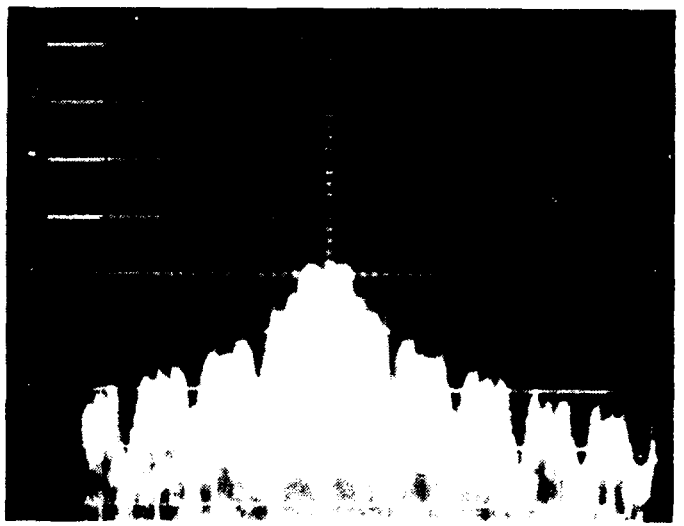

c. Code A_4

X Scale - 1 MHz/div
Y Scale - 10db/div

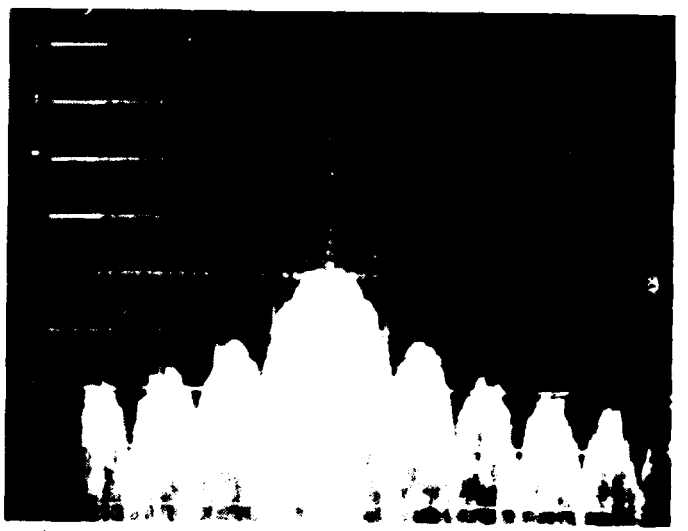

d. Code B_4

X Scale - 1 MHz/div
Y Scale - 10db/div

FIGURE 22 - MULTIPLEXED NOISE CODE SPECTRUM

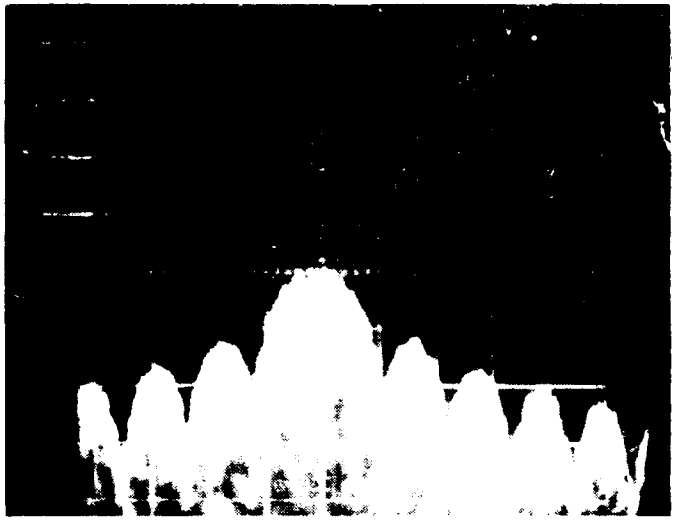

a. Code A_6

X Scale - 1 MHz/div
Y Scale - 10db/div

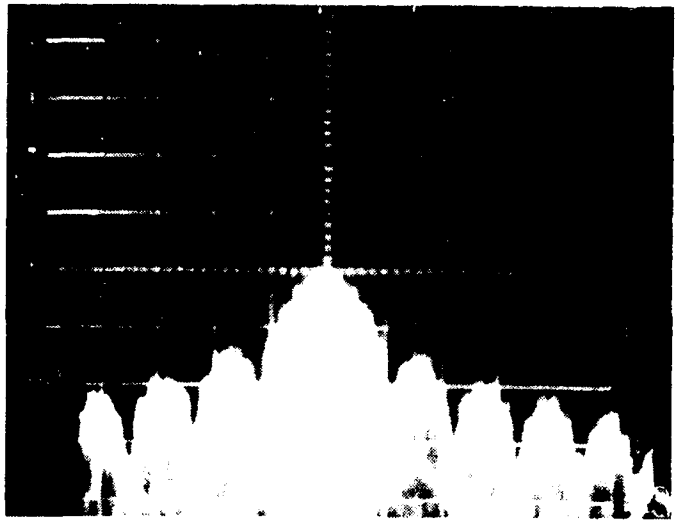

b. Code B_6

X Scale - 1 MHz/div
Y Scale - 10db/div

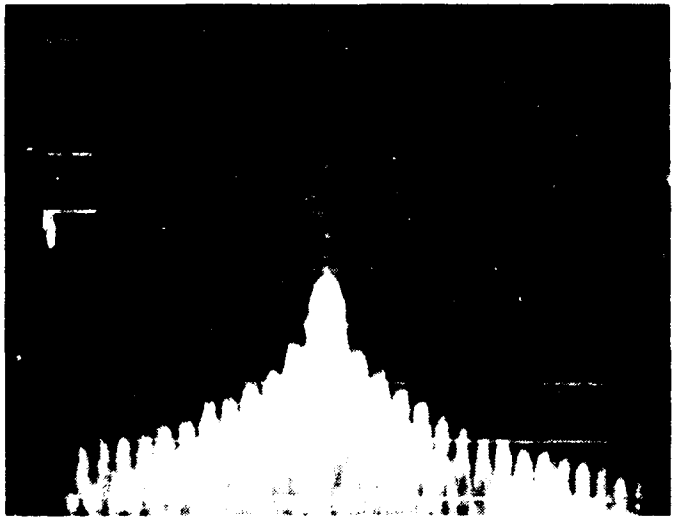

c. Code A_6

X Scale - 3 MHz/div
Y Scale - 10db/div

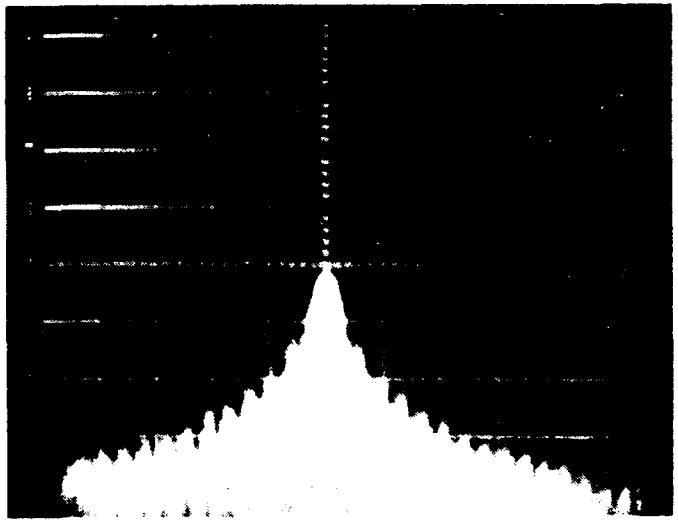

d. Code B_6

X Scale - 3 MHz/div
Y Scale - 10db/div

FIGURE 23 - MULTIPLEXED NOISE CODE SPECTRUM

A detailed description of a spread spectrum orthogonal TDMA multiple-access system concept is contained in Appendix C. Basically, each user has his associated time slot established and maintained synchronous at a common central station or node where the time slots could be either pre-assigned or adaptively selected. Non-interference between users then results since each users spread spectrum signal correlates to zero by all of the remaining users in the system. For system test demonstration purposes, system synchronization will be assumed (different simultaneous users will be timed or slaved to each other using a common clock).

The functional TDMA system described in Appendix C was configured as shown in figure 24 where the buffers and variable attenuators simulate the propagation path loss and facilitated adjusting the relative signal levels between the two user signals at various different values. The remaining functional blocks are the same as those employed for the autocorrelation and crosscorrelation function measurements.

The hardware test setup used for the correlation function tests was reconfigured to conform to the functional test diagram illustrated in figure 24. Measurements of the detected signal plus a second interfering user were then made at the integrator output using a calibrated oscilloscope. The integrator input was photographed simultaneously with the integrator output using a dual beam trace to locate the sample point and illustrate how the operating functions of the multiplier and summing networks perform in the presence of a desired plus interfering signal. In addition, the interference-plus-signal and the signal alone were photographed at the phase detector input for the various different interference-to-signal levels used in the tests to further illustrate and clarify the system performance obtained in the presence of a strong interfering second user.

The interference free detected signal is shown in figure 25 which integrates to an amplitude of 56mv at the output sample point. The reference amplitude is larger for these tests as a result of receiving an order of mini circuit lab double balanced mixers (used to phase modulate the RF carrier) which have a higher output level than the phase modulators employed for the correlation function tests. With the interfering (2nd user) signal level adjusted to equal that of the desired signal at the input to the phase detector, the level of the desired input signal was attenuated by various amounts to simulate different path losses for the tests. Recorded measurements were made at interference-to-signal levels of 30, 40, and 46db for values of τ equal to 5, -1, 11, 20 and 8. In addition, the integrator output and input where photographed with the desired signal removed to verify that the measured output levels are due completely to the presence of the desired signal. The results are shown in figures 26 through 34. In all cases, the interfering signal was essentially completely rejected as can be seen in the photos corresponding to S=0 and solid detection was obtained at every level of interference. A double exposure was taken in the photos of the integrator output where the second exposure was made with the input to the scope removed to accent the zero volt baseline. The detected output of the system corresponds to the amplitude difference of the two exposures at the sample point. Although they were not recorded, similar results were obtained for tests made using the other available time slots.

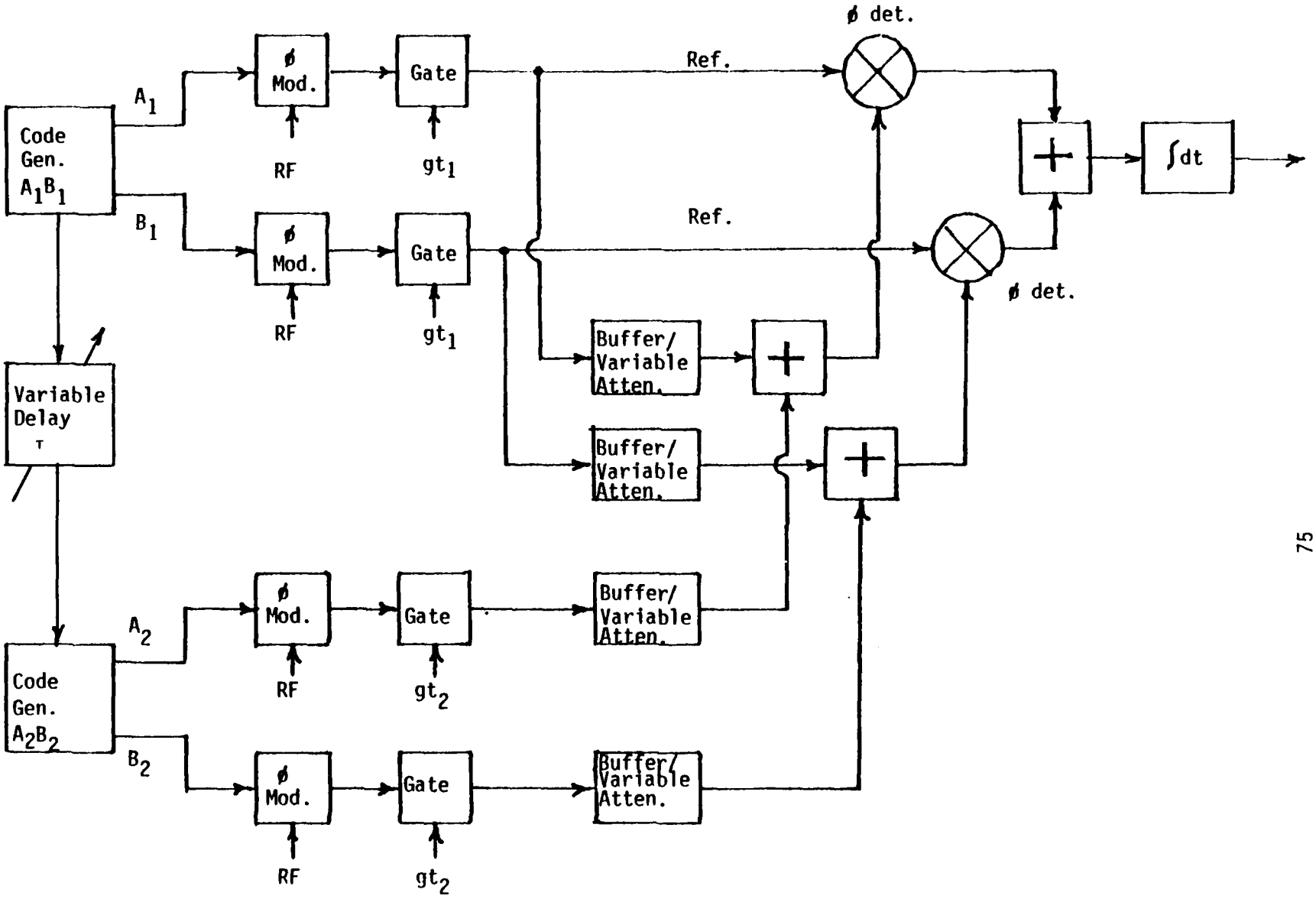

FIGURE 24 - MULTIPLE ACCESS TEST CONFIGURATION (2 USERS)

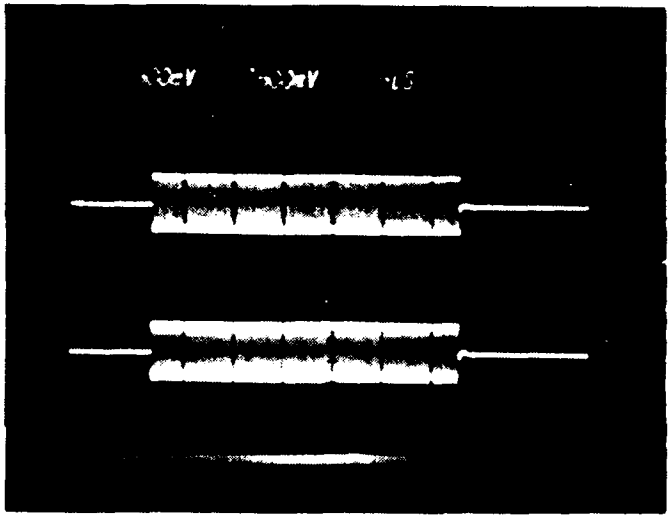

a. Channel a Signal Only (Top)
Channel b Signal Only (Bot)

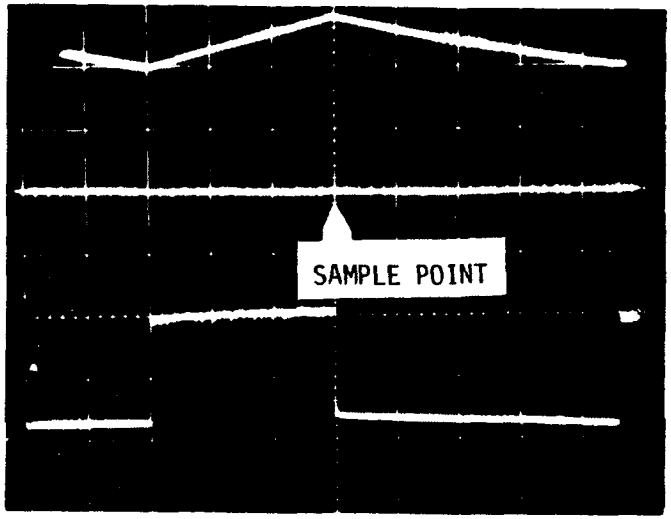

b. Integrator Output (Top) No Interference
Integrator Input (Bot)
X scale - 10 μs/div
Y scale - 20mv/div (Top) 50 mv/div(Bot)

FIGURE 25 - SIGNAL PLUS INTERFERENCE (2nd USER) PERFORMANCE

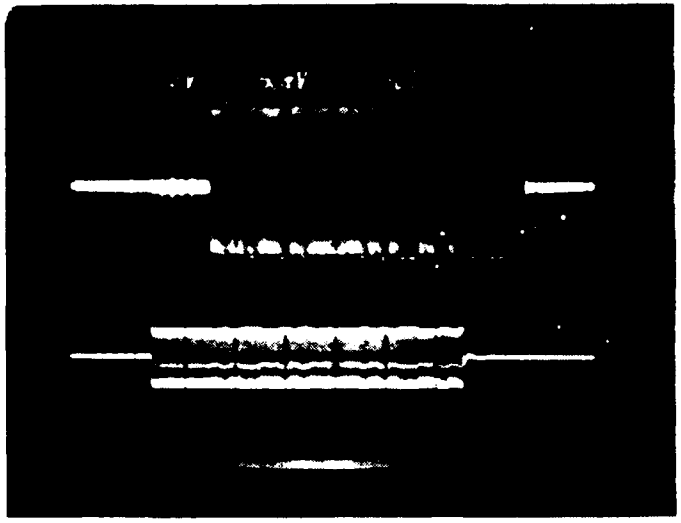

a. Interference + Signal (Top) I/S = 30db
Signal Only (Bot.)

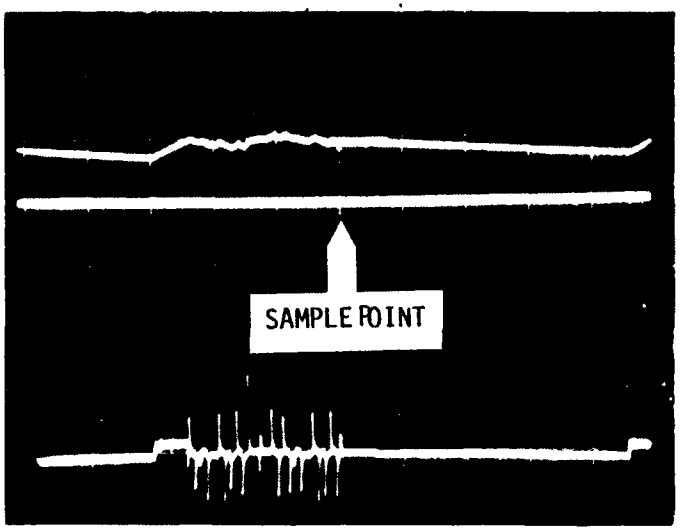

b. Integrator Output (Top) I/S = 30db
Integrator Input (Bot)
X scale - 10μs/div
Y scale - 2mv/div (Top) 50 mv/div (Bot)

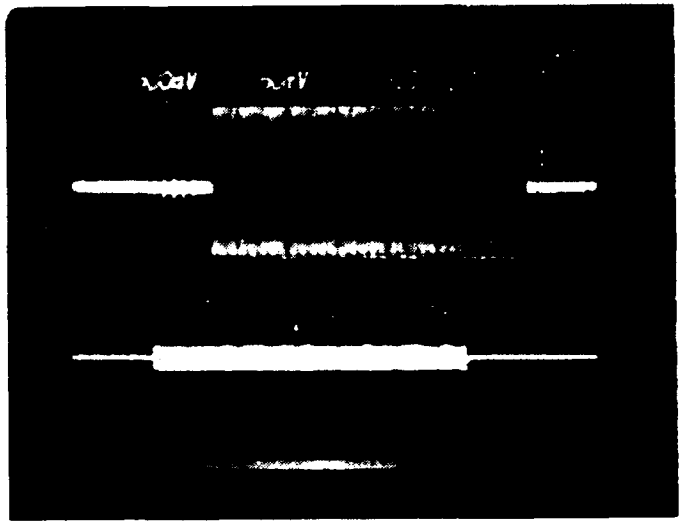

c. Interference + Signal (Top) I/S=40db
Signal Only(Bot)

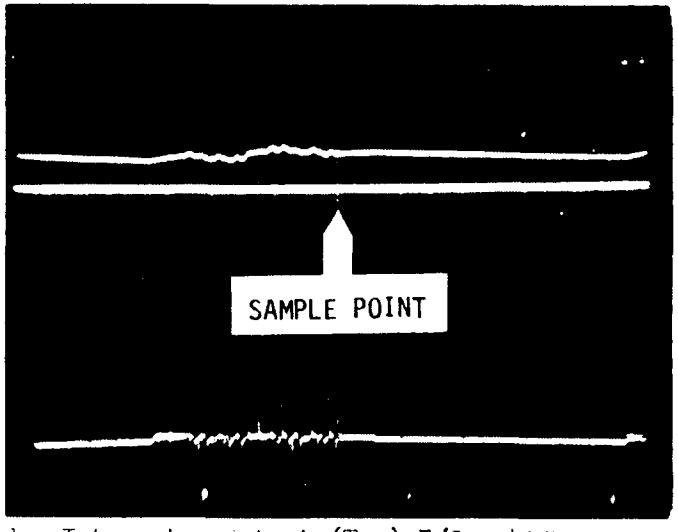

d. Integrator Output (Top) I/S = 40db
Integrator Input (Bot)
X scale - 10μs/div
Y scale - 2 mv/div (Top) 50 mv/div(Bot)

FIGURE 26 - SIGNAL PLUS INTERFERENCE (2nd ORDER) PERFORMANCE $\tau = 5$

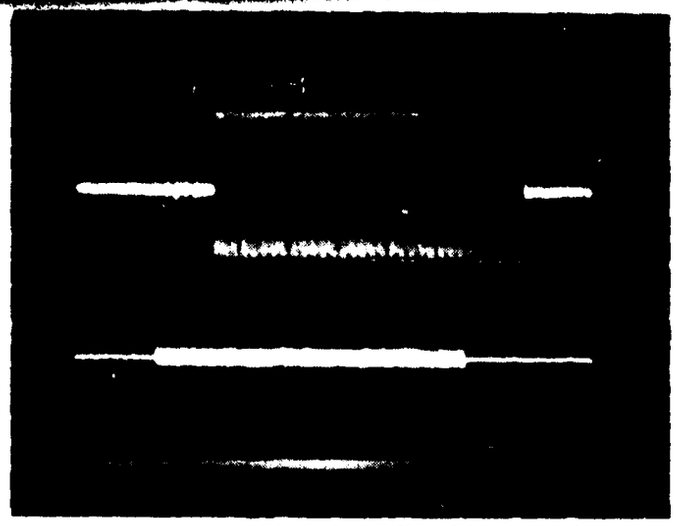

a. Interference + Signal (Top) I/S =46db
Signal Only (Bot)

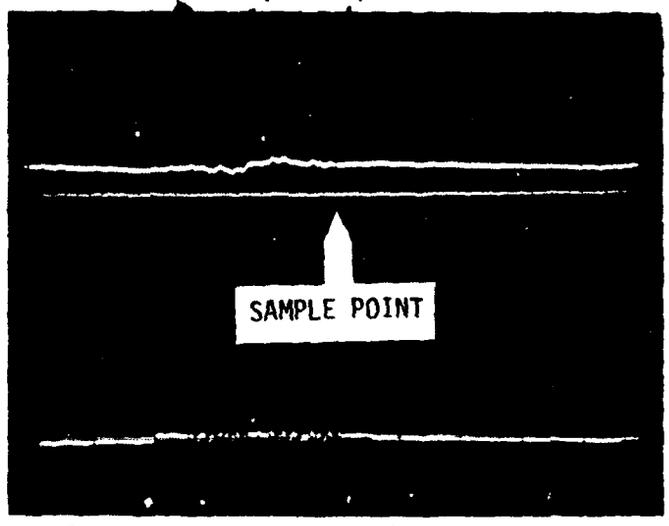

b. Integrator Output (Top) I/S = 46db
Integrator Input (Bot)
X scale - 10 μs/div
Y scale - 2mv/div (Top) 50mv/div (Bot)

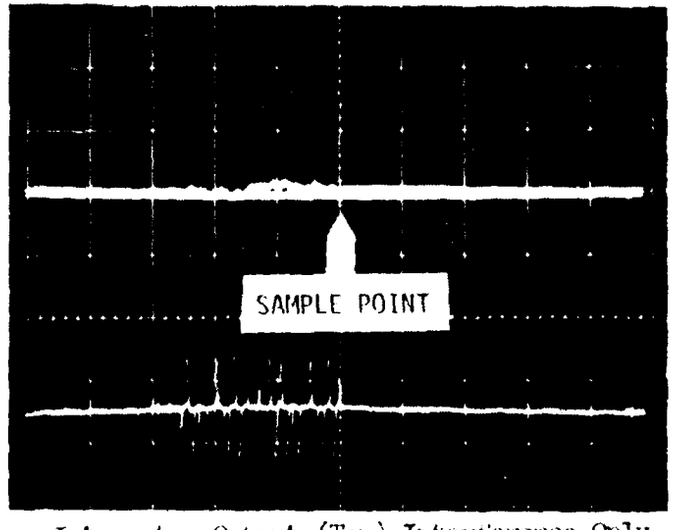

c. Integrator Output (Top) Interference Only
Integrator Input (Bot) Interference Only
X scale - 10 μs/div
Y scale - 2mv/div (Top) 50mv/div(Bot)

FIGURE 27 - SIGNAL PLUS INTERFERENCE (2nd USER) PERFORMANCE $\gamma = 5$

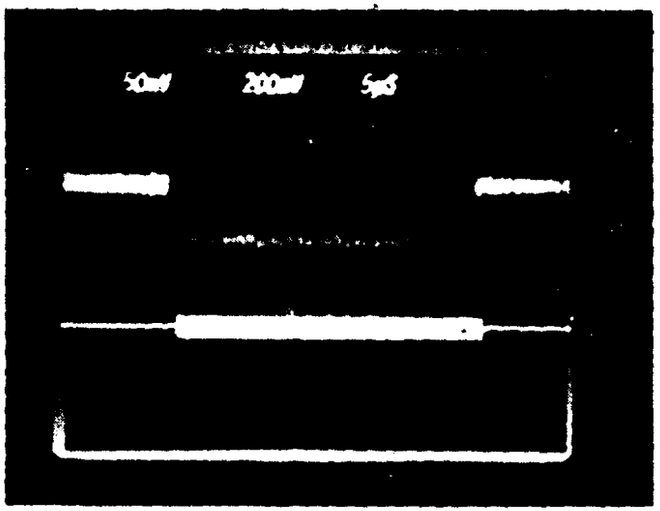

a. Interference + Signal (Top) I/S=30db
Signal Only (Bot)

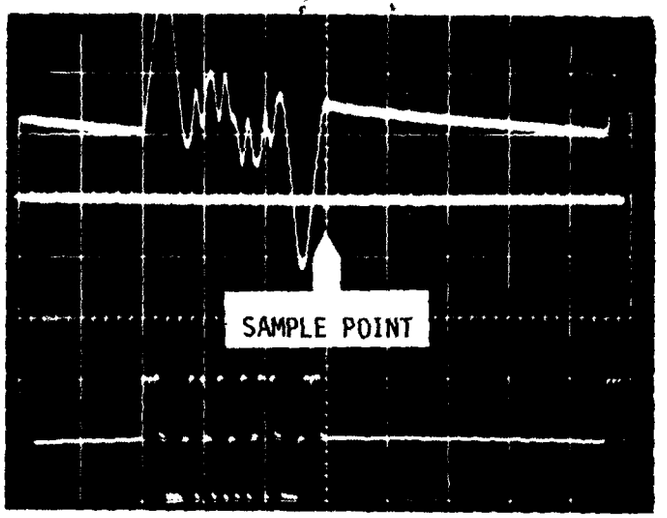

b. Integrator Output (Top) I/S = 30db
Integrator Input (Bot)
X scale - 10μs/div
Y scale - 1mv/div(Top) .1v/div(Bot)

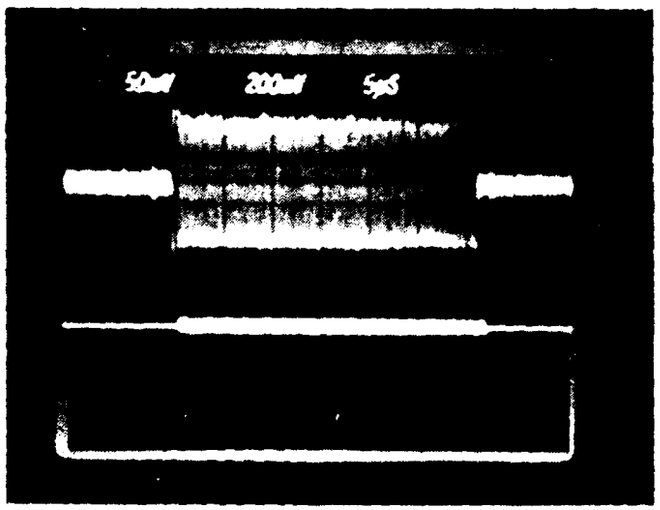

c. Interference + Signal (Top) I/S =40db
Signal Only (Bot)

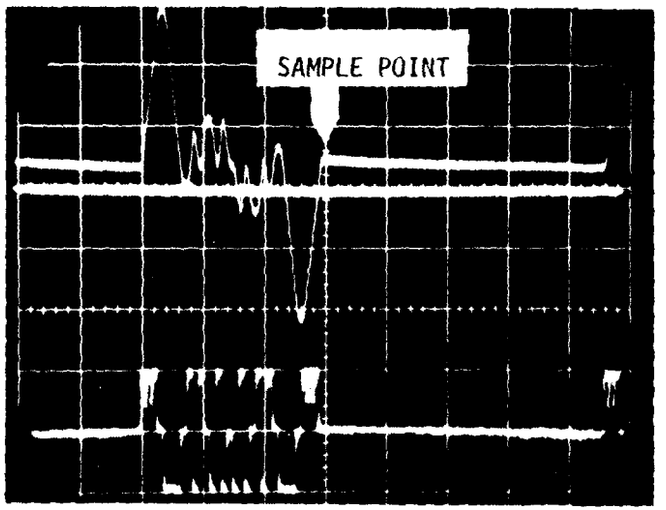

d. Integrator Ouput (Top) I/S = 40db
Integrator Input (Bot)
X scale - 10μs/div
Y scale - 1mv/div(Top) .1v/div(Bot)

Figure 28 - Signal Plus Interference (2nd User) Performance - $\tau = -1$

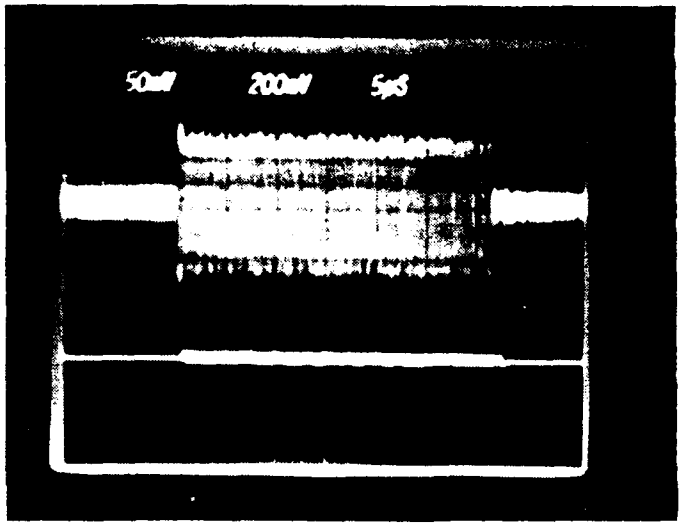

a. Interference + Signal (Top) I/S=46db
Signal Only (Bot)

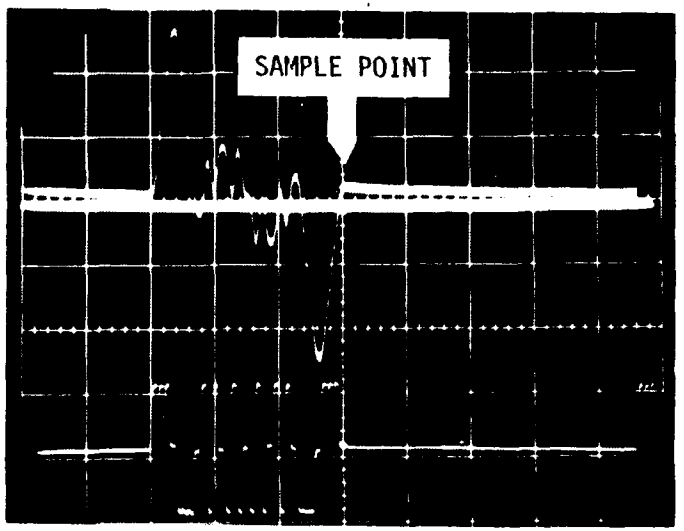

b. Integrator Output (Top) I/S = 46db
Integrator Input (Bottom)
X scale - 10μs/div
Y scale - 1mv/div(Top) .1v/div(Bot)

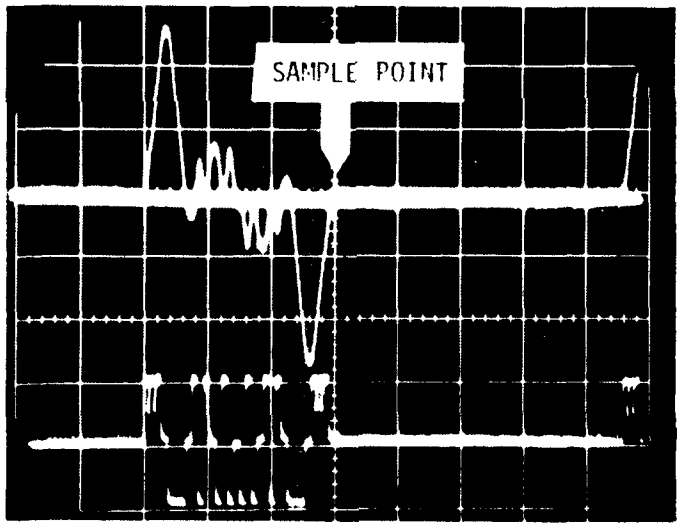

c. Integrator Output(Top)Interference Only
Integrator Input(Bot) Interference Only
X scale - 10 μs/div
Y scale - 1mv/div(Top) .1mv/div(Bot)

Figure 29 - Signal Plus Interference (2nd User) Performance - $\tau = 1$

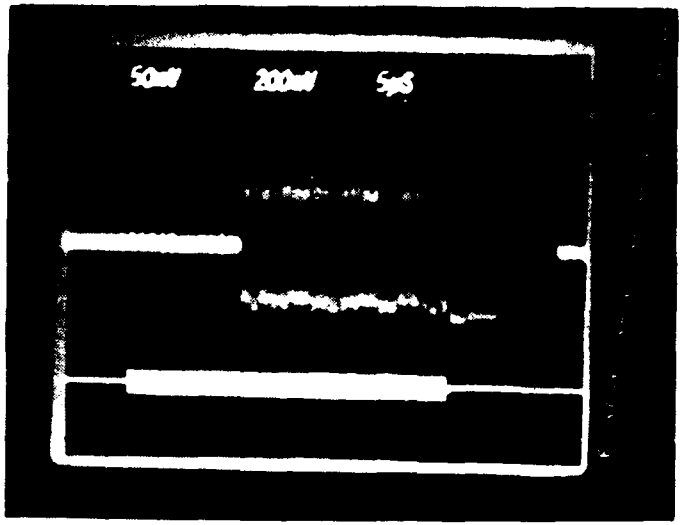

a. Interference + Signal (Top) I/S = 30db
Signal Only (Bot)

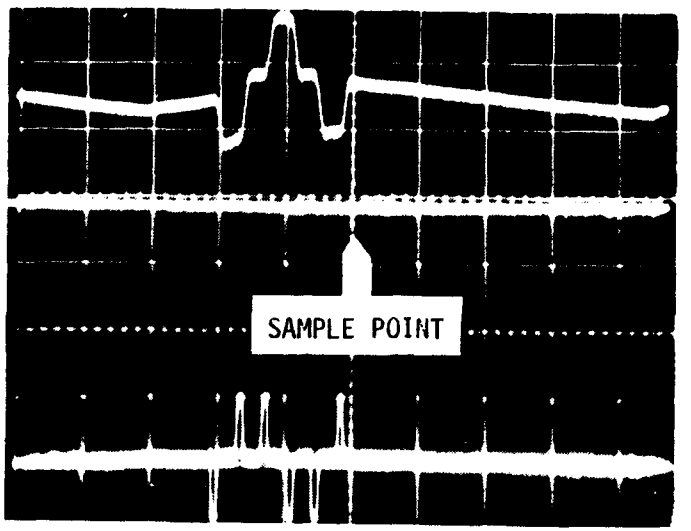

b. Integrator Output (Top) I/S = 30db
Integrator Input (Bot)
X scale - 10μs/div
Y scale - 1mv/div(Top) .1v/div(Bot)

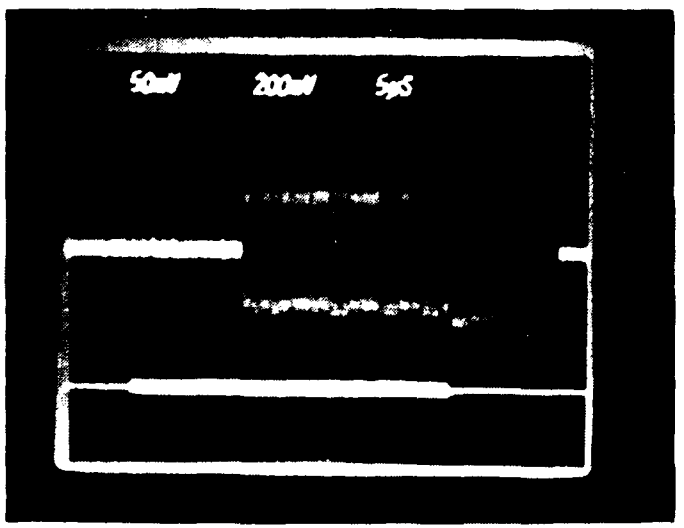

c. Interference + Signal (Top) I/S = 40db
Signal Only (Bot)

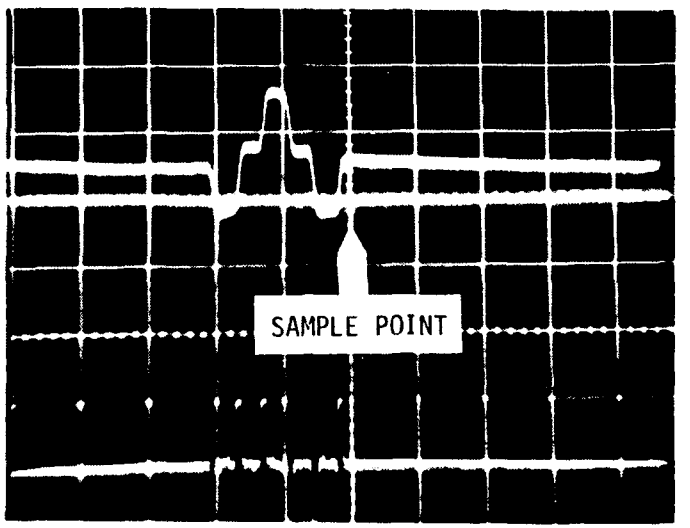

d. Integrator Output (Top) I/S = 40db
Integrator Input (Bot)
X scale - 10μs/div
Y scale - 1mv/div(Top) .1v/div(Bot)

Figure 30 - Signal Plus Interference (2nd User) Performance τ=11

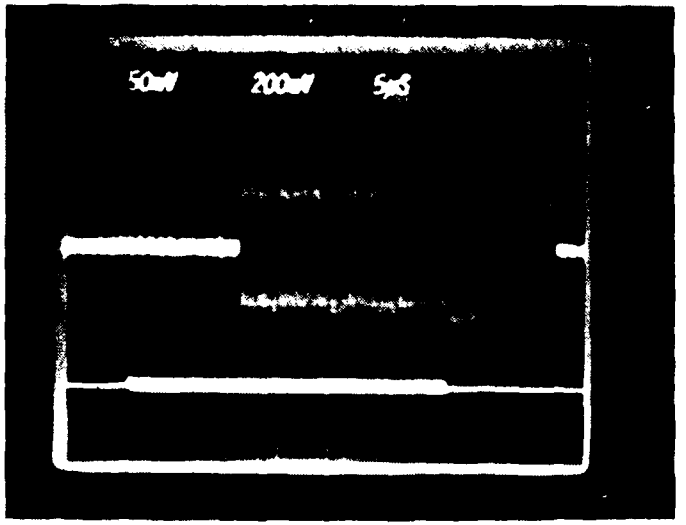

a. Interference Plus Signal (Top) I/S=46db
Signal Only (Bot)

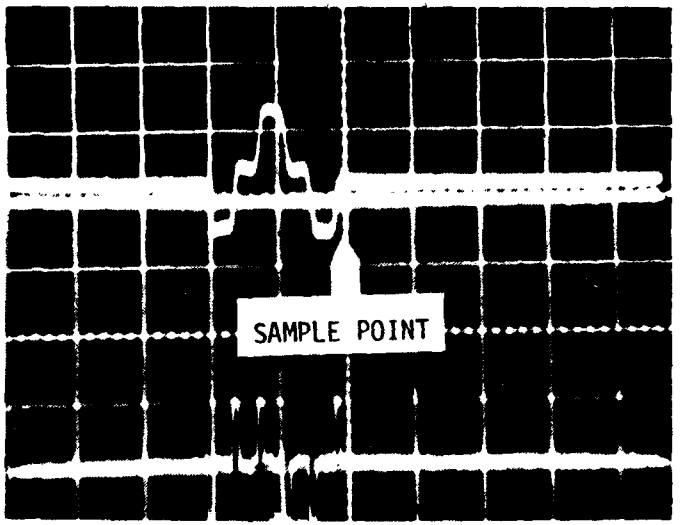

b. Integrator Output (Top) I/S = 46db
Integrator Input (Bot)
X scale - 10μs/div
Y scale - 1mv/div(Top) .1v/div(Bot)

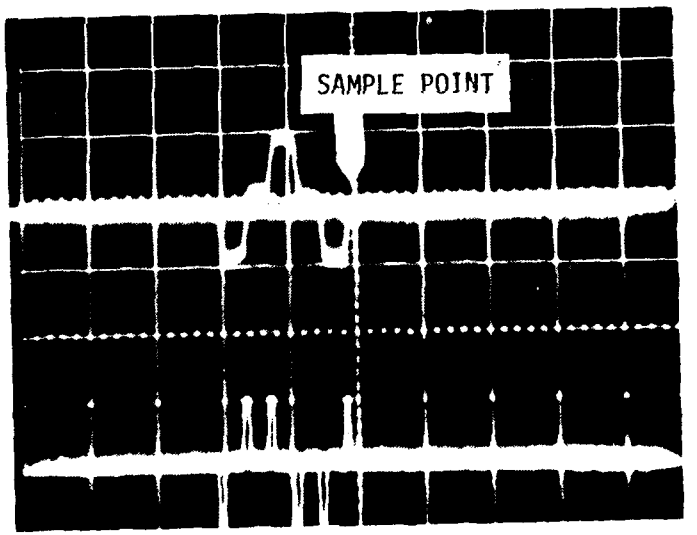

c. Integrator Output (Top) S = 0
Integrator Input (Bot)
X scale - 10μs/div
Y scale - 1mv/div(Top) .1v/div(Bot)

Figure 31 - Signal Plus Interference (2nd User) Performance τ=11

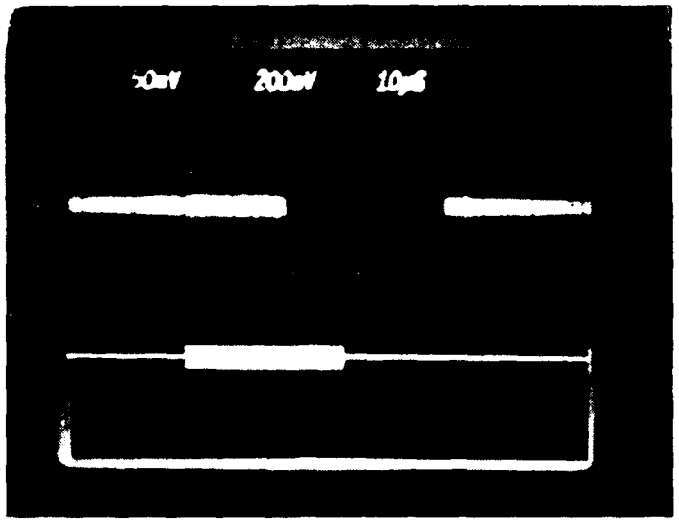

a. Interference + Signal (Top) I/S =30db
Signal Only (Bottom)

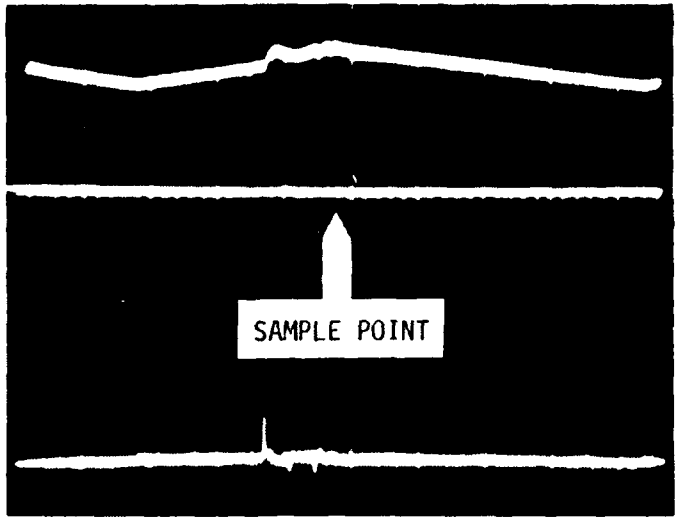

b. Integrator Output (Top) I/S = 30db
Integrator Input (Bot)
X scale - 10μs/div
Y scale - 1mv/div(Top) .1v/div(Bot)

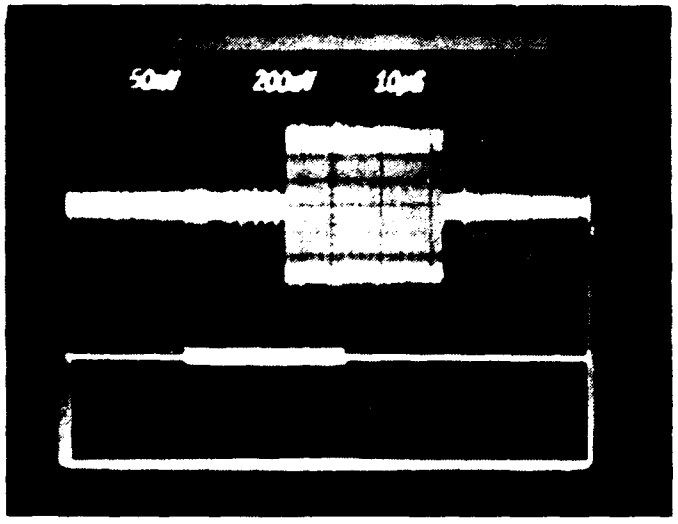

c. Interference + Signal (Top) I/S = 40db
Signal Only (Bot)

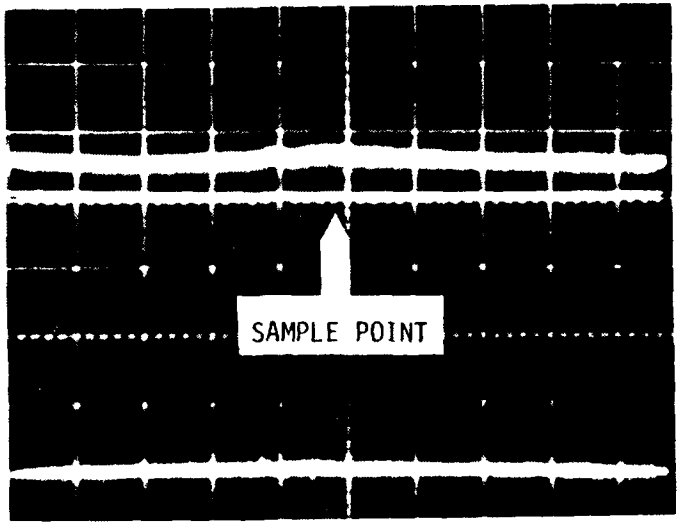

d. Integrator Output (Top) I/S = 40db
Integrator Input (Bot)
X scale - 10μs/div
Y scale - 1mv/div(Top) .1v/div(Bot)

Figure 32 - Signal Plus Interference (and User) Performance τ=20

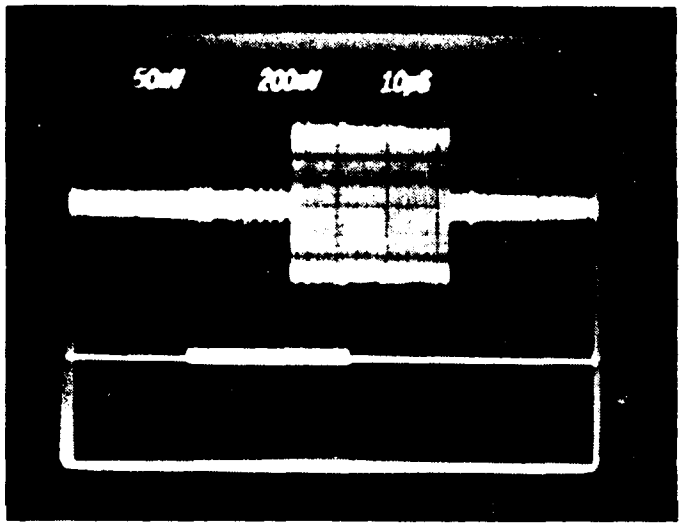

a. Interference + Signal (Top) I/S =46db
Signal Only (Bot)

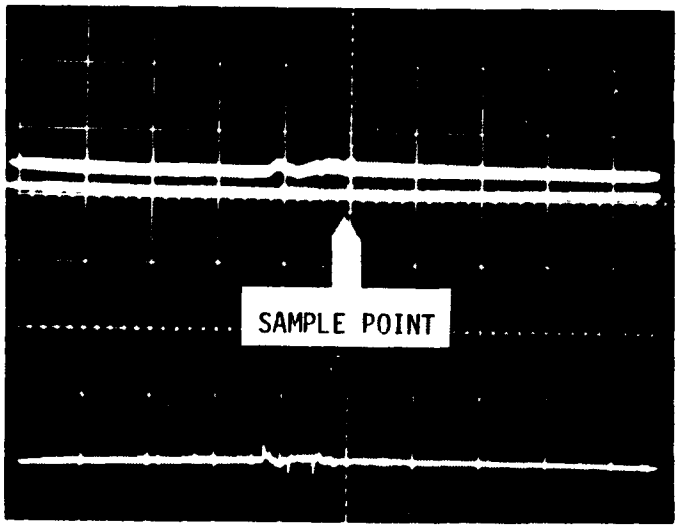

b. Integrator Output (Top) I/S = 46db
Integrator Input (Bot)
X scale - 10μs/div
Y scale - 1mv/div(Top) .1v/div(Bot)

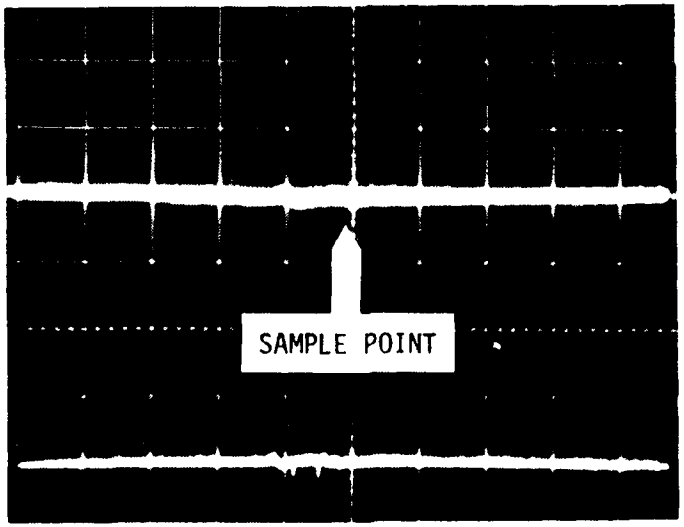

c. Integrator Output (Top) S = 0
Integrator Input (Bot)
X scale - 10μs/div
Y scale - 1mv/div(Top) .1v/div(Bot)

Figure 33 - Signal Plus Interference (2nd User) Performance τ=20

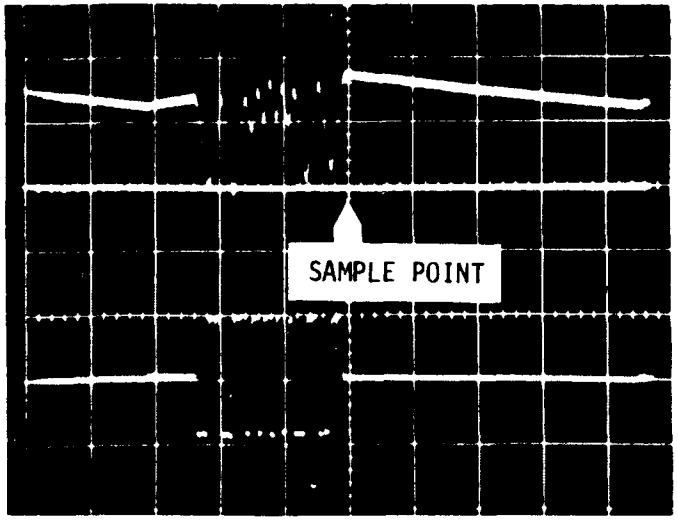

a. Integrator Output (Top) I/S = 30db
Integrator Input (Bot)
X scale - 10μs/div
Y scale - 1mv/div(Top) .1v/div(Bot)

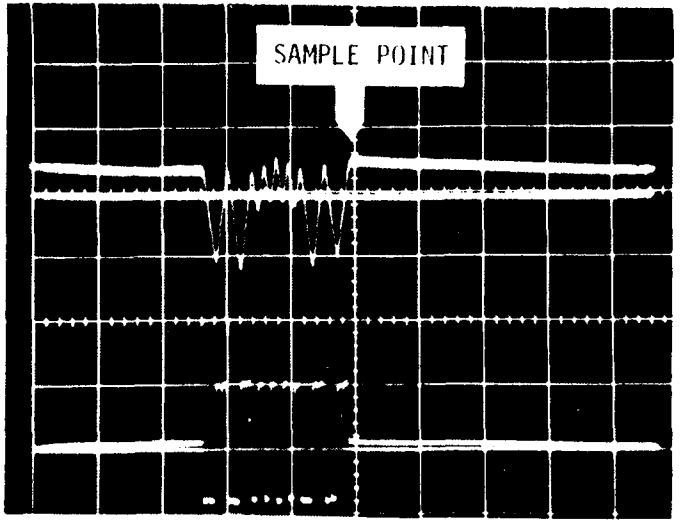

b. Integrator Output (Top) I/S = 40db
Integrator Input (Bot)
X scale - 10μs/div
Y scale - 1mv/div(Top) .1v/div(Bot)

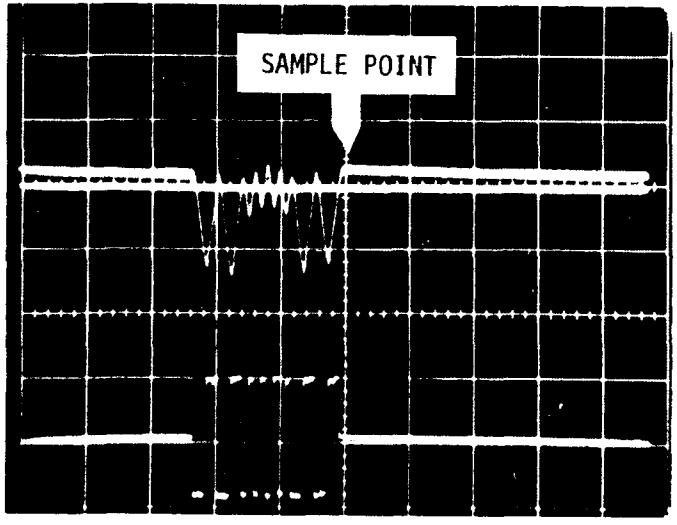

c. Integrator Output (Top) I/S = 46db
Integrator Input (Bot)
X scale - 10μs/div
Y scale - 1mv/div(Top) .1v/div(Bot)

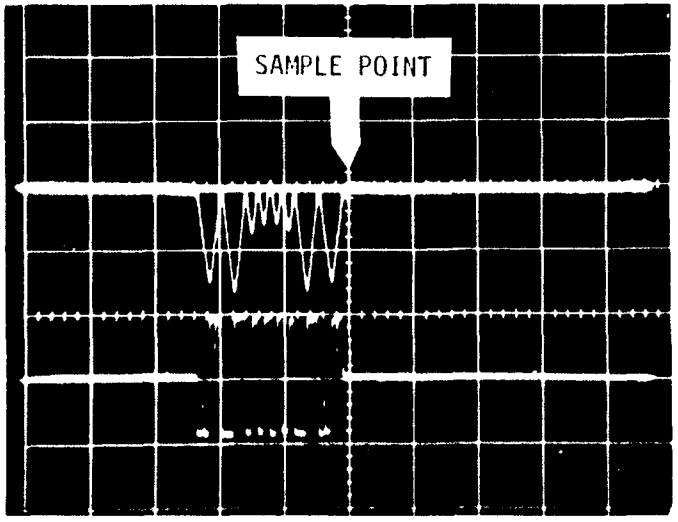

d. Integrator Output (Top) S = 0
Integrator Input (Bot)
X scale - 10μ/div
Y scale - 1mv/div(Top) .1v/div(Bot)

Figure 34 - Signal Plus Interference (2nd User) Performance 1-8

These results demonstrate the feasibility of implementing a spread spectrum (noise coded) orthogonal TDMA multiple user communication system using available hardware. Detecting a desired signal in the presence of a second interfering user operating in the same spread spectrum frequency band that is 46db stronger (which corresponds to receiving an interfering signal whose power level is 40,000 times stronger than the received power of the desired signal) is equivalent to having an interfering source $\sqrt{40000} = 200$ times closer than the transmitter of the desired signal. Hence a potential interferer (2nd user) could be as close as 260 feet away and still not prevent maintaining communications with a desired user that is 10 miles away.

Even better results would be anticipated using the constructed code generators if the subsystem elements available for detection such as the amplifiers and phase detectors had greater dynamic range and more sensitive and stable oscilloscopes and pulse generators were available. An interference rejection capability of 46db is, however, considered very good and will hopefully encourage further development and more elaborate testing of the full orthogonal TDMA potential inherent in multiplexed noise codes. It should be pointed out that there is no counterpart that exists in state-of-the-art technology. Only multiplexed noise codes as a code class are capable of compressing to a lobeless impulse.

Ordered components (power dividers and combiners) were not received in time to enable completing TDMA tests involving 3 or more simultaneous users. These tests, however, are expected to be completed at the Electronic Technology and Devices Laboratory in the future as an in-house research effort.

· Orthogonal CDMA Concept

Orthogonal Code Division Multiple-Access (CDMA) can also be realized for a system which utilizes multiplexed noise codes. Different unique noise codes can be utilized by the users of a multiple-access system without encountering an intolerable amount of self-interference (theoretically there would be zero self-interference or orthogonal operation). This functionally unique concept is possible since code subclasses exist for which the crosscorrelation between any two codes of the subclass is zero at $\tau=0$. Four bit and eight bit orthogonal code subclasses were identified in paragraph 3b(3) of the report. These codes or other established orthogonal subsets such as the group of five codes utilized for this research effort can be used to implement a CDMA system. The excellent results obtained for the crosscorrelation function measurements establish that near orthogonal CDMA operation should also be feasible using practical hardware. To confirm this, several multiple-access system tests were performed using two and three users simultaneously occupying the same frequency band while operating in the same single time slot with each user employing a different code pair of the orthogonal code subset.

AD-A114 033 JOINT TACTICAL COMMUNICATIONS OFFICE FORT MONMOUTH NJ F/G 9/4
MULTIPLEXED NOISE CODES - A UNIQUE CODE CLASS.(U)
APR 82 F S GUTLEBER
UNCLASSIFIED TTO-ENG-002-82 NL

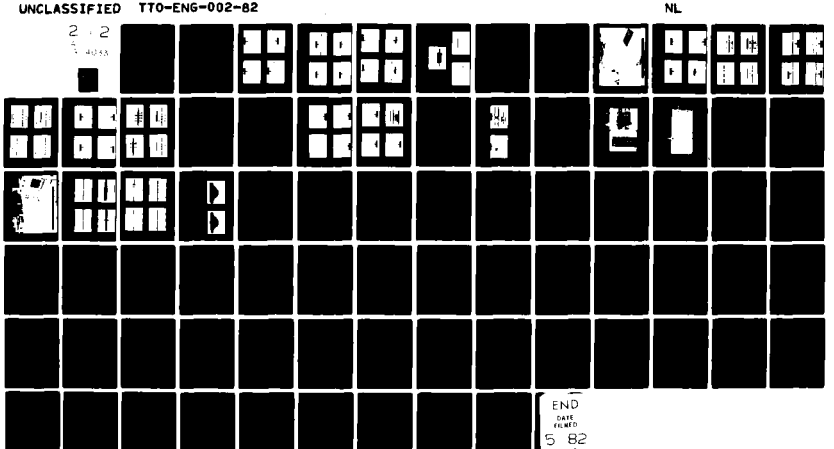

A detailed description of a spread spectrum orthogonal CDMA multiple-access system concept is contained in Appendix D. The system implementation is similar to that used to obtain TDMA with two important fundamental differences. After establishing synchronous timing by having all the users connected via a common central, all of the users adjust their timing to operate in a single common time slot with each user employing a different code. There is no interference between the users since each users spread spectrum code cross-correlates to zero by all of the other users in the system. For test demonstration purposes, system synchronization was assumed and timing was provided using a common clock for the individually generated codes.

The CDMA system described in Appendix D was configured as shown in figure 35 for the tests using 2 users. This is the same as the functional test setup used for the TDMA tests. The only difference is that no delay or time difference (i.e. τ=0) between the users is employed and code generator no. 2 provides a different code than code generator no. 1. As before, the buffers and variable attenuators simulate the propagation path loss and facilitate adjusting the relative signal levels between the two user signals to various different values.

The hardware test setup used for the TDMA tests was reconfigured by simply using different appropriate generated codes for code generators nos. 1 and 2 and setting τ at zero. As was done for the TDMA tests, measurements of the detected desired signal in the presence of a second strong interfering user were made at the integrator output using a calibrated oscilloscope and the intergrator input was photographed simultaneously using a dual beam trace. The integrator input photo is provided to locate the sample point and illustrate how the operating functions of the phase detectors and summing network perform in the presence of a desired plus interfering signal. The interference plus signal and the signal alone were also photographed at the phase detector input to further illustrate and clarify the system performance obtained in the presence of a strong interfering second user.

Tests were made using code pairs A_3B_3, A_4B_4 and A_6B_6. Using each different possible combination of these codes, measurements were made at the integrator output for interference-to-signal levels of 30, 40 and 46db. In addition, the integrator output and input were photographed with the desired signal removed to verify that the interference is essentially eliminated or integrates to zero in the output. Hence, the measured output levels are due completely to the presence of the desired signal. The results are shown in figures 36, 37 and 38 and as for the TDMA tests, the interfering signal is essentially completely rejected and solid detection was obtained in all of the tests performed. As was done for the integrator output measurements made in the TDMA tests, a double exposure was taken where the second exposure was made with the input to the scope removed to accent the zero volt baseline or reference. Figure 39 shows the interference plus signal and signal alone at interfering levels that are 30, 40 and 46db stronger than the desired signal. This was only recorded for the A_4B_4 vs A_3B_3 combination since the result would be the same (in terms of the relative amplitudes) for all the CDMA tests involving 2 users.

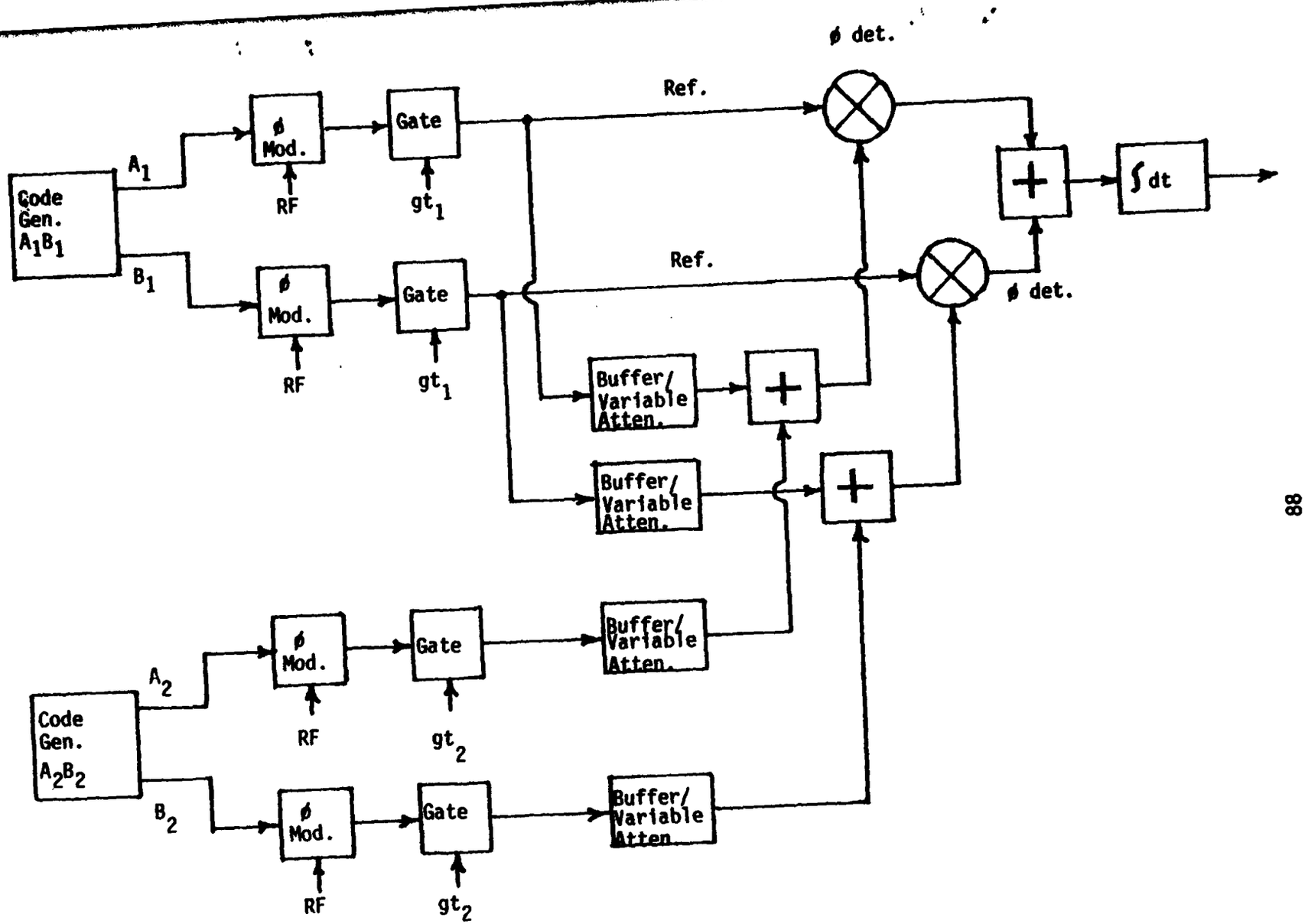

FIGURE 35 - MULTIPLE ACCESS TEST CONFIGURATION (2 USERS)

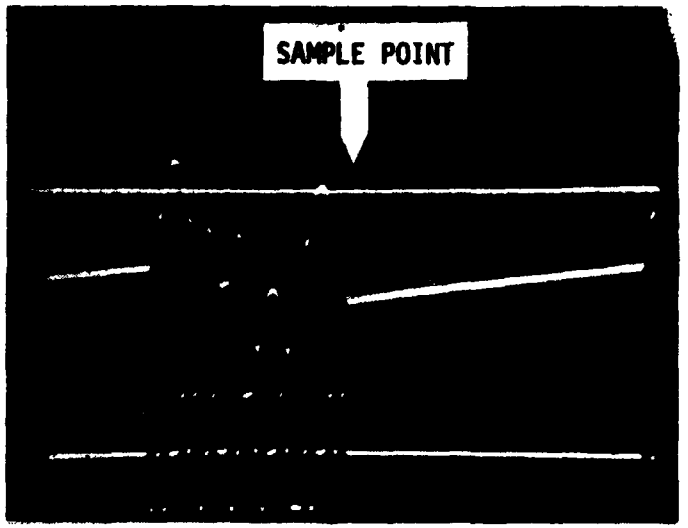

a. Integrator Output (Top)
Integrator Input (Bot) I/S = 30db
X scale - 10μs/div
Y scale - 1mv/div(Top) .1v/div (Bot)

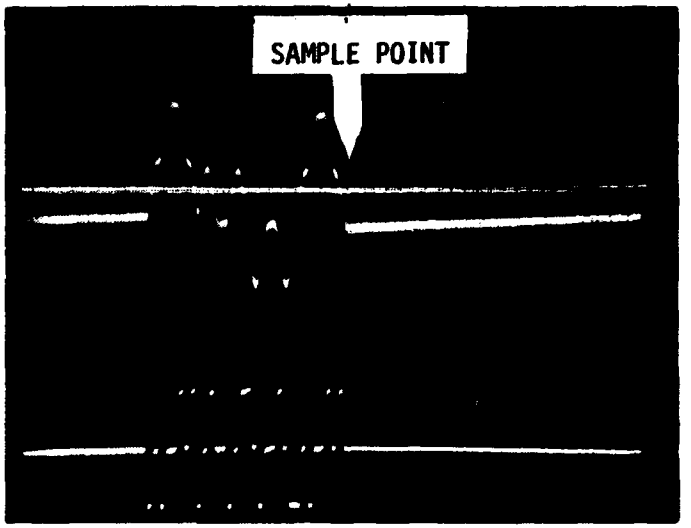

b. Integrator Output (Top)
Integrator Input (Bot) I/S = 40db
X scale - 10μs/div
Y scale - 1mv/div(Top) .1v/div (Bot)

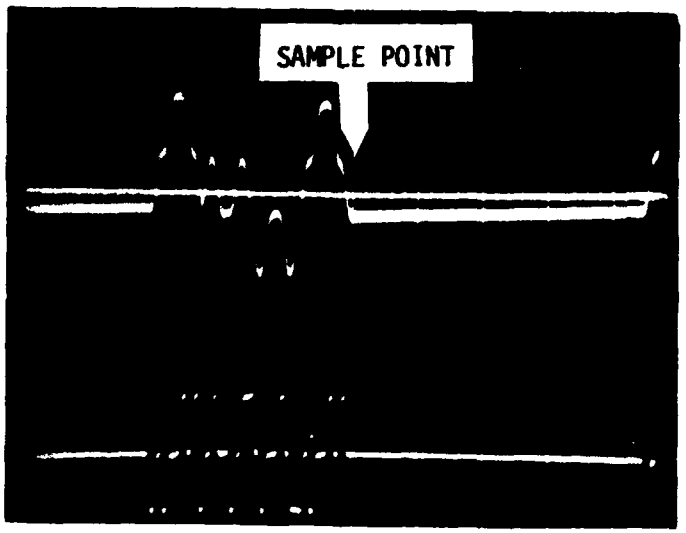

c. Integrator Output (Top)
Integrator Input (Bot) I/S = 46db
X scale - 10μs/div
Y scale - 1mv/div(Top) .1v/div (Bot)

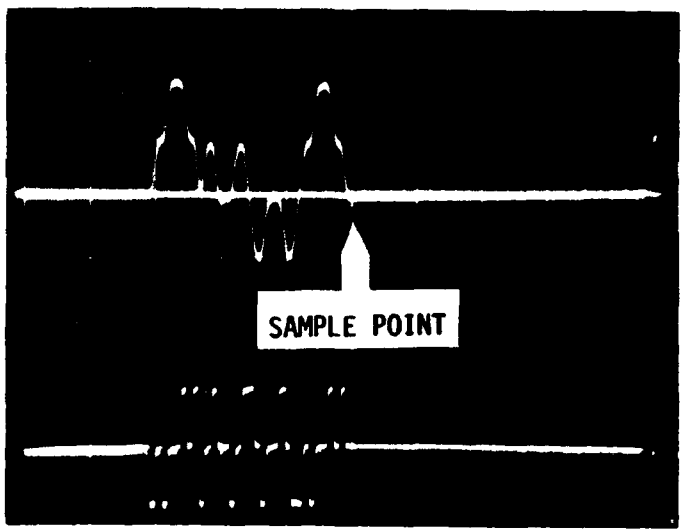

d. Integrator Output (Top)
Integrator Input (Bot) S = 0
X scale - 10μs/div
Y scale - 1mv/div(Top) .1v/div (Bot)

Figure 36 - Signal Plus Interference (2nd User) Performance A_4B_4 vs. A_6 B_6

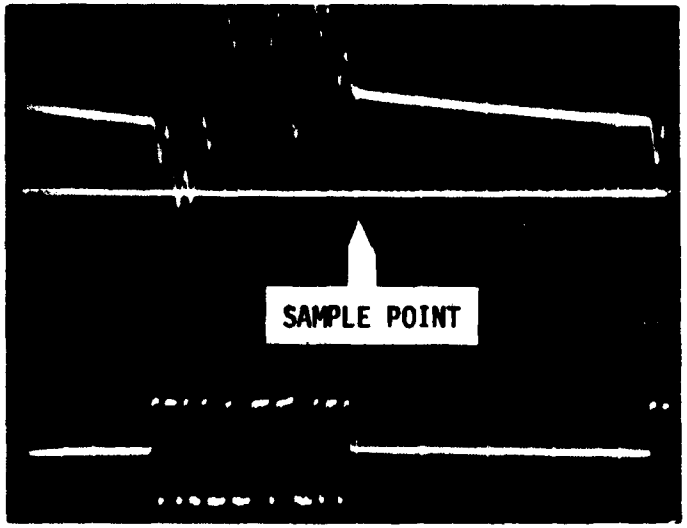

a. Integrator Output (Top)
Integrator Input (Bot) I/S = 30db
X scale - 10μs/div
Y scale - 1mv/div(Top) .1v/div(Bot)

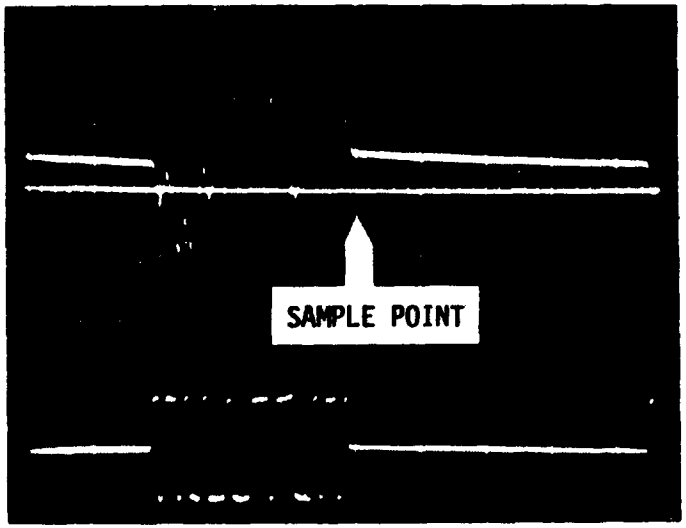

b. Integrator Output (Top)
Integrator Input (Bot) I/S = 40db
X scale - 10μs/div
Y scale - 1mv/div(Top) .1v/div(Bot)

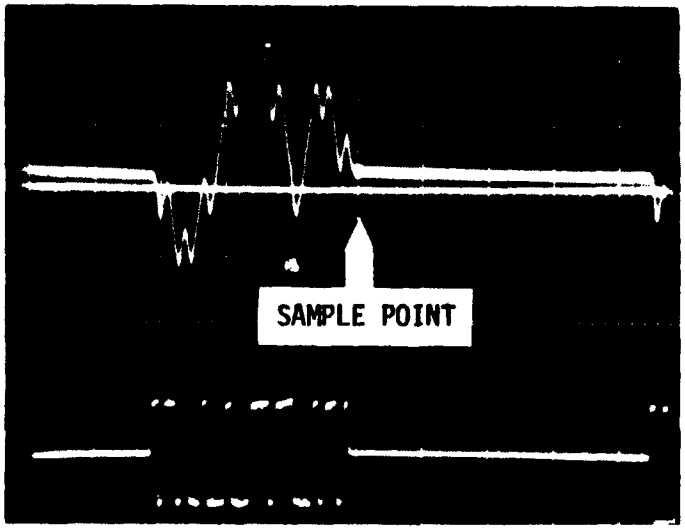

c. Integrator Output (Top)
Integrator Input (Bot) I/S = 46db
X scale - 10μs/div
Y scale - 1mv/div(Top) .1v/div(Bot)

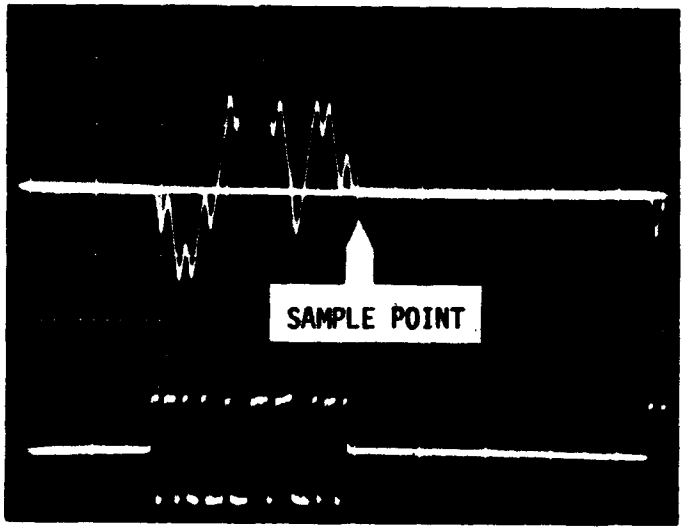

d. Integrator Output (Top)
Integrator Input (Bot) S = 0
X scale - 10μs/div
Y scale - 1mv/div(Top) .1v/div(Bot)

Figure 37 - Signal Plus Interference (2nd User) Performance A_3B_3 vs. A_6B_6

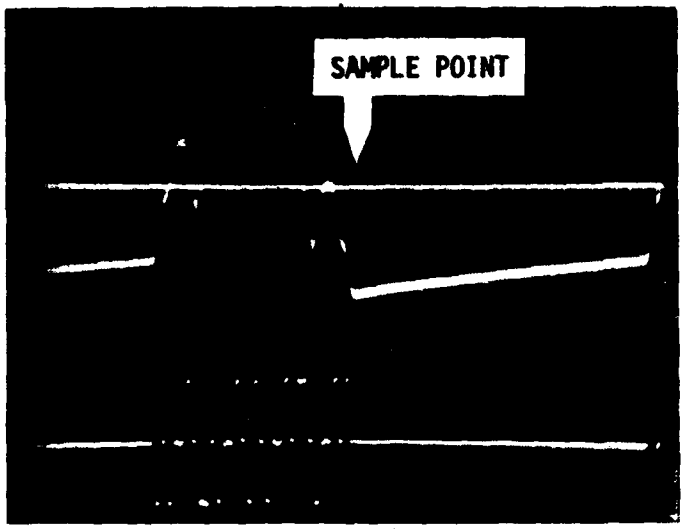

a. Integrator Output (Top)
Integrator Input (Bot) I/S = 30db
X scale - 10μs/div
Y scale - 1mv/div(Top) .1v/div(Bot)

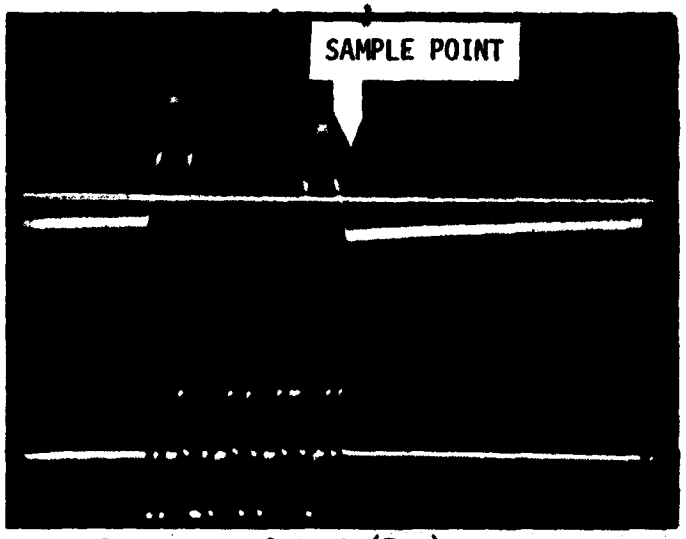

b. Integrator Output (Top)
Integrator Input (Bot) I/S = 40db
X scale - 10μs/div
Y scale - 1mv/div(Top) .1v/div(Bot)

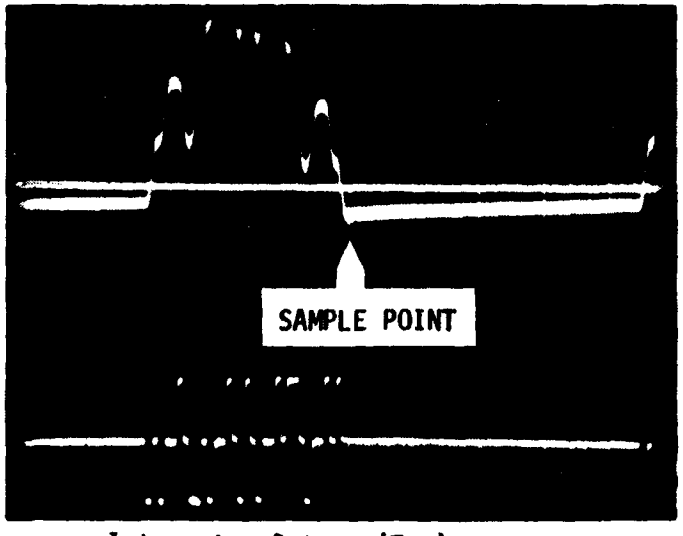

c. Integrator Output (Top)
Integrator Input (Bot) I/S = 46db
X scale - 10μs/div
Y scale - 1mv/div(Top) .1v/div(Bot)

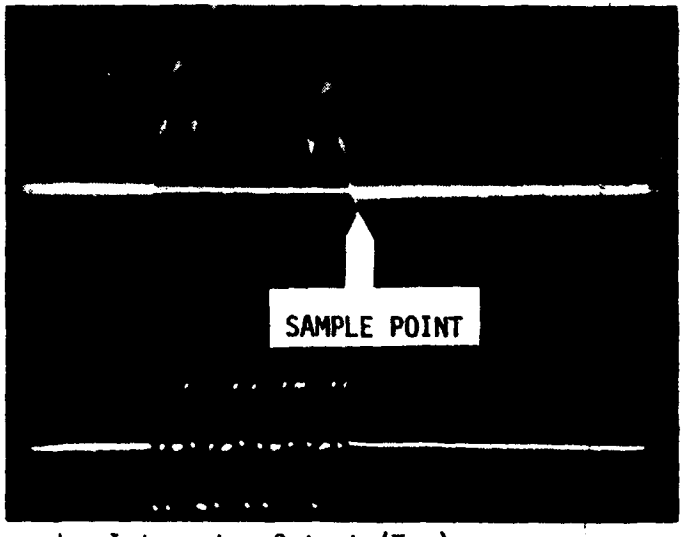

d. Integrator Output (Top)
Integrator Input (Bot) S = 0
X scale - 10μs/div
Y scale - 1mv/div(Top) .1v/div(Bot)

Figure 38 - Signal Plus Interference (2nd User) Performance A_4B_4 vs. A_3B_3

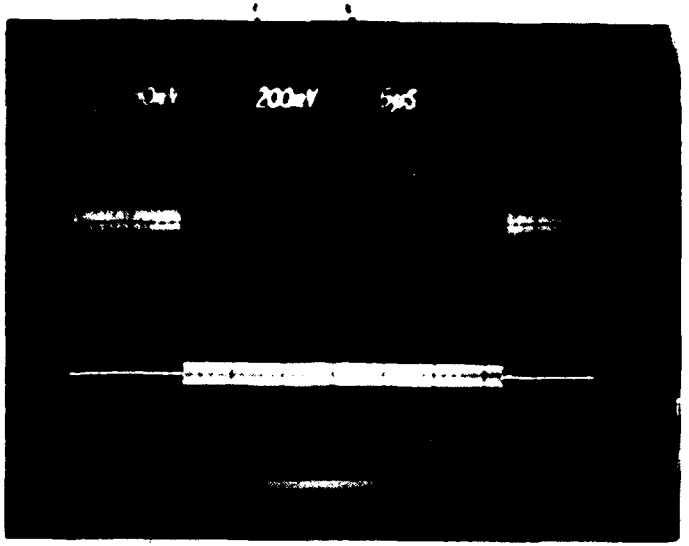

a. Interference + Signal (Top) I/S=30db
Signal Only (Bot)

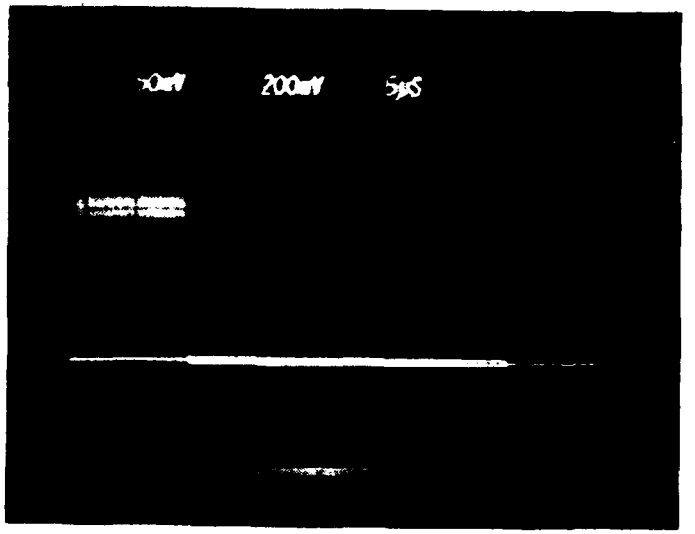

b. Interference + Signal (Top) I/S=40db
Signal Only (Bot)

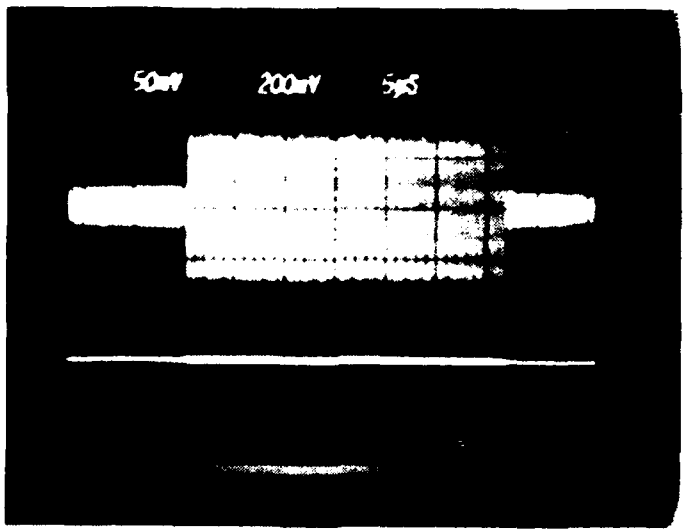

c. Interference + Signal (Top) I/S=46db
Signal Only (Bot)

Figure 39 - Signal Plus Interference (2nd User) Performance A_1B_1 vs. A_2B_2

Tests involving two simultaneous interferers (3 users) were also completed for the CDMA multiple-access configuration. The CDMA system described in Appendix C was configured as shown functionally in figure 40 for the tests involving 3 users. This is the same as for the tests involving two users except that now two interfering sources are combined with the desired signal prior to detection. All three code generators are time synchronous by virtue of using the same reference clock signal to provide the code frame timing with each code generator providing a different code pair.

A photograph of the physical test configuration employed which corresponds to the functional block diagram presented in figure 40 is shown in figure 41. Basically, it is the same as the test configuration employed for 2 users except for the addition of a third generated code which is combined with the 2nd interfering users coded signal. With the signal strength of the two interfering users adjusted to the same level, the combined interfering signal level was made equal to that of the desired signal. Tests were then conducted using code pairs A_3B_3, A_4B_4 and A_6B_6. Measurements were made at the integrator output and input with each code employed as the desired signal and the remaining two as interferers for a combined interference-to-signal level of 30, 40 and 46db. The procedure employed was identical to that utilized for the previous CDMA tests using one interferer. Photographs were also taken of the interference plus signal and signal alone (figures 43, 45 and 47) at the phase detector inputs for each interference-to-signal level employed in the tests and for each test condition. As for all prior multiple-access tests, this was recorded to provide additional clarification of the interference rejection performance associated with the fundamental CDMA multiple-access concept.

The test results are shown in figures 42, 44 and 46 and as was the case for all prior multiple-access testing, the interference is essentially completely rejected and solid detection was obtained in all of the 3 user CDMA multiple-access tests performed.

The results obtained for both the two user and three user CDMA system tests demonstrate the feasibility of implementing a spread spectrum (noise coded) orthogonal CDMA multiple user communications system using practical available hardware. The concept can provide LPI and ECCM protection while simultaneously reducing self-interference to very low acceptable levels for the most critical EMC requirements anticipated for military multiple-access communications. In addition, the CDMA concept can be utilized to perform a switching function. That is, line to line or group to group switching can be achieved using multiplexed noise codes in place of the normally used frequency filters, time gates or space division switching. A multiplexed noise coded switching system is described in detail in Appendix E and the test results obtained on this research program demonstrate conclusively that its implementation is feasible using existing available hardware. A major advantage associated with switching using orthogonal noise codes is that the system would automatically accommodate both digital and analogue inputs. A separate large and expensive space division switching matrix would not be required to switch analogue input signals.

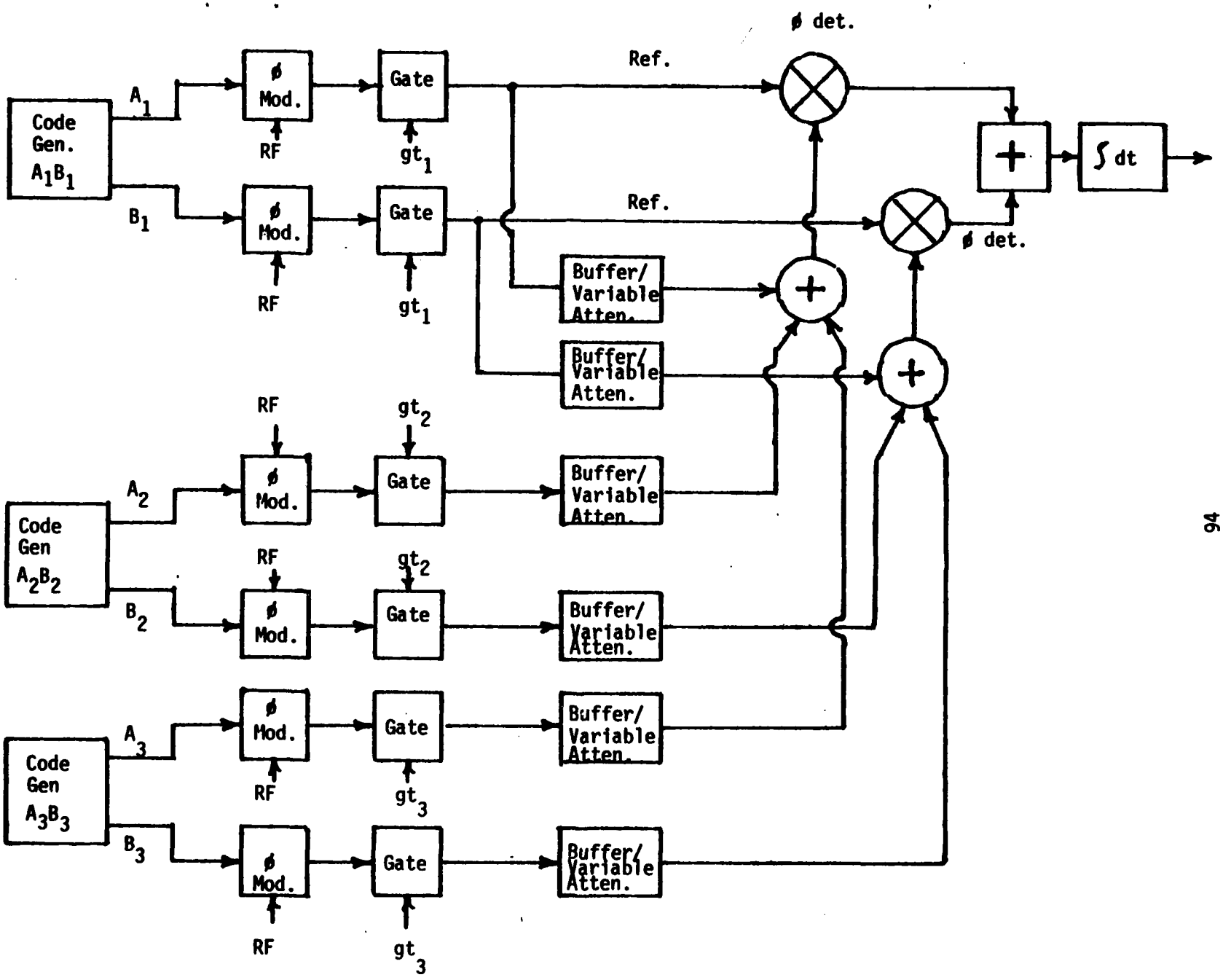

FIGURE 40 - MULTIPLE ACCESS TEST CONFIGURATION (3 USERS)

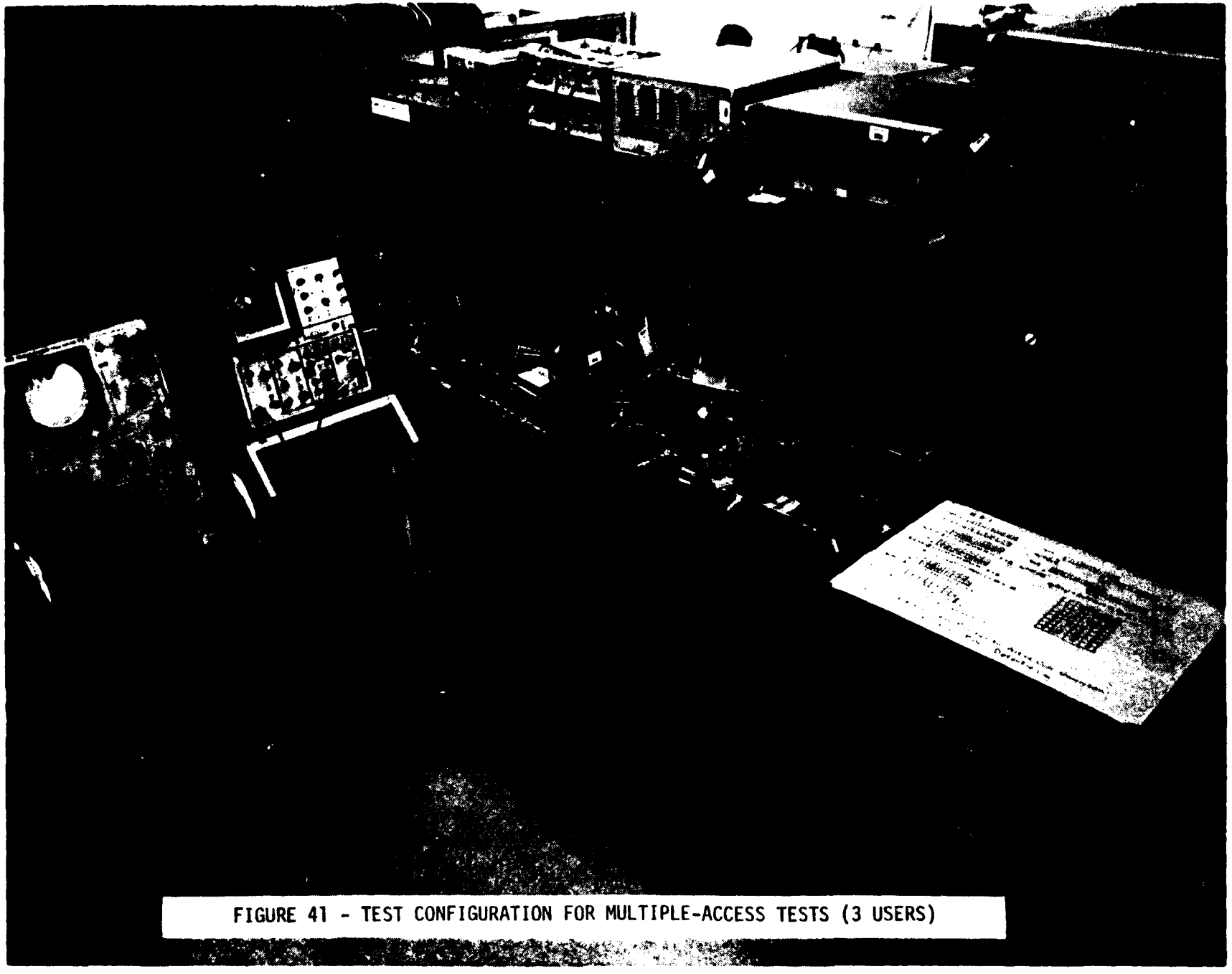

FIGURE 41 - TEST CONFIGURATION FOR MULTIPLE-ACCESS TESTS (3 USERS)

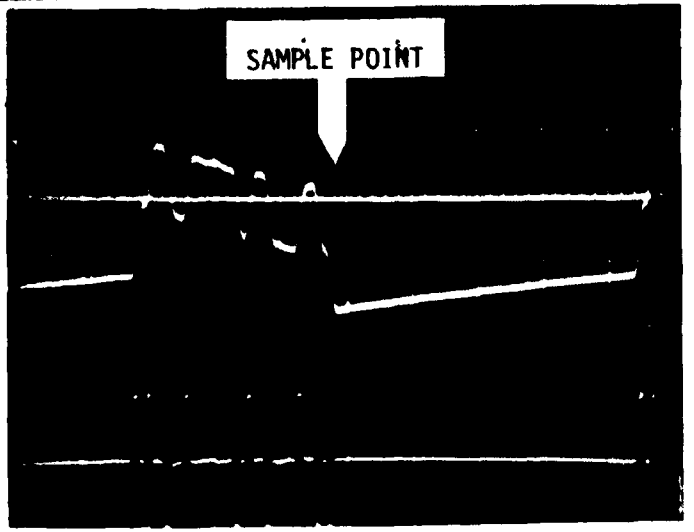

a. Integrator Output (Top)
Integrator Input (Bot) I/S = 30db
X Scale-10μs/div
Y Scale-1mv/div (Top) .1v/div(Bot)

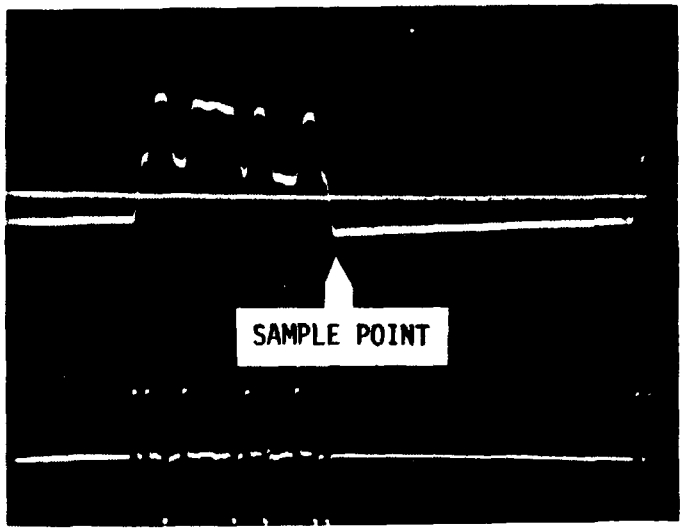

b. Integrator Output (Top)
Integrator Input (Bot) I/S = 40db
X Scale-10μs/div
Y Scale-1mv/div (Top) .1v/div(Bot)

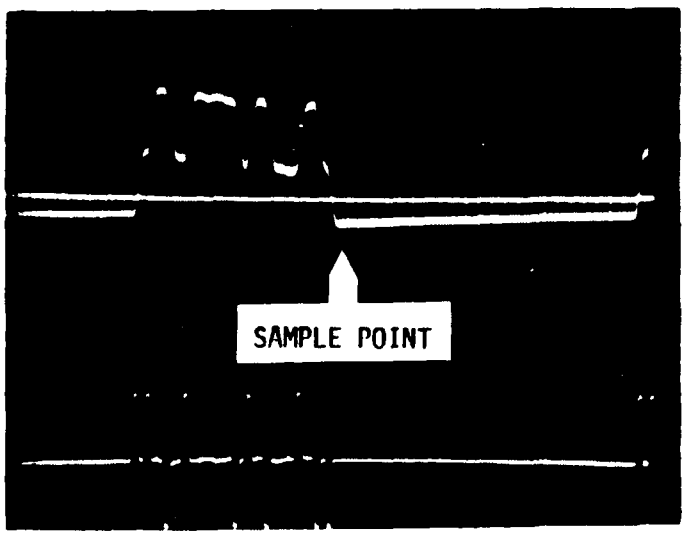

c. Integrator Output (Top)
Integrator Input (Bot) I/S = 46db
X Scale-10μs/div
Y Scale-1mv/div (Top) .1v/div(Bot)

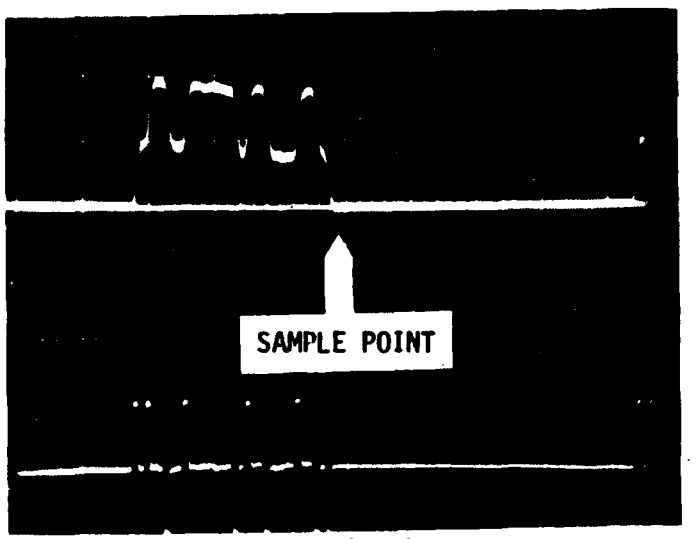

d. Integrator Output (Top)
Integrator Input (Bot) S = 0
X Scale-10μs/div
Y Scale-1mv/div (Top) .1v/div(Bot)

FIGURE 42 - SIGNAL PLUS MULTIPLE INTERFERENCE PERFORMANCE ($A_3B_3+A_6B_6$)vs. A_4B_4

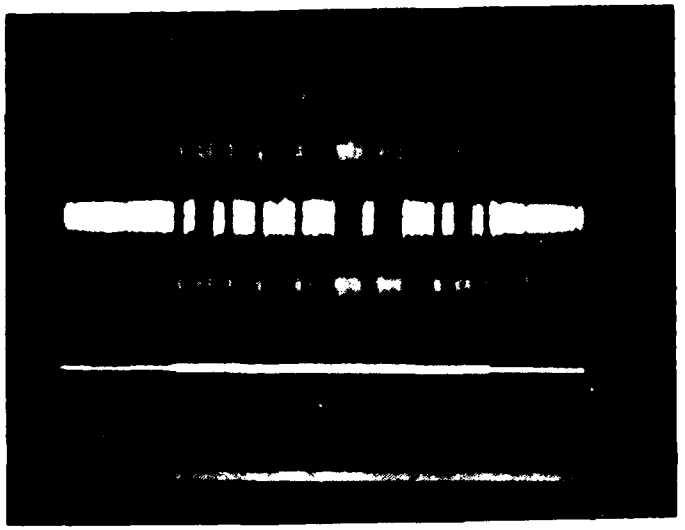

a. Interference (B_3+B_6)+ Signal B_4 (Top)
Signal Only A_4 (Bot)
I/S = 46db

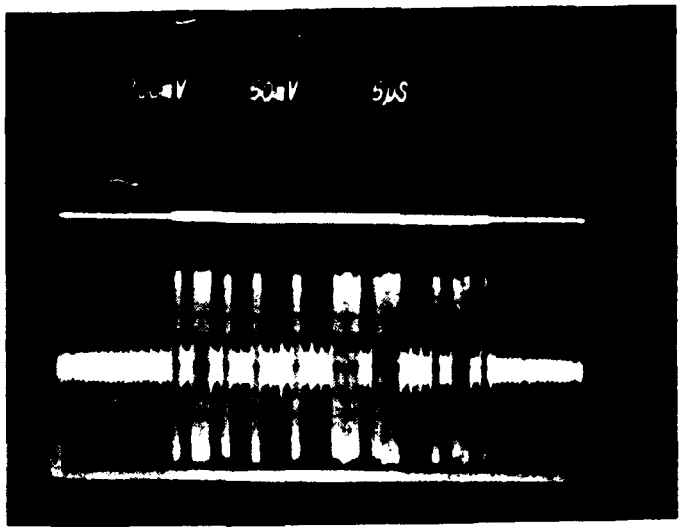

b. Signal Only B_4 (Top)
Interference (A_3+A_6)+ Signal A_4 (Bot)
I/S = 46db

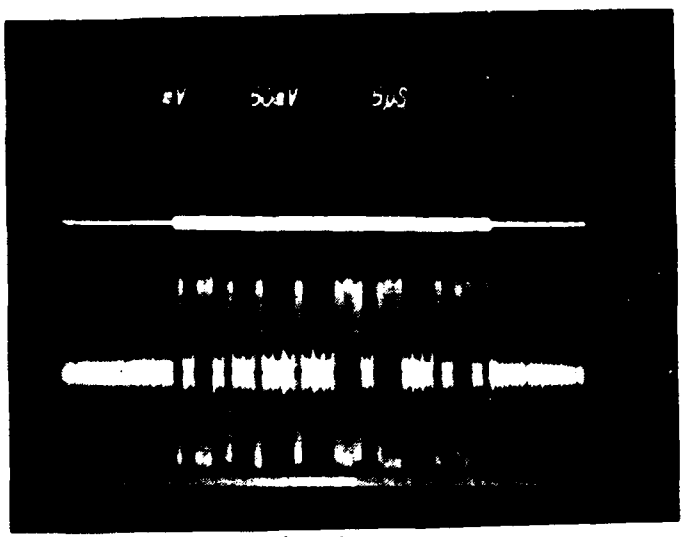

c. Signal Only B_4 (Top)
Interference (A_3+A_6)+Signal A_4 (Bot)
I/S = 40db

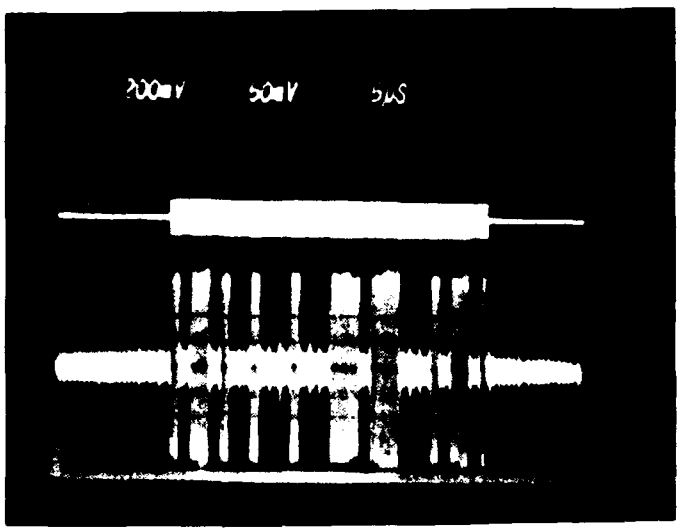

d. Signal Only B_4 (Top)
Interference (A_3+A_6)+ Signal A_4 (Bot)
I/S = 30db

FIGURE 43 - SIGNAL PLUS MULTIPLE INTERFERENCE PERFORMANCE (A_3B_3+A_6B_6) vs. A_4B_4

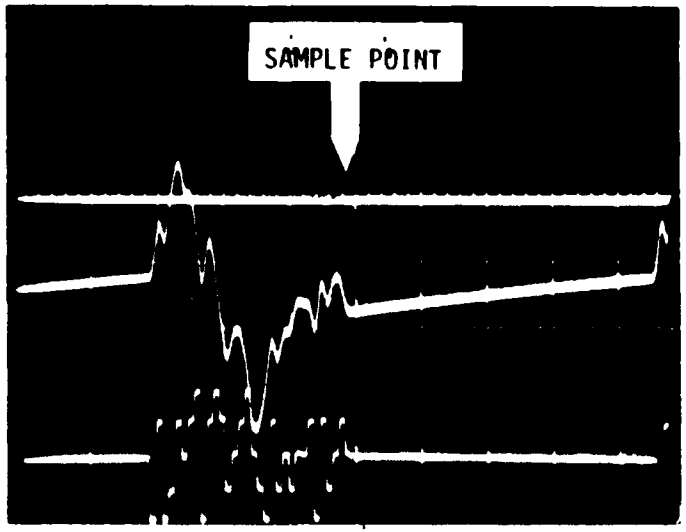

a. Integrator Output (Top)
Integrator Input (Bot) I/S = 30db
X Scale-10μs/div
Y Scale-1mv/div (Top) .1v/div(Bot)

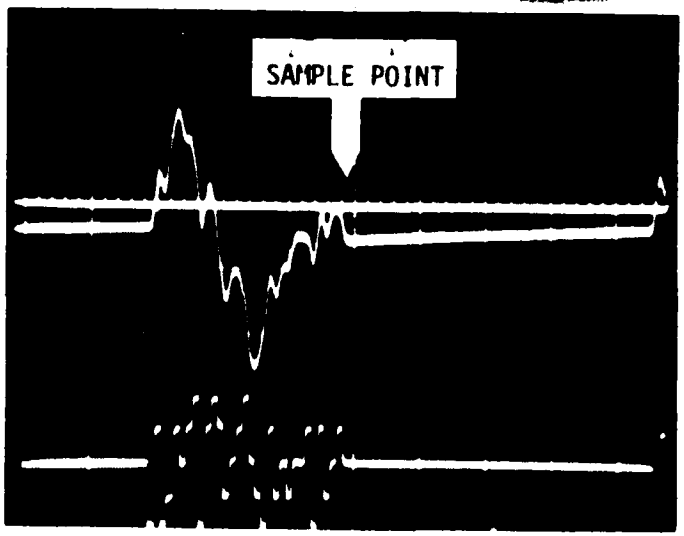

b. Integrator Output (Top)
Integrator Input (Bot) I/S = 40db
X Scale-10μs/div
Y Scale-1mv/div (Top) .1v/div(Bot)

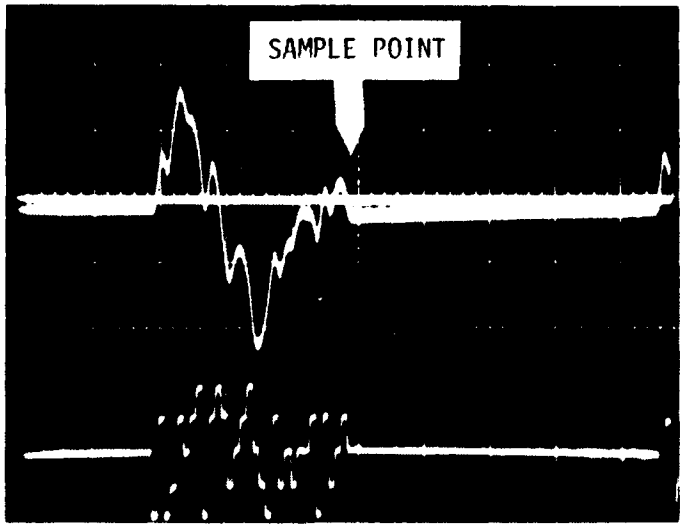

c. Integrator Output (Top)
Integrator Input (Bot) I/S = 46db
X Scale-10μs/div
Y Scale-1mv/div (Top) .1v/div(Bot)

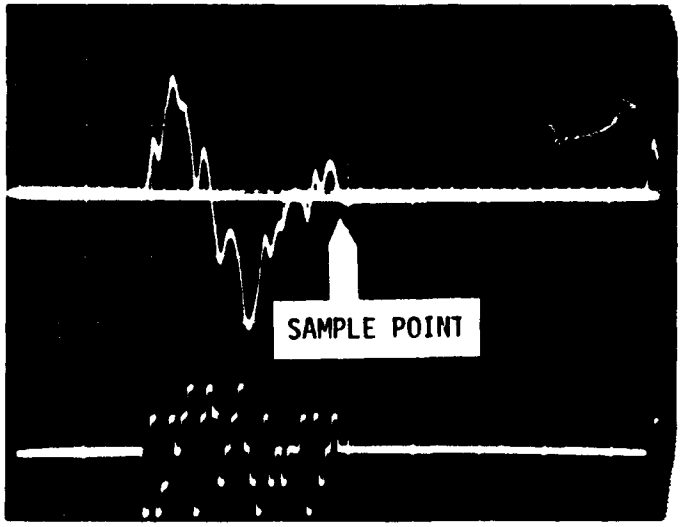

d. Integrator Output (Top)
Integrator Input (Bot) S = 0
X Scale-10μs/div
Y Scale-1mv/div (Top) .1v/div(Bot)

FIGURE 44 - SIGNAL PLUS MULTIPLE INTERFERENCE PERFORMANCE ($A_3B_3+A_4B_4$) vs. A_6B_6

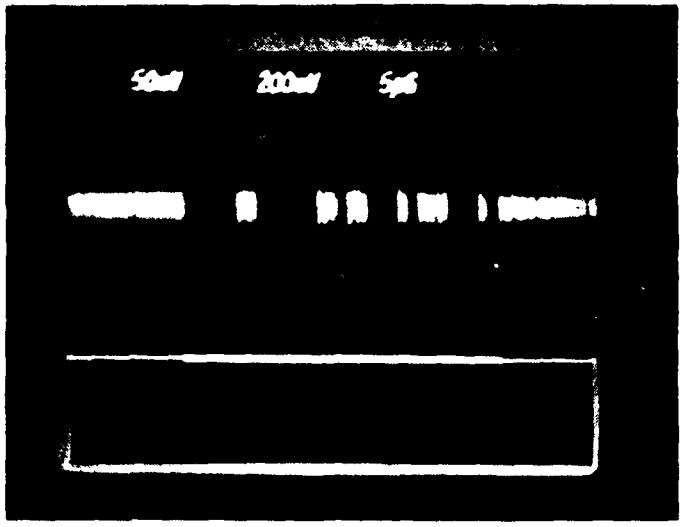

a. Interference (B_3+B_4)+ Signal B_6 (Top)
Signal Only A_6 (Bot)
I/S = 46db

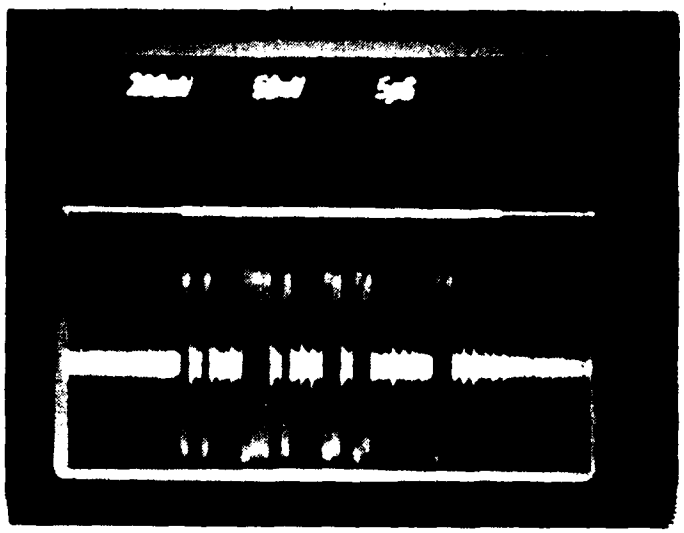

b. Signal Only B_6 (Top)
Interference (A_3+A_4)+ Signal A_6 (Bot)
I/S = 46db

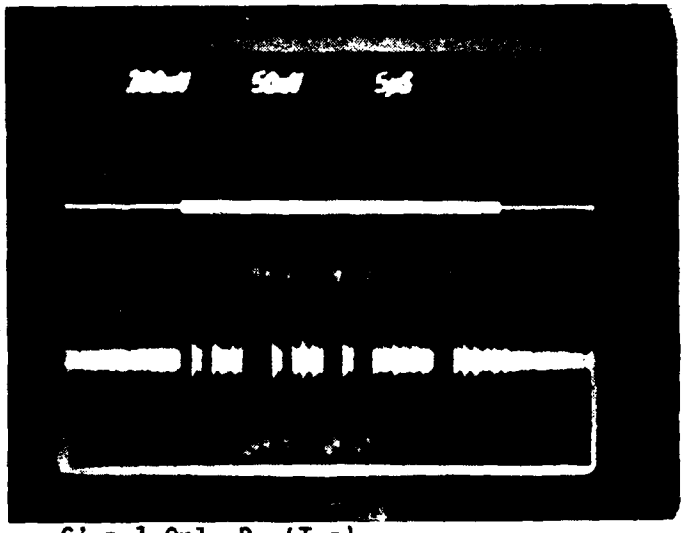

c. Signal Only B_6 (Top)
Interference (A_3+A_4)+ Signal A_6 (Bot)
I/S = 40db

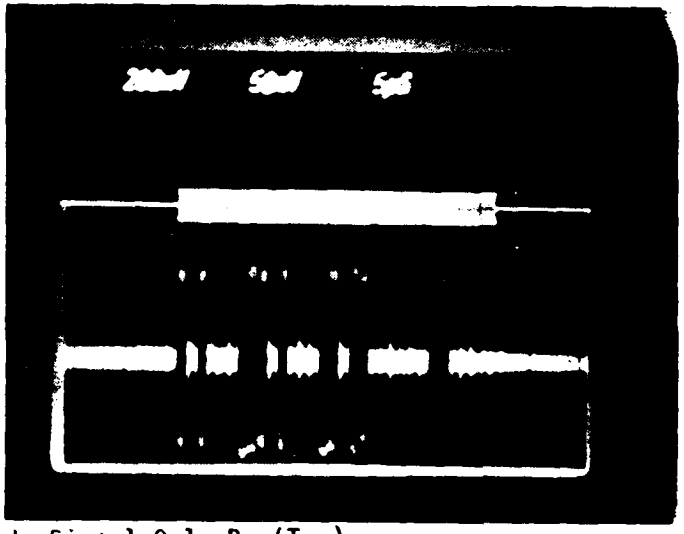

d. Signal Only B_6 (Top)
Interference (A_3+A_4)+ Signal A_6 (Bot)
I/S = 30db

FIGURE 45 - SIGNAL PLUS MULTIPLE INTERFERENCE PERFORMANCE (A_3B_3+A_4B_4) vs. A_6B_6

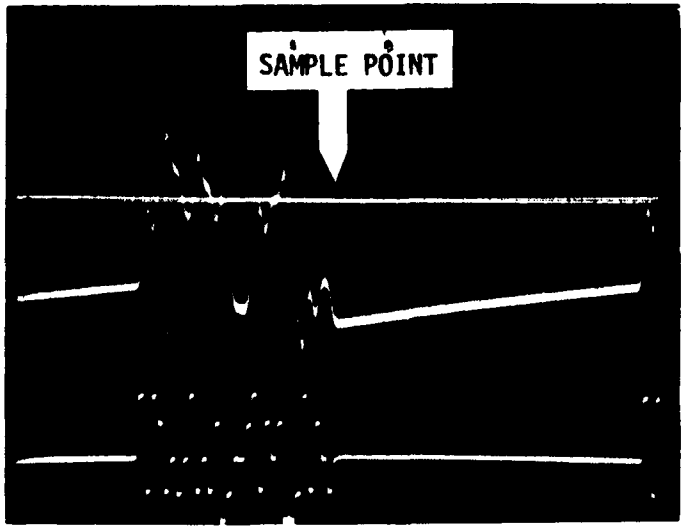

a. Integrator Output (Top)
Integrator Input (Bot) I/S = 30db
X Scale-10μs/div
Y Scale-1mv/div (Top) .1v/div(Bot)

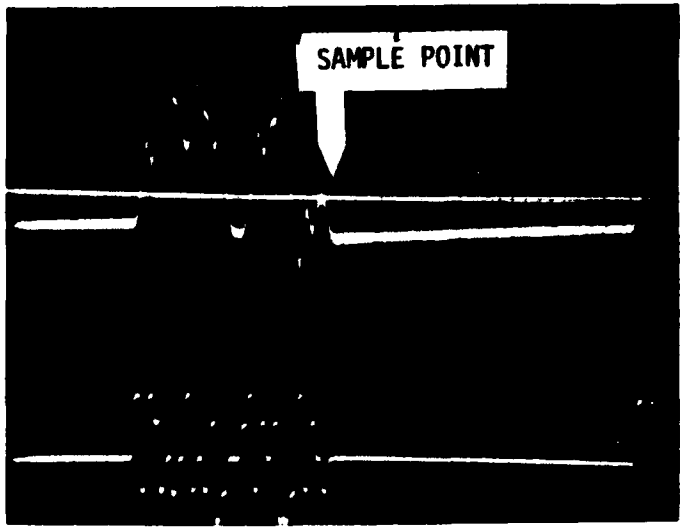

b. Integrator Output (Top)
Integrator Input (Bot) I/S = 40db
X Scale-10μs/div
Y Scale-1mv/div (Top) .1v/div(Bot)

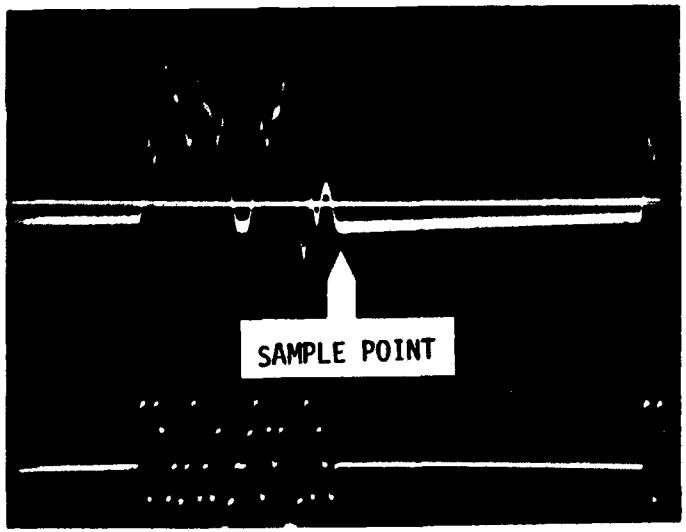

c. Integrator Output (Top)
Integrator Input (Bot) I/S = 46db
X Scale-10μs/div
Y Scale-1mv/div (Top) .1v/div(Bot)

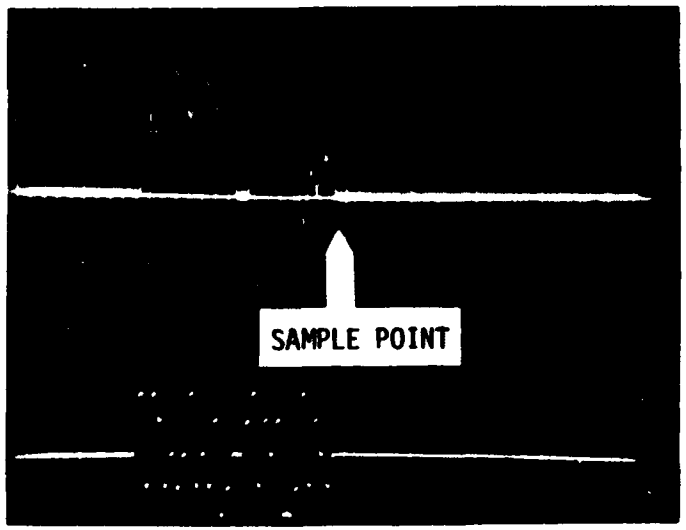

d. Integrator Output (Top)
Integrator Input (Bot) S = 0
X Scale-10μs/div
Y Scale-1mv/div (Top) .1v/div(Bot)

FIGURE 46 - SIGNAL PLUS MULTIPLE INTERFERENCE PERFORMANCE ($A_4B_4+A_6B_6$) vs. A_3B_3

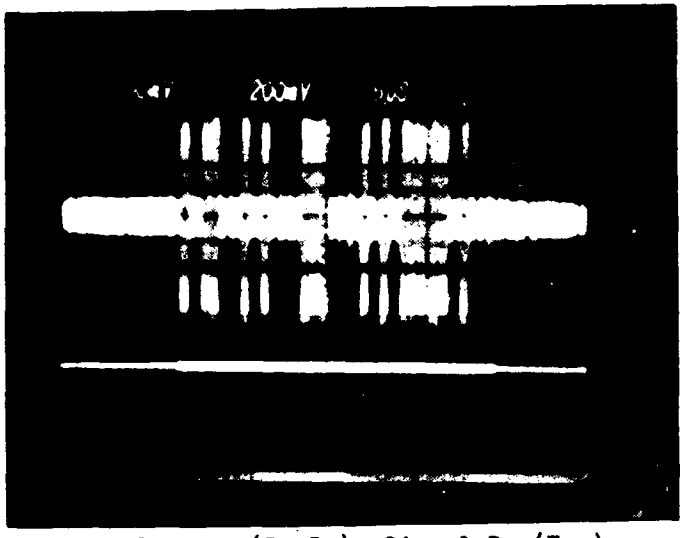

a. Interference (B_4+B_6)+ Signal B_3 (Top)
Signal Only A_3 (Bot)
I/S = 46db

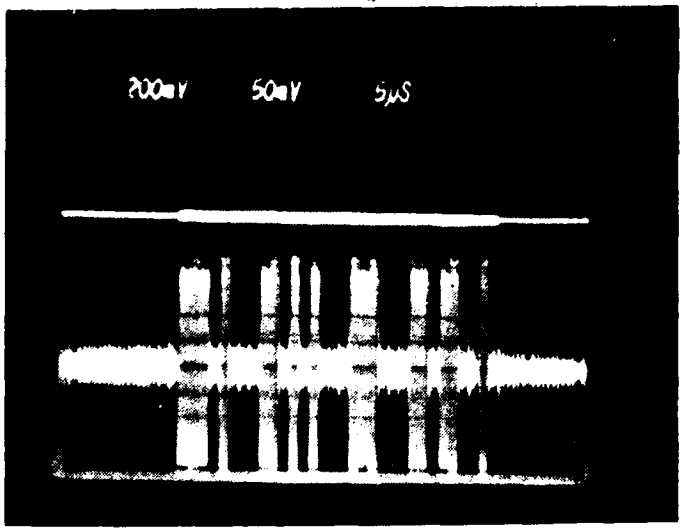

b. Signal Only B_3 (Top)
Interference (A_4+A_6)+ Signal A_3 (Bot)
I/S = 46db

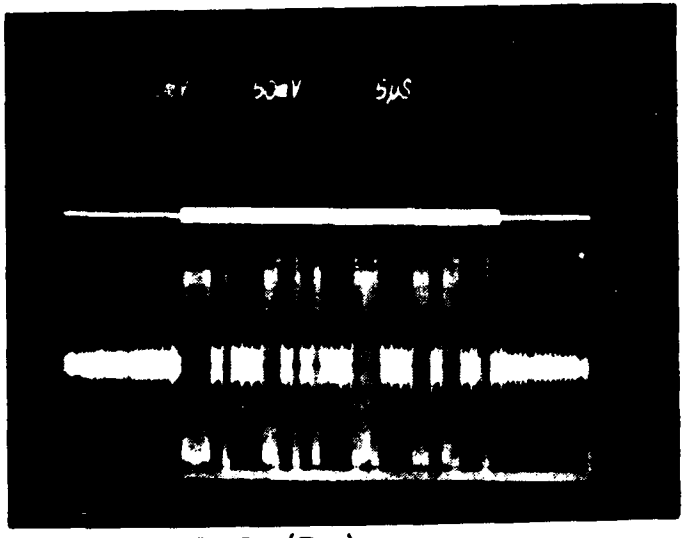

c. Signal Only B_3 (Top)
Interference (A_4+A_6)+ Signal A_3 (Bot)
I/S = 40db

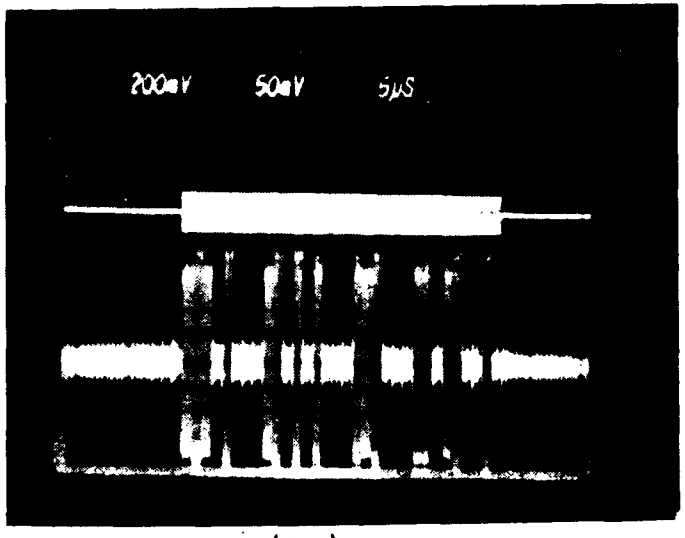

d. Signal Only B_3 (Top)
Interference (A_4+A_6)+ Signal A_3 (Bot)
I/S = 30db

FIGURE 47 - SIGNAL PLUS MULTIPLE INTERFERENCE PERFORMANCE (A_4B_4+A_6B_6) vs. A_3B_3

(6) C.W. Interference Canceling Test

Interference rejection concepts that are theoretically capable of completely canceling C.W. and pulse interference while retaining the desired signal at its peak detected level were described in detail in paragraph 3b(6) and Appendix B. How realistic these claims are when practical hardware is employed was determined by making appropriate measurements using a test configuration which conforms to canceling C.W. interference for a system that employs active coherent detection such as described in Appendix B.

A functional block diagram of the test configuration is presented in figure 48. The test was confined to using only one code of a code pair (code B_3) since two matched delay lines were not available to delay both codes of a mate pair by the same amount. In spite of this restriction, excellent results were obtained since the residue level of the delayed signal that remained after integration (this would normally be subtracted out by the mate code independent of its level) was negligible for the specific code used and at the delay introduced by the available delay line. The variable delay comprised a 3.6 sec fixed SAW delay line in tandem with a variable phase shifter.

Measurements were made at the integrator output and input with a C.W. interference signal adjusted to be 30db stronger than the desired signal as shown in figure 49d. The detected output signal plus interference is shown in figure 49a with the phase adjusted to null or cancel the C.W. interference. The C.W. interference is seen to be virtually totally eliminated. A double exposure was used in the photograph of the integrator output where the second exposure was taken with the input to the scope removed to accent the zero volt reference. The measuring sensitivity and limited dynamic range inherent in the available equipment and components prevented obtaining an absolute measurement of the C.W. attenuation realized. To further illustrate the nulling capability of the concept, however, the integrator input and output was photographed with the C.W. interference removed which is shown in figure 49c. The difference in the output with the C.W. interference present and absent is essentially not detectable. The test was also shown to several observers who viewed the integrator output directly on the oscilloscope and they could not discern whether or not the C.W. interference was present.

A photograph was made of the integrator output and input with the delayed path disconnected as shown in figure 48b to demonstrate that there is only a very slight loss in the desired signal. An overlap of 28½ bits for code B_3 results in a net level after integration (i.e. crosscorrelation value) of only ½ compared to a peak level of 32 for the desireed signal.

The C.W. interference canceling test described above was repeated with the C.W. interference level 20db stronger than the desired signal at the input to the canceler. This test was made to illustrate the functional operations in more detail. The results are shown in figure 50 and as for the previous test, the C.W. interference is virtually totally eliminated.

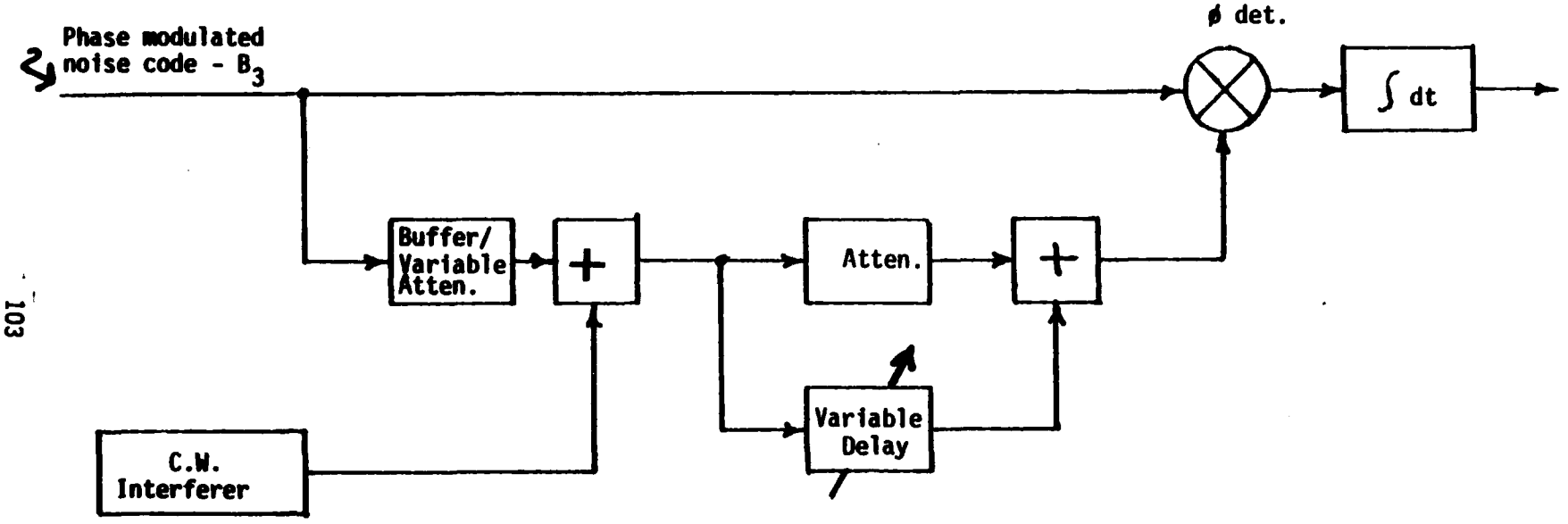

FIGURE 48 - C.W. INTERFERENCE CANCELING TEST

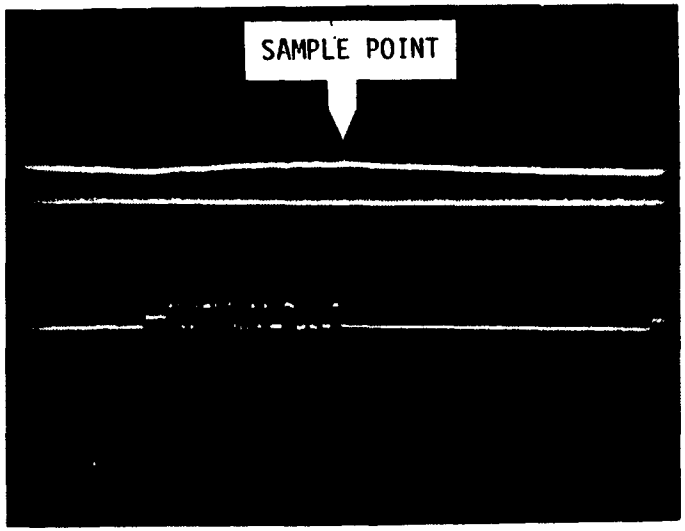

a. Integrator Output (Top)
Integrator Input (Bot) cw/s = 30 db
X scale - 10 μs/div
Y scale - 1 mv/div (Top) 5 mv/div (Bot)

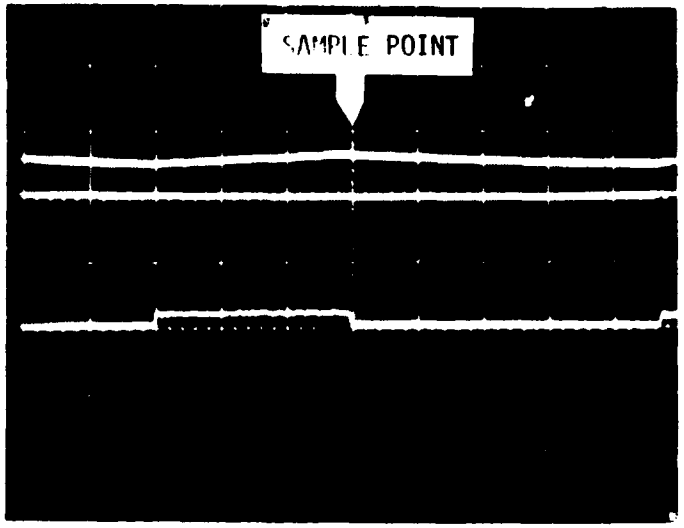

b. Integrator Output (Top) } Delay Path
Integrator Input (Bot) } Disconnected
X scale - 10 μs/div
Y scale - 1 mv/div (Top) 5 mv/div (Bot)

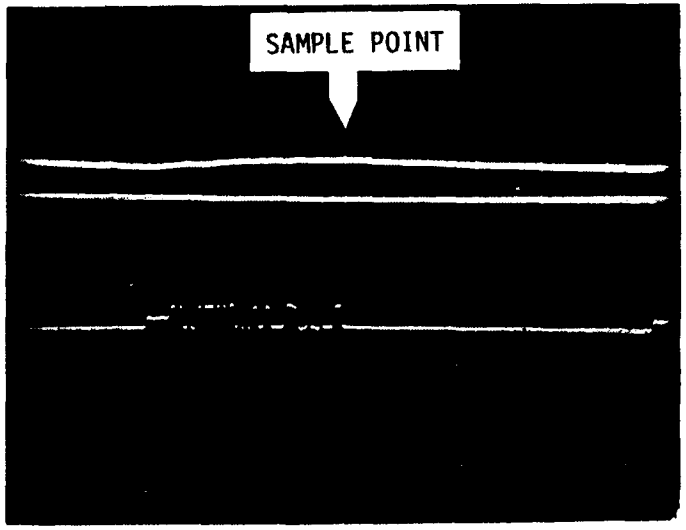

c. Integrator Output (Top)
Integrator Input (Bot) c w removed
X scale - 10 μs/div
Y scale - 1 mv/div (Top) 5 mv/div (Bot)

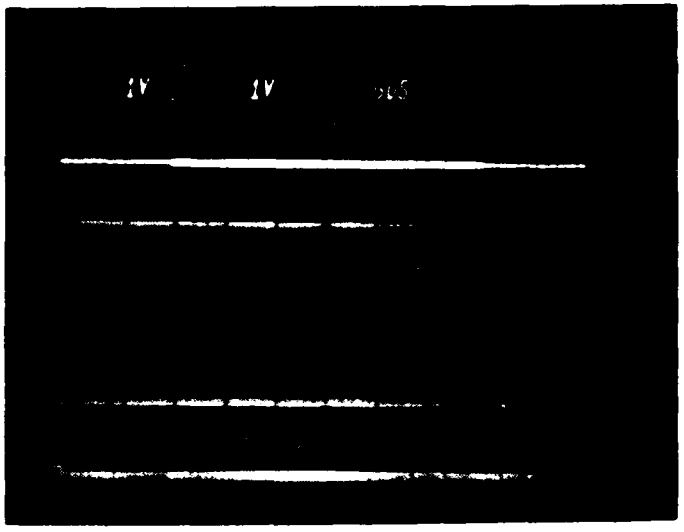

d. Signal Only (Top)
cw Interference & Signal (Bot)
cw/s = 30 db

FIGURE 49 - CW INTERFERENCE CANCELING SPREAD SPECTRUM SYSTEM PERFORMANCE

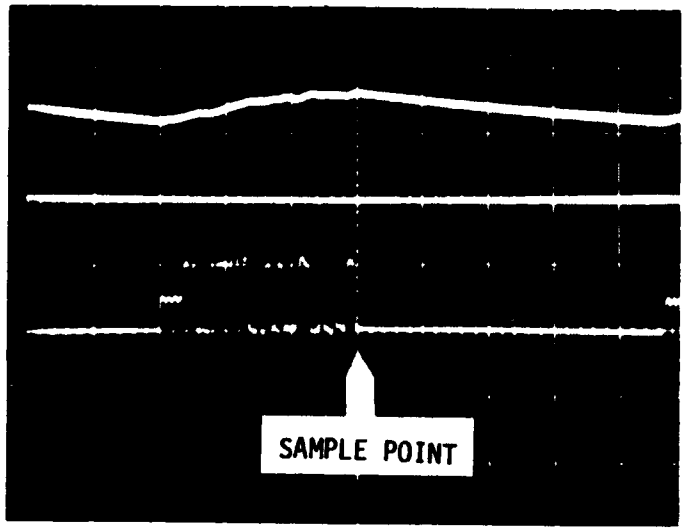

a. Integrator Output (Top)
Integrator Input (Bot) cw/s = 20 db
X scale - 10 μs/div
Y scale - 1 mv/div (Top) 5 mv/div (Bot)

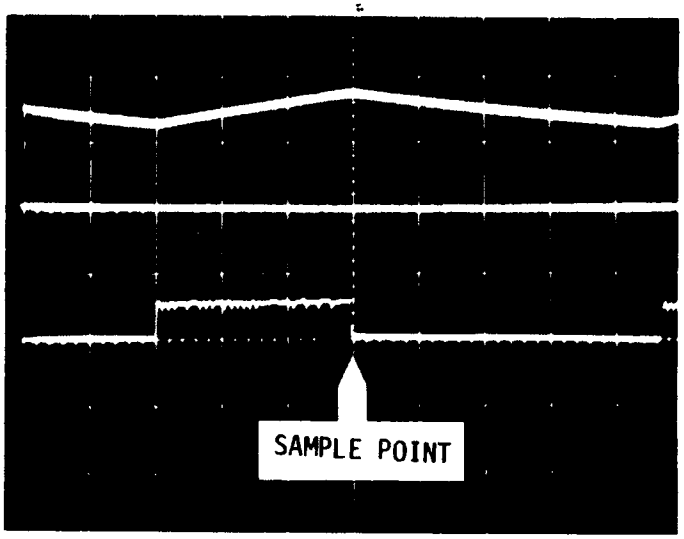

b. Integrator Output (Top) } Delay Path
Integrator Input (Bot) } Disconnected
X scale - 10 μs/div
Y scale - 1 mv/div (Top) 5 mv/div (Bot)

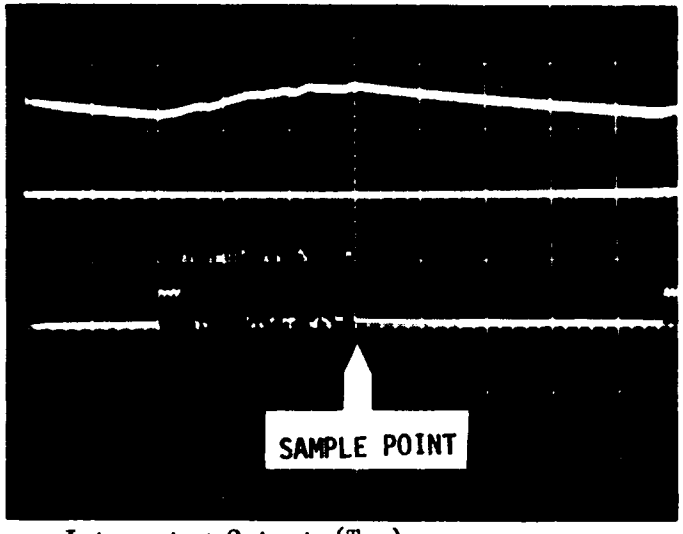

c. Integrator Output (Top)
Integrator Input (Bot) c w removed
X scale - 10 μs/div
Y scale - 1 mv/div (Top) 5 mv/div (Bot)

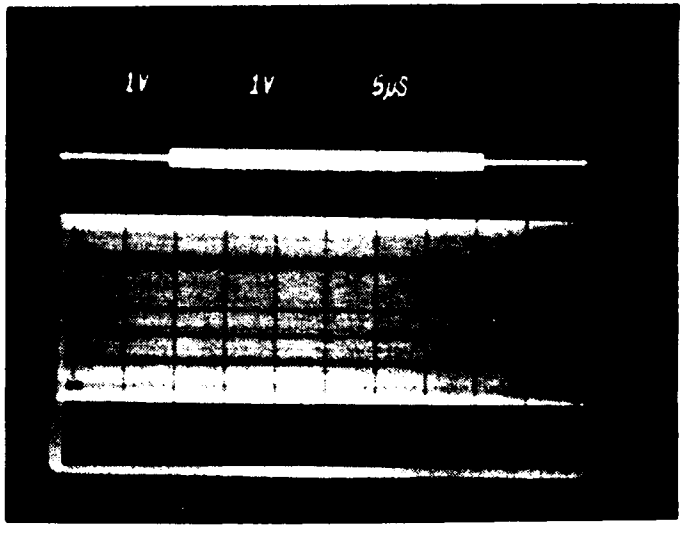

d. Signal Only (Top)
cw Interference & Signal (Bot)
cw/s = 20 db

FIGURE 50 - CW INTERFERENCE CANCELLING SPREAD SPECTRUM SYSTEM PERFORMANCE

A photograph of the integrator input and output was also taken with the delay path disconnected and the desired signal removed (i.e. only the C.W. interference was present) to identify the level of interference that would be present in the output when an interference canceler is not used. The result is shown in figure 51 where the bandwidth spreading of the C.W. is evident in the photos of the integrator input. Figures 51a and 51b were taken at two arbitrary C.W. frequencies within the 1MHz bandwidth of the coded spread spectrum signal. In addition to illustrating further the effectiveness of the interference nulling canceler, the measured levels can be used to confirm that spread spectrum multiplexed noise codes provide an A/J Power gain margin equal to the time-bandwidth product or equivalently the number of code bits n. The voltage gain margin would equal $\sqrt{n}$.

Referring to figure 51a, the peak output C.W. level is 2.8mv and from figure 50 the output peak signal level is 1.6mv when the input signal-to-interference level corresponds to -20db.

Hence:

$$\left(\frac{S}{I}\right)_o = \frac{1.6}{2.8} = .57 = \gamma_o$$

Where:

$\left(\frac{S}{I}\right)_o = \gamma_o$ = output signal-to-noise voltage ratio

Since the input signal-to-noise ratio is -20db for this case

$$\left(\frac{S}{I}\right)_i = .1 = \gamma_i$$

Where:

$\left(\frac{S}{I}\right)_i = \gamma_i$ = input signal-to-noise voltage ratio

Or the improvement realized between the output and input signal-to-noise voltage ratios γ_o/γ_i is

$$\frac{\gamma_o}{\gamma_i} = \frac{.57}{.1} = 5.7$$

which is essentially equal to the square root of the time-bandwidth product or $\sqrt{n}$ as it should be.

$$\sqrt{n} = \sqrt{32} = 5.6$$

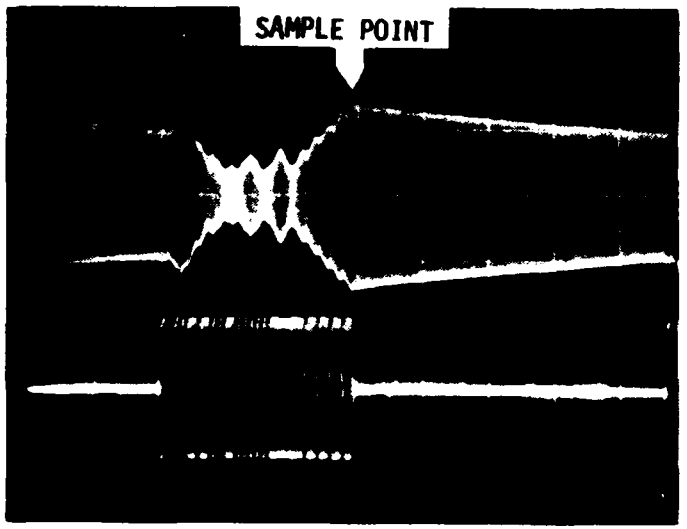

a. Integrator Output (Top) } cw only
Integrator Input (Bot) }
X scale - 10 μs/div
Y scale - 2 mv/div (Top) 50 mv/div (Bot)

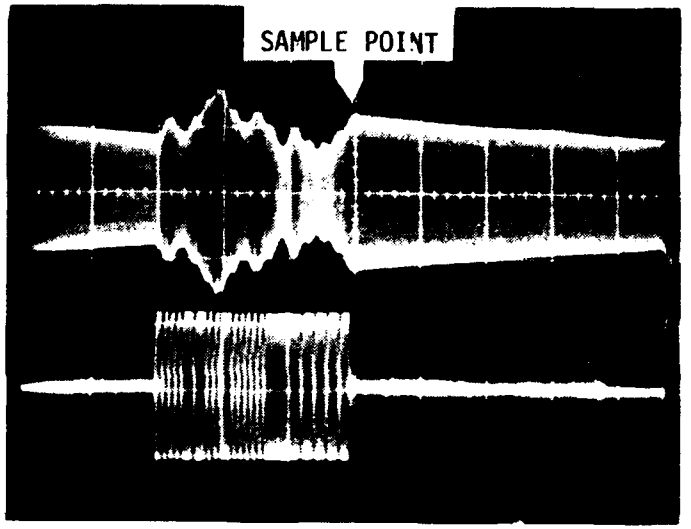

b. Integrator Output (Top) } cw only
Integrator Input (Bot) } freq changed
X scale - 10 μs/div
Y scale - 2 mv/div (Top) 50 mv/div (Bot)

FIGURE 51 - CW INTERFERENCE IN OUTPUT WITH DELAY PATH DISCONNECTED AND SIGNAL REMOVED

Likewise, when the input signal-to-interference ratio $(S/I)_i$ is -30db, the output detected signal level is .5mv as can be seen in figure 49a.

Hence:

$$\gamma_o = \frac{.5}{2.8} = .178$$

$$\gamma_i = -30db = .0316$$

And

$$\frac{\gamma_o}{\gamma_i} = \frac{.178}{.0316} = 5.63$$

This interference reduction capability is automatically realized for a noise coded spread spectrum system and is part of the reason such an effective null was realized using the C.W. interference canceler.

c. Passive (SAW Device) Configurations

(1) Implementation

A passive code generator and pulse compressor was fabricated as a surface acoustic wave (SAW) device using a mask designed for operation at 70MHz with a 10Mb/s code rate. The mask consisted of two parallel 32 bit multiplexed noise coded transducers (code pair $A48_4$) with synchronous bidirectional transducers located at each end of the coded transducers. A non-optimum aperture of 37λ had to be employed because of the limited size of available acoustic substrates plus a software limitation in the mask generating equipment. The mask (a 2x2 inch chrome on glass) was fabricated with an e-beam pattern generator which was controlled from software generated by an Applicon II computer.

The mask was used to print acoustic circuit patterns on ST-X quartz substrates using the photolithographic technique described in reference 38 of the bibliography. One pair of these devices was then mounted in a metal can (as a preliminary prototype design) and bonded with two mil gold wire to connect the transducers to the terminal connectors via appropriate matching circuits. Either the right or left transducers were removed depending on whether a code generator or pulse compressor type device was being implemented. A photograph of this device is shown in figure 52. Preliminary testing of the (SAW) code generator and compressor revealed that although the codes appeared to compress properly, better isolation between the transducers was required in addition to matching with a low Q (less than 10) high inductive circuit which resulted from the use of the undersized (non-optimum) aperture design.

As a second iteration, a pair of the (SAW) devices were mounted in machined out aluminum fixtures as shown in figure 53. The overall size of the fixtures were 2"x4"x1" and they were designed for ease of matching with good electromagnetic feedthrough isolation using deep hollow chambers.

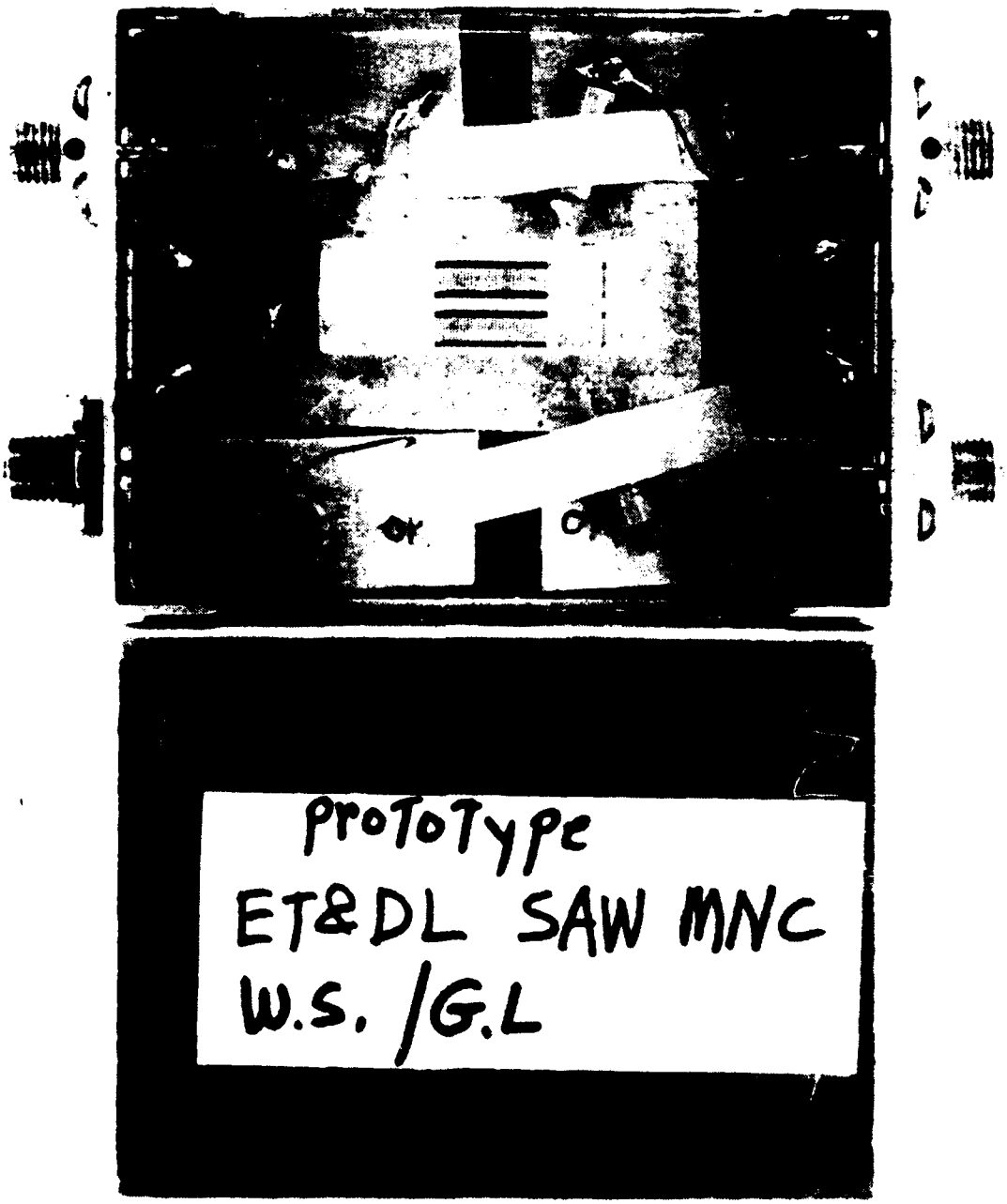

Figure 52 - Surface Acoustic Wave Code Generator/Compressor (metal can enclosure)

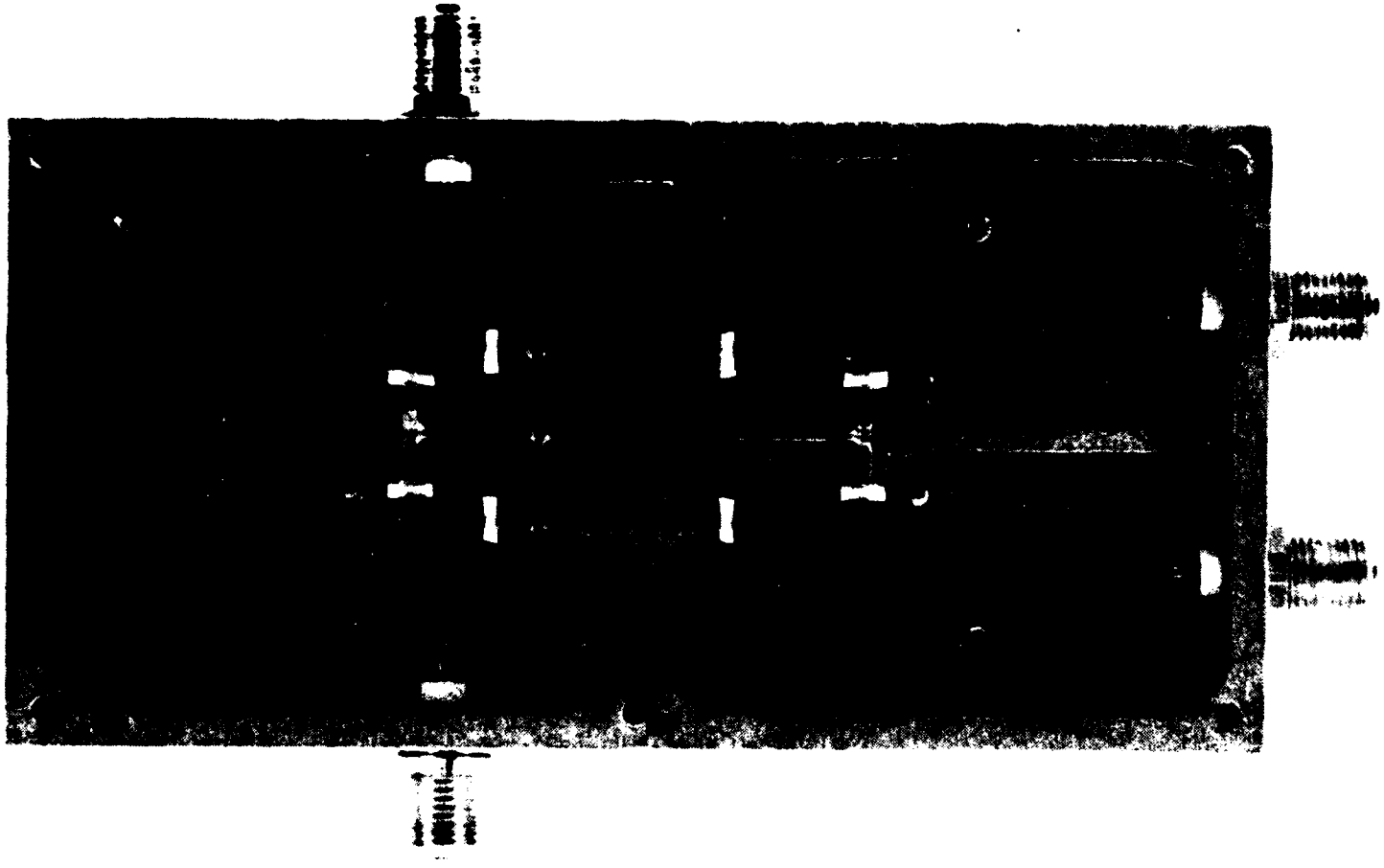

Figure 53 - Surface Acoustic Wave Code Generator/Compressor (machined enclosure)

In addition, the acoustic channels, as well as the input transducers were isolated with thin metal shields placed in close proximity with the acoustic substrate. The substrate itself was placed in a hollow metal cavity to minimize stray capacitance. A Piconics PV (582K3F) type tunable coil was found to provide the low Q and high inductance value (1.2-4 h) required for a good match.

(2) Autocorrelation Function Measurements

The test configuration illustrated in figure 54 was used to evaluate the (SAW) code generator and pulse compressor performance. Since the autocorrelation function is automatically provided as a function of time at the output of the compressor, a calibrated oscilloscope is all that is needed in conjunction with the (SAW) devices to obtain a measurement of the autocorrelation function sidelobes. The amplifiers are used to isolate the devices and overcome their insertion loss. A pulse generator provides a narrow pulse which is used to drive the two (SAW) generators (one for each code forming a mate pair). The (SAW) compressors are identical to their respective code generators but are each driven from the opposite end since their code structure must be a time-reversed replica of the input code to pulse compress the input signal (i.e. provide a matched filter). The summed outputs of the two code compressors then yields the composite autocorrelation function.

A photograph of the physical test configuration employed which corresponds to the functional block diagram illustrated in figure 54 is shown in figure 55. The fabrication and testing of the multiplexed code pair A_4B_4 involved several iterations before obtaining a final (SAW) device whose insertion loss was considered low enough to support system evaluation and testing. The results obtained after each stage of improvement is shown in figure 56 with the final result (figure 56d) having a measured sidelobe plus noise level 30db below the main lobe peak value. A photograph of individually generated and compressed codes of the mate code pair is shown in figure 57. Although better matching and packaging reduced the insertion loss considerably and provides a device that could be used for system performance tests, the residual noise level would still prevent obtaining an accurate measurement of the sidelobes and could yield misleading or inaccurate system test results. In view of this, it was considered expedient to delay fabricating additional SAW devices until larger quartz substrates were received which would permit obtaining stronger coupling (i.e., provide a lower insertion loss). The larger substrates never arrived in time to be utilized, however, which prevented fabricating the additional SAW devices required for performing system tests and crosscorrelation function measurements.

(3) Multiplexed Noise Code Spectrum

A photograph was taken of the spectrum of code pair A_4B_4 (generated with the SAW device) using an AIL Model 607 Spectrum Analyzer. The results are shown in figure 58 where it can be seen that (as was the case for active code generation) the spectrum is spread by the number of code bits 32. The code chip rate is 10Mb/s and the bandwidth of the spread specturm is about 10MHz whereas the information bandwidth is 312KHz ($10^7 \div 32$).

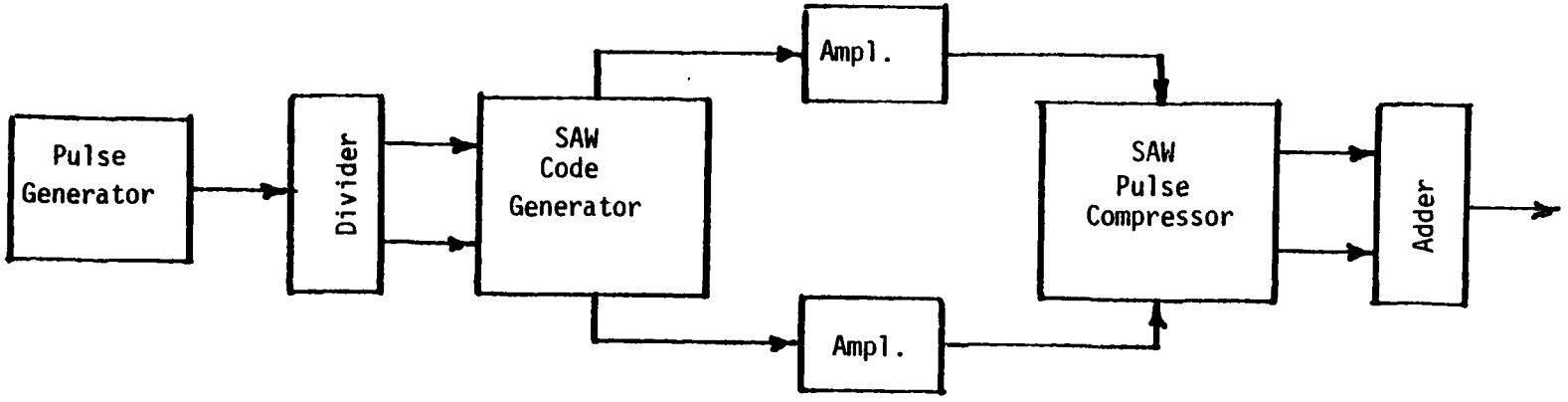

FIGURE 54 - AUTOCORRELATION FUNCTION TEST CONFIGURATION

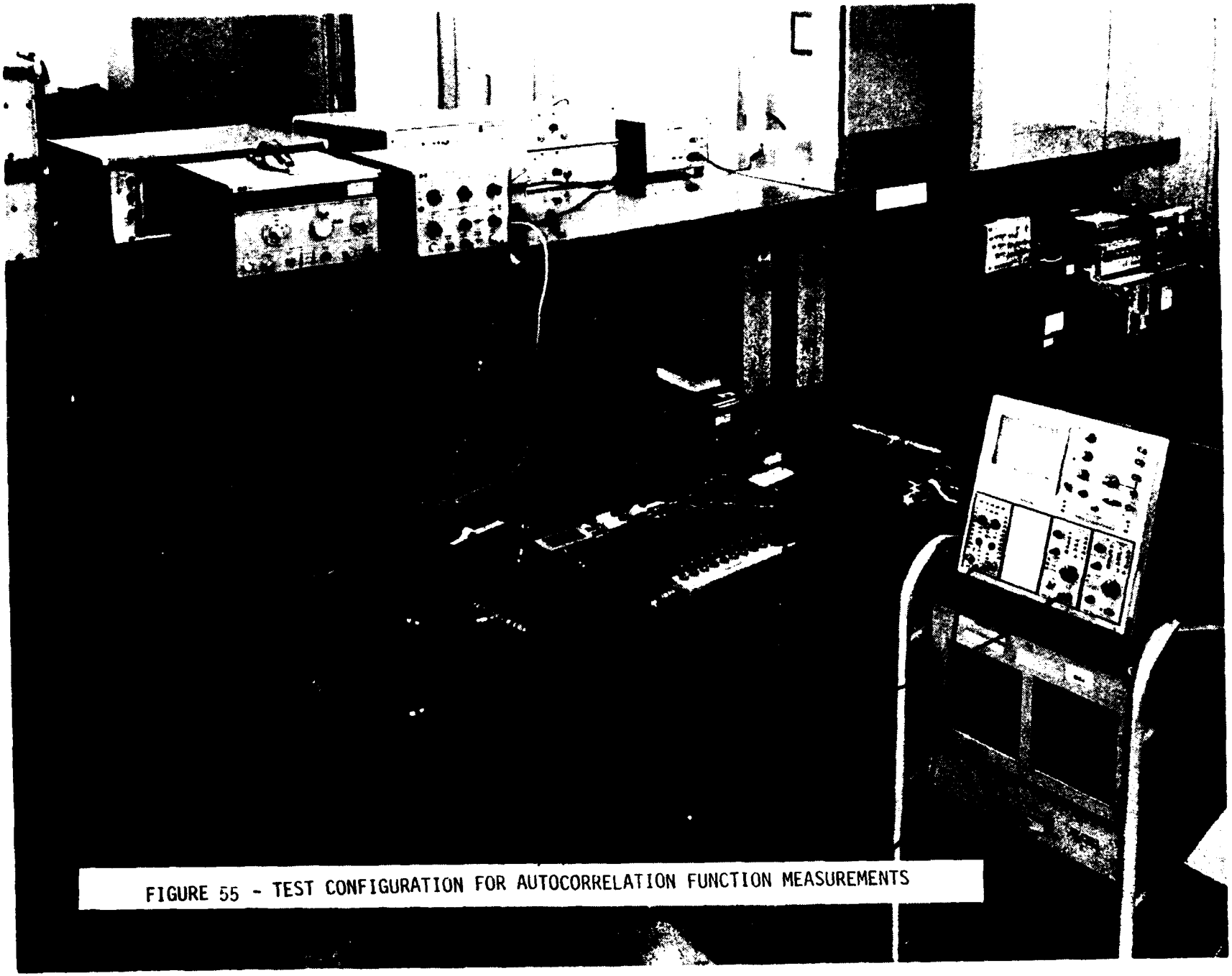

FIGURE 55 - TEST CONFIGURATION FOR AUTOCORRELATION FUNCTION MEASUREMENTS

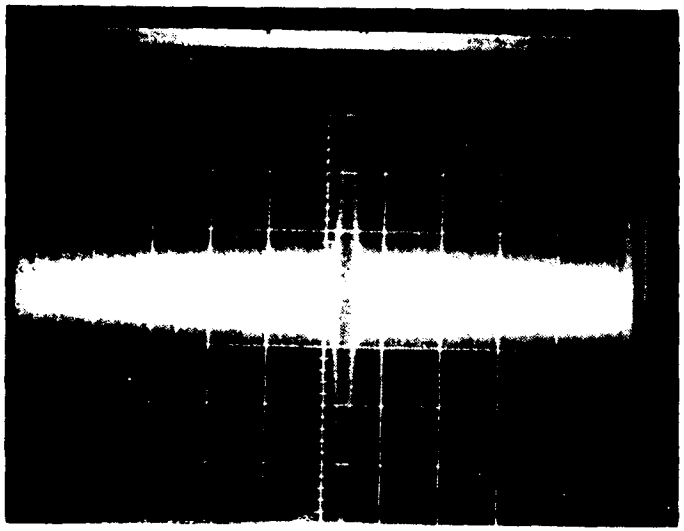

a. No Matching
Metal Can

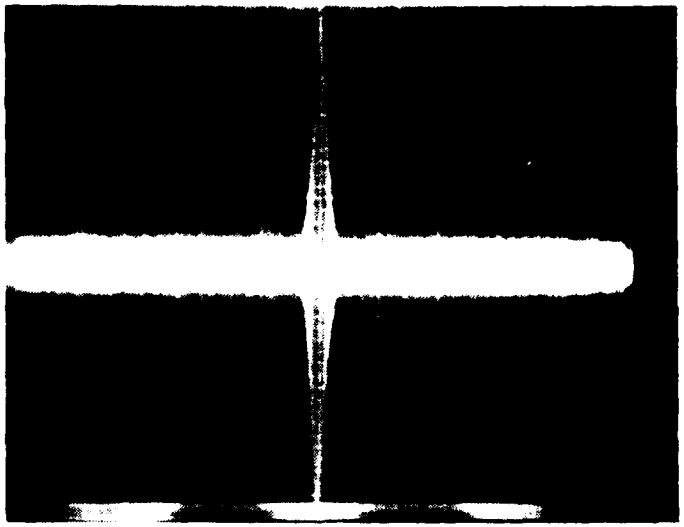

b. Matched (Core Inductor)
Metal Can

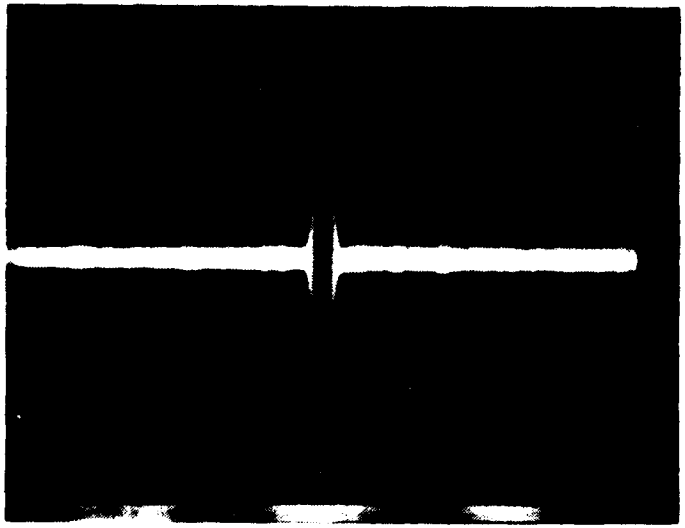

c. Matched (Variable Inductor)
Packaged

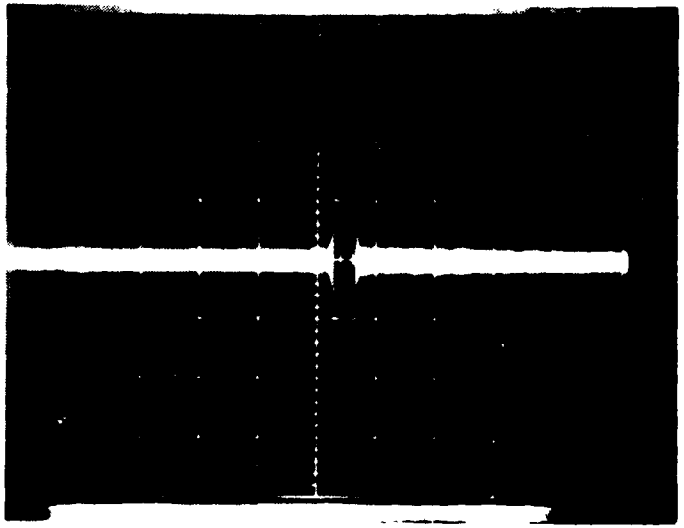

d. Same as c but with Matched Cable
Pairs

Figure 56-Composite (Summed) Compressed Multiplexed Noise Code Pair A_4 B_4

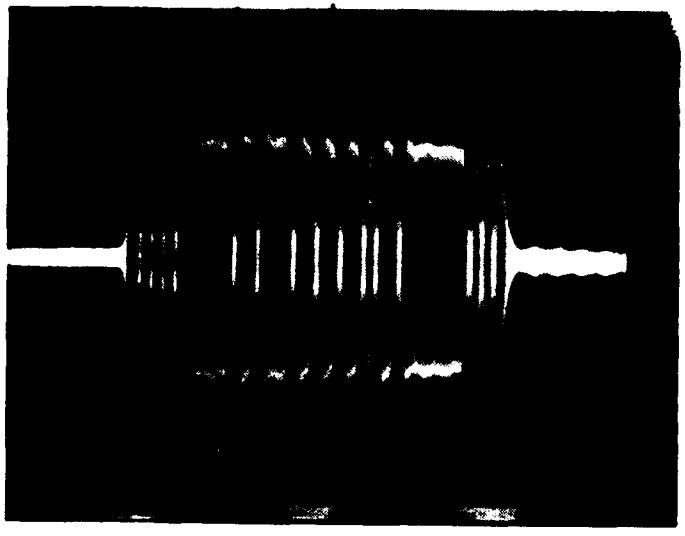

a. Code A_4 (Generated)

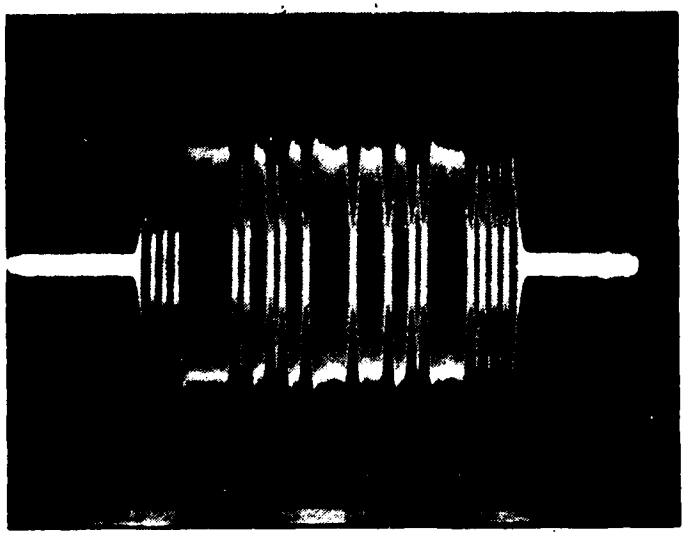

b. Code B_4 (Generated)

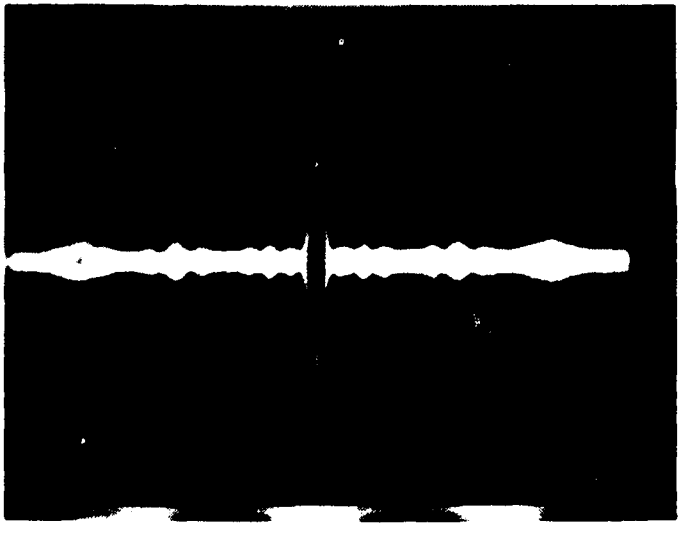

c. Code A_4 (Compressed)

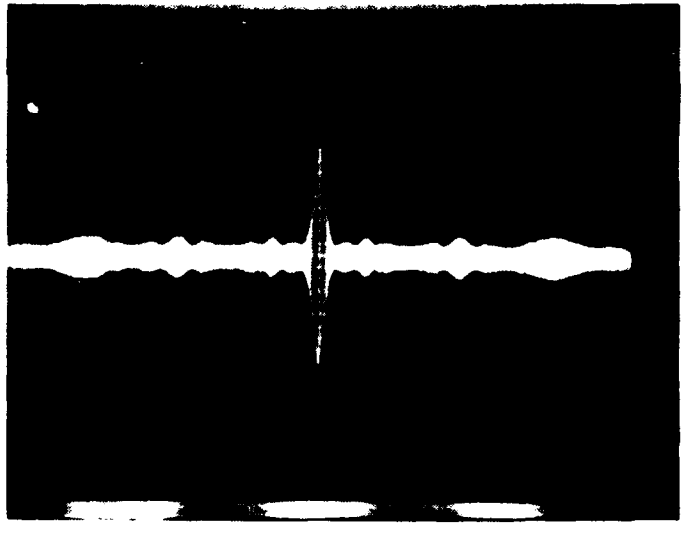

d. Code B_4 (Compressed)

Figure 57 -SAW Device Generation & Compressi[illegible] of Code Pair A_4 B_4

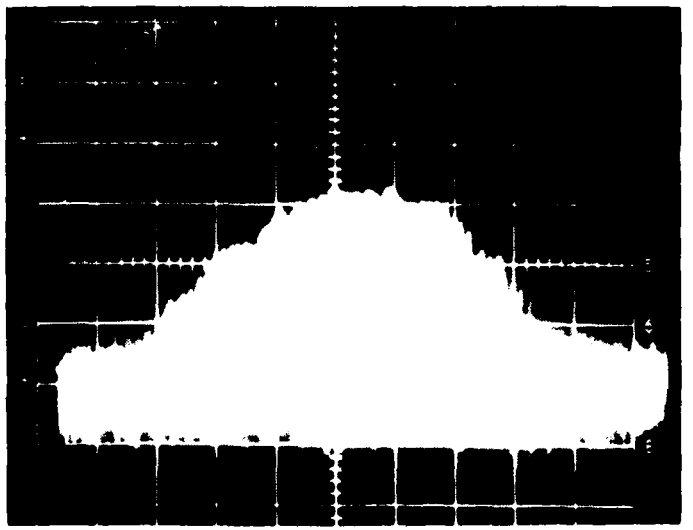

a. Code A_4

X Scale - 3 MHz/div
Y Scale - 10db/div

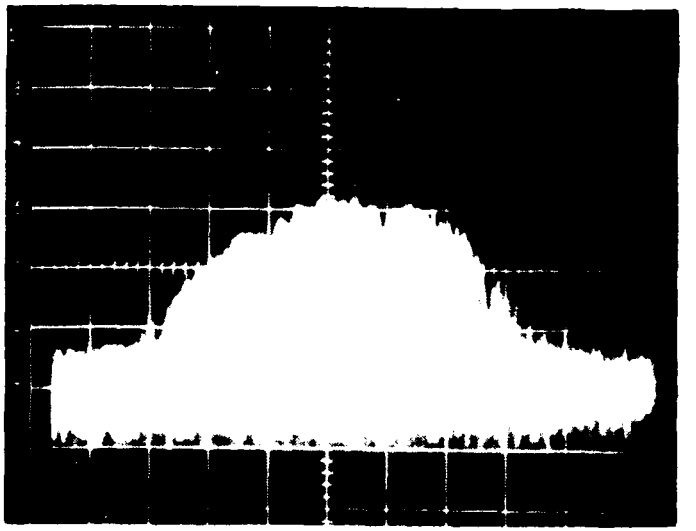

b. Code B_4

X Scale - 3 MHz/div
Y Scale - 10db/div

FIGURE 58 - MULTIPLEXED NOISE CODE SPECTRUM (SAW CODE GENERATOR)

(4) Future Plans

The ET&D Laboratory intends to fabricate and test additional SAW code generators and pulse compressors with internal funds when larger quartz substrates (ordered under the research grant) are received. When this is accomplished, the SAW devices will be subjected to system tests analogous to those employed using the active code generator/matched filter detector configurations with engineering support provided by the TRI-TAC Office. An important advantage associated with the use of SAW devices for performance testing is the relative ease with which multiple-access simulations can be accommodated in conjunction with the fact that the output of the passive pulse compression filter (i.e., matched filter) is the auto-correlation function of the input code. The large quantity of peripheral test equipment and components that were necessary for performing system tests using active code generators would not be required which should enable system tests using passive configurations to utilize more than 3 simultaneous users. The largest number of users that could be accommodated for testing would only be limited by the number of passive code generators and pulse compressors that are fabricated.

5. Test Equipment and Components

a. Equipment Fabricated at ET&D Laboratory

(1) Active Code Generators
32 bit code pair implemented with
TTL DM 47165N 8 bit shift registers

(2) Integrator
Low Pass R-C Filter

(3) Linear Adder
Balanced Resistive Combiner

(4) Passive Code Generator/Pulse Compressor
32 bit code pair implemented using
surface-acoustic-wave (SAW) device

b. Instruments and Components

(1) Digital Data Simulator Model 900SP
SRC Division/Moxon Incorporated

(2) Signal Generators
Model 8654A Hewlett Packard
Model 608F Hewlett Packard

(3) Pulse Generators
Model 214A Hewlett Packard
Model 8012B Hewlett Packard
Model 8004 Hewlett Packard

(4) Oscilloscopes
Model 7504 Tektronix Inc.
Model 7104 Tektronix Inc.
Type 502A Tektronix Inc.

(5) Amplifiers
Avantec UTC5 111M
EIN RF Power Amplifier, Model 5006

(6) Variable Attenuators
Step-Telonic Ind. Inc., Model TG-950
Continuous - Weinschel Eng., Model 933
Weinschel Eng., Model 905

(7) Phase Shifter
Merrimac Type PS-4-60

(8) D.C. Supplies
Hewlett Packard, Model 721A
Hewlett Packard, Model 6218A
Lambda, Model LS515
Kepco, (0-20V)

(9) Phase Detectors
Merrimac, Model PCM-3

(10) Power Dividers/Combiners
Merrimac PDM-20-300
Anzac T-1000
Hewlett Packard 11549A
Mini Circuits Model ZSC-2-1W

(11) Phase Modulators
Mini Circuit Lab - Miniature Double Balanced Mixers,
Model ZMY-1

(12) RF Switch
Watkin Johnson SPST, Model S-1

(13) Spectrum Analyzer
AIL Model 707

6. CONCLUSIONS.

The various fundamental concepts which define the requirements for obtaining lobeless compression, an orthogonal noise code subclass, and basic general code expansion concepts was described and theoretically verified. In addition, a relatively complete coverage of the various unique attributes inherent in multiplexed noise codes was disclosed. In essence, a practical unified theory and explanation of these codes was presented to teach the principles involved and illustrate the magnitude of the gains that are realizable from noise codes that are capable of compressing to a lobeless impulse and which are available in abundance. The theoretical treatment has demonstrated that the concepts and applications are all technically sound.

In order to verify that the advertised performance could be obtained with practical hardware required that multiplexed noise codes be fabricated and tested. This was accomplished for codes that were implemented actively using shift registers and also passively using SAW device technology.

o Active Configurations

An orthogonal subset of 32 bit mate pair codes was implemented with shift registers and tested using a coherent (correlation) detector in appropriate test configurations. This first involved measuring the autocorrelation function of one of the code pairs and then measuring the crosscorrelation function between all of the generated codes at $\tau = 0$. The largest single measured sidelobe of the autocorrelation function was down from the main lobe by 40 db (10,000/1) with most of the sidelobes down by about 50 db (100,000/1). The cross correlation value between the codes comprising the orthogonal subset was -60 db (1,000,000/1) in all cases. These results are very impressive when compared to the best one can achieve, even theoretically, using state-of-the-art direct sequence P-N codes. A 63 bit P-N code has its largest sidelobe down by only 19 db and an orthogonal subclass of direct sequence P-N codes that comprises different or unique codes is non-existent.

Measuring the spectrum of the code mate pairs verified that they do indeed spread the information band by a factor equal to the time bandwidth product (equivalently by the number of code bits N) which demonstrates that the codes provide a power gain margin or A/J protection ratio of 64 (32 for each code of the pair). This was confirmed as part of the C.W. interference canceling test.

The excellent results obtained for both of the correlation measurement tests indicate that orthogonal multiple-access operation should be feasible. This capability was demonstrated by performing TDMA and CDMA tests where in the TDMA version, all the users employ the same code but select different available time slots and in the CDMA version, the same single available time slot is used by everyone in the system with a different unique noise code assigned to each user. An interference rejection capability in excess of 46 db (or 40,000/1) was verified for both the TDMA and CDMA configurations. In the TDMA tests, a second user occupying any arbitrarily chosen available time slot did not interfere with the detection of the desired signal while

having a signal strength 46 db stronger than that of the desired signal. In the CDMA tests, one and two potentially interfering users employing different codes did not interfere with the detection of the desired signal while having a signal strength 46 db stronger than that of the desired signal.

The last test performed using an active configuration demonstrated that C.W. interference can be virtually totally eliminated while retaining the desired signal at its peak detected level using the interference canceling concepts described in this report. This unique result is realizable by virtue of the fact that multiplexed noise codes are capable of compressing to a lobeless impulse which facilitates obtaining a replica of the interference that does not interfere with the signal detection operation while being adjusted in phase to completely subtract or cancel the input interference. Experimental confirmation of the fact that multiplexed noise codes automatically provide a power gain margin or protection ratio equal to the number of code bits n was also made using the C.W. interference test set up. A measurement of the output and input signal-to-interference ratios made with the interference canceler disconnected showed in an improvement equal to the number of code bits n.

o Passive Configurations

The SAW device fabrication of a multiplexed noise code pair (which involved several iterations) provided a final device whose measured sidelobe plus noise level was 30 db below the main lobe. Although improved matching and packaging reduced the insertion loss considerably, the residual noise level still prevented obtaining an accurate measurement of the sidelobes and could yield misleading or inaccurate system test results. It was therefore considered expedient to postpone the fabrication of additional SAW devices until larger quartz substrates (which would enable obtaining an optimum design) became available. The larger substrates, however, never arrived during the allocated time for the research grant which prevented performing system tests and crosscorrelation function measurements using the passive configurations.

In view of the excellent results obtained using the active configurations, and the promising results obtained thus far in fabricating a SAW device code generator and compressor, the ET&D Laboratory intends to pursue the development and testing of multiplexed noise code generators and compressors. They plan to fabricate additional SAW devices when larger quartz substrates (ordered under the research grant) are received. These devices will then be subjected to system tests analogous to those employed using the active configurations with engineering support provided by the TRI-TAC Office.

Although most of the unique attributes inherent in multiplexed noise codes have been disclosed in this research program, there is more to exploit which has not been addressed. Multi-amplitude, multilevel and multidimensional multiplexed noise codes have been conceived that can provide code subclasses with additional unique properties. Continued investigations could result in the discovery of subclasses of these codes whose crosscorrelation function values are significantly less than $\sqrt{n}$ for all values of τ. This would enable the practical realization of asynchronous CDMA operation. Also, the multidimensional codes (this code class is simultaneously coded in phase and time) have the potential of providing an impulse ambiguity or uncertainty function (a code structure that is simultaneously lobeless in time (range) and frequency (doppler)). These concepts are described and their performance capabilities theoretically verified in the appropriate reports listed in the bibliography.

7. RECOMMENDATIONS

In view of the successful test results obtained on this research program in conjunction with the fact that multiplexed noise codes (as a code class) have the potential to provide an optimum design solution for numerous diversified applications in the communications science field, it is strongly recommended that appropriate government agencies utilize research funds to support further more advanced development and testing of multiplexed noise codes to establish their full capability. These codes would impact very little on the overall cost of systems while being capable of meeting the stringent and critical requirements of future communications systems. In fact, they would most likely offer substantial cost savings and provide superior performance over alternate attempts at satisfying the requirements of future systems.

ACKNOWLEDGEMENTS

The author wishes to express his gratitude to Major General James M. Rockwell and Dr. Robert E. Frese for their endorsement of his application for the Secretary of the Army's Research and Study Fellowship, to Mr. Brian Charnick for nominating him and to Dr. Clarence G. Thornton, Mr. V.G. Gelnovatch and Mr. Elio Mariani for making available the research facilities of the Electronic Technology and Devices Laboratory at Fort Monmouth, which included fabricating the necessary code generators/ matched filters and providing the work area, test equipment and peripheral devices needed to conduct the various system tests.

Special appreciation is extended to Mr. William J. Skudera, Mr. Granville LeMeune and Mr. Charles Heinzman for their direct involvement in device fabrication, procurement of required components, equipment evaluation and their assistance in performing the system tests. The success of this research program would not have been possible without their special expertise and support. In addition, Mr. Skudera, who designed the SAW devices, provided paragraph 4.c.(1) which describes their implementation.

Thanks are also extended to the many individuals at several of the various laboratories and centers of ERADCOM and CORADCOM at Fort Monmouth who so willingly loaned some of the required test equipment and peripheral devices. This includes Mr. Vincent Organic, Mr. Bert Bramble, Mr. Daniel Hadden, Mr. Joseph McCray, Dr. Arthur Ballato, Mr. Theodore Lukaszek, and Mr. Richard Tilton.

The author is also gratefully indebted to Mrs. Patricia Dowd for typing the complete final report.

APPENDIX A

General Code Mate Pair Expansion Concept

Verification that code mate pairs a and b expanded by the following general relationship results in a new mate pair A and B.

$$A = a(t), b(t+\tau_o) \quad (1)$$

$$B = a(t), \overline{b(t+\tau_o)} \quad (2)$$

where:

Code a = $a_1, a_2, a_3 \ldots a_n$.

Code b = $b_1, b_2, b_3 \ldots b_n$

$\bar{x}$ = complement of x (i.e., 1011 becomes 0100)

τ_o = a time delay of τ_o sec.

A code mate pair comprises two codes which satisfies the following equations

For a code pair a and b

$$\varphi_a(\tau) = -\varphi_b(\tau)$$

$$\text{for all } \tau \neq 0 \quad (3)$$

where:

$\varphi_a(\tau)$ = autocorrelation function of code a

$\varphi_b(\tau)$ = autocorrelation function of code b

Employing equations (1) and (2) results in

$$A = a_1, a_2, \ldots a_n, \ldots\ldots, b_1, b_2, \ldots b_n$$

$$B = a_1, a_2, \ldots a_n, \ldots\ldots, \overline{b_1}, \overline{b_2}, \ldots \overline{b_n}$$

which for clarity will be graphically presented as codes with code bit widths of Δ_o and a delay τ_o equal to $n + \Delta$.

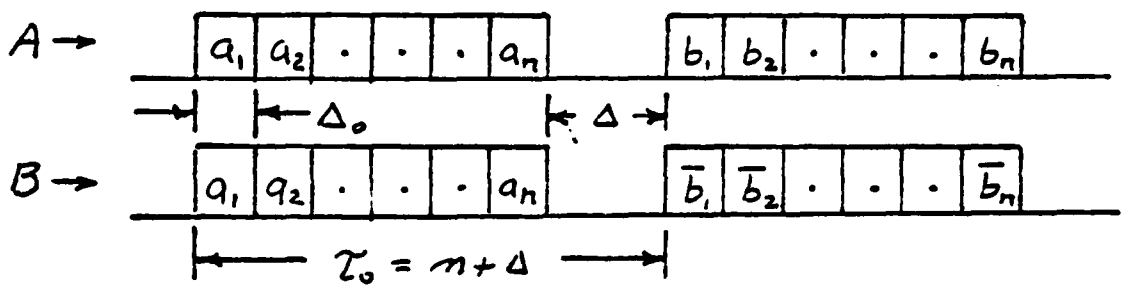

The autocorrelation function of Code A is then given by:

$$\phi_A(\tau) = \frac{1}{n}\sum_{i=1}^{n-\tau} a_i\, a_{(i+\tau)} + \frac{1}{n}\sum_{i=1}^{n-\tau} b_i\, b_{(i+\tau)}$$

$$\text{for } 0 \le \tau \le (n-1)$$

$$+ \frac{1}{n}\sum_{i=1}^{\tau-\Delta} b_i\, a_{(i+n-\tau+\Delta)}$$

$$\text{for } (\Delta+1) \le \tau \le (n-1+\Delta)$$

$$+ \frac{1}{n}\sum_{i=1}^{2n+\Delta-\tau} a_i\, b_{(i-n+\tau-\Delta)}$$

$$\text{for } (n+\Delta) \le \tau \le (2n-1+\Delta) \qquad (4)$$

And the autocorrelation function of Code B is:

$$\phi_B(\tau) = \frac{1}{n}\sum_{i=1}^{n-\tau} a_i\, a_{(i+\tau)} + \frac{1}{n}\sum_{i=1}^{n-\tau} \overline{b_i}\, \overline{b_{(i+\tau)}}$$

$$\text{for } 0 \le \tau \le (n-1)$$

$$+ \frac{1}{n}\sum_{i=1}^{\tau-\Delta} \overline{b_i}\, a_{(i+n-\tau+\Delta)}$$

$$\text{for } (\Delta+1) \le \tau \le (n-1+\Delta)$$

$$+ \frac{1}{n}\sum_{i=1}^{2n+\Delta-\tau} a_i\, \overline{b_{(i-n+\tau-\Delta)}}$$

$$\text{for } (n+\Delta) \le \tau \le (2n-1+\Delta) \qquad (5)$$

Since an autocorrelation function is an even function, that is $\phi(\tau) = \phi(-\tau)$, it is not necessary to define $\phi_A(\tau)$ or $\phi_B(\tau)$ for negative values of τ.

The first two terms of $\phi_A(\tau)$ and $\phi_B(\tau)$ in equations (4) and (5) sum to zero for all $\tau \neq 0$ since they define the autocorrelation functions of codes a and b or codes a and $\overline{b}$ which by definition form code mates.

Now let the 3rd and 4th terms of equation (4) be given by A_3 and A_4 and the 3rd and 4th terms of equation (5) be given by B_3 and B_4.

Then since

$$a_i\, b_j = -a_i\, \overline{b}_j \tag{6}$$

$$\phi_{A_3}(\tau) = -\phi_{B_3}(\tau) \qquad \text{for all } \tau \neq 0 \tag{7}$$

$$\phi_{A_4}(\tau) = -\phi_{B_4}(\tau) \qquad \text{for all } \tau \neq 0 \tag{8}$$

or

$$\phi_A(\tau) = -\phi_B(\tau) \qquad \text{for all } \tau \neq 0 \tag{9}$$

And the expanded code pair A and B form a new code mate pair.

Note that any a_i and b_j code bit can be zero and that τ_o can assume *any value*. When τ_o is less than the length of the first code (a or b) forming the expanded code, partial or complete interleaving of the code bits occur. The above proof verifies that equations (1) and (2) gurantee a new expanded mate pair for any degree of interleaving or butting for codes a and b.

APPENDIX B

Interference Canceling Spread Spectrum System Concepts

1. A C.W. Interference Canceling Spread Spectrum System Employing Active Coherent Detection

The implementation of a C.W. Interference canceler that uses coherent detection consists of a variable delay line (whose order of magnitude is equal to the compressed code bit width τ) and a linear adder. A functional block diagram of the canceler as utilized in a transmission link is shown in Figure B1. During the presence of C.W. interference at any frequency in the input bandwidth of the system , the delay device $(\tau + \epsilon)$ is varied in delay until the phase of the output interference is exactly 180° out of phase with its phase at the input. Adding the input to the output then results in the complete cancelation of the interference while causing no degradation at all in the output signal level. The retention of the desired signal level is readily demonstrated with an example.

Consider the following 4 bit multiplexed noise code pair

code a 1 0 0 0

code b 1 0 1 1

where 0 signifies +1

1 signifies -1

Then without the C. W. canceler interposed between the receiver and demultiplexer; the coherent matched filter detector would result in the following

For the code a channel

$$\begin{array}{rl} & 1\ 0\ 0\ 0 \\ \times & 1\ 0\ 0\ 0 \\ \hline \sum_a & +1+1+1+1 = +4 \end{array}$$

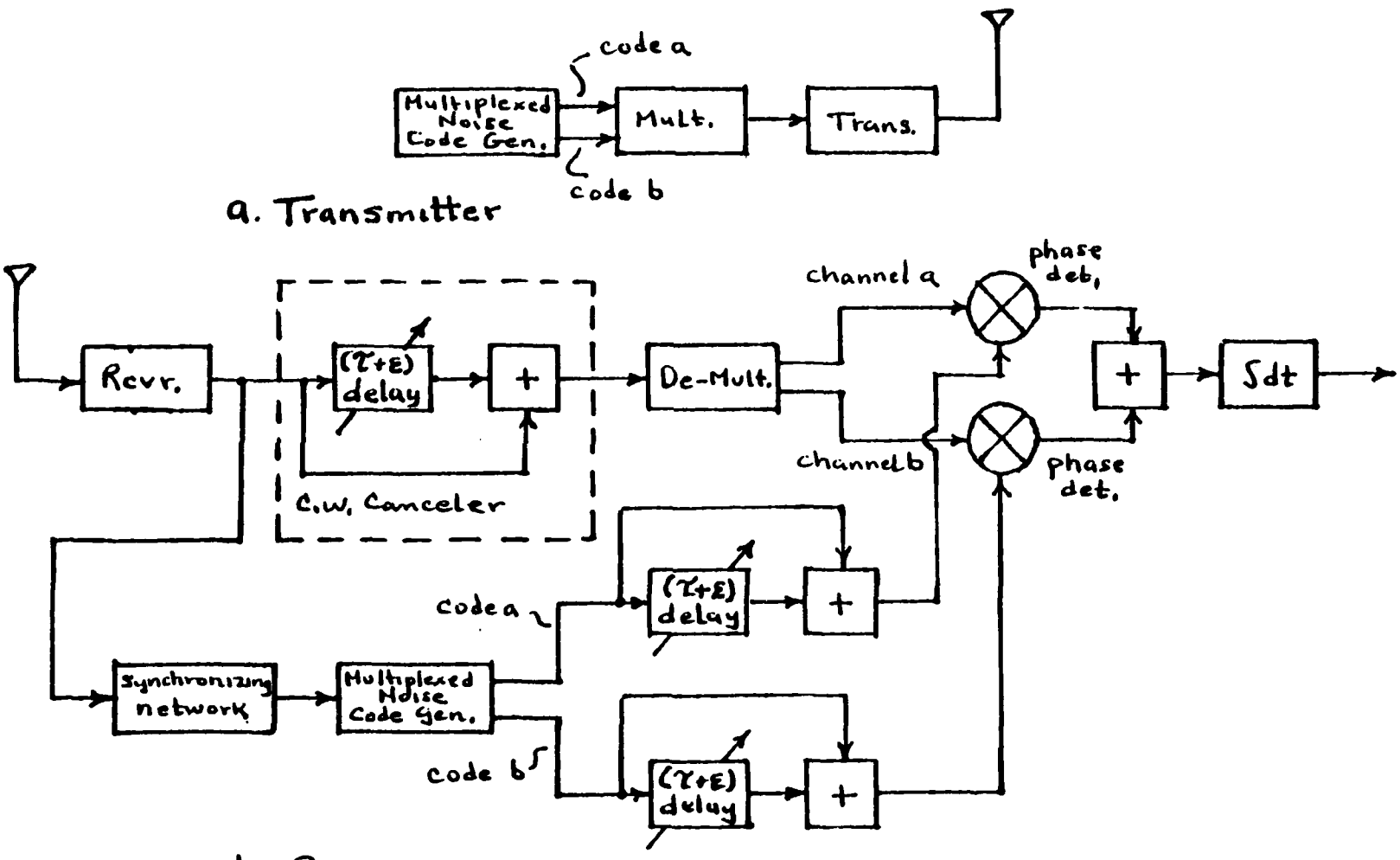

Fig. B1- C.W. Interference Canceling Spread Spectrum System

For the code b channel

$$\begin{array}{r} 1\ 0\ 1\ 1 \\ \times\ 1\ 0\ 1\ 1 \\ \hline \end{array}$$

$$\sum_b \quad +1+1+1+1 = +4$$

Or the total output signal level is

$$\sum_T = \sum_a + \sum_b = 4 + 4 = 8$$

where

$1 \times 1 = +1$

$0 \times 0 = +1$

$0 \times 1 = -1$

$1 \times 0 = -1$

The output signal voltage is eight times larger than the input signal voltage as a result of coherently summing the eight code bits. Since the input noise is uncorrelated during each code bit interval, the output noise voltage would sum on a root mean square or rms basis, hence the output noise voltage would be $\sqrt{8}$ times larger than the input noise. The output signal-to-noise voltage ratio $(\frac{S}{N})_o$ is therefore enhanced by $8/\sqrt{8}$ over the input signal-to-noise voltage ratio $(\frac{S}{N})_i$

In general

$$(\frac{S}{N})_o = \sqrt{n} \quad (\frac{S}{N})_i$$

or $$(\frac{P}{N})_o = n \quad (\frac{P}{N})_i$$

where

n = total number of code bits

$(\frac{P}{N})_i$ = input signal-to-noise power ratio

$(\frac{P}{N})_o$ = output signal-to-noise power ratio

When the interference canceler is interposed between the receiver and demultiplexer, the composite signal entering the coherent detectors becomes

For the code a channel

$$\begin{array}{r} 1\ 0\ 0\ 0 \leftarrow \text{code a signal} \\ +\quad 1\ 0\ 0\ 0 \leftarrow \text{delayed code a signal} \\ \hline \end{array}$$

$$e_a = 1 \cdot 0^2 0^2 0$$

where

e_a = input to the detector for code a

The exponent indicates the amplitude

$0^K = +K$

$1^K = -K$

A dot signifies a zero amplitude

For the code b channel

$$\begin{array}{rl} & 1\ 0\ 1\ 1 \leftarrow \text{code b signal} \\ + & \quad 1\ 0\ 1\ 1 \leftarrow \text{delayed code b signal} \\ \hline e_b = & 1 \cdot\ \cdot\ 1^2 1 \end{array}$$

where

e_b = input to the detector for code b

The summed (integrated)output of the phase detector for channel a now becomes

$$\begin{array}{rl} & 1 \cdot 0^2 0^2 0 \\ \times & 1\ 0\ 0\ 0 \\ \hline \sum_a & +1 \cdot +2 +2 = +5 \end{array}$$

And the integrated output of the phase detector for channel b is

$$\begin{array}{rl} & 1 \cdot\ \cdot 1^2 1 \\ \times & 1\ 0\ 1\ 1 \\ \hline \sum_b & +1 \cdot\ \cdot +2 = +3 \end{array}$$

Or the total output signal level is

$$\sum_T = \sum_a + \sum_b = 5 + 3 = +8$$

Hence there is no loss in the output signal level due to the presence of the delayed signal. Since the canceler doubles the noise power as a result of adding the delayed noise to the input noise, there would be a net 3 db degradation in the output signal-to-noise ratio when compared to operating without the interference canceler. This 3 db loss in $\left(\frac{S}{n}\right)$ could however be regained by simply delaying the reference signal by $(\tau \mp \varepsilon)$ and using it to coherently detect the delayed portion of the composite input signal.

In this case, the output of the detector corresponding to the delayed reference becomes

For channel a, the integrated output is

$$\begin{array}{r} 1 \cdot 0^2 0^2 0 \\ \times \quad 1\ 0\ 0\ 0 \\ \hline \end{array}$$

$$\Sigma_a \quad \cdot \cdot +2+2+1 = +5$$

And for channel b, the integrated output is

$$\begin{array}{r} 1 \cdot \cdot 1\ 1 \\ \times \quad 1\ 0\ 1\ 1 \\ \hline \end{array}$$

$$\Sigma_b \quad \cdot \cdot \cdot +2+1 = +3$$

Or the total output of the detector for the delayed portion of the input signal is

$$\Sigma_T = \Sigma_a + \Sigma_b = 5 + 3 = +8$$

Coherently adding this to the detected undelayed signal then enhances the output signal-to-noise power ratio by 2 or regaines the 3 db loss incurred when summing in the C.W. canceler.

To further illustrate this point, consider the actual operation of the coherent detector as shown in Figure 1. The summed reference and its delayed replica are the same as the composite input signal.

Multiplying and integrating in the channel a detector then produces

$$\begin{array}{r} 1 \cdot 0^2 0^2 0 \\ \times\ 1 \cdot 0^2 0^2 0 \\ \hline \end{array}$$

$$\Sigma_a \ +1 \ \cdot +4+4+1 = +10$$

And multiplying and integrating in channel b filter results in

$$\begin{array}{r} 1 \cdot \cdot 1^2 1 \\ \times\ 1 \cdot \cdot 1^2 1 \\ \hline \end{array}$$

$$\Sigma_b \ +1 \ \cdot \cdot +4+1 = +6$$

Or the total output signal level is now

$$\Sigma_T = \Sigma_a + \Sigma_b = +16$$

Since the input noise is uncorrelated from bit to bit, it will sum in the integrator on an rms basis. Therefore for channel a

$$\begin{array}{l} N_i\ N_i\ N_i\ N_i\ N_i \\ \times\ 1\ \cdot\ 0^2\ 0^2\ 0 \\ \hline N_i\ \cdot + 2N_i + 2N_i + N_i \end{array}$$

or

$$N_a = \sqrt{N_i^2 + 4N_i^2 + 4N_i^2 + N_i^2}$$

$$= \sqrt{10}\, N_i$$

And for channel b

$$\begin{array}{l} N_i\ N_i\ N_i\ N_i\ N_i \\ \times\ 1\ \cdot\ \cdot\ 1^2\ 1 \\ \hline N_i\ \cdot\ \cdot\ 2N_i\ N_i \end{array}$$

or

$$N_b = \sqrt{N_i^2 + 4N_i^2 + N_i^2}$$

$$= \sqrt{6}\, N_i$$

And the total noise in then

$$N_T = \sqrt{N_a^2 + N_b^2}$$

$$= \sqrt{16}\, N_i$$

The resultant output signal-to-noise voltage ratio is therefore

$$\left(\frac{S}{N}\right)_o = \frac{16\, S_i}{\sqrt{16}\, N_i} = \sqrt{16}\, \left(\frac{S}{N}\right)_i$$

Or the output $\left(\frac{S}{N}\right)$ power ratio is improved by 16

$$\left(\frac{P}{N}\right)_o = 16\, \left(\frac{P}{N}\right)_i$$

which is an improvement of 2/1 over the case where only the undelayed signal is detected or again we see that the 3 db loss incurred by the canceler has been regained.

It is important to note that the length of the code structure is immaterial and simple 4 bit or even 2 bit noise code pairs enable the total cancelation of a strong C. W. interferer to be achieved.

It should be evident that several C.W. cancelers of the type illustrated can be utilized in tandem to totally eliminate multiple C.W. interference.

It should also be mentioned that slowly varying C.W. could be readily accommodated by forming a closed loop whereby the output interference level would be continuously monitored in some type of null detector and the variable delay ($\tau + \varepsilon$) adjusted until the interference was canceled and retained at a null position. A practical system would, in fact, require some type of interference monitor while adjusting the delay to affect a null.

2. A Pulse Interference Canceling Spread Spectrum System Employing Passive Pulse Compression

The hardware implementation of a pulse interference canceler using passive pulse compression consists of a variable delay line (whose order of magnitude is equal to the compressed code bit width τ) and a linear adder which follows the summed output of the pulse compression matched filters for the multiplexed noise code pair. A functional block diagram of the canceler as utilized in a transmission link is shown in figure B2. During the presence of an interfering pulse, the delay device ($\tau + \varepsilon$) is varied in delay until the phase of the interfering pulse in time slot T_o (this time slot is gated out and represents the selected time interval for detecting the received signal) is exactly 180^o out of phase with its phase at the input. Adding the input to the output and gating out the resultant signal in time interval T_o then results in the total cancellation of the pulse interference with the output peak signal level remaining the same as at the input to the canceler. In essence, because the noise code employed is capable of lobeless compression, the simple operation described provides a coherent replica of the interfering pulse exclusive of the desired signal which facilitates subtracting out the interference completely (regardless of its relative level) without reducing the desired signal. This proposed concept is readily clarified with an example.

Consider the following 4 bit multiplexed noise code pair a and b as being utilized over the transmission link with a and b orthogonally multiplexed over 2 channels.

Code a - 1 0 0 0

Code b - 1 0 1 1

And assume the presence of a strong interfering pulse x with $x >> 1$ occuring during the third code bit of code a.

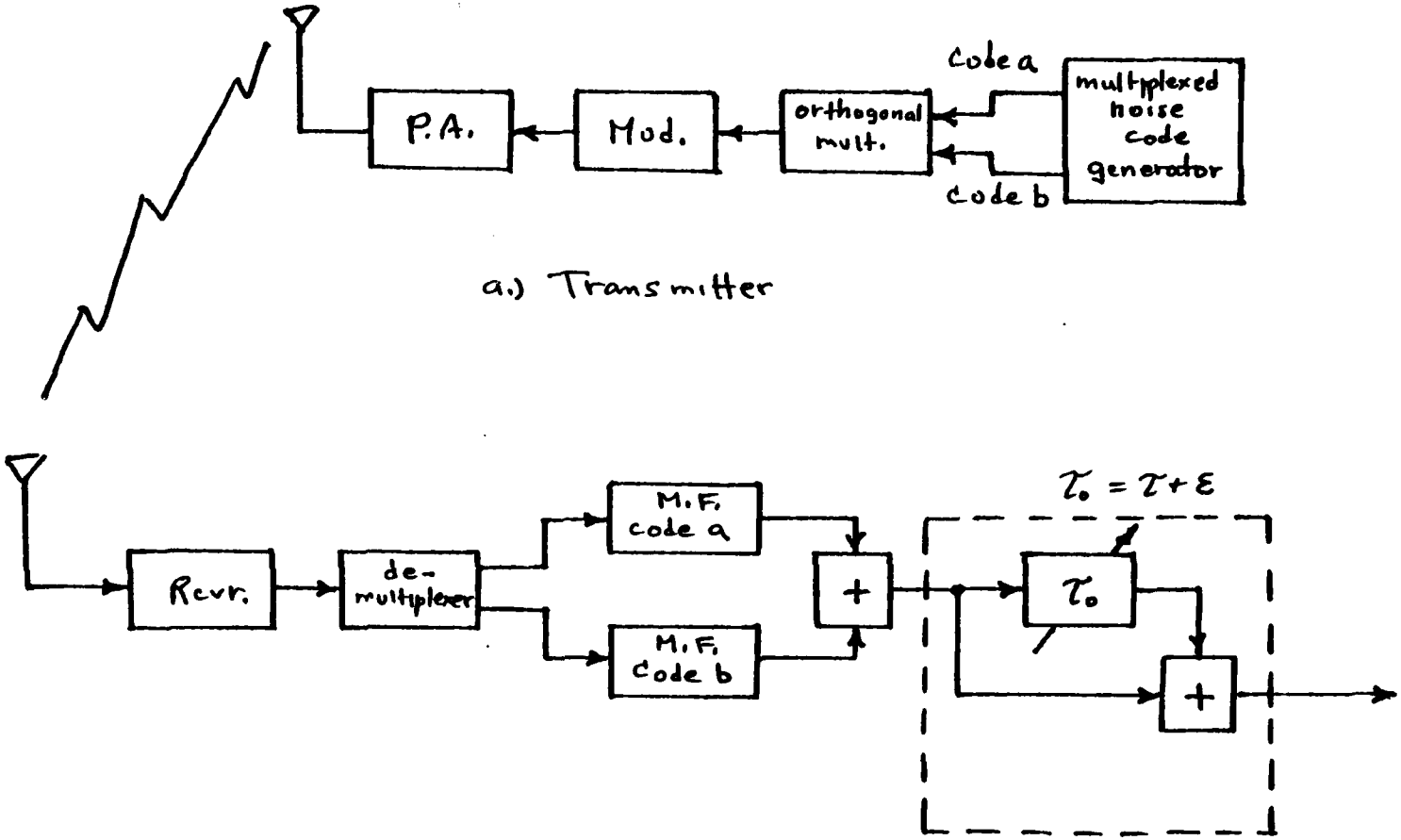

Figure B2 – Pulse Interference Canceling Spread Spectrum System

Compressing code a results in

$$
\begin{array}{l}
\ \overset{x}{} \\
1\ 0\ 0\ 0 \\
\ \overset{x}{} \\
1\ 0\ 0\ 0 \\
\ \overset{x}{} \\
1\ 0\ 0\ 0 \\
\ \overset{\bar{x}}{} \\
\hline
0\ 1\ 1\ 1 \\
\hline
\end{array}
$$

$$
\begin{array}{l}
\ x\ x_4 x\ - \\
1\ .\ 0\ 0^{\ }0\ x\ 1 \\
\ \overset{x}{} \\
\end{array}
$$

where 0^{y} signifies an amplitude of $(y + x)$

$$\bar{x} = -x$$

Compressing code b yields

$$
\begin{array}{l}
0\ 1\ 0\ 0 \\
0\ 1\ 0\ 0 \\
1\ 0\ 1\ 1 \\
\hline
0\ 1\ 0\ 0 \\
\hline
\end{array}
$$

$$0\ .\ 1\ 0^{4}1\ .\ 0$$

And adding the two outputs results in

$$
\begin{array}{l}
\phantom{1\,.\,0\,0^{4}0\,x\,1}\ x\ x\ x\ - \\
1\ .\ 0\ 0^{4}0\ x\ 1 \\
\underline{0\ .\ 1\ 0^{4}1\ .\ 0} \\
\phantom{1\,.\,0\,0^{4}0\,x\,1}\ x_8\ - \\
\ .\ .\ x\ 0^{8}x\ x\ .
\end{array}
$$

Note that the amplitude of the desired signal has increased by 8 whereas the interfering pulse has spread (coherently) over 4 time slots with no increase in level during the time slot containing the desired signal.

Delaying this compressed signal by $\tau_o = \tau + \varepsilon$ and adding it to itself then yields

$$
\begin{array}{l}
\overset{x}{0}\overset{-}{} \\
x\ 0^{8}x\ x \\
\qquad \overset{x}{0}\overset{-}{} \\
\qquad x\ 0^{8}x\ x \\
\hline
x\ 0^{8}0^{8}\overset{-}{x}^{2}x \\
\qquad \leftarrow\!| \quad |\!\leftarrow T_0
\end{array}
$$

where ε represents a vernier time or phase shift that inverts x

And applying a gate around T_0 provides an interference free signal that has the same amplitude as when no interference was present. Actually either or both of the interference free pulses could be gated out. The gate position T_0 is shown delayed one bit to account for the situation where the interfering pulse occurred during the last bit.

It should be mentioned that if the frequency of the interfering pulse was varied from pulse to pulse from an interfering pulse train, then a closed loop could be easily formed whereby the output interference would be continuously monitored using an appropriate type of null detector and the variable delay ($\tau + \varepsilon$) adjusted to maintain the interference at a null or zero level.

3. A Pulse Interference Canceling Spread Spectrum System Employing Active Coherent Detection

The hardware implementation for a pulse interference canceler that employs coherent detection consists of two variable delay lines (whose order of magnitude for the delay is equal to the width τ of each code bit), a second active coherent (matched filter) detector and a linear adder. A functional block diagram of the canceler as utilized in a transmission link is shown in Figure B3. During the presence of an interfering pulse, the vernier portion of the delay devices ε are varied in delay until the phase of the interference in the delayed channel is exactly 180^0 out of phase with the phase of the interference in the undelayed channel. Simply adding the detector outputs of the two channels then completely cancels the interference while leaving the desired signal at its peak value. In essence, because the noise code is capable of lobeless compression, the simple implementation described provides a coherent replica of the interference exclusive of the desired signal which facilitates subtracting out the interference completely (regardless of its level) without reducing the level of the desired signal. This concept is readily clarified with an example.

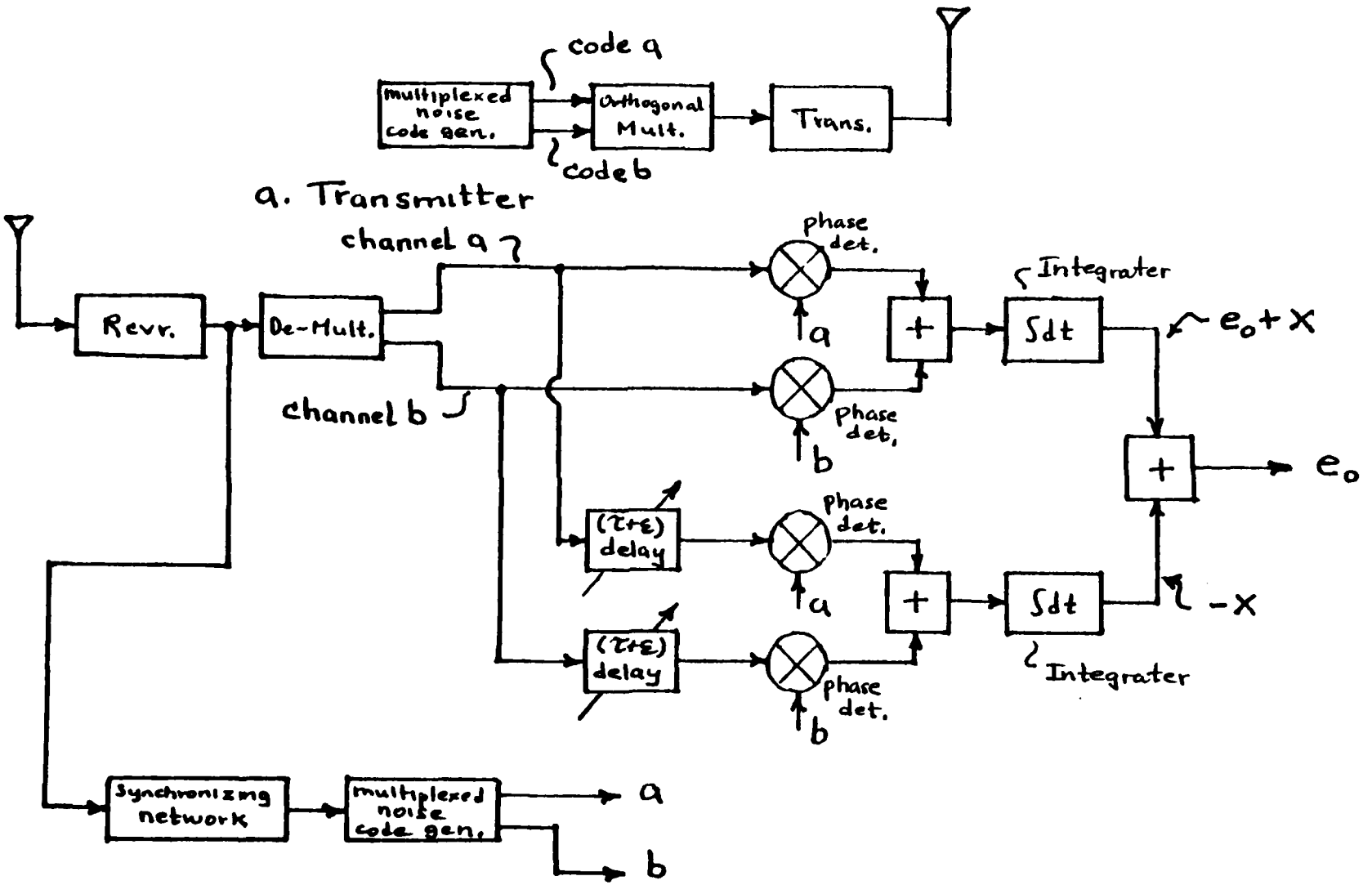

b. Receiver with Active Coherent Detection

FIG. B3 - Pulse Interference Canceling Spread Spectrum System

Consider the following 4 bit multiplexed noise code pair a and b as being utilized over the transmission link with codes a and b orthogonally multiplexed over 2 channels.

Code a - 1 1 1 0

Code b - 0 0 1 0

And assume the presence of a strong interfering pulse x with x >> 1 occuring during the third code bit of code a.

a = 1 1 (1+X) 0

b = 0 0 1 0

Coherently detecting this composite signal in the undelayed channels results in

For code a

$$\begin{array}{r} 1\ 1\ (1+X)\ 0 \\ X\ 1\ 1\ \ 1\ \ 0 \\ \hline \end{array}$$

$$\phi_a(0) = \sum +1+1(+1+X)+1 = +4+X$$

For code b

$$\begin{array}{r} 0\ 0\ 1\ 0 \\ X\ 0\ 0\ 1\ 0 \\ \hline \end{array}$$

$$\phi_b(0) = \sum +1+1+1+1 = +4$$

Hence

$$\phi_T(0) = 8 + X$$

And coherently detecting the delayed input signal yields

For code a

$$\begin{array}{r} 1\ 1\ (1+X)\ 0 \\ X\ 1\ 1\ 1\ \ 0 \\ \hline \end{array}$$

$$\phi_a(1) = \sum \cdot +1+1(-1+X) \cdot = +1+X$$

For code b

$$\begin{array}{r} 0\ 1\ 0\ 0 \\ X\ 0\ 1\ 0\ 0 \\ \hline \end{array}$$

$$\phi_b(1) = \sum \cdot -1-1+1 \cdot = -1$$

Hence

$$\phi_T(1) = X$$

which provides a coherent replica of the interference that is completely free of the desired signal. Adjusting the vernier portion of the delay ε then results in X being equal and opposite to its value in the undelayed channel and the simple linear addition of the two channels results in completely canceling the interference.

$$e_o = \phi_T(0) + \phi_T(1)$$

$$= S + X - X = S$$

If the frequency of the interfering pulse is varied from pulse to pulse of an interfering pulse train, then a closed loop can be formed whereby the output interference would be monitored using an appropriate type of null detector and the variable delay $(\tau + \varepsilon)$ continuously adjusted to maintain the interference at a null or zero level.

APPENDIX C

An Orthogonal Spread Spectrum TDMA Mobile Subscriber Access System

1. Introduction.

A concept is described that identifies a new approach for implementing an orthogonal mobile subscriber access TDMA system which utilizes noise codes to optimize transmission efficiency and simultaneously obtain a large degree of A/J protection. The result is realized by using noise codes that compress lobelessly in conjunction with obtaining a synchronous time reference in space for all the users that access the system.

2. Concept Description.

a. General. The basic approach is illustrated in Figure C1 where user No. 1 is connected with 1' via time slot 1, 2 with 2' via time slot 2, 3 with 3' via time slot 3, etc. Each user pair has their associated time slot (or pair of time slots for time multiplexed duplex operation) established and maintained synchronous at a common central station or node. The time slots may be preassigned or adaptively selected.

Since the intended application is for mobile random access, omni-directional antennas must be used. This would result in self-interference between the mobile users (i.e., over the direct paths) since only the time multiplexed access signals emanating from the central are rendered totally non-interfering. In order to retain the system orthogonal, all transmissions from the various users to the central are in one frequency band and those from the central to the mobile users are in a different frequency band. This causes the mobile users to only be receptive to transmissions from the central which then provides a space time reference for all of the mobile users. The various channels existing in the transmitted output from the central are kept orthogonal using a loop back synchronous timing scheme.

The proposed concept may be applied to the signaling and control traffic, the message traffic, or both. It will be described in terms of available access channels (these may represent either a group of user address channels for call-up signaling traffic or the available channels for communicating with message traffic) to facilitate presenting the technique as a general concept for application in any ground mobile TDMA communication system.

b. Timing. The basic philosophy involved in obtaining a synchronous mobile user is illustrated in Figure C2. A pulsed timing signal is transmitted to the central and returned to the mobile user with a frequency shift equal to twice the doppler frequency. This signal ($f + 2f_d$) is then compared in phase or time with the clock standard prf frequency ($f_o + f_{do}$) that is simultaneously received from the central node and the output of the time discriminator is used to control the loop V.C.O. This frequency is changed until upon lock, its frequency is equal to ($f_o - f_{do}$). In this state, the frequency of all of the users would arrive at the Central Node with a synchronous frequency equal to f_o and can be time multiplexed into any available time slot at the central.

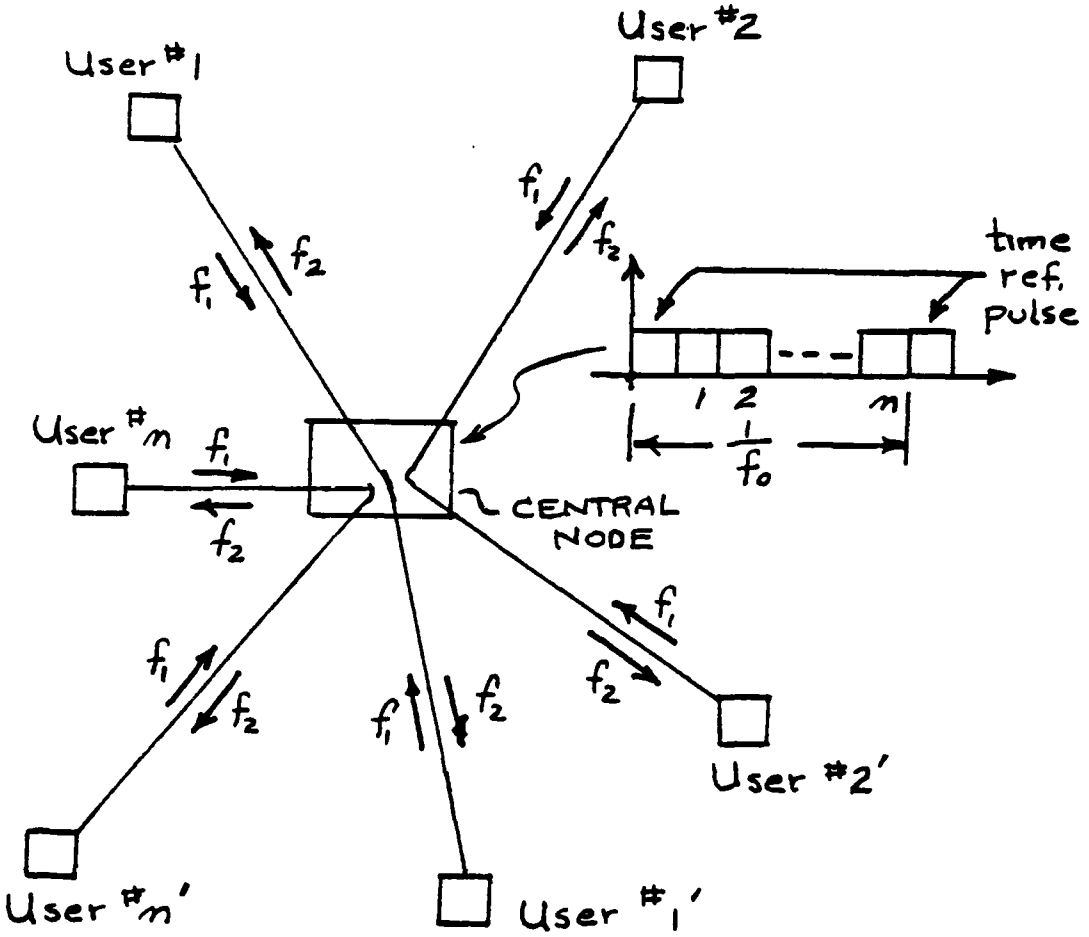

FIGURE C1 - Ground Mobile Access System Employing Orthogonal TDMA

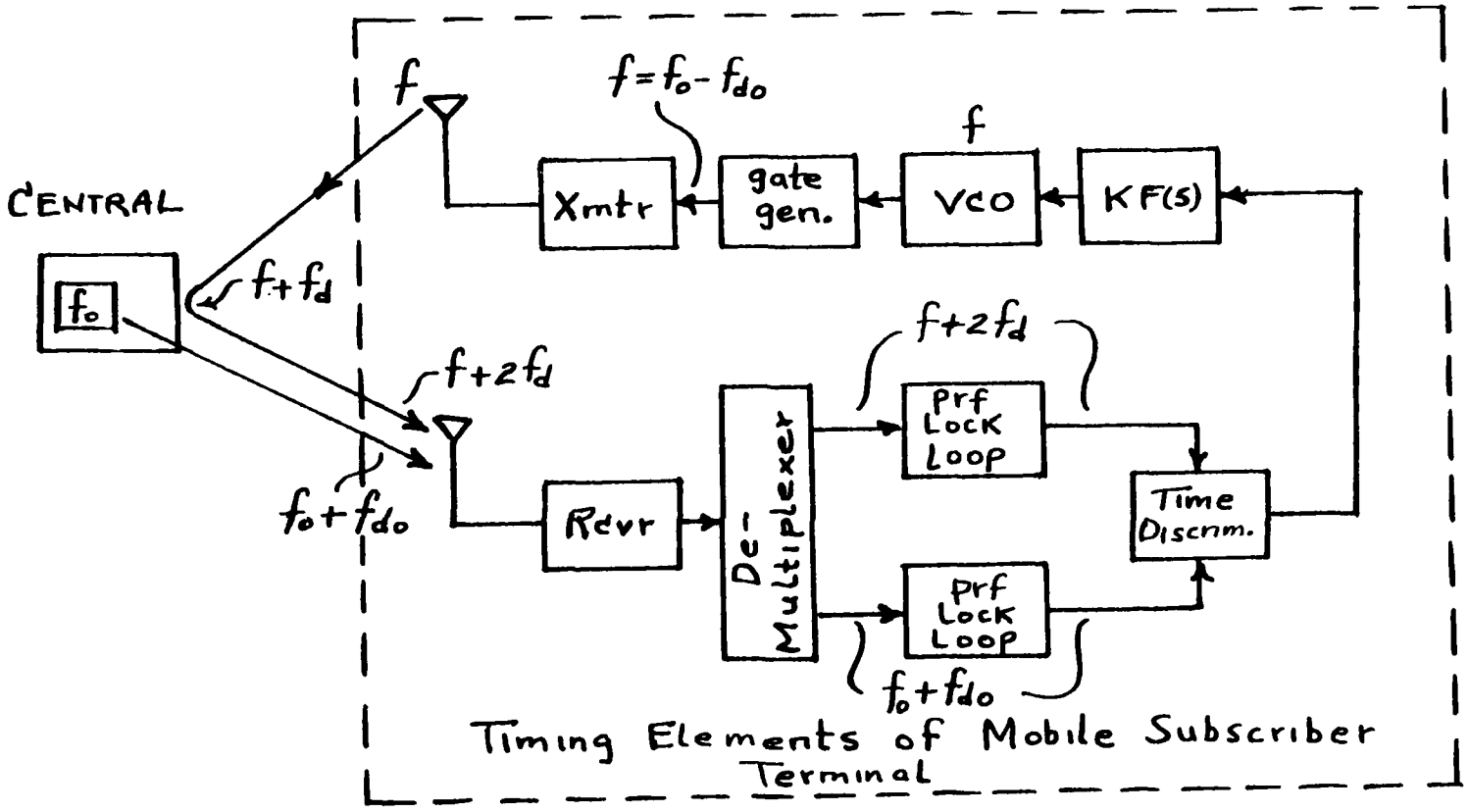

FIGURE C2 - Loop Back Synchronous Timing Subsystem

The implementation requires using a separate orthogonal channel for the loop signal frequency f. This is demultiplexed from the central clock signal and the demultiplexed outputs are then compared in a loop time discriminator whose output is filtered and used to control the V.C.O. The frequency f of the V.C.O. is automatically changed until the loop around transmission is synchronized.

When the transmission loop is locked: The time discriminator output is zero, and

$$f + 2f_d = f_o + f_{do} \tag{1}$$

Since the path to and from the central node is the same

$$f_d = f_{do} \tag{2}$$

Hence

$$f = f_o - f_{do} \tag{3}$$

Therefore, the signal frequency received from each mobile user at the Central is

$$f + f_d = f_o - f_{do} + f_d = f_o$$

c. Spread Spectrum Coding. Since the proposed system is orthogonal in operation, perfect (lobeless) noise codes may be utilized to great advantage. A jamming protection ratio that is equal to the number of accesses may be obtained with no required increase in bandwidth (or spectrum) beyond that needed to accommodate the number of accessing channels. If a system was designed to accommodate 1000 access channels, then a 1000 bit noise code could be utilized which would result in reducing the power of a jammer by 1000/1 or 30db over a TDMA system using no coding and the same peak power. Two methods of generating and compressing perfect noise codes involves multiplexed coding and multidimensional coding. Their utilization in the proposed mobile TDMA system will now be illustrated.

(1) Multiplexed Codes. Perfect noise codes are codes which comprise an impulse autocorrelation function (i.e., codes which compress to a single impulse containing no lobes) are realizable by employing multiplexed mate code pairs that meet the following conditions. The autocorrelation function of the two codes forming a mate pair must be of equal magnitude and opposite sense for all values of time outside of the main lobe. Expressed mathematically: For two mate pair codes a and b

$$\varphi_a(\tau) = -\varphi_b(\tau)$$

for all $\tau \neq 0$

where $\varphi_a(\tau)$ = autocorrelation function of code a

$\varphi_b(\tau)$ = autocorrelation function of code b

When two codes meet this requirement, then the simple linear sum of their orthogonally multiplexed matched filter outputs results in compressing the composite code structure into a single impulse.

A general functional block diagram of a communication link employing multiplexed coding is shown in Figure C3 The specific method of orthogonally separating the mate pair codes is immaterial and may involve TDM, FDM, horizontal and vertical antenna polarization or quadrature phase modulation. Better approaches exist for generating and compressing multiplexed codes and are described in several granted and pending patents and technical reports. A preferred approach would depend on the specific application and user requirements.

Let us now utilize the following example multiplexed code pair in the proposed TDMA system.

Code a = 0001

Code b = 0100

where:

0 indicates a plus (+)

1 indicates a minus (-)

Consider three users accessing the system with the selected (either preassigned or adaptively) channels occupying the first, third and fourth time slot positions. Different amplitudes will be assumed for the separate single channel users accessing the system to demonstrate that utilizing perfect noise codes enables the system to operate completely free of self-interference even for large differences in received power levels. The amplitudes and phases of the three users arriving at the Central will be taken to be +2, +4, -1.

If each of the separate users employs the proposed perfect noise code, then the composite signal received at the Central would be as shown below.

The code (a) composite signal would be:

Time Slot	-3	-2	-1	+1	+2	+3	+4
User #1	0^2	0^2	0^2	1^2			
User #2			0^4	0^4	0^4	1^4	.
User #3				1	1	1	0
Σ(a)	0^2	0^2	0^6	0	0^3	1^5	0

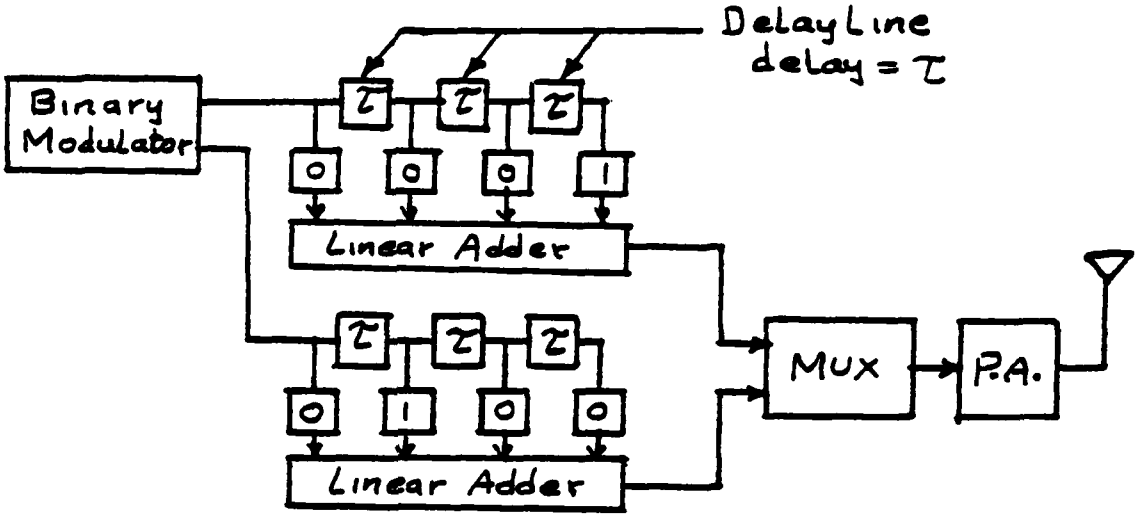

a.) Multiplexed Coder / Transmitter

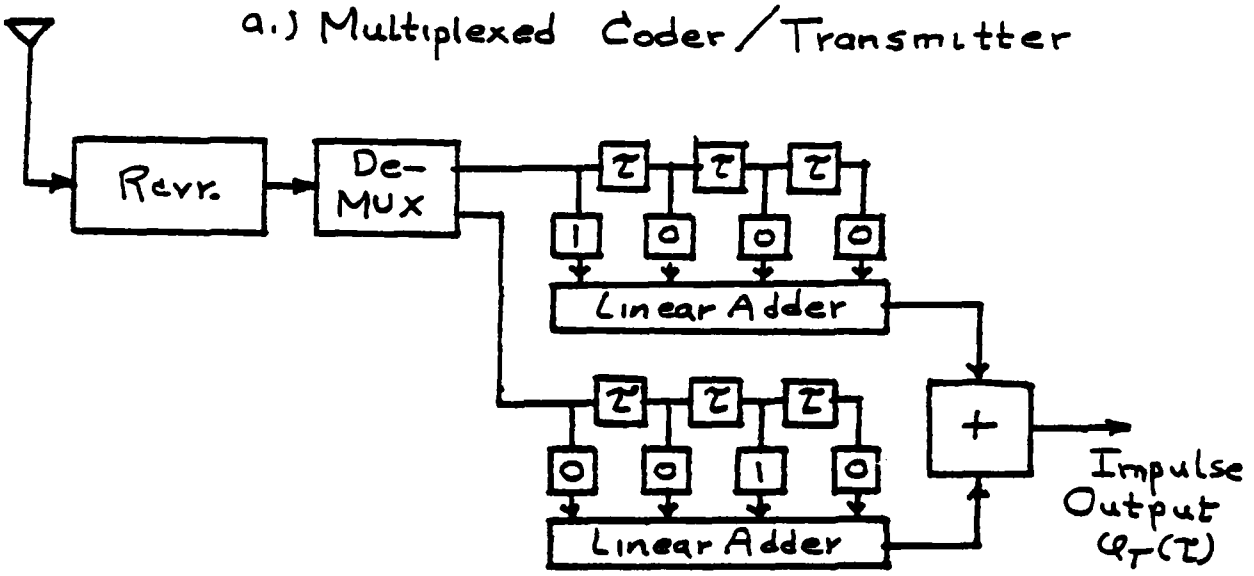

b.) Multiplexed Pulse Compressor / Receiver

Code a = 0 0 0 1 $\quad \varphi_a(\tau) = 1 \cdot 0\,0^4\,0 \cdot 1$

Code b = 0 1 0 0 $\quad \varphi_b(\tau) = 0 \cdot 1\,0^4\,1 \cdot 0$

$\varphi_T(\tau) = \cdots 0^8 \cdots$

Figure 3 - Multiplexed Code Transceiver

where the exponent indicates the amplitude

The code (b) composite signal would be:

Time Slot	-3	-2	-1	+1	+2	+3	+4
User #1	0^2	1^2	0^2	0^2			
User #2			0^4	1^4	0^4	0^4	
User #3				1	0	1	1
Σ(b)	0^2	1^2	0^6	1^3	0^5	0^3	1

The composite outputs are now pulse compressed in their respective matched filters and linearly added.

Pulse compressing Σ code (a) results in:

Time Slot		-3	-2	-1	+1	+2	+3	+4	+5	+6	+7
Pulse Comp. Filter	1	1^2	1^2	1^6	1	1^3	0^5	1			
	0		0^2	0^2	0^6	0	0^3	1^5	0		
	0			0^2	0^2	0^6	0	0^3	1^5	0	
	0				0^2	0^2	0^6	0	0^3	1^5	0
Filter Output $\Sigma\varphi_a(\tau)$		1^2	.	1^2	0^9	0^6	0^{15}	1^2	1	1^4	0

And pulse compressing Σ code (b) results in:

Time Slot__		-3	-2	-1	+1	+2	+3	+4	+5	+6	+7
Pulse Comp. Filter	0	0^2	1^2	0^6	1^3	0^5	0^3	1	·		
	0		0^2	1^2	0^6	1^3	0^5	0^3	1		
	1			1^2	0^2	1^6	0^3	1^5	1^3	0	
	0				0^2	1^2	0^6	1^3	0^5	0^3	1
Filter Output $\Sigma\varphi_b(\tau)$		0^2	·	0^2	0^7	1^6	0^{17}	1^6	0	0^4	1

The linear sum of the two matched filter outputs then yields:

Time Slot	-3	-2	-1	+1	+2	+3	+4	+5	+6	+7
$\Sigma\varphi_a(\tau)$	1^2	·	1^2	0^9	0^6	0^{15}	1^2	1	1^4	0
$\Sigma\varphi_b(\tau)$	0^2	·	0^2	0^7	1^6	0^{17}	1^6	0	0^4	1
$\Sigma\varphi_T(\tau)$	·	·	·	0^{16}	·	0^{32}	1^8	·	·	·

Note that the compressed information bits of the three separate users are totally non-interfering (each has compressed to its proper amplitude and phase) and each received signal voltage is increased by a factor of eight. The factor of eight is simply the time-bandwidth product or equivalently, the number of noise code bits contained in each information bit. The signal-to-noise power ratio or the signal-to-jammer power ratio in a hostile environment is increased by the time-bandwidth product (*i.e., the protection ratio*).

A gated automatic gain control loop (AGC) would now adjust the individual channel signals to the same level for re-transmission to the mobile users. The composite group of TDMA channels would be noise coded again as a multiplexed noise code pair (this could be either the same as or different than the received noise code structure) in a hostile environment. Similar demultiplexing and matched filter detection in each user receiver would result in the non-interfered with reception of all the channel signals. Each user would then simply gate out his selected time slot prior to demodulation of the information to provide an output that is totally non-interfered with by the other users in the system and which simultaneously provides a protection against jammers equal to the number of accesses with no required increase in bandwidth.

APPENDIX D

An Orthogonal CDMA System

1. Introduction.

Normally the utilization of different noise codes for the users of a mobile subscriber multiple-access system results in non-orthogonal operation. That is, self-interference is inherent in the system operation and although each interfering signal is reduced by the time-bandwidth product, interfering users in close proximity are generally intolerable. A unique characteristic of the specific class of multiplexed noise codes, however, enables a system implementation which operates orthogonally (with zero self-interference) even though a different unique code is utilized by each user in the system. Cancellation of the interference with either antenna or signal processing (these type of solutions are employed in other proposed methods of minimizing or eliminating the near-far ratio self-interference disadvantage that is inherent in noise coded multiple-access systems) is not required in the concept proposed here.

The property of multiplexed noise codes as a class that is of primary significance for the proposed concept is that code subclasses exist whereby the cross-correlation between any two unique multiplexed noise codes of the subclass is always zero at $\tau = o$. Although spurious lobes exist whose averaged (rms) value has an amplitude that is down by at least the square root of the code sequence length (i.e. the time-bandwidth product), the absence of any cross-correlation value in the same time slot (at $\tau = o$) for all the codes enables the implementation of a synchronously timed system that operates orthogonally (i.e. with zero self-interference).

2. Concept Description.

A typical deployment for the system which illustrates the requirements needed to establish a synchronously timed system is shown in Figure D1. All the users in the system adjust their timing (synchronously) such that their coded signal of n bits arrives at a common central node during the time interval T_o. Communicating via a central provides a common time reference for achieving a synchronously timed system. The nth time bit or time slot corresponds to $\tau = o$ and all communications of each user occurs in this single same time slot.

Since the intended application is for mobile random access, omni-directional antennas would generally be used. This would result in self-interference between the users over direct paths since only the synchronized access signals emanating from the central are rendered totally non-interfering. In order to retain the system orthogonal, all the transmissions from the various users to the central are in one frequency band and those from the central to the mobile users are in a different frequency band. This causes the mobile users to only be receptive to transmissions from the central which then provides a space time reference for all of the users. The various accessing signals are kept

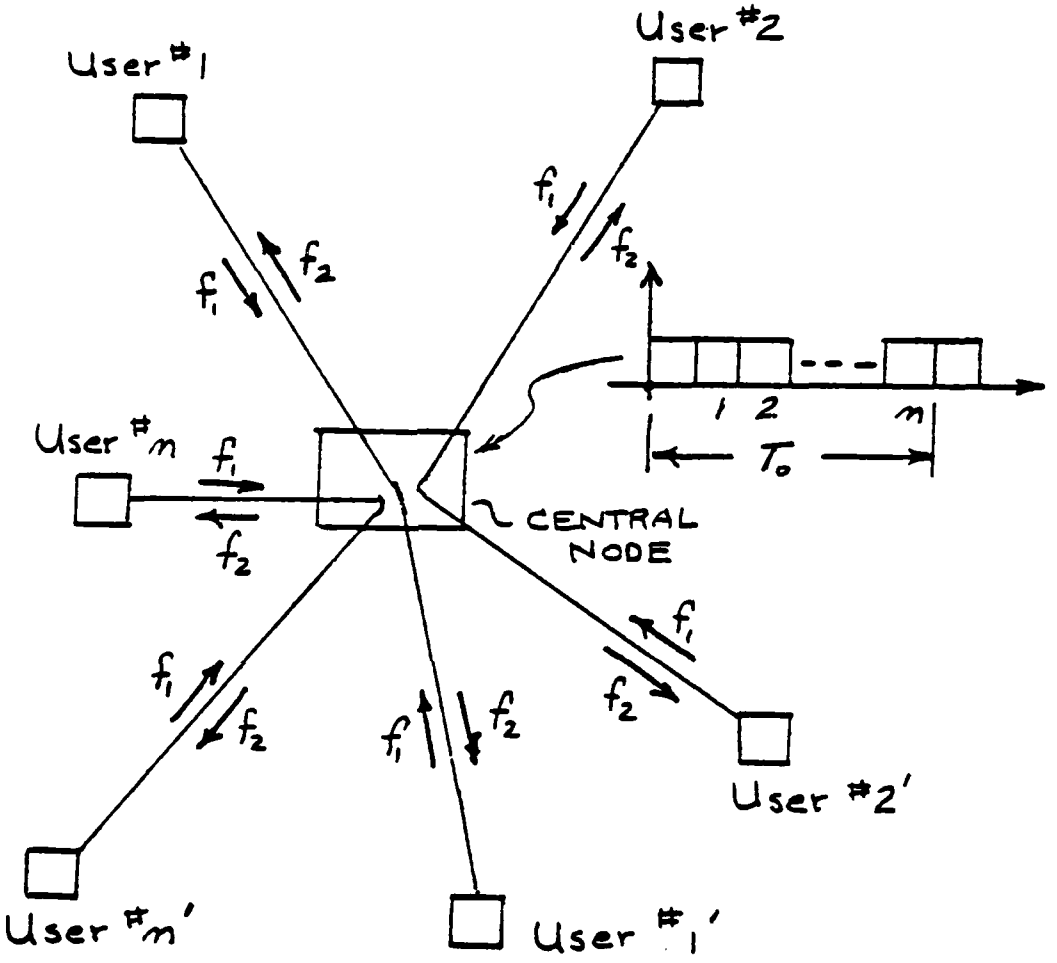

FIGURE D1 - Ground Mobile Access System Employing Orthogonal CDMA

orthogonal (synchronously timed to the single time slot) using a loop back synchronous timing scheme at each user terminal identical to that employed for the TDMA approach as described in Appendix C.

Although all of the received different unique noise codes arrive and are re-transmitted during the same time, they are rendered non-interfering when pulse compressed (matched filter detected) and gated. This unique property is an inherent characteristic of specific multiplexed noise code subclasses. Multiplexed noise codes are codes formed with mate pairs that comprise an impulse autocorrelation function (i.e., noise codes which compress to a single impulse containing no lobes).

A general functional block diagram of a communication link employing multiplexed codes is shown in Figure D2. The specific method of orthogonally separating the mate pair codes is immaterial and may involve TDM, FDM, horizontal and vertical antenna polarization or quadrature phase modulation. Better implementation means exist for generating and compressing multiplexed codes and are described in several granted and pending patents and technical reports. A preferred code generation/compression technique would depend on the specific application and user requirements.

Subclasses of these codes which possess the required advertised characteristic of having a crosscorrelation value of zero at $\tau=0$ were found to exist in sufficient quantity to support the practical implementation of an orthogonal multiple-access system as described in this appendix. Hand calculations of the crosscorrelation function of four and eight bit multiplexed mate code pairs (8 bit and 16 bit noise codes) resulted in identifying 8 unique codes for the four bit code pairs and 16 unique codes for the 8 bit code pairs whose crosscorrelation value between any two or more codes of the subclass is zero at $\tau=0$. The specific codes forming the sub-classes are shown in Tables D1 and D2 where the codes identified in table D1 form a sub-class of 4-bit multiplexed codes and the codes identified in table D2 form a sub-class of 8-bit multiplexed codes.

Demonstrating the validity of the proposed system concept requires establishing that the crosscorrelation between any 2 or more codes identified in either tables D1 or D2 is zero at $\tau=0$. This was accomplished in paragraph 3b(3) of the report and will not be repeated here.

3. Conclusion.

A totally new conceptual approach to multiple-access was described for which orthogonal operation was demonstrated to be possible when utilizing a code division multiple access concept with each user employing a different unique noise code structure for his own address. This was rendered possible by discovering that code subclasses of the broad class of multiplexed noise codes exist which have the unique property of having a crosscorrelation value of zero at $\tau=0$ between all of the codes of the subclass. The two subclasses identified which were for four bit and eight

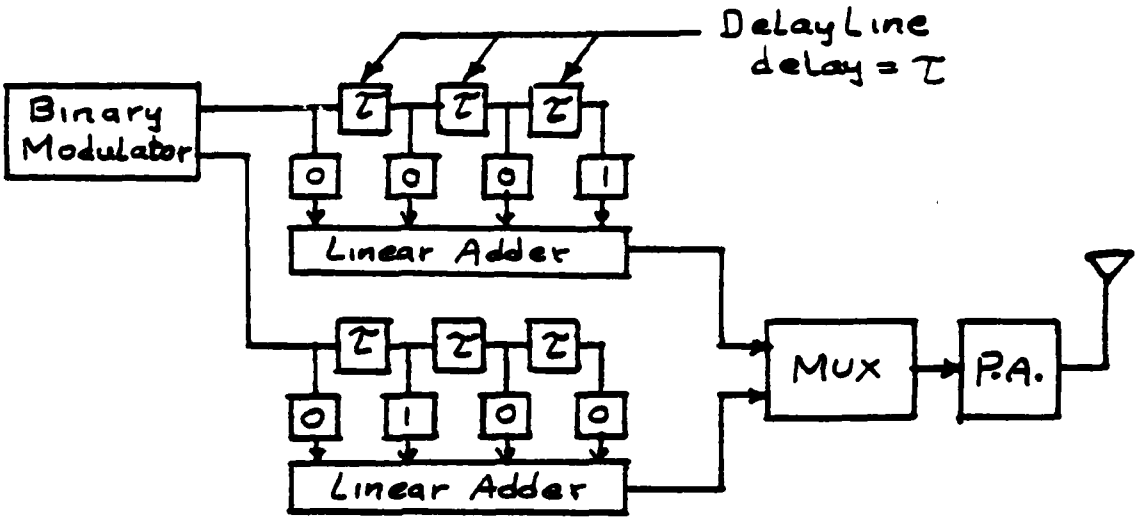

a.) Multiplexed Coder / Transmitter

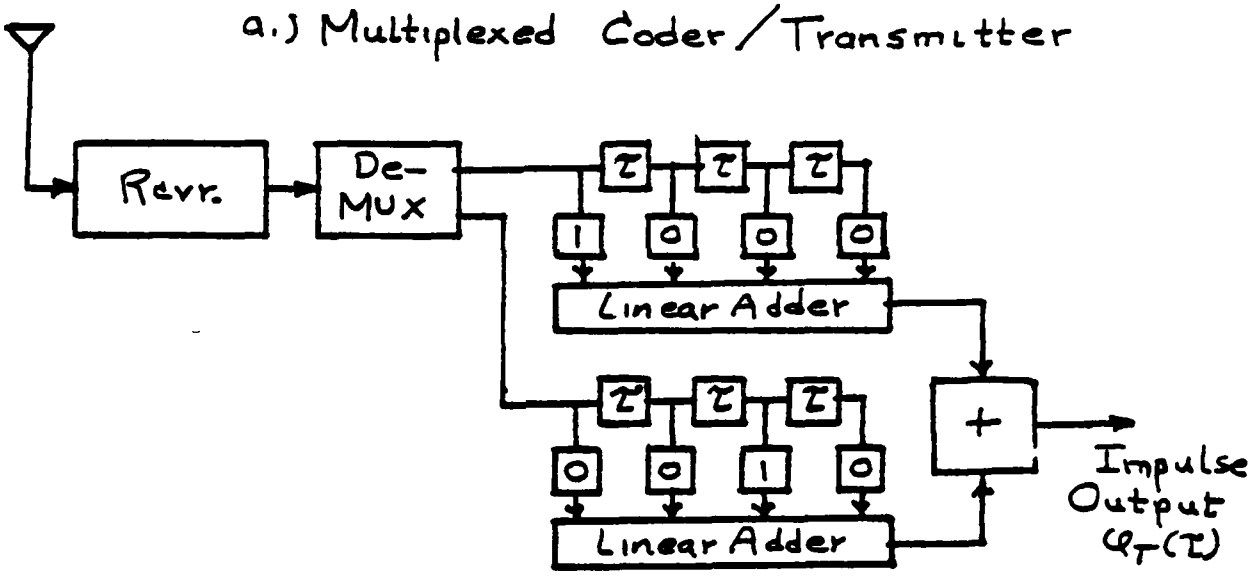

b.) Multiplexed Pulse Compressor / Receiver

Code a = 0 0 0 1 $\quad \varphi_a(\tau) = 1 \cdot 0\, 0^4\, 0 \cdot 1$

Code b = 0 1 0 0 $\quad \varphi_b(\tau) = 0 \cdot 1\, 0^4\, 1 \cdot 0$

$\varphi_T(\tau) = \cdots 0^8 \cdots$

Figure D2 - Multiplexed Code Transceiver

Code Pair No.	Code a	Code b
1	1 0 0 0	1 0 1 1
2	0 0 1 0	1 1 1 0
3	0 1 0 0	0 1 1 1
4	0 0 0 1	1 1 0 1
5	1 0 0 0	0 1 0 0
6	0 0 1 0	0 0 0 1
7	0 1 0 0	1 0 0 0
8	0 0 0 1	0 0 1 0

Table D1 - Sub Class of 4 Bit Multiplexed

Noise Codes with Zero Crosscorrelation at $\tau = 0$

(Code Set #1)

Code Pair No.	Code a	Code b
1	1 0 1 0 0 0 1 1	1 0 0 1 0 0 0 0
2	1 0 0 0 0 1 0 0	1 0 0 0 1 0 1 1
3	0 1 0 0 1 0 0 0	1 0 1 1 1 0 0 0
4	0 0 0 1 0 0 1 0	0 0 0 1 1 1 0 1
5	1 1 0 1 0 0 0 1	1 1 0 1 1 1 1 0
6	1 1 1 1 0 1 1 0	0 0 1 1 1 0 1 0
7	0 1 0 0 0 1 1 1	0 1 0 0 1 0 0 0
8	0 1 1 1 0 1 0 0	1 0 0 0 0 1 0 0
9	0 1 1 1 1 0 1 1	1 0 0 0 1 0 1 1
10	1 1 1 0 1 1 0 1	0 0 0 1 1 1 0 1
11	0 0 1 0 1 1 1 0	1 1 0 1 1 1 1 0
12	1 0 1 1 1 0 0 0	0 1 0 0 1 0 0 0

Table D2 - Sub Class of 8 Bit Multiplexed

Noise Codes with Zero Crosscorrelation at $\tau = 0$

(Code Set #2)

bit code pairs verify the existence of subclasses of codes with the required unique properties and demonstrates the associated operational capability. Establishing multiplexed code subclasses for time-bandwidth products (or equivalently code lengths) greater than 16 requires the utilization of a computer and allocated research time and funds.

APPENDIX E

A Multiplexed Noise Coded Switching System

1. Introduction.

A unique switching system is described which performs line to line or group to group switching using multiplexed noise codes in place of the normally used frequency filters, time gates, or space division switching. These prior art approaches are in general more complex, bulky, and vulnerable to noise interference (impulse and random), crosstalk, and the unauthorized interception of messages. In addition, the proposed method of switching automatically accommodates both digital and analogue input signals making it ideally suited for communication systems that are transitioning from analogue to digital signal structures or which must accommodate both.

Perhaps the most important advantage associated with noise coded switching is that the noise codes can serve a multi-purpose function that is capable of satisfying the most difficult requirements associated with tactical communication systems. The codes can be utilized to perform the signaling function of a mobile access system with little or no self-interference, provide a large degree of A/J protection, enjoy a low probability of intercept (LPI) and meet communications security requirements while interoperating directly with a multi-channel switching system that automatically switches the code to any required destination point over trunk lines.

Switching is accomplished by setting an input line code generator and an output line pulse compressor (or equivalently matched filter) to the same code pair which automatically directs the specific signal applied to the input line to the selected output line that is matched to the input code. The use of particular subclasses of multiplexed noise codes provides a system which operates orthogonally (with no interference between any of the input/output lines) while utilizing a different unique code for each selected input/output set of lines.

The unique property of multiplexed noise codes as a class that is of primary significance for the proposed concept is that subclasses exist whereby the crosscorrelation between any two unique noise codes of the subclass is always zero at $\tau = 0$. Although spurious lobes exist whose (rms) value has an amplitude that is down by at least the square root of the code sequence length (i.e. the time-bandwidth product), the absence of any crosscorrelation value in the same compressed time slot (at $\tau = 0$) for all the codes enables the implementation of a system that operates orthogonally while using different noise codes to perform the switching function.

2. Concept Description

A functional block diagram of the noise coded switch is shown in figure E1. An input line S_1 through S_n or a group of these input lines are selected using the code selectors. The required output line or lines (determined from the system switching algorithm) are then established by setting the matched filter decoder to the appropriate codes with a second set of code selectors. An input signal S_i modulated by a generated code pair a_i and b_i will only transfer to the selected output line whose matched filter pair is matched to a_i and b_i and be totally non-interfering with all of the other output lines.

A functional block diagram which illustrates the operation of the line to line switch in more detail is presented in figure E2. The role of the switch controller, clock and gate (these were omitted in figure E1 for clarity) is illustrated in this figure. A clock is required, but only for the purpose of starting all of the generated codes at the same time and generating a gate which will gate all of the output lines at $\tau = 0$ ($\tau = 0$ corresponds to the time of occurrence for the compressed noise code). The code selection is accomplished by the switch controller which is integral to a switch processor. Any input line x is assigned to a signal S_i by selecting a mate code pair a_i and b_i. These codes are then used to modulate (this is a simple multiplier or mixer) the signal to be switched S_i and is then fed to a linear adder. A separate adder is used for codes a and b. Each adder is connected to a simple 2 wire bus which is tapped by all of the output lines. Line y is then selected as the output line by configuring its corresponding matched filters to compress the codes a_i and b_i to a lobeless impulse (i.e., the matched filters coherently compress the multiplexed noise code pair applied to line X).

Subclasses of these codes which possess the required advertised characteristics of having a crosscorrelation value of zero at $\tau = 0$ were found to exist in sufficient quantity to enable their utilization for switching with no interference occuring between any of the input/output lines (i.e., with zero crosstalk). Two specific sets of codes forming the subclasses are shown in tables D1 and D2 of Appendix D where the codes identified in table D1 form a subclass of 4 bit multiplexed codes and the codes identified in table D2 form a subclass of 8 bit multiplexed codes.

3. System Capacity

It is anticipated that the quantity of available unique noise codes per defined subclass (codes whose crosscorrelation value equals zero at $\tau = 0$) will be greater than the time-bandwidth product (possibly by a large factor) for moderate to large time-bandwidth values (i.e., 50 to 1000). The two subclasses established are both equal to the time-bandwidth product

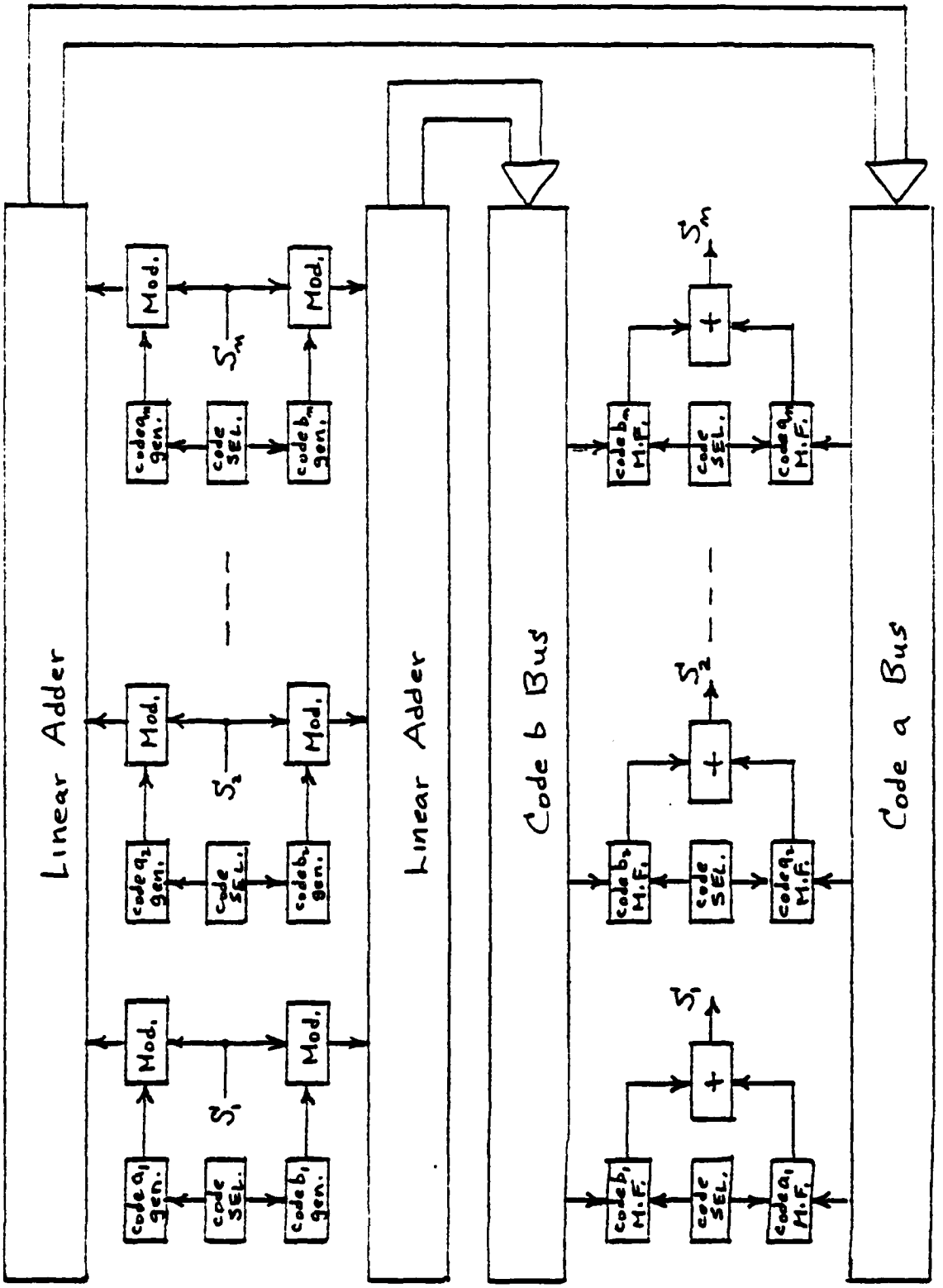

Figure E1— Multiplexed Noise Coded Switching System

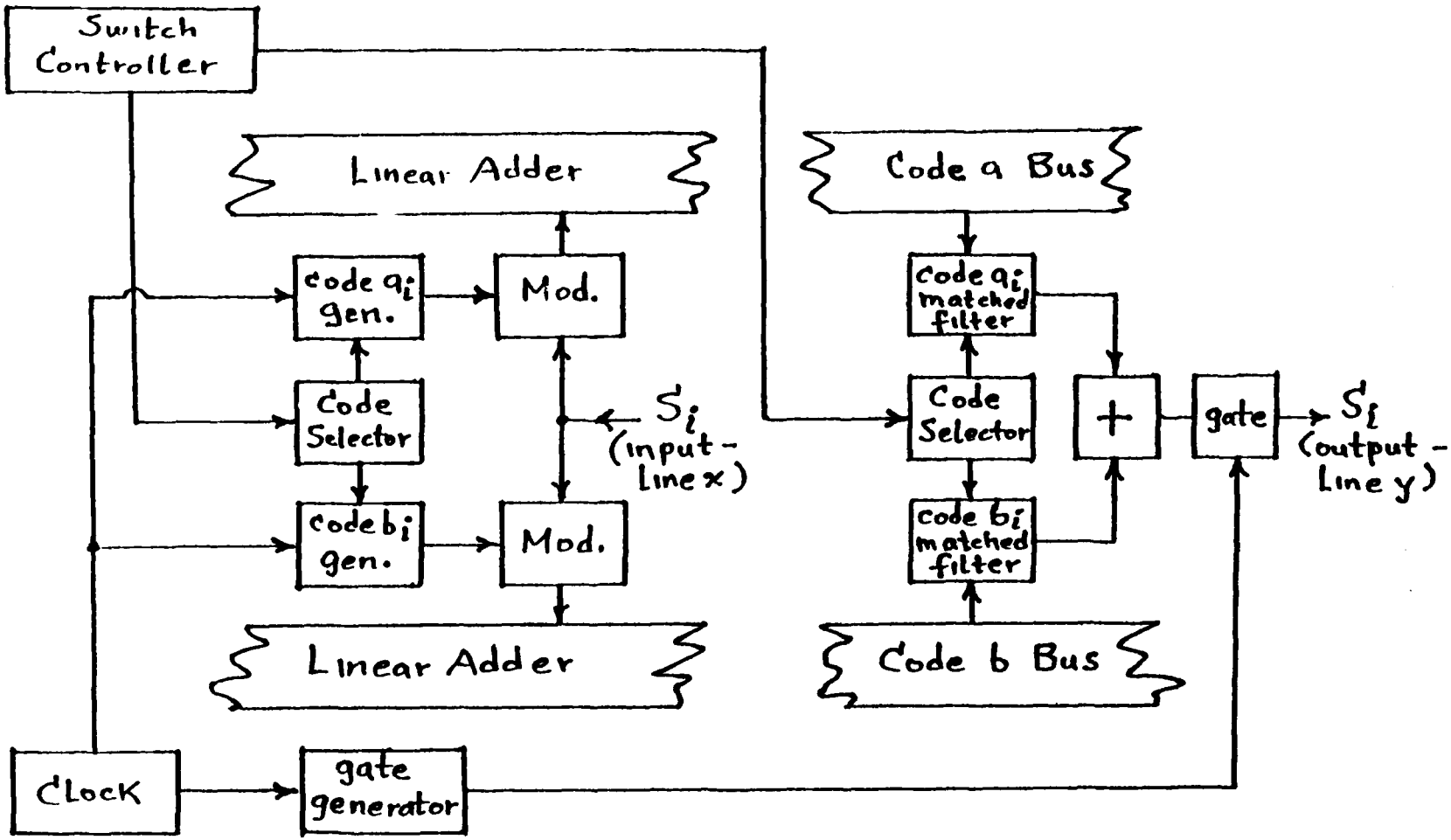

Figure E2 - Line-to-Line Switch Operation

(T x B = n = no. of code bits) even though the quantity of perfect noise codes that could be generated are rather limited for four bit and eight bit code pairs. As the code bit quantity increases to moderate values, the number of different multiplexed noise codes that can be generated rapidly approaches infinity as a result of the various general expansion rules that have been discovered for the general class of multiplexed noise codes. It is therefore reasonable to assume that for any application, the required number of code bits would never be greater than the required number of bits switched in a digital switch using gates and would most likely be significantly less which would make a coded switched system less complex. In addition, very large switch line capacities that would be impractical for pure time gate switching (due to bandwidth and bit rate limitations) would become practical using coded switching as established in this appendix.

It should also be mentioned that even larger quantities of noise codes would become available to make up a subclass for any given application if some degree of non-orthogonal operation is allowed. The performance would be slightly degraded, but this would occur gracefully.

4. Conclusion

A totally new conceptual approach to switching was described for which orthogonal operation was demonstrated to be possible when utilizing a multiplexed noise coded line selection scheme with each selected input/output line employing a different unique noise code structure. This was rendered possible by discovering that code subclasses of the broad class of multiplexed noise codes exist which have the unique property of having a crosscorrelation value of zero at $\tau = 0$ between all of the codes of the subclass. The two subclasses identified which were for four bit and eight bit code pairs verify the existence of a subclass of codes with the required unique properties and demonstrates the associated operational capability. Establishing multiplexed code subclasses for time-bandwidth products greater than 16 requires the utilization of a computer and allocated research time and funds.

BIBLIOGRAPHY

1. Gutleber, Frank S., A Unique Pulse Interference Canceling Spread Spectrum System, FSG-163, 3 Feb 81.

2. ——— A Unique C.W. Interference Canceling Spread Spectrum System, FSG-161, 27 Aug 80.

3. ——— A Multiplexed Noise Coded Switching System, FSG-160, 1 Feb 80.

4. ——— An Orthogonal CDMA System, FSG-158, 17 Oct 79.

5. ——— A Unique Non-Orthogonal Mobile Subscriber Access System, FSG-157, 17 Sep 79.

6. ——— A Pulse Compressor for Multiplexed Noise Codes Generated with Transposed Codes, FSG-156, 8 Aug 79.

7. ——— A Multiplexed Noise Code Generator Utilizing Transposed Codes, FSG-155, 3 Aug 79.

8. ——— An Orthogonal Spread Spectrum TDMA Mobile Subscriber Access System, FSG-144, 6 May 77.

9. ——— A Self-Adaptive Mobile Subscriber Access System Employing TDMA, FSG-142, 26 Jul 76.

10. ——— A Combined ECCM/Diversity Tropospheric Transmission System, FSG-140, 5 May 76.

11. ——— A Multi-Level Mate Pair Code Compressor for Multiplexed Interleaved Noise Codes, FSG-133, Feb 75.

12. ——— A General Multilevel/Multiplexed Noise Code Generator Employing Interleaving, FSG-132, Feb 75.

13. ——— A Mate Pair Code Compressor for Multilevel/Multiplexed Codes Expanded by Butting, FSG-131, Feb 75.

14. ——— A General Multilevel/Multiplexed Noise Code Generator Employing Butting, FSG-130, Feb 75.

15. ——— A Basic (KERNEL) Multilevel/Multiplexed Noise Code Mate Pair Set, FSG-129, Feb 75.

16. ——— Multi-Dimensional Coding, FSG-125, Jul 74.

17. ——— A Bi-Orthogonal PCM System Employing Multiplexed Noise Codes, FSG-116, Jun 72.

18. ——— A TDMA Communications System Employing Perfect Noise Codes, FSG-115, Jun 72.

19. ——— Multiplexed Coding, USAECOM Memorandum Report, United States Army Electronics Command, Apr 70.

20. ——— A Passive Matched Filter for Compressing Interleaved Multiplexed Noise Codes, FSG-102, Nov 69.

21. ——— A Passive Code Generator for Interleaved Multiplexed Noise Codes, FSG-101, Nov 69.

22. ——— A Passive Multiplexed Impulse Autocorrelation Function System, FSG-86, Jan 69.

23. ——— Multiplexed Pseudo Noise Codes with Space Taper, FSG-76, Mar 68.

24. ——— Code Expansion Generator, FSG 26-71, Sep 67.

25. ——— Noise Modulated Pulse Compression System, FSG 25-70, Sep 67.

26. ——— Double Multiplexed Impulse Autocorrelation Function System, FSG 18-63, Jun 67.

27. ——— A Passive Matched Filter for Pulse Compressing Multiplexing Codes, FSG 5-50, Jan 67.

28. ——— A Passive Mate Code Pair Generator, FSG 3-48, Dec 66.

29. ——— Amplitude Weighted Multiplexed Impulse Autocorrelation Function System, FSG-45, Sep 66.

30. ——— A Unique Hardware Method of Implementing Multiplexed Code Pairs, FSG-38, Aug 65.

31. ——— A Multiplexed Pseudo-Noise Code Class, FSG-32, Nov 63.

32. ——— Coding for Multiple Access Systems, FSG-31, Nov 63.

33. ——— A Class of Code Pairs which Contain Implulse Auto-correlation Properties when Utilized with a Multiplexed Correlation Detector, FSG-30, Oct 63.

34. ——— A Time Multiplexed Detector, FSG-29, Oct 63.

35. ——— A Frequency Multiplexed Correlation Detector, FSG-28, Sep 63.

36. ——— Multiplexed Impulse Correlation Function, FSG-8, Mar 80.

37. ——— A Method of Achieving a Delta or Impulse Correlation Function, FSG-6, Feb 60.

38. Skudera, William J., & Granville LeMeune, Acoustic Surface Wave Fabrication Techniques and Results, TR ECOM-4333, August 1975.

39. Jauregui, S., A Theoretical Study of Complementary Binary Code Sequences and a Computer Search for New Kernals, PhD Dissertation, Naval Postgraduate School, Monterey, California, May 1962.

40. Golay, M. J., Complementary Series, IRE Trans. on Info. Theory, Vol. IT-7, April 1961.

RELATED PATENTS

1. Gutleber, Frank S., Code Generator To Produce Permutations of Code Mates, Patent No. 3,461,451, Aug 12, 1969.

2. ——— Impulse Correlation Function Generator, Patent No. 3,518,415, June 30, 1970.

3. ——— Means And Method To Obtain An Impulse Autocorrelation Function, Patent No. 3,519,746, July 7, 1970.

4. ——— An Amplitude Weighted Multiplexed Impulse Autocorrelation Function System, Patent No. 3,634,765, Jan 11, 1972.

5. ——— Time Division Multiple Access Communications System, Patent No. 3,908,088, Sept 23, 1975.

6. ——— Multiplexed Pseudo Noise Pulse Burst Codes With Space Taper, Patent No. 3,917,999, Nov 4, 1975.

7. ——— Code Generator To Produce Permutations of Code Mates, Patent No. 3,947,674, Mar 30, 1976.

8. ——— Impulse Correlation Function Generator, Patent No. 3,955,197, May 4, 1976.

9. ——— Self-Adaptive Mobile Subscriber Access System Employing Time Division Multiple Access, Patent No. 4,215,244, July 29, 1980.

10. ——— Impulse Autocorrelation Function Code Generator, Patent No. 4,245,326, Jan 13, 1981.

11. ——— Combined ECCM/Diversity Tropospheric Transmission System, Patent No. 4,270,207, May 26, 1981.

12. ——— Bi-Orthogonal PCM Communications System Employing Multiplexed Noise Codes, Patent No. 4,293,953, Oct 6, 1981.

13. ——— Orthogonal Spread Spectrum Time Division Multiple Accessing Mobile Subscriber Access System, Patent No. 4,301,530, Nov 17, 1981.

14. Speiser, J.M. and H.J. Whitehouse, Surface Wave Transducers With Sidelobe Suppression, Patent No. 3,551,836, Dec 29, 1970.

15. ——— Surface Wave Multiplex Transducer Device With Gain and Sidelobe Suppression, Patent No. 3,723,916, Mar 27, 1973.